BRNO UNIVERSITY OF TECHNOLOGY FACULTY OF CHEMISTRY

CHEMISTRY & LIFE 2015

Brno University of Technology • Faculty of Chemistry
September 2 - 4, 2015

Conference proceedings

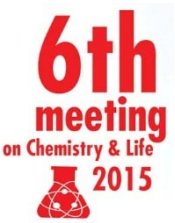

The Sixth Meeting on Chemistry and Life took place at Brno University of Technology, Faculty of Chemistry on Sept. 2-4, 2015. The conference was held under the auspices of the rector of Brno University of Technology, prof. Petr Štěpánek. The scientific level of the conference was guaranteed by the dean of the Faculty of Chemistry, prof. Martin Weiter. The konference was visited by the outstanding experts from abroad (G. H. Pollack and A. Crosby from USA, K. Kovar from Switzerland,, L.E Melymuk from Canada and J. Hofman from the Czech Republic) who presented plenary lectures and by more than 200 other participants from the Czech Republic and 8 other countries. The conference was also attended by companies collaborating with the faculty in the area of contracted research and business activities.

Table of Contents

SPECTRAL ANALYSIS OF LASER PRINTS FOR FORENSIC INVESTIGATION

MICHAELA BELOVIČOVÁ* MICHAL ČEPPAN, ÁGNES BARÁTHOVÁ and SIMONA ŠIMONOVÁ

Slovak University of Technology in Bratislava, Faculty of Chemical and Food Technology, Department of Graphic Arts Technology and Applied Photochemistry, Institute of Natural and Synthetic Polymers, Radlinského 9, 812 37 Bratislava, Slovak Republic
michaela.belovicova@stuba.sk

An important part of forensic analysis of questioned documents is identification or verification of documents. Questioned documents include handwritten documents, but also printed documents and photocopies of printed documents. Currently, almost all offices and households are equipped with laser or inkjet printer and the frauds committed in the context of the document are not uncommon, in fact they represent a large domain of forensic science. Printing inks are usually made of four different colorants (cyan, magenta, yellow and black – CMYK), which together with different combination form the whole spectrum of colors. Laser printers use toner or liquid ink dry resin. Due to technological progress and economic factor the original cartridges (original manufacturer) are filled with new ink (recycled, other manufacturer), which have different chemical composition and are often less expensive. Therefore, the resolution prints on basis of chemical analysis gets still difficult.

As a suitable method for obtaining spectral data of laser toner printer is the FTIR analysis. The use of attenuated total reflection (ATR) accessories in conjunction with Fourier transform infrared (FTIR) spectrometers provides the opportunity of non-destructive analysis with simple or no preparation of samples[1]. However, the problem of this method is that visually resolution of obtained spectra is not unambiguous, what can be attributed to the fact, that different types of toner have very similar chemical composition. Because it is an industrial secret, available resources are unable to provide sufficient information about the detailed composition of the toner, resp. information of the proportions of ingredients in the toner. A common type of forgery consist in materially altering an existing writing or adding a new writing. These changes can be characterized by means of optical spectroscopy[3]. In this work the reflection spectra in Vis and NIR region were measured to obtained more information, which can help to distinguish the different types of toners. Given the similarity of the most commercial used inks, and difficulty monitoring of the spectral change more efficient chemometric methods – PCA[4] (Principal Component Analysis) may be utilized for resolution of spectra set of toners.

In this work forty-eight samples of laser prints from different types of cartridges produced by nine manufacturers were studied (Table 1).

For the analysis of different types of toner was made a model target consisting of solid surfaces 1 cm × 1 cm (Fig. 1).

Table 1
The list of analyzed toner cartridges

	toner	toner label	printer
1	Xerox	006RO1451	docucolor 250
2	HP	CC530A	color LJ CP2025
3	KM	TN114	KM
4	Nash NRG	NRG	Nashuatec Dsc428
5	KM	toner for 1350w	KM PagePro1350w
6	IBM	InfoTech	IBM Infoprint 1312
7	Nash NRG	NRG	Nashuatec Dsm660
8	HP	Q6511X	HP LJ 2420dn
9	HP	C4092A	LBP-810
10	HP	Q2612A	LJ 3050 pcl6
16	KM	di2011	KM Dialta Di2011
17	HP	C7115X	LJ 1200 series
18	HP	CE505X	LJ III P 2055D
19	HP	Q5949X	LJ 1320
20	HP	Q2613X	LJ 1300
21	KM BH	C220far	C220
22	KM BH	C220čier	C220
23	KM	Toner-KM BH 36	KM BH 36
24	HP	92295A	HP LJ Series II
25	HP	92298A	HP LaserJet 4M
26	Epson	XC11NF	Epson Aculaser CX11NF
28	Canon	lbp3360-100%toner	Canon LBP3360
29	HP	C4092A	HP LJ 1100
30	Canon	lbp3360-95%toner	Canon LBP3360-95
35	Xerox	Xerox 3220/3210	Xerox WC 3220/3210
37	HP	Q5949A	HP LJ 1320
38	HP	Q5949A	LJ 1320
39	Canon	CN716	Canon mf 8040 cn
40	HP	C4127X	HP LJ 4000
41	HP	CE255A	HP LJ P 3015
42	Samsung	SCX 4200	Samsung SCX-4200
43	Nashuatec	dt50blk885014	Nashuatec dsm660
45	HP	n-hp-05A, CE505A	LJ P2055D
46	HP	HP 15A	HP LJ 1200 Series
47	HP	CC530A	LJ 1200 series
48	Canon	C-exv11 integral	ir2870
49	Canon	C-exv21 integral	ir c2880/c3380 pcol5c
50	Canon	C-exv21 integral	ir c2880/c3880 ufr II
56	Canon	C-exv22	ir 5055N
57	Grand Print	GP-U215	Lexmark X215
58	Canon	C-exv3	Canon iR2200
59	HP	92274A	HP LJ 4L
60	Samsung	ML-1610D2	Samsung ML-1610
61	HP	HP35A	HP LJ P1005
62	HP	LJ 49X	HP LJ 1320
63	Canon	Cartridge M	Canon smartBase PC 1270D
66	HP	M 3027 m/p	HP LJ 3005
67	HP	CE285AD	HP LJ M1212nf MFP

Fig. 1. **Model target**

The reflection spectra of laser prints in the Infrared region (IR) were collected using Excalibur FTS 3000MX (Digilab, USA) spectrometer with ATR adapter with diamond crystal.

The obtained spectra (Fig. 2) of laser prints were analyses at 4 cm^{-1} resolution. For each spectrum were 100 scans were acquired over the range of 4,000 to 600 cm^{-1}. Raw spectra were adjusted before further analysis with baseline correction, interpolation and normalization of spectra to minimize the impact of noise and downforce of diamond crystal using the Unscramble X program. The samples were measured three times and then averaged. For the resolution of toner in the IR region the most important is the region of the "fingerprints" region (1754–600 cm^{-1}) and was then used in further analyzes (Fig. 3). According to the visual comparison of obtained FTIR spectra, the samples of laser toners could be divided into two groups. With available information about composition, we found that this separation is caused by the presence of one of the main component in toner-polymer binder. The commonly used types of toner binder[5] are – styrene copolymers of acrylic resins (e. g. styrene polymethyl methacrylate), styrene

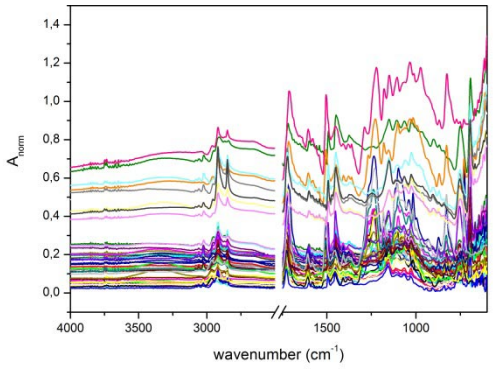

Fig. 2. **Obtained raw FTIR spectra without correction**

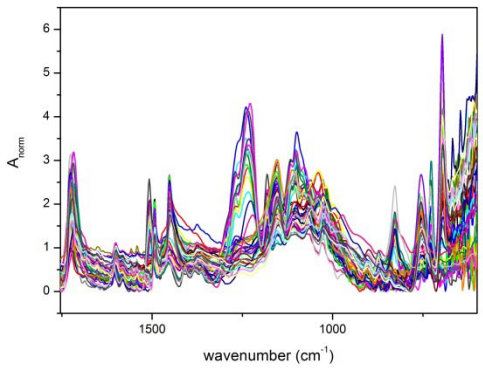

Fig. 3. **Adjusted FTIR spectra, fingerprints region (1754–600 cm^{-1})**

copolymers of butadiene or polyesters. Two types of polymers – polyester resin and styrene acrylate copolymer were confirmed in the group of our samples. The measured spectra were compared with spectral database NICODOM. The absorption bands confirmed for polyester resin match with polyethylene terephthalate. This type of polymer was assigned to the 15 samples of all mentioned toner cartridges. The rest of the samples show presence of second main polymer – styrene/acrylic copolymer. Acrylic acid has a carbonyl group which shows very significant peak at around 1700 cm^{-1} which corresponds to C=O bond in the carboxylic acid substituent group. Styrene and styrene sulfonic acid has phenyl group which shows a significant peak at around 690 cm^{-1} which is due to benzene ring bending. Styrene has a series of peaks at 3082 m 3059, and 3027 cm^{-1} which corresponds to C-H stretches in the phenyl ring[7]. Powder toners are mixtures of several types of chemical compounds such as a colorant (dye or pigment), binding agent, and additives (e. g. fused silica). The spectral differences in IR region are caused by a modified matrix polymer of toner by adding various additives to improve its properties[8].

UV-Vis and NIR spectra were measured with an Ocean Optics fibre optic spectrophotometer consisting of HiRes spectrometer HR 4000CG, UV-Vis light source DH-2000-BAL and standard reflection/backscattering probe with reflection accessory with 45°/45° geometry and NIR halogen light source HL-2000-FHSA with Ocean Optics NIR256-2.5 detector in the wavelength range 240–800 nm for UV-Vis region and 1000–2300 nm for NIR region. For each measurement, the detector was calibrated on the blank paper near the printed area, which largely excluded the influence of the background of the spectral data. Spectra were averaged from three measurements. The raw UV-Vis spectra were interpolated with steps of 2 nm, smoothing with Savitzky-Golay algorithm, normalized and baseline corrected. NIR spectra were adjusted at same way, plus SNV (Standard Normal Variete) and detrending[9] of data set. In the UV-Vis and NIR region (Fig. 5a, 5b) we can see a very similar spectral recording of samples containing different type of polymer. Simple visual resolution is not possible.

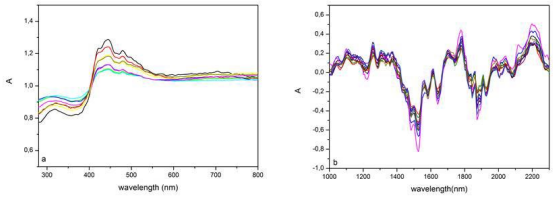

Fig 5. **a) UV-Vis spectra of laser toner after adjustment, b) NIR spectra of samples of laser toner after adjustment**

The spectral data obtained with modern spectrophotometers are difficult to interpreting data sets containing a large amount of information. One of the most common multivariate statistical methods of data analysis is the Principal Component Analysis. PCA creates linear combination of the original spectral variables, called eigenvectors or principal components (PCs). These variables successively account for increasing amount of variation in the data[10]. The firs principal component account for as much of the variability in the data as possible, and each succeeding component accounts for as much of the remaining variability as possible. The results of PCA are showed in terms of component scores and loadings graphs[11]. Our samples of laser

toners were submitted to PCA analysis which makes it possible to compare sets of samples. Representation of spectra in the score graph classified the spectra set into two clusters (Fig. 6). This distribution corresponds to the previous visual sorting of FTIR spectra and reflects the polymer binders in toners, which are most important contributors to the IR spectra of toners. In order to assess the classification potential of PCA with regard to the spectra of unknown toners, the measured spectra of laser prints were divided into the "Training set" (blue spectra/dots, 8 spectra), which are known samples, and "Test set" (green spectra/dots, 40 spectra) representing the new, unknown samples. The PCA analysis was performed using the "Training set" spectra. Then, the set of "Test set" spectra was projected onto the PCA scatter plot of "Training set" spectra (Fig. 7). Objects lying in a given cluster are similar and not similar with samples from other clusters. As can be seen on the Fig. 7, the PCA is able to classify "unknown" toners into corresponding to clusters.

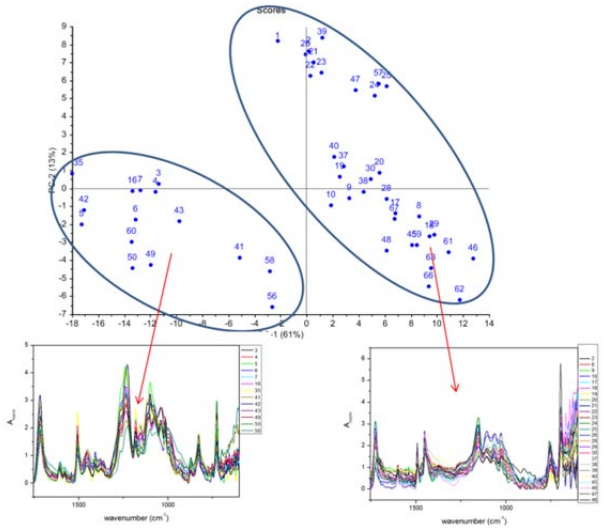

Fig. 6. **PCA dividing of laser toner samples (IR region)**

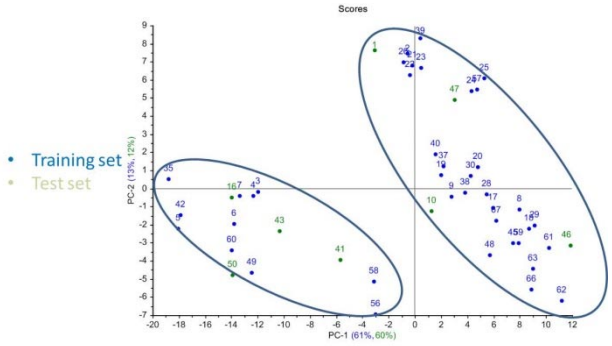

Fig. 7. **PCA training set (green) and test set (blue)**

The aim of this study was linking the two methods: chemometric PCA method and FTIR and Vis-NIR spectral analysis of laser prints toner from different manufacturers. The obtained results suggest the potential of this approach in classification of laser prints and as a tool for identification of questioned prints.

This work was supported by the Slovak Research and Development Agency under the contract no. APVV-0324-10. This publication is the result of the project implementation: Center of Excellence for Security Research ITMS code: 26240120034 supported by the Research & Development Operational Program funded by the ERDF. Michaela Belovičová was also supported by an internal STU grant.

REFERENCES

1. Boyd S., Kirkwood J.: Agilent Technologies, Inc., Publication number si-01374 (2011).
2. A. de Koeijer, J., J. M. de Moel, J.: Identifying black toner using FTIR and pyrolys-GC/MS. Problems of Forensic Sciences XLVI: 413–427. (2001).
3. Somma F., Aloe P., Spagnolo S. G.: Defects in UV-Vis-NIR reflectance spectra as method for forgery detections in writing documents. J. Phys.: Conference Series Volume 249, Number 1. (2010).
4. Muehlethaler, C., Massonnet, G., Esseiva, P. The application of chemometrics on Infrared and Raman spectra as tool for the forensic analysis of paints. Forensic Sci. Int. 209: 173–182. (2011).
5. The Anatomy of a Toner, online resource: http://www.gallifordconsulting.com/The%20Anatomy%20of%20a%20Toner.pdf.
6. Chen Z.: The crystallization of poly (ethylene terephthalate) studied by thermal analysis and FTIR spectroscopy. Ph.D. thesis, University of Birmingham, ID Code: 4251, (2013).
7. Akyildiz, H. I., Effect of styrene sulfonic acid on solubility of poly (acrylic acid-co-styrene-co-styrene sulfonic acid). Online resource: http://www.lib.ncsu.edu/resolver/1840.16/6821. (2011).
8. Trzcińska B. M., Classification of black powder toners on the basis of integrated analytical information provided by Fourier transform infrared spectrometry and X-ray fluorescence spectrometry. J. Forensic Sci., Jul, *51* (4): 919–24. (2006)
9. Barnes R. J., Dhanoa M. S., Lister S. J.. Standard normal variate transformation and de-trending of near-infrared diffuse reflectance spectra. Appl. Spectrosc.; 43: 772–777. (1989).
10. Egan J. W., Morgan S. L., Bartick E. G., Merrill R. A., Taylor H. J.: Forensic discrimination of photocopy and printer toners. II. Discriminant analysis applied to infrared reflection-absorption spectroscopy. Anal Bioanal Chem 376: 1279–1285. DOI 10.1007/s00216-003-2074-z. (2003).
11. Online resource: http://www.ludesi.com/pca/. (2010).

PREPARATION AND STABILITY OF LIPOSOME PARTICLES WITH ENCAPSULATED NATURAL UV FILTERS

JITKA BOKROVÁ, PETRA MATOUŠKOVÁ, RENATA PAVELKOVÁ and IVANA MAROVÁ

Brno University of Technology, Faculty of Chemistry, Materials Research Centre, Purkyňova 118, 612 00 Brno, Czech Republic
xcbokrova@fch.vutbr.cz

Abstract

Photoprotective agents are compounds that can prevent skin damage caused by exposure to UV light. Encapsulation enables controlled released of these photoprotective compounds from the particles applied on the skin surface as well as protection of actives against enviromental threats.

Presented work is focused on possibilities of encapsulation natural UV filters in liposome micro- and nanoparticles. Beta carotene, tocopherol, vitamin C and catechin were packed into liposomes using several types of techniques. The efficiency of encapsulation was evaluated by HPLC/UV-VIS and spectrophotometrical methods. Size of prepared particles was determined by dynamic light scattering. Stability of particles was determind using zeta potential. Long-term stability of particles in water and oil as well as in model cosmetic emulsion was evaluated. Moreover, sedimentation stability of emulsion containing liposomes was studied too. To analyse sun protection factor (SPF) spectrophotometry was used.

In this work it was found that selected natural UV filters were packed into liposomes with high encapsulation efficiency. All of tested liposomes with actives exhibited excellent stability. Prepared particles with encapsulated UV filters could be used as ingredients for sunscreen products and also for daily cosmetics.

Keywords

Liposome, UV filter, encapsulation.

Introduction

1. Encapsulation

Encapsulation is a process to entrap active agents within a carrier material and it is a useful tool for cosmetic and/or pharmaceutical industry, enabling protection and controlled release of several active agents. The encapsulation of some bioactive compounds in micro- or nanoparticles has been investigated of various reasons, e. g. protection from oxidative decomposition and evaporation, odor masking or merely to act as support to ensure controlled release.

A large number of microencapsulation method have been developer in order to be adapted to different types of active agents and shell materials, generating particles with a variable range of size, shell thicknesses and permeability, providing a tool to modulate the release rate of the active principle[1].

Liposomes are spherical bilayer vesicles that are spontaneously formed when phospholipids are dispersed in aqueous solution. They are widely used as carriers of both hydrophilic molecules in aqueous compartments and lipophilic ones in the bilayers, but also amphiphilic molecules. In addition, the use of liposomes for encapsulation of various types of antioxidants is an attractive approach to overcome their physicochemical stability concerns (sensibility to oxygen, light, temperature, and volatility) and their reduced bioavailability which is due to low solubility in water[2].

2. UV filters

The exposure to UV radiation can generate harmful reactive oxygen species (ROS) in the skin. In particular, UVB radiation (290–320 nm) penetrating the skin to a depth of 160–180 μm, can cause erythema and sunburns and trigger off the induction of oxidative stress, DNA damage and premature aging of skin. UVA radiation (320–400 nm) can penetrate deeper into the epidermis and dermis of the skin (around 1 mm) and advance the generation of singlet oxygen and hydroxyl-free radicals, which can harm proteins, lipids and DNA. Furthermore, UVA is 10 times more efficient than UVB at causing lipid peroxidation.

Usually, endogenous enzymatic and nonenzymatic antioxidants (AOs) are able to inhibit the action of ROS; but sometimes excessive and chronic exposure to UV radiation makes these defences inadequate causing many adverse effects like premature skin aging and melanoma. In order to reduce the risk of injury, more effective action is the filtering of sunny rays using sunscreen capable to absorb radiant energy in UVB and UVA range.

Chemical sunscreens are usually organic aromatic compounds conjugated with carbonyl group which absorb ultraviolet rays and release lower energy rays; in this way they prevent the skin from damaging effects of UVB and UVA. However, UV absorption may activate organic sunscreens and they may consequently interact with cutaneous molecules, causing adverse skin reactions like dermatitis or photosensitivity reactions. Thus, in recent years the great interest of photoprotection is addressed in using natural products for their higher tolerability and for their negligible environmental impact[3].

In cosmetic field polyphenols appear particularly promising because they are characterized by an absorption spectrum which can filter UV radiations so reducing the penetration of the radiations into the skin and consequently lowering inflammation, oxidative stress and DNA damaging effects. Moreover, they have anti-inflammatory, immunomodulatory and antioxidant properties, so they can react with free radicals produced by UV radiation (singlet oxygen and hydroxyl free-radicals) and inhibit or retard their harmful effects[4].

Beta-carotene

Beta-carotene is one of the isoprenoid compounds named carotenoids. It is a red-orange pigment found in fruits, vegetables and green leafy plants. Beta-carotene is able to quench singlet oxygen without degradation and reacts with free

radicals, such as peroxyl, hydroxyl and superoxide radicals. Carotenoids have consistently been shown to prevent or decrease oxidative damage to DNA, lipids and proteins. As a result, beta-carotene is used in the prevention and treatment of many diseases that develop with the participation of oxidative stress[5].

Catechin

Catechins are a group of polyphenolic compounds that extensively occur in the plants. They are widely used as nutraceutical for enhancing human health, pharmaceutical formulations and in ointments or cosmetics for increasing the product shelf life. Catechins can be extracted, isolated from plant sources and delivered in suitable form. The principal catechins are shown to have the ability in many animal and *in vitro* models to protect the skin from the adverse effects of UV radiation, including lowering the risk of skin cancers. It has been suggested that catechins may favorably supplement sunscreen protection and be useful in skin diseases associated with solar UV radiation-induced inflammation, oxidative stress and DNA damage[6].

Vitamin E

Vitamin E consists of 8 molecular forms, 4 tocopherols, and 4 tocotrienols. The molecules consist of a hydrophobic prenyl tail that inserts into membranes and a polar chromanol head group exposed to the membrane surface. The major function of vitamin E is to prevent lipid peroxidation. When an ROS attacks membrane lipids, a peroxyl radical may form that can create more peroxyl radicals, resulting in a chain reaction that may threaten the structural integrity of the membrane. Tocopherols and tocotrienols scavenge the peroxyl radical, ending the chain reaction. Vitamin E may also quench singlet oxygen. Once oxidized, vitamin E can be regenerated back to its reduced form by L-ascorbic acid, allowing it to be reactivated without creating a new membrane structure.

Vitamin E is important for protecting the lipid structures of the stratum corneum and for protecting stratum corneum proteins from oxidation. The lipophilic nature of vitamin E makes it attractive for application to and absorption into skin. Several studies have documented photoprotective effects when vitamin E was topically applied to animal skin[7].

Vitamin C

Ascorbic acid is known for its antioxidant potential, its regulation in collagen production and for its action on the improvement of UV-induced modifications in skin relief and ultrastructure. It also acts on regeneration of vitamin E[8].

Methods

Liposomes were prepared manually from mixture of egg lecithin and cholesterol using ultrasonic homogenization. For preparation of enriched liposomes lipid extract from salmon was used.

The efficiency of encapsulation was determined by HPLC/UV-VIS (beta-carotene, vitamin C, vitamin E) and by spectrophotometry (catechin). Stability of the particles was followed in water and in a model cosmetic emulsion. The physicochemical evaluation of particles (size and zeta potential) was analyzed by dynamic light scattering. Sedimentation stability of emulsion containing liposomes was evaluated by analytical centrifugation. Sun protection factor (SPF) of individual components was tested too.

Results and discussion

Liposomes with encapsulated bioactive compound were prepared from mixture of egg lecithin and cholesterole using ultrasonic homogenization. For preparation of enriched liposomes extract from salmon was used.

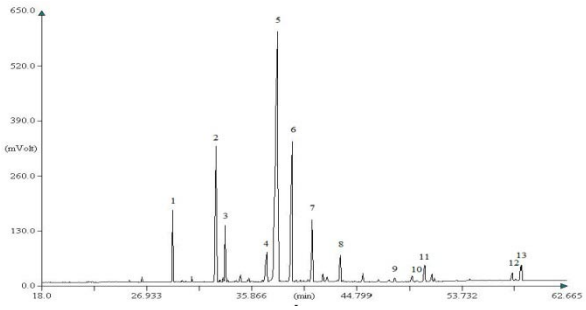

Fig. 1. **Salmon extract content chromatogram**

Table 1
Fatty acids content in salmon extract

sample number	fatty acid	FA content [%]
1	C14:0	3.55
2	C16:0	13.12
3	C16:1 n9c	3.5
4	C18:0	3.18
5	C18:1 n9c	48.81
6	C18:2 n6c	15.67
7	C18:3 n3	6.18
8	C20:1	2.42
9	C20:3 n3	0.38
10	C20:5 n3	0.16
11	C22:0	1.95
12	C22:6 n3	0.14
13	C24:1	0.96

Lecithin was partly replaced by salmon extract in enriched liposomes. PUFA represented 75 % of total fatty acids content in salmon extract (Fig. 1, Table 1).

In Fig. 2 encapsulation efficacies of different types of liposomes and active compounds were compared. The best results were reached using vitamin C and beta-carotene. In general, encapsulation effectiveness was similar in both types of liposomes.

The size and stability of prepared particles was analyzed by dynamic light scattering. The size of both liposomes and enriched liposomes was found in range of 200–800 nm. Encapsulated substance did not affect the size of particles.

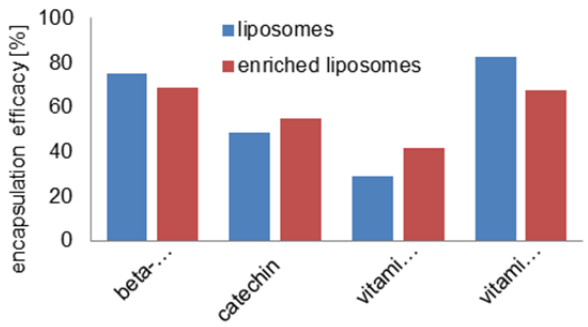

Fig. 2. **Encapsulation efficacy of prepared particles**

The values of zeta potential were used for characterization of particle stability. Zeta potential of all particles was ranging from –30 to –40 mV. The less stable were empty particles, after encapsulation of bioactive compound the stability of particles increased substantially.

Prepared particles were monitored in terms of long-term stability, too. As the most stable environment for particles water was found. The released amount of bioactive compound after 1 month did not exceed 30 %. Long-term stability of particles stored in model cosmetic emulsion was lower, but still sufficient.

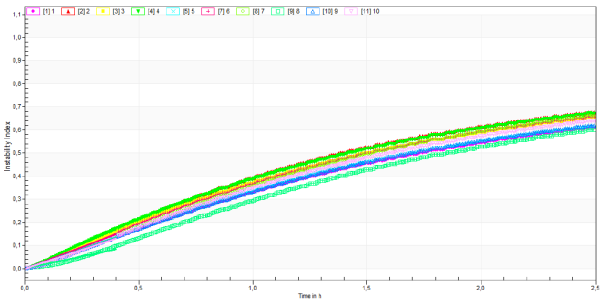

Fig. 3. **Instability index of emulsions with different types of liposomes**

The sedimentation stability of model cosmetic emulsion with liposomes was analyzed by analytical ultracentrifugation. Results were expressed in terms of the instability index (Fig. 3) It was found, that neither type of particle or encapsulated substance does not affect the sedimentation stability. For enhanced stability of emulsion carbomer can be add.

To analyse sun protection factor of individual components spectrophotometry was used[9]. The highest SPF was found for lecithin, the major component of liposomes.

Table 2
Sun protection factor of individual components

sample	sample concentration [mg·ml^{-1}]	SPF
Eusolex 9020	0.01	1.42 ± 0.07
Eusolex 2292	0.15	10.18 ± 0.27
cholesterole	2.24	0.05 ± 0.01
lecithine 10	2.28	4.44 ± 0.12
lecithine 40	8.3	17.53 ± 0.09
salmon extract	4.06	0.01 ± 0.21
vitamin E	3.54	3.81 ± 0.03
beta-carotene	0.42	4.98 ± 0.23
vitamin C	0.76	1.31 ± 0.00
catechin	0.94	1.75 ± 0.00
palm oil 0.1	0.02	6.14 ± 0.09
olive oil 0.1	0.02	2.72 ± 0.01
coconut oil 0.1	0.02	1.65 ± 0.02
coconut oil 0.5	0.1	2.92 ± 0.07

Conclusion

Encapsulation could be a promising alternative for the enlargement of stability and controlled release of selective active compounds. Substances as beta-carotene, catechin and some vitamins show high antioxidant activity as well as photoprotective properties,which makes them possible active ingredients of commercial sunscreeen formulations.

This work was supported by project „Materials Research Centre – Sustainability and Development“ No. LO1211 (Ministry of Education, Youth and Sport of the Czech Republic).

REFERENCES

1. Martins, Isabel M., Maria F. Barreiro, Manuel Coelho a Alírio E. Rodrigues. *Chemical Engineering Journal*, *245*, 191–200 (2014).
2. Xia, Shuqin, Chen Tan, Yating Zhang, Shabbar Abbas, Biao Feng, Xiaoming Zhang a Fang Qin. *Colloids and Surfaces B: Biointerfaces*. *128*, 172–180 (2015).
3. Stevanato, Roberto, Mariangela Bertelle a Sabrina Fabris. *Regulatory Toxicology and Pharmacology*, *69* (1), 71–77 (2014).
4. Gregoris, Elena, Sabrina Fabris, Mariangela Bertelle, Luigi Grassato a Roberto. *International Journal of Pharmaceutics*, 405 (1–2), 97–101 (2011).
5. Kasperczyk, Sławomir, Michał Dobrakowski, Janusz Kasperczyk, Alina Ostałowska, Jolanta Zalejska-Fiolka a Ewa Birkner. *Toxicology and Applied Pharmacology*, 280 (1), 36–41 (2014).
6. Primavesi, Laura, Marta Piantanida a Valerio Pravettoni. *Polyphenols in Human Health and Disease*. Elsevier, 849 (2014).
7. Pinnell, Sheldon R. *Journal of the American Academy of Dermatology*, 48 (1) 1–22 (2003).
8. Gaspar, L. a P. Campos. *International Journal of Pharmaceutics*, 343 (1–2) 181–189 (2007).
9. Pachuau, Lalduhsanga a C. Malsawmtluangi. *Journal of Applied Pharmaceutical Science*, 3 (09) 150–151 (2013).

ASSESSMENT OF ANTIOXIDANT PROPERTIES OF DIFFERENT TYPES OF HERBS BY EPR AND UV-VIS SPECTROSCOPY

LENKA BUTOROVÁ[a, b], MARTIN POLOVKA[b], BLANKA TOBOLKOVÁ[b], EVA VÍTOVÁ[a] and GABRIELA KŘEMENOVÁ[c]

[a]*Brno University of Technology, Faculty of Chemistry, Department of Food Science and Biotechnology, Purkyňova 118, 612 00 Brno,*
[b]*National Agricultural and Food Centre, VÚP Food Research Institute, Department of Chemistry and Food Analysis, Priemyselná 4, 824 75 Bratislava,*
[c]*The Medicinal Herbs Centre, Údolní 74, 602 00 Brno*
xcbutorova@fch.vutbr.cz

Introduction

Currently, there is an increasing interest in complex characterization of medical plants and isolation of their main bioactive components including antioxidants. Herbs are rich sources of natural antioxidants, which are mainly responsible for their health benefits e.g. anticarcinogenic, antimutagenic or anti-inflammatory. The antioxidant effect of herbs is mainly attributed to phenolic compounds such as flavonoids and phenolic acids. These compounds can help preventing oxidative damages caused by free radicals, retard the progress of chronic diseases or lipid oxidative rancidity in foods. Therefore herbs have been used for centuries to flavour and conserve food, to treat health disorders and to prevent diseases[1–4]. The first step of effective isolation of antioxidants from herbs is the extraction, which must be fast, simple and inexpensive, but also sensitive to respective bioactive components, environmental friendly and easy to automate. To do so, the optimalization of extraction process is necessary[5].

The aim of this study was to perform the assessment of antioxidant properties of various types of herbs commonly available in Czech Republic in different extraction solvents by using modern spectroscopic techniques – UV-VIS NIR and EPR spectroscopy.

Examined samples

Ten selected medical herbs: sage (*Salvia officinalis* SO), lemon balm (*Melissa officinalis* MO), narrowleaf plantain (*Plantago lanceolata* PL), rosemary (*Rosmarinus officinalis* RO), lavender (*Lavandula augustifolia* LA), peppermint (*Mentha piperita* MP), oregano (*Origanum vulgare* L. OV), St John's wort (*Hypericum perforatum* HP), hyssop (*Hyssopus officinalis* HO) and garden angelica (*Archangelica officinalis* AO) were analysed. Herbs were harvested in their full ripeness in The Medicinal Herbs Centre (Brno, Czech Republic) by experienced agronomists during the summer 2014. After harvest herbs were immediately dried on trays at 30 °C and stored in paper bags until analysis.

Preparation of extracts

For analysis 0.5 g of homogenized herbs was placed into centrifuge tubes for solvent extraction. 20 ml of selected solvent (50 % acetone, 50 % ethanol, distilled water or dimethylsulfoxide – DMSO) was added to test portion of herbs. After that mixture was shaken on a shaker 60 min at 150 rpm and laboratory temperature, centrifuged at 15 000 rpm at 20 °C for 10 minutes, filtered through a fluted filter into a dark vial and stored in the refrigerator at 5 °C during analysis. Two extracts of every herbs were prepared, every sample was analysed two times (number of repeatitions, n = 4).

UV-VIS experiments

The entire UV-VIS experiments were performed using UV-VIS-NIR spectrophotometer Shimadzu 3600 with accessories.

Total phenolic content was determined applying Folin-Ciocalteau modified method[6]. Exactly 200 µl of concentrated/diluted herbal extract, 15.8 ml of distilled water and 1 ml of Folin-Ciocalteau reagent were mixed. After 10 min 3 ml of 20% sodium carbonate was added and after 60 min the absorbance of final solution was measured at 765 nm in 1cm quartz cuvette. Standard solutions of gallic acid were used for calibration curve construction and the results were expressed as gallic acid equivalents (GAE, g/kg).

Total flavonoids content (TFC) was determined by modified method using 2-aminoethyl-diphenylborate reagent[7]. 3 ml of extract was mixed with 150 µl of 1 % 2-aminoethyl-diphenylborate in ethanol directly in a quartz cuvette. After 10 minutes final solution was measured at 404 nm against a reference (concrete solvent). Standard solutions of rutin were used for calibration curve construction and the results were expressed as rutin equivalents (RE, g/kg).

Colour characteristics (colour coordinates L*, a* and b*) of extracts were performed directly from measured spectra by means of ColourLite Panorama Shimadzu software (LabCognition Analytical Software, Germany) under standardized conditions: D65 day light illuminant and 10° standard observe angle. Sample spectrum was scanned at wavelength 200–1000 nm, with 0.5 nm interval and slit width 1 nm. 1mm quartz cuvette was used for measurements.

EPR experiments

All experiments were performed using a portable X-band EPR spectrometer e-scan (Bruker, Germany) with accessories.

Antioxidant activity of extracts was tested by 2,2´-azino-bis(3-ethyl-benzothiazoline-6-sulphonic acid cation radical ($ABTS^{\bullet+}$) assay. $ABTS^{\bullet+}$ radical-scavenging activity assay was prepared on this way: 300 µl of diluted sample was mixed with 700 µl of the solution of $ABTS^{\bullet+}$ in water (initial concentration c = 0.1 mmol/l). The mixture was purged with 2 ml of air and immediately transferred into the EPR flat cell. EPR measurements started exactly 3 min after $ABTS^{\bullet+}$ addition and a set of 10 EPR spectra was recorded in time domain during 15 min. Radical-scavenging activity was expressed as a TEAC (Trolox equivalent antioxidant capacity) value. TEAC values were calculated for concentration value $ABTS^{\bullet+}$ (double

integral of EPR spectra) measured at 10.5 min after addition radical into the system.

The capability of extracts components to terminate the hydroxyl radicals (•OH) generated by chemical reaction directly in the experimental system via thermal decomposition of potassium persulfate ($K_2S_2O_8$) radical initiator in the presence of 5,5-dimethyl-1-pyrroline-N-oxide (DMPO) as spin trap was investigated. Aqueous solutions of 100 µl DMPO (25 µl DMPO/840 µl distilled water), 200 µl 0.1 M sodium phosphate buffer (pH = 7), 300 µl herbal extract and 250 µl 0.1 M $K_2S_2O_8$ were mixed together, then purged with 2 ml of air and immediately transferred into EPR flat cell. The time course of EPR spectra was monitored for 30 minutes. As reference, particular solvent, which was used for preparation of herbal extracts, was added instead herbal extract. If we use this system we observe antioxidant activity as a results of competing reactions between the spin trap DMPO and antioxidants present in sample by formation of spin adduct DMPO-OH dominantly. Antioxidant activity of samples tested by technique of spin trapping in the presence of DMPO / $K_2S_2O_8$ **was expresed as %RS value (radical scavenger, % extinguished radicals)[8], which directly reflects the antioxidant ability to eliminate radicals produced in experimental system.**

Results and discussion

Obtained results confirmed expected dependence of all the monitored characteristics on solvent used, as previously also proved for isolation of valuable components from spelt flours[9]. The extraction yields as well as the total content of polyphenols and flavonoids, and last but not the least antioxidant properties of herbs under study are inversely proportional to the values of relative permittivity of the solvents, taken as a measure of polarity. This fact indicates that preferably, the non-polar components are extracted. The observed tendency is also demonstrated on Fig. 1, proving the decrease in antioxidant properties in the following order 50 % acetone > 50% ethanol > DMSO > distilled water.

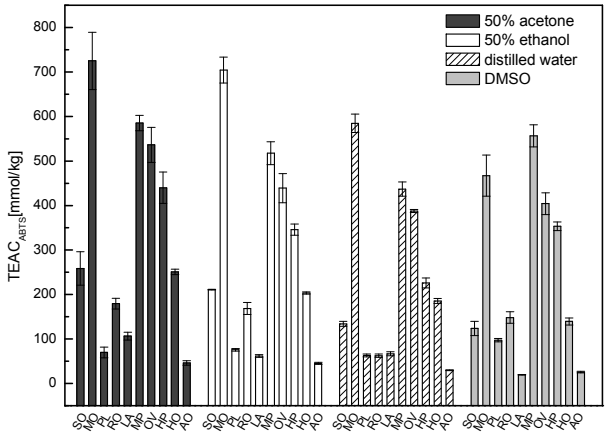

Fig. 1. **Dependence of ABTS$^{•+}$ radical-scavenging ability of medical herbs extracts on extraction solvent. The abbreviations of individual herbs are explained in the main text**

Based on the results we can conclude that 50 % acetone was the most appropriate solvent for the extraction of antioxidant compounds selected herbs. It allows obtain the maximum content of antioxidants from herbs and therefore it is suitable for routine analytical work, but from the food point of view it is not suitable due to its flammability, irritation effect and volatility. Extracts in 50 % ethanol and/or distilled water are rather interesting in light of implementation into food industry.

As regards the comparison of properties of individual herbs, practically identical trend is obvious for all the solvents used. The concentration of polyphenols, flavonoids as well as radical-scavenging properties decreased in general in the following order: MO > MP > OV > HP > SO > HO > RO > PL > LA > AO.

Statistical analysis also confirmed that total content of polyphenols and flavonoids correlate well with total antioxidant activity determined using ABTS$^{•+}$ assay. This trend is also shown in Table 1. for aqueous extracts of herbs. It confirms generally known fact that polyfenolic compounds and flavonoids are mainly responsible for antioxidant properties of herbs[2]. This tendency was observed in all examined solvents. Pearson correlation coefficients decreased in following direction DMSO > 50% ethanol > distilled water > 50% acetone comparing $TEAC_{ABTS•+}$ vs. TPC and/or $TEAC_{ABTS•+}$ vs. TFC.

There was also found a strong positive correlation between the values of TPC and TFC for all selected solvent. Pearson correlation coefficients acquired values 0.882 for aqueous extracts, 0.912 for ethanol extracts, 0.943 for acetone extracts and 0.982 for DMSO extracts of herbs. It suggests the fact that flavonoids are fractions of phenolic compounds[10]. Different values of Pearson correlation coefficients within each extraction system may be influenced polarity and donor-acceptor properties of solvents, which influence largely yields and process of extraction.

Table 1
Correlation matrix of the antioxidant and color characteristics of aqueous extracts of individual herbs

	TPC	TFC	L*	a*	b*	$TEAC_{ABTS•+}$	%RS
TPC	1	0.882	0.725	0.238	0.738	0.977	0.627
TFC	0.882	1	0.711	0,087	0.798	0.834	0.624
L*	0.725	0.711	1	0.498	0.946	-0.806	0.731
a*	0.238	0.087	0.498	1	0.241	0.372	0.125
b*	0.738	0.798	0.946	0.241	1	0.782	0.855
$TEAC_{ABTS•+}$	0.977	0.834	0.806	0.372	0.782	1	0.637
%RS	0.627	0.624	0.731	0.125	0.855	0.637	1

Additionally, correlation analysis showed relationship among colour coordinate b* (which determines representation

of yellow and/or blue colour in herbal extracts) and TPC, TFC and $TEAC_{ABTS^{\bullet+}}$ values. This tendency was obvious for all investigated extraction systems. Even positive values of colour coordinate b* were noted in all herbal extracts, suggesting dominant proportion of yellow colour in individual extracts. It is known that the yellow colouration of herbs is due to the presence of carotenoids and flavonoids (mainly flavonols, chalcones or aurones), which are also known for their antioxidant properties[11]. Probably recorded correlation indicates this fact.

In order to perform detailed analysis of the character of the isolated compounds and to find closer relationships among parameters, additional liquid chromatography experiments are in progress. All the experimental data will be after finishing of experiments processed by multivariate statistics.

This contribution is the result of the project implementation "Establishment of a HiTech Centre for Research on Formation, Elimination and Assessment of Contaminants in Food" supported by the Research & Development Operational Programme funded by the ERDF. The Medicinal Herbs Centre in Brno is gratefully acknowledged for samples provision.

REFERENCES

1. Mishra S. S., Patel K. K., Raghuwaski N., Pathak A., Panda P. P., Girhupunje K., Patro Ch. N.: Ann. Biol. Res. *2*, 1 (2011).
2. Miser-Salihoglu E., Akaydin G., Caliskan-Can E., Yardim-Akaydin S.: J. Nutr. Food Sci. *3,* 5 (2013).
3. Paur J., Carlsen M. H., Halvorsen B. L., Blomhoff R., in: *Herbal Medicine: Biomolecular and Clinical Aspects*, Chap. 2, CLR Press, (2011).
4. Saxena M., Saxena J., Nema R., Singh D., Gupta A.: J. Pharmacogn Phytochem. *1,* 6 (2013).
5. Gupta A., Naraniwal M., Kothari V.: IJANS. *1,* 1 (2012).
6. Chaovanalikit A., Wrolstad R. E.: J. Food Sci. *69*, 1 (2004)
7. Jiang P., Burczynski F., Campbell C., Pierce G., Austria J. A., Briggs C. J.: Food Res. Int. *40*, 3 (2007).
8. Zalibera M., Rapta P., Staško A., Brindzová L., Brezová V.: FRA *43,* 5 (2009).
9. Polovka M., Kajdi F., Tobolková B., Suhaj M.: Acta Agron Óvariensis *53*, 1 (2011).
10. Petrussa E., Braidot E., Zancani M., Peresson C., Bertolini A., Patui S., Vianello A.: Int. J. Mol. Sci. *14* (2013).
11. Davies K. in: *Plant pigments and their manipulation*. Oxford: Blackwell, 2004.

USING OF ARGON-HYDROGEN PLASMA AS A TOOL FOR REMOVING OF CORROSION LAYERS FROM BRONZE SAMPLES

PETRA FOJTÍKOVÁ*, LUCIE ŘÁDKOVÁ, DRAHOMÍRA JANOVÁ, JAN KOPLÍK and FRANTIŠEK KRČMA

Brno University of Technology, Faculty of Chemistry, Purkyňova 118, 612 00 Brno
xcfojtikovap@fch.vutbr.cz

The presented research is focused on the protection of cultural heritage objects. Their conservation procedure includes sanative/remedial and preventive part. Both parts include the collection of steps leading to protection of historical value of the archaeological object (artefact) and minimalization of the intervention action necessity[1].

The application of low temperature low pressure plasma, so called plasma chemical reduction, is the aim of presented research. History of plasma chemical reduction goes back to the end of the 20th century, especially to the 80th years. The first application of plasma chemical reduction was done by the group around V. D. Daniels[2]. Nowadays, the method is used in some workplaces in the Europe; for example at Central Bohemian Museum in Roztoky[3] (Czech Republic), Swiss National Museum in Zürich[4] (Switzerland) or at Technical University in Athens[5] (Greece). The experimental apparatus used for the current research was constructed according to design proposed by S. Veprek[6] and it was further improved.

The bronze alloy was chosen for the presented study because there is only very limited knowledge about plasma treatment of such alloy however there is a huge number of excavated bronze archaeological objects and it is necessary to conserve them and to keep them for future generations. Because there is impossible to optimize any treatment procedure on original objects (they have unvaluable historical value and also every object has its individual corrosion history and corrosion layers composition), the model samples were prepared. The used bronze composition was 96.4 % of copper and 3.6 % of tin (determined by energy dispersive X-ray fluorescence spectrometer (EDXRF – EX-6600). The corrosion layers were prepared on bronze plates with dimension of 10 × 50 mm according to the following procedure. The samples were cleaned by ethanol, dried by hot air flow and stored to the ambient soil in Brno climatic conditions for two years. After that, the samples (with model corrosion layers) were carefully excavated, dried in the vacuum dryer at the temperature of 60 °C and finally they were stored in the special bags (approximate size of 100 × 100 mm). Each bag was made of a special foil with barrier properties using hand heat sealing tongs. Together with the sample, the oxygen and moisture absorbers were added to the bag. The samples were stored under these conditions at laboratory temperature up to their plasma chemical treatment.

As it was already mentioned in the previous section, the experimental apparatus for plasma chemical reduction (Fig. 1) was inspired by S. Veprek[6] and further improved to decrease mainly heat stress to the sample during the treatment. Also more in situ diagnostic technics were implemented and whole system was computer based using the specially designed software.

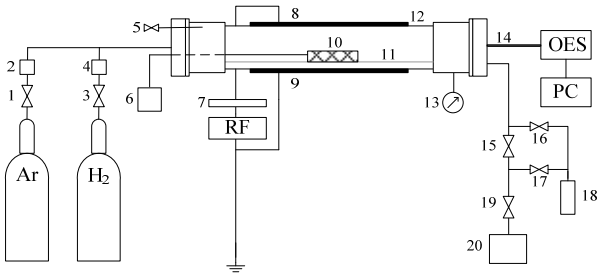

Fig. 1. **Schematic drawing of plasma chemical apparatus:** 1, 3 – valves; 2, 4 – mass flow controller; 5 – aeration valve; 6 – thermocouple; 7 – matching network; 8, 9 – outside placed copper electrodes; 10 – sample; 11 – glass holder; 12 – quartz reactor; 13 – capacitance gauge; 14 – optical fiber; 15, 16, 17 – on/off valves; 18 – liquid nitrogen trap; 19 – butterfly valve; 20 – rotary oil pump

The cylindrical quartz glass reactor of dimension of 100 × 900 mm was an apparatus core. The working gas mixture supply was realized via two mass flow controllers for argon and hydrogen separately. This allowed setting the working gas mixture with variable composition. The simple aeration valve was mounted to the flange of reactor body. The pressure in the reactor ws measured bycapacitance gauge connected to the end of reactor. The whole reactor was continuously pumped by rotary oil pump through the liquid nitrogen trap condensating the process products, mainly hydrochloric acid and water. Two outer copper electrodes were mounted on the outer reactor wall by glass fibre. One electrode was grounded; the second one was connected through the matching network with radio frequency generator (operating frequency of 13.56 MHz and maximum power of 1200 W). The treated sample was placed on the glass holder at position close to the reactor center. The K-type thermocouple was mounted at the sample surface by stainless steel wire. The light emitted from the discharge was measured by optical emission spectrometer Ocean Optics HR4000 with 2400 gr/mm grating connected to PC equipped by Spectra Suite software. The spectra were measured from pumping side of reactor at its axis.

The plasma chemical treatment conditions were specific for every treated sample how ever some parameters were fixed for the whole presented serie. The experimental conditions are reviewed in Tables 1 and 2.

Table 1 The experimental conditions

argon mass flow	10 sccm
hydrogen mass flow	40 sccm
max. sample temperature	120 °C
treatment duration	90 minutes
pressure before treatment	~ 20 Pa
operational pressure	~ 150 Pa

Table 2
The delivery power and mode of plasma generation useed for each experiment

	delivery power [W]	*mode
sample 1	100	continuous
sample 2	200	continuous
sample 3	300	continuous
sample 4	400	continuous
sample 5	100	pulse
sample 6	200	pulse
sample 7	300	pulse
sample 8	400	pulse

Various active particles like ions, radicals, excited molecules are generated in the active plasma discharge. These species can react with the sample surface. The reaction of atomic hydrogen (active discharge) with oxygen (corrosive layer) forms OH radical (consequently reduced to water) that can be used for the process monitoring by in situ optical emission spectrometry[7]. The emission spectra in the range of 250–350 nm were measured every minute (during the first 30 minutes) and then every five minutes (30–90 minutes) up to the end of experiment. The relative intensity of OH radicals was calculated from the part 306–312 nm because of potential overlap by other molecular bands and finally the time dependence of intensity was created.

The sample temperature was continuously measured by thermocouple. Because bronze is very temperature sensitive material due to tin presence, the temperature of 120 °C was selected as the maximal allowed. Such low temperature (significantly under the tin melting point) was selected because sample surface is locally (at atomic scale) overheated by impact of heavy particles, mainly ions. So, if the sample temperature becomes attack the critical value (120 °C), the power dissipated to plasma was decreased until the sample temperature have steady tendency. Whereas the absolute power value was modified in continuous mode, the duty cycle was changed in pulsed mode. The duty cycle of 99 % at the beginning of the process decrease in dependence of the sample temperature.

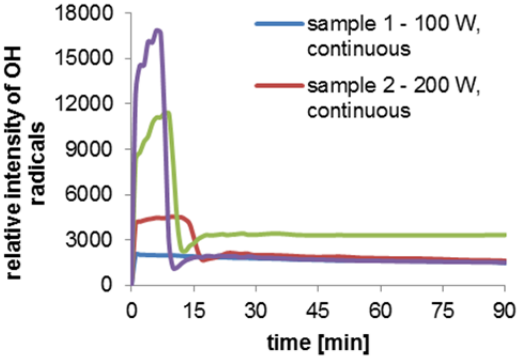

Fig. 1. **Time dependence of the OH radical relative intensity for samples 1–4 treated using the continuous mode of plasma**

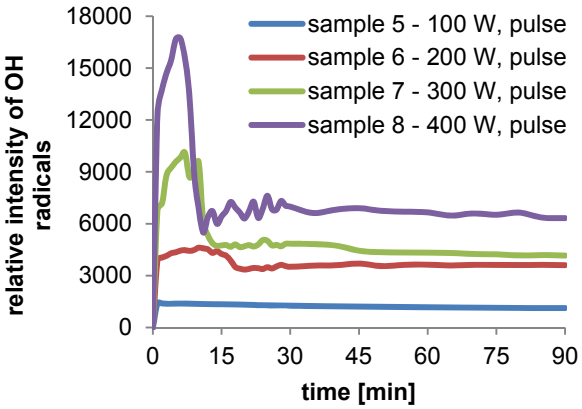

Fig. 2. **Time dependence of the OH radical relative intensity for samples 5–8 treated using pulsed discharge mode**

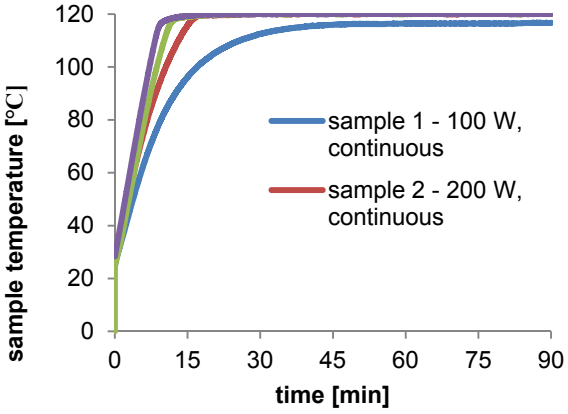

Fig. 3. **Time dependence of sample temperature for samples 1–4**

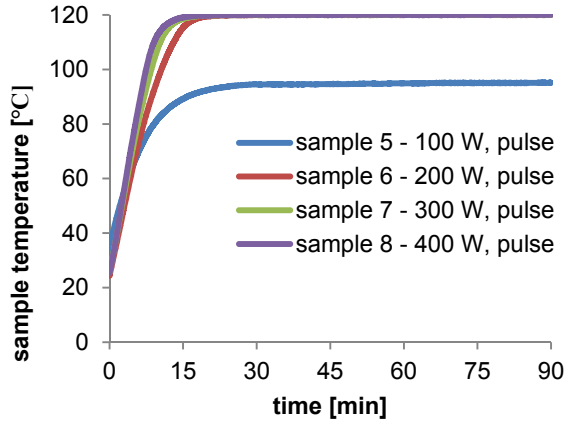

Fig. 4. **Time dependence of sample temperature for samples 5–8**

The process of plasma chemical reduction is possible considered as successful if the maximum of relative intensity of OH radicals is created and the decrease follows (Fig. 1 and Fig. 2)[8].

The maximum of OH radical relative intensity was not created in the case of sample 1 (delivery power 100 W). The delivery power 100 W in continuous mode thus was evaluated as undesirable for the plasma chemical corrosion layers removal. The same situation can be seen also in the case of sample 5 treated at similar dissipated power.

From the results (Fig. 3 and Fig. 4) is evident that delivery power 100 W in the continuous as well as in the pulsed mode is safe and it is not necessary to limited it but corrosion layers are not reduced, as it is visible from (Fig. 1 and Fig. 2).

The material analyzes were performed by a scanning electron microscope (SEM) Philips XL 30 before and after the plasma treatment (without removal of the corrosion products resudui). The samples surface morphology was gained by the backscattered electron detector using 20 keV accelerating voltage. Simultaneously, the chemical composition was measured by energy dispersive x-ray analysis (EDX) Edax analyzer. Average value of ten measurements was performed on the each sample, each from area of 3.45 × 4.45 μm. The presence of 19 elements was proved, most of them was determined at trace level, only. The highest content was obtained for oxygen, copper and tin. The decrease of oxygen content (Fig. 5), as well as the increase of copper and tin content, corresponds with results of optical emission spectroscopy.

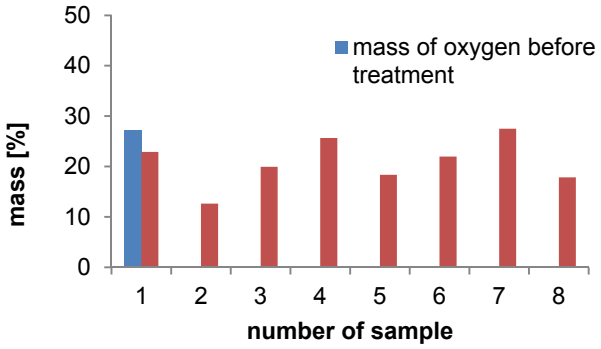

Fig. 5. **Relative mass abundance of oxygen before and after plasma chemical reduction**

Oxygen from corrosion layer reacts with atomic hydrogen (both neutral and ionic) from plasma and creates OH radical detectable by OES. Oxygen is removed form the corrosion products layer and thus the relative oxygen abundance at the object surface decreases. Due to this fact, the abundance of tin and copper (main bronze alloy compounds) increases. The decrease of oxygen content in every measurement is important fact. However, the oxidation after measurnements may causes the different oxygen content (Fig. 5).

Eight bronze samples with the same corrosion layers were created for the presented study. Results show that the lowest applied power is undesirable for the succesfull corrosion layers removal because there is too low concentration of hydrogen active species. The best results were obtained for the highest applied power. Because of low temperature treatment necessity, the mean power was modified during the treatment to keep the maximal predetermined sample temperature. Both mean power modificatiuon modes (i.e. absolute power value decrease in continuos mode or decrease of duty cycle in pulsed mode) were found as possible ways how to keep the maximal sample temperature.

This research has been conducted within the project DF11P01OVV004 "Plasma chemical processes and technologies for conservation of archaeological metallic objects", founded by the Ministry of Culture of the Czech Republic.

REFERENCES

1. Benešová J. et al.: Konzervování a restaurování kovů, Chap. 1, p. 22, Technické muzeum v Brně, Brno, 2011 – in Czech.
2. Daniels V. D., Holland L., Pascoe W.: Stud. in Conserv. 24, 85 (1979).
3. Webpage of Středočeské muzeum v Roztokách u Prahy available from: http://www.muzeum-roztoky.cz/, [15.7.2015] – in Czech.
4. Schmidt-Ott K., Boissonnas V.: Stud. in Conserv. 47, 81 (2002).
5. Novakovic J., Papadopoulou O., Vassiliou P., Filippaki E., Bassiakos Y.: Anal. and Bioanal. Chem.. 395, 2235 (2009).
6. Vepřek S., Patscheider J., Elmer J.: Plasma Chem. and Plasma P.. 5, 201 (1985).
7. Krčma F., Cihlář M., Klíma M.: Proceedings of ICPIG XXVII, Eindhoven University of Technology, Eindhoven, Contr. No. 08-225 (4p.), 2005.
8. Rašková Z.: Optická emisní spektroskopie plazmochemické konzervace archeologických nálezů. Master thesis, Brno University of Technology, Brno, 2001 – in Czech.

POSSIBILITIES OF USING ENERGY BY-PRODUCTS AS RAW MATERIALS FOR HYDROTHERMAL REACTION

LUCIE GALVÁNKOVÁ and TOMÁŠ OPRAVIL

Brno University of Technology, Faculty of chemistry, Purkyňova 464/118, 602 00 Brno, Czech Republic
xcgalvankova@fch.vutbr.cz, opravil@fch.vutbr.cz

Keywords
Coal fly ash, hydrothermal reaction, zeolites, alkali activator, cation exchange capacity.

Abstract
The aim of this contribution is the study of possibilities of processing energy by-products, especially coal fly ash, by hydrothermal treatment. Thanks to hydrothermal conditions and proper alkali activation of fly ashes we can obtain new materials, mainly zeolites. The results of hydrothermal synthesis are influenced by many factors, while temperature of reaction, solution/fly ash ratio and different concentration of alkali activator (NaOH) were examined. Phase composition of prepared samples was characterized by X-ray diffraction (XRD) and scanning electron microscopy (SEM). Also the ability of exchanging Mg^{2+} cations of prepared samples was determined.

1. Introduction

Energy demands of our society increases every year. This trend is connected with producing of huge amount of solid wastes called secondary by-product. One of the most important by-products is coal fly ash generated during combustion of coal in power stations. Since this inorganic material comprises 5–20 % of the mass of the coal, large amount of coal fly ash is produced every year. There are many reasons for exploiting fly ash, which include reducing the cost of waste disposal together with reducing of space required for storage. Another significant advantage is income from the sale of this by-product instead of spending money for landfill it. Another big advantage of using fly ash is the possibility of replacing natural primary materials in some applications. The major application of the coal fly ash is his use for cement or concrete manufacturing. This can be done because of the unique composition of coal fly ash, which contains large amount of SiO_2 an Al_2O_3 and has pozzolanic property after reaction with lime. The coal fly ash is also used for manufacturing bricks, special ceramics, asphalt and aerated concrete. The rest of coal fly ash is disposed of in landfills or lagoons which can results in polluting soils and groundwater. For these and many other reasons, researchers all over the world working on finding new techniques and utilization for energy by-products[1, 2, 3, 4, 5].

Synthesis of zeolites from coal fly ashes is one of a number of potential applications for obtaining valued industrial products. This is possible thanks to composition of fly ash, where the main components are amorphous aluminosilicate glasses. Fly ash then shows compositional similarities to some volcanic materials, which are precursors of natural zeolites. Natural zeolites are mined all over the world, but most of industrially used zeolites are synthesized in alkaline mediums with different sources of silicon and aluminium. Both types of zeolites natural and synthetic ones are used as catalysts, selective adsorbents and ion exchangers. Hence they are used in many fields such as pollution control, petroleum refining, agriculture and purification of gases, etc. Producing of zeolites from coal fly ash is a quite cheap way how to get zeolites. Höller and Wirsching was the first scientist who synthesized zeolites from fly ash in 1985. Since then many techniques of converting fly ash to zeolites have been investigated and published[5, 6, 7, 8, 9, 10]. The most common method used for conversion of fly ash into zeolites is hydrothermal treatment of mixture of fly ash and alkali solution such as sodium or potassium hydroxide. This alkaline conversion of fly ash is based on the combination of different activation solution/fly ash ratios, different molarity of alkaline solutions, changing of temperature, pressure and reaction time. By this method are obtained different synthetic zeolites types such as zeolite Na-P1, zeolite A and X, etc. The resulting materials vary widely and are usually formed by a mix of zeolites. The structural heterogeneity limits their applications. To improve limits of applications of prepared zeolites there is an effort to find new synthetic methods or try to improve process of alkaline hydrothermal conversion by changing variable factors[11, 12, 13]. Zeolites prepared from fly ash can be used as ion exchangers for example in process of decontamination of waste water or as adsorbents[13, 14, 15, 16].

In the present study the objective was to investigate an influence of changing conditions of hydrothermal reaction together with changing concentrations of sodium hydroxide (0.5; 1; 1,5 and 2 M) and solution/fly ash ratios (5, 10 and 15 ml/g). Sodium hydroxide was chosen as the cheapest and highly effective activation reagent. Synthesized products were compared on the basis of structural characteristics and cation exchange capacity.

2. Experimental

2.1. Materials

Coal fly ash was obtained from Počerady, a Czech coal-fired power plant using electrostatic precipitators. X-ray diffraction analyses revealed that the major crystalline phases in the raw fly ash were mullite, quartz, hematite and magnetite together with the amorphous phase. These results are shown in Fig. 1. Sodium hydroxide solutions were prepared by dissolving of NaOH in distilled water.

2.2. Synthetic process

Zeolites synthesis reactions were carried out in Teflon-lined laboratory autoclave placed in conventional drier. Different solution/fly ash ratios (5–20 ml/g), reaction temperature (160–180 °C) together with autogenous pressure (0,6–1 MPa) and NaOH concentration (0,5–2 M) were used. All samples were hydrothermally treated for 24 h. After the

reactions, the products were filtered and washed repeatedly with distilled water and were dried at room temperature.

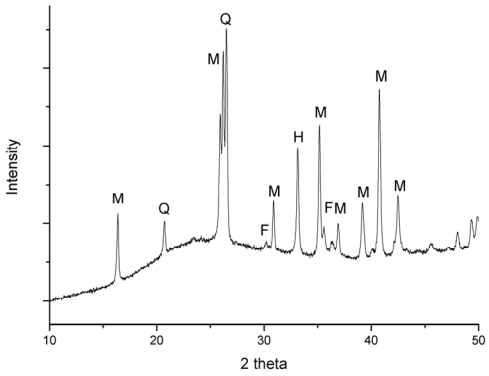

Fig. 1. **XRD pattern of raw fly ash**. **M, Q, F, H stands for mullite, quartz, magnetite and hematite**

2.3. Characterization of products

The phase composition of prepared samples was characterized by X-ray diffraction (XRD, Empyrean, Pananalytical) and morphological analysis was performed on selected prepared samples by scanning electron microscopy (SEM, ZEISS EVO LS 10).

Cation exchange capacity (CEC) values were determined using method by Gillman. In this method 2.5 g of sample was leached for 60 min with 30 ml of 0.1 M barium chloride solution. After centrifugation the solution above the solid sample was poured. This procedure was repeated thrice. After that, the sample was leached for 120 min with 30 ml of 0.02 M magnesium sulfate solution. Amount of magnesium ions in leachate was determined by inductively coupled plasma atomic emission spectrometer (ICP-OES, ULTIMA 2, HORIBA Scientific). The results were expressed as miliequivalents per 100 g of solids.

3. Results and discussion

3.1. Effect of solution/fly ash ratio

Effect of changing solution/fly ash ratio (5, 10 and 20 ml/g) was examined on samples prepared by mixing 0,5M sodium hydrogen solution with raw fly ash. Fig. 2 shows the XRD patterns of samples synthesized at 160 °C for 24 h. The major produced zeolitic phases were identified as zeolite Na-P1 ($Na_6Al_6Si_{10}0_{32}\cdot 12H_2O$) and analcime ($NaAlSi_2O_6\cdot H_2O$). Beside these two new phases, XRD pattern also shows presence of mullite, quartz and hematite. These phases remained even after the hydrothermal treatment. We can say that with increasing solution/fly ash ratio amount of zeolitic phases increase together with decreasing amount of crystalline phases from the raw fly ash. Zeolite Na-P1 is the typical product produced during the hydrothermal treatment of fly ash. This zeolite is classified into the gismondine group and in pure form achieves high-CEC values. The second produced zeolite analcime belongs into the analcime group. This zeolite has smaller pores than zeolite Na-P1 so can be expected lower CEC values. Fig. 3 shows the XRD patterns of samples prepared at 180 °C at 24 h. The trend of increasing amount of zeolitic phases at the expense of decreasing amount of mullite and quartz is the same as for the samples prepared at 160 °C.

Creation of zeolites is promoted by higher solution/fly ash ratio and increasing temperature. This can be explained by the solubility of Si and Al into the alkaline solution. Higher temperature and increasing amount of NaOH per 1 g of fly ash increases the solubility of phases present in raw fly ash which supports creation of zeolitic phases. Higher temperature promotes producing analcime instead of zeolite Na-P1, which arises at lower temperature. Changed parameters of hydrothermal reaction have probably no effect of amount of hematite and magnetite present in fly ash.

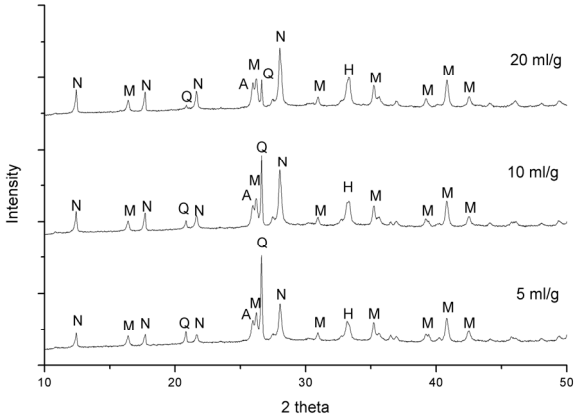

Fig. 2. **XRD patterns of samples synthesized at 160 °C** (synthesis conditions – 0.5 M NaOH solution, 24 h, s/f ratio: 5, 10 and 20 ml/g). **N = zeolite Na-P1, A = analcime**

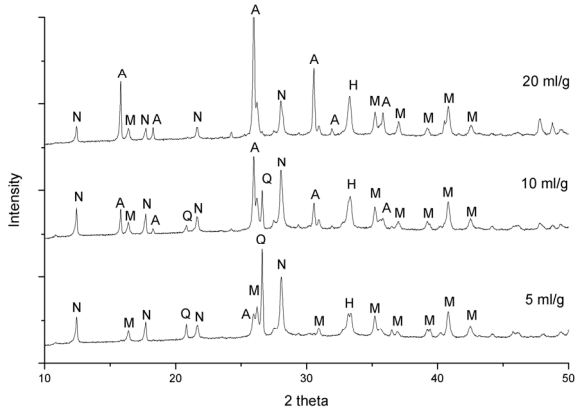

Fig. 3. **XRD patterns of samples synthesized at 180 °C** (synthesis conditions – 0.5 M NaOH solution, 24 h, s/f ratio: 5, 10 and 20 ml/g)

3.2. Effect of concentration of NaOH

Samples for evaluating effect of NaOH concentration to formation of zeolites was prepared with solution/fly ash ratio value 20 ml/g. Effect of concentration was examined for two different temperatures of reaction 160 °C and 180 °C. Fig. 4 represents XRD patterns for samples prepared at 160 °C. Main zeolitic phases are zeolite Na-P1 and analcime. In a sample prepared with the highest concentration 2 mol/dm^3 there is a third zeolitic phase called carbobystrite ($Na_8Al_6Si_6O_{24}CO_3{\cdot}4H_2O$). This zeolite belongs into cancrinite group. This zeolite was also present in samples prepared at 180 °C and NaOH concentration higher than 1 mol/dm^3 (Fig. 5). Generally, increasing NaOH concentration and reaction temperature rapidly increase amount of analcime and decreases amount of zeolite Na-P1 and amounts of mullite and quartz. Samples prepared using 2 M solution of NaOH exhibit some differences from this trend. Quantity of analcime decrease together with small increase of quantity of zeolite Na-P1 and creating the carbobystrite and in the case of sample prepared at 180 °C zeolite MAP ($Na_8Al_8Si_80_{32}{\cdot}15{,}17H_2O$). This zeolite belongs to the same group like zeolite Na-P1 and it has very similar structure. Named conditions probably favor creation of P zeolites, but for accurate explanation must be done some more experiments.

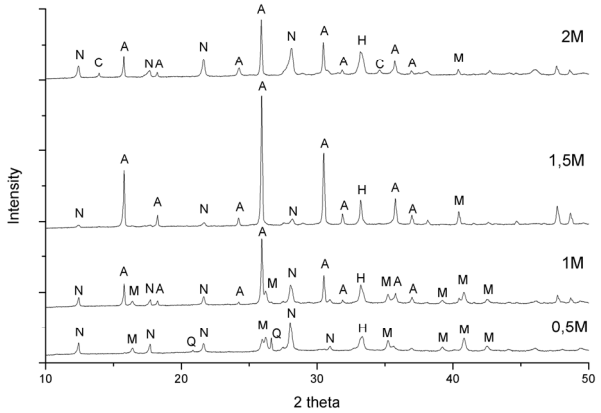

Fig. 4. **XRD patterns of samples synthesized at 160 °C** (synthesis conditions – s/f ratio: 20 ml/g, 24 h, NaOH concentrations: 0.5; 1; 1.5 and 2 M). **C = carbobystrite**

The morphology of raw fly ash before and after hydrothermal treatment is shown on Fig. 6. The fly ash particles before the hydrothermal treatment had spherical shape and smooth surface. Their surface is covered with aluminosilicate glass created during the combustion of coal. The surface of particles became rough after the alkaline hydrothermal treatment. This indicates that the new zeolitic phases deposited on the surface of fly ash particles.

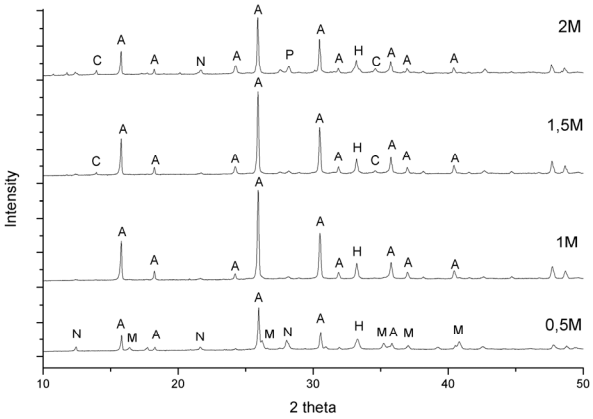

Fig. 5. **XRD patterns of samples synthesized at 180 °C** (synthesis conditions – s/f ratio: 20 ml/g, 24 h, NaOH concentrations: 0.5; 1; 1.5 and 2 M). **P = zeolite MAP**

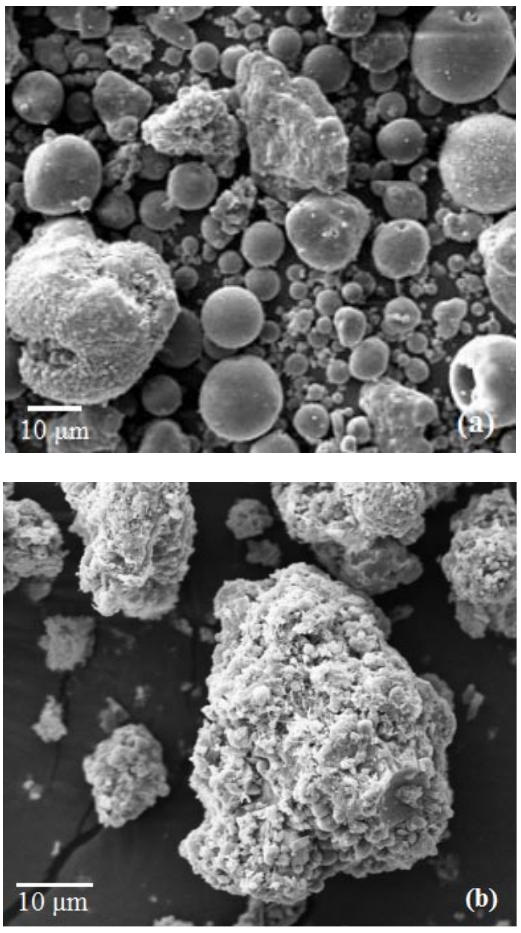

Fig. 6. **SEM image of fly ash**
a) before the hydrothermal treatment
b) after hydrothermal synthesis (synthetic conditions – NaOH concentration: 2 M, temperature: 180 °C, s/f ratio: 20 ml/g, 24 h)

3.3 Cation exchange capacity (CEC)

CEC value of raw fly ash was determine to a value 3.51 meq/100 g. The results of determined CEC values for samples prepared with solution/fly ash ratio 20 ml/g are shown in Table 1. The higher CEC values were measured for samples prepared at lower temperature and NaOH concentration. This trend corresponds with amount of P zeolites present in samples. The highest CEC value was determined in sample prepared at 160 °C using 1 M solution of sodium hydroxide. This means that even when the amount of prepared zeolitic phases is higher, especially analcime, the CEC value mainly depends on a type and structure of synthesized zeolite.

Table 1
CEC values for exchanging Mg^{2+} cations obtained for prepared samples

Samples	NaOH [mol·dm^{-3}]	Temperature [°C]	CEC [meq/100 g]
A_160	0.5	160	335.92
A_180	0.5	180	314.73
B_160	1	160	339.21
B_180	1	180	215.44
C_160	1.5	160	281.86
C_180	1.5	180	221.25
D_160	2	160	292.07
D_180	2	180	241.64

4. Conclusions

Effect of variable factors affecting alkaline hydrothermal synthesis of zeolites from coal fly ash was examined. Examined variable factors were solution/fly ash ratio, temperature and autogenous pressure of hydrothermal reaction and NaOH concentration. Presented results show that the type of synthesized zeolite mainly depends on temperature and pressure of hydrothermal reaction and concentration of sodium hydroxide solution. The most proper solution/fly ash ratio for synthesizing zeolites was determined on 20 ml/g.

Zeolite Na-P1 and analcime were synthesized using NaOH as activation agent. Creation of zeolite Na-P1 is preferred by lower reaction temperature (160 °C) together with lower concentration of NaOH solution (0.5 M and 1 M). In opposite increasing temperature and NaOH concentration rapidly increase the amount of analcime. Besides these two zeolites, zeolite MAP and carbobystrite was synthesized using high NaOH concentration and high temperature. Amount of crystalline phases present in raw fly ash is decreasing with increasing NaOH concentration, temperature of reaction and solution/fly ash ratio. Only hematite and magnetite stayed unreacted.

CEC values of prepared samples increase rapidly in comparison with the CEC value of raw fly ash. The highest exchange capacity for Mg^{2+} cations reached samples containing bigger amount of zeolite Na-P1.

Hydrothermal treatment of coal fly ash using sodium hydroxide as activation agent, seems to be the right way for synthesize low-cost zeolites, which can be used mainly as ion exchangers. Application of these zeolites depends on their type and structure. Both can be controlled by reaction conditions from which length of hydrothermal reaction remains as next challenge.

This study was supported by project of Materials Research Centre on Faculty of Chemistry, Brno University of Technology – sustainability and development r.c. LO1211 with financial support of National program of sustainability I (The Ministry of Education, Youth and Sports).

REFERENCES

1. Ahmaruzzaman M.: Prog. Energy Combust. Sci. *36*, 327 (2010).
2. Yao Z. T., Ji X. S., Sarker P. K., Tang J. H., Ge L. Q., Xia M. S., Xi Y.: Earth-Sci. Rev. *141*, 105 (2015).
3. Lutze D., Vom Berg W.: *Handbuch Flugasche im Beton: Grundlagen der Herstellung und Verwendung,* Verl. Bau und Technik, Düsseldorf, 2004.
4. Molina A., Pool C.: Miner. Eng. *17*,167 (2014).
5. Inada M., Eguchi Y., Enomoto N., Hojo J.: Fuel *84*, 299 (2005).
6. Querol X., Moreno N., Umaña J. C., Alastuey A., Hernández E., López-Soler A., Plana F.: Int. J. Coal Geol. *50*, 413 (2002).
7. Miyake M., Tamura Ch., Matsuda M.: J. Am. Ceram. Soc. *85*, 1873 (2002).
8. Murayama N., Yamamoto H., Shibata J.: Int. J. Miner. Process. *64*, 1 (2002).
9. Sommerville R., Blissett R., Rowson N., Blackburn S.: Int. J. Miner. Process. *124*, 20 (2013).
10. Bayuseno A. P., Schmahl W. W., Müllejans T.: J. Hazard. Mater. *167*, 250 (2009).
11. Wang Ch. F., Li J. S., Wang L. J., Sun X. Y.: J. Hazard. Mater. *155*, 58 (2008).
12. Hollman G. G., Steenbruggen G., Janssen-Jurkovičová M.: Fuel *78*, 1225 (1999).
13. Bukhari S. S., Behin J., Kazemian H., Rohani S.: Fuel *140*, 250 (2015).
14. Xu R.: *Chemistry of zeolites and related porous materials: Synthesis and structure*. John Wiley, Singapore, 2007.
15. Auerbach S. M., Carrado K. A., Dutta P. K.*: Handbook of zeolite science and technology*. M. Dekker, New York, 2003.
16. Camblor M. A.: Macla *6*, 19 (2006).

UV-VIS SPECTRAL CHARACTERISTICS OF HUMIC SUBSTANCES IN CHERNOZEMS

MAGDALENA HABOVÁ and LUBICA POSPISILOVA

Department of Agrochemistry, Soil Science, Microbiology and Plant Nutrition, Faculty of Agronomy, Mendel University in Brno, Czech Republic
habova.mh@seznam.cz

Ultraviolet and visble spectra are widely used for evaluation of humic substances quality. Object of our study were HA isolated from ten subtypes of *Chernozems* intensively used in agriculture. Spectra were recorded within the range 200–700 nm. Absorbance indexes were calculated at: 253/203, 253/230, 250/365, 253/410, 465/665 a 255/465 nm.

Humic substances represent a highly complex and refractory materials. Their chemical composition depends on plants residues, and intensity of humification and mineralization processes[1]. The predominant fraction of humic substances are humic acids, which can act as scavengers for various kinds of contaminants[2, 3]. Humic acids (HA) have a high intensity of light absorbance in UV-VIS spectral range. For this reason HA were isolated from ten subtypes of *Chernozems.* These soils are intensively used in agriculture and they occupy in the Czech Republic around 11 % of agricultural lands.

Standard methods for isolation and chemical properties determination were used[3]. Basic soil characteristics shown that soil reaction of studied samples was neutral. Stronger acidity was determined in *Arenic Chernozem* (Žabčice). Cation exchange capacity varied from middle to high, except *Arenic Chernozem* (Žabčice), when the values were low. Soils were heavy textured, except both samples of *Arenic Chernozems,* which were light textured. Conductivity of soil solution was low and soils were not salty. Low carbonates content was found in most studied samples.

As it is evident from Fig. 1 the highest content of humic acids was found in *Phaeoic Chernozem* (Dubany). HA content decreased in the following order: *Phaeoic Chernozem* > *Haplic Chernozem* (Hrušovany) > *Haplic Chernozem* (Bořetice) > *Luvic Chernozem* (Praha and Unčovice) > *Calcaric Chernozem* (Velešovice) > *Anthropic Chernozem* (Velešovice) > *Haplic Chernozem* (Bratčice) > *Arenic Chernozem* (Březí) > *Arenic Chernozem* (Žabčice). Humification degree (HD) was calculated as a ratio HA/TOC * 100 and varied from low to middle (12.5–30 %). The highest values of humification degree (more than 27 %) were found in *Phaeoic Chernozem* (Dubany) and *Haplic Chernozem* (Hrušovany).

Results also showed differences in absorbance and calculated indexes values. The lowest absorbance was characteristic arenic subtypes of Chernozems. Higher values were achived in *Phaeoic Chernozems*. Increasing of *A253/A203* and *A253/A230* ratios indicated higher ability of HA for substitution in aromatic, hydroxyl, carbonyl and carboxyl groups. Decreasing of both ratios is typical for substitution in aliphatic groups. Higher values of ratios *A250/A365* and *A254/A410* are typical for aromatic and high molecular compounds. One of the most important calculated index was the A465/A665 ratio. Low values of *A465/A665* and *A264/A465* ratios are typical for highly aromatic and condensed compounds. According to A465/A665 ratio quality of HA decreasing in order: *Anthropic Chernozem* (Velešovice) > *Calcaric Chernozem* (Velešovice) > *Haplic Chernozem* (Hrušovany) > *Luvic Chernozem* (Praha and Unčovice) > *Phaeoic Chernozem* > *Arenic Chernozem* (Žabčice) > *Haplic Chernozem* (Bořetice) > *Arenic Chernozem* (Březí) > *Haplic Chernozem* (Bratčice) > *Arenic Chernozem* (Březí). Correlation between HA content *A253/A203* was found ($n = 90$, $\alpha = 0.05$, $r_{crit} = 0.217$). Reversed correlation between HA content and *A465/A665* ratio was found ($n = 90$, $\alpha = 0.05$, $r_{crit} = 0.217$).

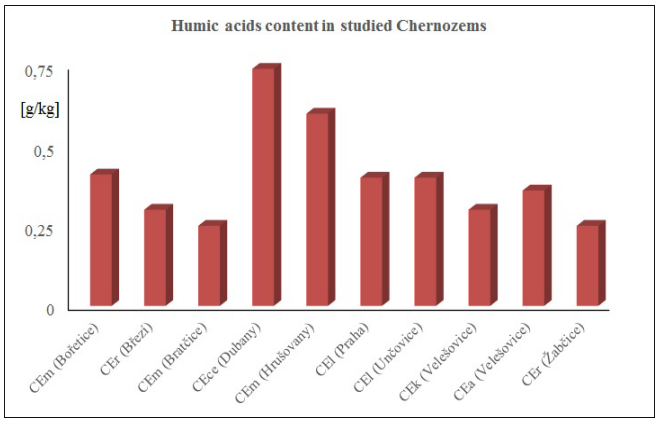

Fig. 1. **Average content of humic acids in studied soil types**

This work was supported by projects NAZV QJ 1210263 and IGA SP 2150691.

REFERENCES

1. Stevenson F. J.: Humus chemistry genesis, composition, reactions, Wiley Interscience Publication, New York. 445 p. (1982).
2. Senesi N.: Nature of interactions between organic chemicals and dissolved humic substances and the influence of environmental factors. In: Organic substances in soil and water: Natural components and their influence on contaminant behaviour, Chapter 4, Royal Soc. of Chemistry, London. 73–101 (1993).
3. Pospíšilová L., Tesařová M.: Organický uhlík obhospodařovaných půd. Acta Folia II. Universitatis Agriculturae et Silviculturae Mendelianae Brunensis, Brno. 0–41 (2009).

HYBRID ORGANIC-INORGANIC PEROVSKITE SOLAR CELLS WITH PRINTED PHOTO-ANODE

MICHAL HATALA*, PAVOL GEMEINER and MILAN MIKULA

Department of Printing Arts Technology and Photochemistry, Faculty of Chemical and Food Technology SUT in Bratislava, Radlinského 9, 821 37 Bratislava, Slovakia
hatalamichal@gmail.com

Perovskite solar cells can be classified as one of the most promising photovoltaic technologies of the 3rd generation of photovoltaic systems. Primary structure is based on solid state Dye Sensitized Solar Cells (ssDSSC), with the exception that these systems employ hybrid organometallic perovskites ($CH_3NH_3MX_3$; M=Sn, Pb; X=F, Cl, Br, I) especially in the role of light harvester. Perovskite can be characterized as a semi-conductive material with a band gap 1.55 eV and thus of very good absorption in the whole range of visible light spectrum. Excitons, formed by absorption of radiation, exhibit weak binding energy (0.03 eV), which allows their rapid dissociation even at the room temperature. The resulting free charge carriers have high mobility and can have diffuse length up to 1000 nm. These noteworthy features of perovskites allow achieving high photovoltaic performance. Initially, the perovskite served as a sensitizer (Fig. 1) of mesoporous TiO_2 layer in standard DSSC (I). Due to its high charge mobility it was not required to form a monomolecular layer as in the case of dyes.

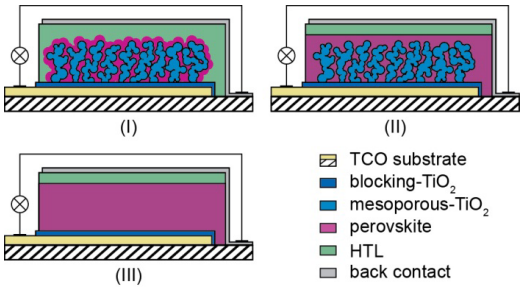

Fig. 1. **Basic structures of PSC** [1]

Besides the sensibilisation function, the ability of hole conduction allowed to use the perovskite infiltrated in the mesoporous TiO_2 layer as a primary hole transport material (HTM) (II) combined with commonly used polymer HTM. The simple functional structure n-TiO_2/p-perovskite, in the case of additional HTM omission, can be understood also as a heterojunction solar cell either with the mesoporous or planar TiO_2 layer. In generally, perovskites can act as p- or n- type semi-conductors, thanks to their ambipolar character, which allows modifying the basic structure, even in terms of the necessity of mesoporous conductive oxide layer[2]. Perovskites can serve also as an electron transporting layer and partially fulfill the function of TiO_2, depending on the structure of the solar cell. The simplest solar cell may also consist of compact oxide, perovskite and polymer HTM layer in a planar configuration (III). In the case of organic photovoltaic systems (OPV), perovskites found their application also as an additional active layer[1, 2]. From the production point of view, the most promising preparation method of perovskite layer is using solution coating techniques. In general perovskites ($CH_3HN_3MX_3$) are prepared by one- or two-step method. By one-step method the mixture of two precursors (MX_2, CH_3NH_3X) in commonly used solvent (dimethylsulphoxide (DMSO), γ-butyrolactone (GBL), N,N-dimethylacetamide (DMAC) or N,N-dimethylformamide (DMF)) is applied. The main disadvantage is a high reaction rate, which can lead to a poorer control of the crystallization process, leading frequently to the disproportionate crystal size, formation of voids and therefore to non-standard process as a whole. By two-step method, firstly applied is the MX_2 solution in dimethylformamide (DMF). The solution of organic salt CH_3NH_3X in isopropanol (IPA) is applied after heating. The insolubility of the first precursor in the second used solvent is a necessary condition. The two-step method should allow an easier process control of crystal formation and a better TiO_2 layer pore filling. As the deposition technique is commonly used spin-coating and dip-coating. The crystallization itself requires highly precise control of coating process (spin velocity, dipping time and annealing temperature) because of its high sensitivity[3, 4]. Ambient conditions, especially humidity, have also a large impact [5, 6].

In the paper we focused on the preparation of the monolithic perovskite solar cells on the rigid glass substrates. The mesoporous titanium dioxide (TiO_2) photoanode was prepared using a screen printing technique. One-step and two-step method were used for the deposition of perovskite layer at ambient conditions. Spin coated precursors contained two elementary components Lead iodide (PbI_2) and Methylammonium iodide (CH_3NH_3I). Metal back contacts were sputtered directly onto perovskite layer or onto subsequently spin-coated HTM.

As the basic substrates were used glass slides coated with transparent conductive oxide layer – fluorine doped tin oxide (FTO). Narrow strip of the FTO conductive layer was removed using etching solution containing hydrochloric acid and zinc dust. This process should prevent unwanted cross contact between the layers on the edge of glass substrate. After the etching, substrates were cleaned using ultrasonic bath in the presence of detergent, rinsed with deionized water and exposed to UV light. On the cleaned substrates were subsequently coated functional layers using screen printing and spin-coating technique. The basic structure is as follows (Fig. 2): blocking-TiO_2, mesoporous-TiO_2, Perovskite, HTM and metal back contact.

Blocking TiO_2 layer is usually prepared from the solution using spin-coating, dip-coating or simple dipping method. We prepared the layer by the sol-gel method using 0.15 M Titanium diisopropoxide bis(acetylacetonate) ($Ti(acac)_2OiPr_2$) (75 wt. % in isopropanol, Sigma Aldrich) in Ethanol (dehydrated 99.8 %, Centralchem) solution. This was spin-coated on the top of masked (adhesive tape) substrate at 2000

rpm for 60 s. The layer was than heated at 125 °C for 5 min. This process was repeated in order to improve the coverage. This is critical to prevent the contact between perovskite and FTO layer, which is the primary role of blocking-TiO_2 layer.

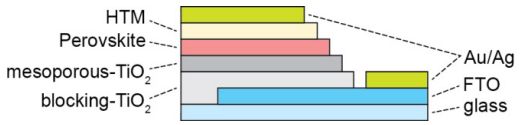

Fig. 2. **Simplified schematic cross section of prepared PSC**

Mesoporous-TiO_2 layer is an essential functional layer in DSSC, ensuring electron transport after their injection from excited dye. In the case of PSC, the mesoporous semi-conductive layer is also engaged in the process of the electron transportation towards the FTO layer. The main difference in structure between DSSC- and PSC- photo-electrode is the actual thickness, which is in order of a microns (up to 20 μm) for DSSC, but submicron for PSC. We prepared the set of screen-printable TiO_2 pastes with different percentage content of TiO_2 nanoparticles (1, 2, 4 and 6 wt. %) in order to achieve required thickness. Except the TiO_2 (21 nm particles, AEROXIDE® TiO_2 P25) the composition included acetic acid (Lachema), distilled water, ethanol (96 %, mikroCHEM), α-terpineol (96 %, Sigma Aldrich) and ethyl cellulose (viscosity 22 mPa.s in toluene:ethanol (80:20) solution, Sigma Aldrich). Dispersions were mixed and homogenized using magnetic stirrer and an ultrasonic bath. Desirable consistency was in the final step attained with an ethanol evaporation at 80–90 °C for 3–4 hours. The actual preparation of layers was carried out by screen printing (54 threads/cm) onto previously prepared FTO substrates coated with blocking-TiO_2 layers. Afterwards, the printed layers were exposed to a temperature of 470 °C for 30 min.

Rheological behavior of prepared pastes were evaluated by measuring of flow (τ [Pa] = f (D [s^{-1}])) (Fig. 3) and viscosity (η [Pa.s] = f (D[s^{-1}])) curves (Fig. 4) using rheoviscosimeter HAAKE VT501 (21 °C, cone 1.0°, φ = 20 mm).

By all prepared dispersions it was shown a decreasing viscosity with increasing shear rate – non-newton, pseudoplastic behavior, which is typical for screen-printable pastes (Fig. 3). Viscosity values at shear rate D = 10 s^{-1} for all four pastes were in the range of 28–43 Pa.s. This agrees with the recommended value[7]. For the screen-printing process is desired, besides pseudoplasticity of pastes, also their time-depending shear-thinning behavior – thixotropy, which can be demonstrated through the hysteresis curves, based on the dimensions of the resulting loops (Fig. 4). Significant thixotropy of all four pastes indicates probably substantial internal structural changes caused by embedded stress.

Thicknesses of printed layers were measured by the image analysis method using images from optical microscope (Fig. 5). Submicron thickness was confirmed for 1(< 0.5 μm), 2 (~ 0.5 μm) and 4 wt. % (> 0.5 μm) TiO_2 nanoparticles concentration pastes.

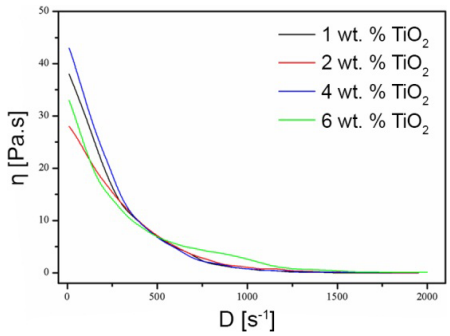

Fig. 3. **Viscosity curves for TiO_2 dispersions with different percentage content of nanoparticles** (1, 2, 4 and 6 wt. %)

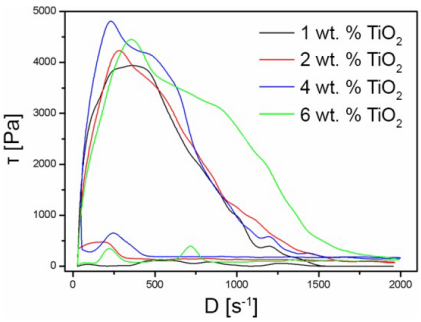

Fig. 4. **Hysteresis of TiO_2 dispersions with different percentage content of nanoparticles** (1, 2, 4 and 6 wt. %) **showed on flow curves**

Perovskite layers were prepared by one- and two-step method from the solutions using spin-coating technique. For one-step process $CH_3NH_3PbI_3$ deposition, PbI_2 (99 %, Sigma Aldrich) and CH_3NH_3I (Solaronix) in 1:1 molar ratio were mixed in DMAC (99.5 %, Alfa Aesar) at 70 °C for 12 hours. The mixture was then coated on the masked mesoporous-TiO_2 layer by spin-coating at 2000 rpm for 120 s. After spin-coating the layers were heated at 100 °C for 5 min. For two-step deposition was in the first step dissolved PbI_2 in DMF (99.8 %, Sigma Aldrich) at 70 °C and spin-coated on the masked mesoporous-TiO_2 layer at 3000 rpm for 20 s and dried at 100 °C for 5 min. In the second step, CH_3NH_3I dissolved in IPA (mikroCHEM) was spin-coated on masked PbI_2 layer at 4000 rpm for 20 s and the layer was heated at 100 °C for 5 min. During the heating of perovskite precursors the organic solvents were evaporated and the layers turned black, which indicated formation of perovskite crystals. The overall process, preparation of precursors, and spin-coating were carried out at ambient conditions (temperature: 20–25 °C, relative humidity: 30–45 %).

The surface structures of resulting perovskite layers were analyzed from the SEM and AFM images (non-contact mode, 100 μm scanner, set point: 0.04 μm, frequency: 1 Hz). Perovskite layers prepared by one-step method (Fig. 6 [a]) showed shapeless crystal structure with noticeable round clusters. In the case of two-step method (Fig. 6 [b]), the

morphology of deposited $CH_3NH_3PbI_3$ is remarkably different. In the SEM images are noticeable cube-like crystals. Besides morphological difference, in our conditions of perovskite deposition, TiO_2 layer is not completely covered with perovskite by the-two step coating procedure. Based on these observations, despite of less ideal crystal shapes, the final solar cells were equipped with one-step method prepared perovskites.

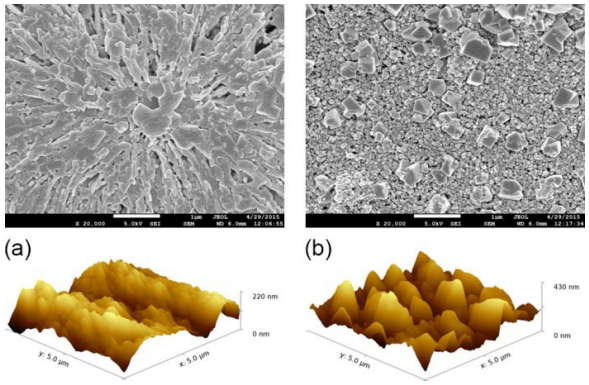

Fig. 6. **Surface** (upwards) **SEM image** (20 000x magnification) **and** (below) **AFM image of $CH_3NH_3PbI_3$ prepared by (a) one-step and (b) two-step method on the mesoporous TiO_2 layer**

HTL was prepared by spin-coating of 2.2'7.7-tetrakis(N,N-di-p-methoxyphenyl-amine)-9,9' spirobifluorene (spiro-MeOTAD) onto masked perovskite layer at 4000 rpm for 30 s. A spiro-MeOTAD solution was prepared by dissolving of spiro-MeOTAD in chorbenzene (Lachema), to which 4-tert-butyl pyridine (TBP) and lithium bis(trifluoromethanesulfonyl)imide (Li-TFSI) were added. Spin-coated layers were dryed at 25 °C under reduced humidity conditions for 12 hours. Finally metal (gold, silver) layers were sputtered on the top of the HTL to form the back contact using magnetron sputtering equipment.

Photovoltaic parameters were evaluated based on the I-V characteristics measurement under irradiation of 88 $mW.cm^{-2}$. Fig. 7 shows I-V characteristics of two solar cells, finished either with silver (Ag) or gold (Au) back-contact.

These characteristics represent two samples with highest reached fill factor (FF). Photo-anodes printed with 4 wt. % TiO_2 nanoparticles concentration pastes. The photovoltaic parameters for these samples are summarized in Table 1.

The results obtained are inferior to the results reported in the literature. We assume that the primary cause could be the cross contact and the subsequently short circuiting of active layers. Inhomogenous perovskite layer may cause the unwanted contact between HTM and TiO_2 layer. The porosity of perovskite layer can be concluded also on the basis of the fact that in case of sputtering the metal electrode directly on the perovskite layer (ommision of HTL), there was no response of finalised solar cells to irradiation. Based on the significant different I–V curves shapes measured for gold and silver electrode, there is also a possibility of short circuiting between sputtered metal back contact and perovskite layer. These problems require further investigation and an optimalisation of layers.

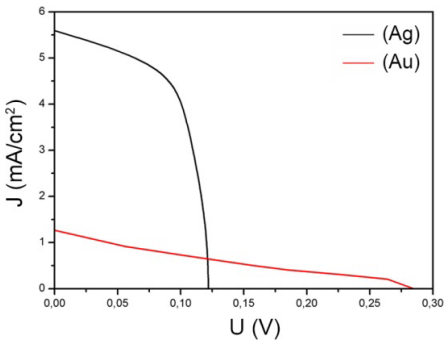

Fig. 7. **I-V characteristics of PSC with silver (Ag) and gold (Au) back contact**

Tabe 1
Short-current density (J_{SC}), open-circuit voltage (U_{OC}), fill factor (FF) and overall conversion efficiency (η) for PSC finalised with silver (Ag) and gold (Au) Back contact

back-contact	J_{SC} ($mA.cm^{-2}$)	U_{OC} (V)	FF (%)	η (%)
silver (Ag)	5.59	0.12	64.08	0.50
gold (Au)	1.27	0.29	22.07	0.09

This work was supported by the Slovak Grant Agency, project VEGA 1/0818/13, and by the National Centrum of Research and Application of Renewable Sources of Energy, ITMS 26240120016, co-financed by the Fund of European Regional Development.

REFERENCES

1. Grätzel M.: The light and shade of perovskite solar cells, Nat. Mater. 13, 838 (2014).
2. Docampo P. et al.: Lessons Learned: From Dye-Sensitized Solar Cells to All-Solid-State Hybrid Devices, Adv. Mater. 26, 4013 (2014).
3. Cohen B.-E.; Gamliel S.; Etgar L.: Parameters influencing the deposition of methylammonium lead halide iodide in hole conductor free perovskite-based solar cells, APL Mat. 2, 081502 (2014).
4. Im J.-H.; Kim H.-S.; Park N.-G.: Morphology-photovoltaic property correlation in perovskite solar cells: One-step versus two-step deposition of $CH_3NH_3PbI_3$, APL Mat. 2, 081510 (2014).
5. Sfyri G. et al.: Study of perovskite solar cells synthesized under ambient conditions and of the performance of small cell modules, Sol. Energ. Mat. Sol. Cells 134, 60 (2014)
6. You J. et al.: Moisture assisted perovskite film growth for high performance solar cells, Appl. Phys. Lett. 105, 183902 (2014).
7. Lin H.; Chang C. P.; Hwu W.; Ger M.: The rheological behaviors of screen-printing pastes, J. Mater. Process. Technol., Vol. 197, Issues 1–3, 284 (2008).

ARE TERRESTRIAL ORGANISMS ABLE TO LIVE IN CONTAMINATED SOIL AFTER FIRE-FIGHTING?

ŠÁRKA HŘIBOVÁ*, MILADA VÁVROVÁ and HELENA ZLÁMALOVÁ GARGOŠOVÁ

Brno University of Technology, Faculty of Chemistry, Institute of Chemistry and Technology of Environmental Protection, Purkyňova 118, 612 00 Brno, Czech Republic xchribovas@fch.vutbr.cz

Abstract

Many fire accident happend in several decades. There were several wildfires and also huge fires of large industry areas or companies in the world. In order to put down the fire, fire-fighting foaming agents (FEAs) are often used. Their good properties, i.e. stability and large active surface of foam, are the reasons of their frequent usage. In fact, these agents are mixtures of several chemical substances as alcohols, perfluorinated hydrocarbons, surfactants, additives and water, of course. An infiltration of FEAs solution occurs after application during firefighting. FEAs are partly captured by the soil particles and causing contamination of the soil environment. Consequently, the soil may be uninhabitable for terestrial organisms during dry seasons. On the contrary, there is known premise about rainy seasons, when the contamination is diluted and rinsed as leachate with low ecotoxicity. The crucial question is, whether the soil environment is suitable for life of indigenous terestrial organisms after direct FEAs application. There was performed test of ecotoxicity with using earthworm *Eisenia Fetida* as chief representative of terrestrial organisms in the study. Soil matrix LUFA 2.3 was selected as a model of natural soil environment. Tested FEAs were follows: Sthamex F-15, Moussol-APS F-15 and Finiflam F-15. For experimental purposes, laboratory installation for infiltration was designed and compiled. Infiltration of three FEAs solutions was done before the ecotoxicity testing. Contaminated soil after infiltration was tested for semi-chronic ecotoxicity and reproduction ecotoxicity then. Introductory results indicates differences between each FEA, caused by various composition. Sthamex F-15 was determined as the most ecotoxic agent at all. Whilst Moussol-APS F-15 was evaluated as the agent with least ecotoxicity effect.

Introduction

The soil forms the upper layer of the Earth´s crust, which is essentially polydisperse system created by soil particles, soil water, soil air and organisms. It can be contaminated via several ways, wherein one of them is just by direct application of chemicals on the surface[1, 2]. This study deals with direct application of FEAs during fire-fighting, especially in case of wildfires and areal fires.

Experimental

There was individually tested contaminated soil by three different foaming agents in the study, namely Sthamex F-15, Moussol-APS F-15 and Finiflam F-15. Infiltration of FEAs solutions was done under laboratory conditions. Each FEA was diluted in concentration of work solution, i.e. 5 % for Sthamex F-15 and 3 % for the other ones. Solutions were left to infiltrate through soil layer in glass column and outcoming filtrates were collected. Standard soil matrices contaminated during infiltration were tested with using earthworm *E. fetida*. Semi-chronic effect and influence on reproduction ability of organism were evaluated at the end of the test.

Materials and methods

Artificial soil. Standard soil matrix LUFA 2.3 (LUFA Speyer Germany) was selected as representative material. LUFA 2.3 is sandy loam soil type. This type of reference soil matrix comes from real nature ecosystems located in Germany used for agriculture purposes with application of no pesticides, biocidal fertilizers or organic manure for five years at least[3, 4, 5].

Tested agents. There were tested three FEAs in the study, namely Sthamex F-15 (STH), Finiflam F-15 (FIN) and Moussol-APS F-15 (MOU)[6, 7, 8]. Selected FEAs are often used by Fire Rescue Unit of South Moravian Region of the Czech Republic. FEAs concentrates were diluted with deionized water to concentrations of commonly used work solutions, thus 5% concentration for STH and 3 % for the other ones. Prepared solutions were used as stock solutions and they were tested for hazardous property H14 (ecotoxicity) with using soil organism *E. fetida* (earthworm).

Test organism. Earthworm *E. fetida* was selected as representative organism for assessment of contaminated soil by selected FEAs. Earthworms can receive toxicants via dermal contact and also via oral income. Adult individuals with evolved annulet and weight fewest 250 mg are needed for test purposes[9].

Experimental design. Experiment was drafted and modeled on infiltration field tests. A column apparatus for infiltration experiment was designed. It was compiled from glass cylinder with specific proportions. Standard soil matrix was placed inside in height of 30 cm. This is an average height corresponding to topsoil height and height used for infiltration experiments being done in-situ. Work solutions of three tested FEAs were individually applied in exact volume onto such prepared matrix[10]. Out-coming filtrates were collected and stored for ecotoxicity testing. When infiltration was done, the soil contaminated during experiment was promptly tested for its ecotoxic activity. Results were already published[11].

Ecotoxicological assessment. Semi-chronic toxicity and reproduction test was performed to assess direct impact of FEA application on soil during fire-fighting. There were prepared contaminated matrices by every single FEA in concentrations of 25, 50 and 100 %. Lower concentrations than 100 % were prepared by mixing of contaminated soil from infiltration experiment with pure standard soil LUFA 2.3. Prepared material was put into testing vessel and 10 suitable test organisms were placed in. Subjects with evolved annulet and weight fewest 250 mg were chosen. All ten organisms were weighed together and total weight was registered.

Appropriate food was put in after addition of earthworms. Horse manure with no medications and growth promoters is

suitable. There was spread 5 grams of food on the surface of soil and then was moistened by distilled water in the vessel. Test vessel was covered by cellophane then and was stored under temperature 20 ± 2 °C and illumination about 800 lux. Test was carried out under light-dark cycles 16 hours light and 8 hours dark. Food was provided once a week during test duration.

After 28-day exposition, living organisms were counted and weighed. Growth inhibition was evaluated. Vessels with tested materials were stored for next 28 days for further testing of influence on reproduction ability of organisms[5, 9, 12, 13].

Results

Result analysis. Semi-chronic assay principle is based on the assessment of growth inhibition or stimulation of organisms. Measured data were evaluated with using software MS Excel. Weight increment was evaluated via comparison of weight of organisms in contaminated environment with total weight of organisms in control test[9, 12]. Appropriate results are listed in Table 1.

Reproduction assay principle is based on the assessment of number of juvenile organisms after one month incubation. Measured data were evaluated with using software MS Excel. Number of juveniles was compared with number in control test. Inhibition of reproduction was evaluated in all assays[13]. Appropriate results are listed in Table 2.

Table 2
Number of living organisms in test vessels and resulting mortality

FEA	Number of juveniles	Mortality [%]
Control	10	0.00
STH 25 %	0	100
STH 50 %	0	100
FIN 25 %	9	10.0
FIN 50 %	10	0.00
MOU 25 %	10	0.00
MOU 50 %	10	0.00

Conclusion

Results of semi-chronic test indicate high ecotoxic activity of contaminated soil matrices by work solutions of FEAs. The biggest ecotoxic effect was observed in the case of Sthamex F-15. Wholly inhibition of growth of organisms was observed for both concentrations, i.e. 25 % and 50 %. Results for Finiflam F-15 are questionable. There was observed inhibition of growth 91.2 % for 25% contamination. On the contrary, lower inhibition 54.7 % was observed for 50% contamination. Moussol-APS F-15 was proved as the least ecotoxic agent. There was observed 4.1% inhibition effect for 25% contamination and 60.9 % inhibition for 50% contamination.

Results of reproduction test correspond with results of semi-chronic test. Sthamex F-15 was proved as the most ecotoxic agent. Any live organism wasn´t found in test vessel both for 25% and 50% contamination. Majority of dead organisms was degraded and only few corpses were found. These results are only supplementary and further testing is needed.

Although contaminated matrices were proved as inappropriate for life of soils organism *E. fetida*, it does not mean, that they are unsuitable for other living organisms such as plants are. This contamination is probably not permanent. Good biodegradability of similar agents was proved in study of Adams et. al.[14].

Outcomes from performed tests are only preliminary and determine direction for more detailed and widespread study for confirmation, possibly refutation of these results.

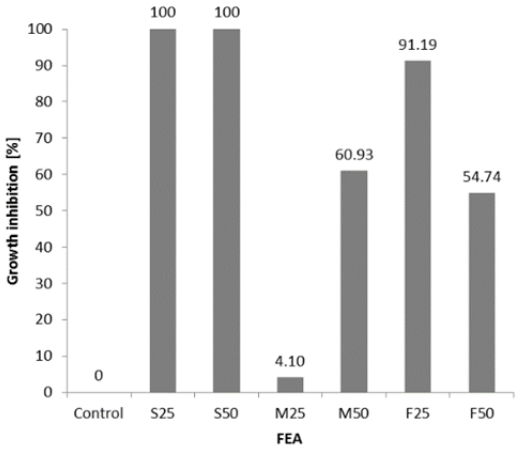

Fig. 1. **Comparison of weight increment with inhibition of growth of test organism E. fetida**

Table 1
Inhibition or stimulation of growth of organism E. fetida

FEA	Initial weight of one organism	Final weight of one organism [mg]	Weight increment of one organism	Growth inhibition [%]	Weight increment [%]
Control	2 359	3 677	139	–	–
STH 25 %	2 117	–	0.00	100	0.00
STH 50 %	2 167	–	0.00	100	0.00
FIN 25 %	2 560	2 670	10.0	91.2	8.80
FIN 50 %	2 723	3 320	60.0	54.7	45.3
MOU 25 %	2 325	3 655	130	4.10	95.9
MOU 50 %	2 459	3 001	50.0	60.9	39.1

This study was supported by the grant no. FCH-S-15_2869 from the Ministry of Education, Youth and Sports of theCzech Republic.

REFERENCES

1. Brady N. C., Weil R. R.: The Nature and Properties of Soils. 14 ed. Pearson-Prentice Hall, Upper Saddle River, NJ. 2008. 990 pp. ISBN: 13-978-0-13-227938-3.
2. Kirkham M. B.: Principles of Soil and Plant Water Relations, 2. Ed., Elsevier, USA, 2014, pp. 579, ISBN 978-0-12-420022-7.
3. LUFA Speyer [webpage on the Internet]. Analyses Data Sheet. Speyer, Germany: LUFA Speyer [updated 2013 May; cited 2014, Aug]. Available form: http://www.lufa-speyer.de/images/stories/bodanalyse.pdf.
4. Ellis S. R., Hodson M. E., Wage P.: The influence of different artificial soil types on the acute toxicity of carbendazim to the earthworm Eisenia fetida in laboratory toxicity tests, European Journal of Soil Biology, Vol. 43, 2007, pp. 239–245, ISSN 1164-5563.
5. ISO 15799, Soil quality – Guidance on the ecotoxicological characterization of soils and soil materials, 2003.
6. FABRIK CHEMISCHER PRÄPARATE VON DR. RICHARD STHAMER GMBH&CO. KG. Product information: STHAMEX F-15 / F-6. Hamburg, 2011, 2 p.
7. ZAHAS S.R.O. Data sheet: Finiflam F-15 3%. Lipník, Czech Republic, 2011, 2 p.
8. FABRIK CHEMISCHER PRÄPARATE VON DR. RICHARD STHAMER GMBH&CO. KG. Product information: MOUSSOL-APS F-15. Hamburg, 2011, 2 p.
9. ISO 11268-2, Soil quality – Effects of pollutants on earthworms – Part 2: Determination of effects on reproduction of Eisenia fetida/Eisenia andrei, 2012.
10. Johnson A.: A Field Method for Measurement of Infiltration. U. S. Geol. Survey Water-Supply Paper 1544-F., 1963, p. F1–F27.
11. Hribova S., Zlamalova Gargosova H., Vavrova M.: Sorption ability of the soil and its impact on environmental contamination, Interdisciplinary Toxicology, Bratislava, 2014, Vol. 7(4), p. 177–183, doi: 10.2478/intox-2014-0025.
12. *Test No. 222: Earthworm Reproduction Test (Eisenia fetida/Eisenia andrei)*, OECD Guidelines for the Testing of Chemicals, Section 2, OECD Publishing, Paris (2004). DOI: http://dx.doi.org/10.1787/9789264070325-en.
13. *Test No. 207: Earthworm, Acute Toxicity Tests*, OECD Guidelines for the Testing of Chemicals, Section 2, OECD Publishing, Paris (1984). DOI: http://dx.doi.org/10.1787/9789264070042-en.
14. Adams R., Simmons D., Hartskeerl K., Koehler M.: Surviving suppression: no detectable impacts of Class A foam on soil invertebrates and some Australian native plants. *Bushfire 2004: earth, wind & fire: fusing the elements: conference proceedings*, Department for Environment and Heritage, Adelaide, South Australia.

LACTIC ACID PRODUCTION FROM WASTE BREAD

HELENA HUDEČKOVÁ and LIBOR BABÁK

Institute of food science and biotechnology,
Faculty of chemistry, Brno university of technology,
Purkyňova 118, 612 00 Brno, Czech Republic
xchudeckova@fch.vutbr.cz

Introduction

Lactic acid is organic acid traditionally used in food and pharmaceutical industries[1]. It has great potential in producing the biodegradable plastics. Polylactic acid (PLA) is alternative to traditional plastics (derived from fossil feed-stocks) but its large-scale applications limited by high price of lactic acid production[2]. For lowering cost of lactic acid production was examinated using of renewable agricultural residues as fermentable substrate, thermophilic microbes for non-sterilised fermentations and trying of some other strategies in downstream separation and purification processes[3, 4, 5].

Food waste offers interesting composition to be a suitable fermentation feed. Globally is wasted many different types of food. The main categories are meat, fruit and vegetable, and bakery products. In the last category is the most abundant bread[6].

Heat and moisture during baking of bread cause starch gelatization, which making bread much more susceptible to microbial attack. Composition of different types of bread is various. Typically 100 g of white bread contains about 50 g of saccharides (about 47 g of it is starch), 37 g of water and 8 g of proteins. Because of it is bread great, comparatively complete source of nutrition for many microorganisms. Because of it we tried to use waste bread as raw material for lactic acid production[6].

Traditional lactic acid producers have optimal temperatures of growing and fermenting about 30 to 40 °C. These temperatures of fermentation are inclinable to contamination by unsolicited microorganisms. It means that raw material have to be sterilized. Therefore we tried to fermentation with thermotolerant *Bacillus coagulans*. Its advantage is that grows and ferments at temperatures from 50 to 60 °C. The other benefits are simple nutrition requirement and production of high optical pure L-lactic acid[7].

The aim of this work was to study production of lactic acid by thermophilic *Bacillus coagulans* on waste bread under non-sterilised conditions. We tried fermentation with two different calues of pH (without adjusting of pH and pH 7.0).

Methods

Raw material

For experiment was used wheat-rye bread (after shelf life). Raw material has not been attacked by mold. Bread was crushed by mixer and chopper. The moisture of bread was 10.21 % (w/w). Content of starch was 64.17 % (w/w).

Enzymes

We used two enzymes, one for liquefaction and second for saccharification. As liquefaciting enzyme was used α-amylase (BAN 240 L) and for saccharification was used glucoamylase (AMG 300 L). Enzymes were provided by Novozyme.

Hydrolysis

200 mL of 15 % (w/v) bread and water suspension was prepared for experiment. Solution pH was adjusted to 5.5. For adjusting pH of bread suspension was used 1 % (w/v) solution of H_2SO_4 and 1 % (w/v) solution of NaOH. Then α-amylase was added to bread suspension and flasks were placed into tempered shaker (Heidolph UNIMAX 1010, Heidolph 1000). After 2 hours of exposure α-amylase was added to the flask glucoamylase. After addition, the suspension was hydrolyzed for 1.5 hours. Hydrolysis took place under 65 °C with stirring 130 min^{-1}.

Microorganisms and cultivation

For fermentation we used bacteria *Bacillus coagulans* CCM 4318 (Czech Collection of Microorganisms, Brno, Czech republic). For preparation of inoculum and growth of bacteria before fermentation was used liquid MRS medium. It was consisted of: glucose (20 $g \cdot L^{-1}$), proteose peptone (10 $g \cdot L^{-1}$), beef extract (10 $g \cdot L^{-1}$), yeast extract (5 $g \cdot L^{-1}$), polysorbate 80 (1 $g \cdot L^{-1}$), ammonium citrate (2 $g \cdot L^{-1}$), sodium acetate (5 $g \cdot L^{-1}$), magnesium sulphate (0.1 $g \cdot L^{-1}$), manganese sulphate (0.05 $g \cdot L^{-1}$), dipotassium phosphate (2 $g \cdot L^{-1}$). Medium was sterilised by autoclaving at 121 °C for 15 minutes. Before inoculating it was tempered to 50 °C.

Inoculum was prepared from freezed culture. We added 20 mL of freezed medium with bacteria to 200 mL of tempered sterile MRS medium. It was cultivated for 48 hours. Conditions of cultivation were 50 °C and 150 min^{-1}. From this inoculum was prepared second inoculum which was used for inoculated of fermentation. Second inoculum was prepared under similar conditions as first. Time of cultivation was 24 hours.

Batch fermentation

The inoculum of *Bacillus coagulans* was diluted to an optical density 1.0 and hydrolysates were inoculated with 20 ml of diluted inoculum. After inoculation, flasks were placed into a tempered shaker (Heidolph UNIMAX 1010, Heidolph 1000). Fermentation took place under 50 °C with stirring 150 min^{-1} for 60 hours. The experiment was taken at two different values of pH – with adjustment to 7.0 and without adjustment. The pH 7.0 was adjusted using 1 % (w/v) solution of NaOH. Time of fermentation was 56 hours.

Analytical methods

Samples were collected periodically during 56 hours of batch experiment. The collected samples were centrifuged at 14,000 min^{-1} for 10 minutes. The supernatants were used for analysis of lactic acid and reducing saccharides in the fermentation medium. Amounts of reducing saccharides were analysed spectrophotometrically by Somogyi-Nelson. Yields of lactic acid were analysed by HPLC.

The lactic acid content was determined using Polymer IEX H form 8 μm (Watrex, CZ) at 60 °C with UV/VIS detector (ECOM LCD 2084). For analyse on HPLC we used as mobile phase $9 \cdot 10^{-3}$ M solution of H_2SO_4 at a flow rate set to

1 mL·min^{-1} and was constant throughout the measurement. Time analysis of lactic acid calibration solution was 15 minutes. For standard solution was observed retention time of the substance. Calibration curve was based on the area of the relevant peak. Concentration of the lactic acid in the samples was determined by conversion via linear regression equation. It was obtained from the calibration curves.

Statistical evaluation of the results

All measured values were determined three times. These three measured values were averaged by function AVERAGE. For calculation of value of the confidence interval was used function CONFIDENCE in Microsoft office Excel 2010 (Microsoft, USA). Was chosen statistical significance level $\alpha = 0.05$.

Results and discussion

We were hydrolysated 15 % (w/v) suspension of wasted bread and distilled water. Concentration of reducing saccharides before fermentation was 67.306 ± 0.004 g·L^{-1} in sample without adjustment of pH. Concentration of reducing saccharides in samples with adjusted pH was 64.889 ± 0.005 g·L^{-1}. After that we inoculated it with *Bacillus coagulans*. Fermentation was terminated after 56 hours. Yields of lactic acid and processes of fermentation were different in individual samples with different pH. We obtained 3.399 ± 0.016 g·L^{-1} of lactic acid in hydrolysate without pH adjustment. In hydrolysate with adjusted pH we obtained 5.60 ± 0.14 g·L^{-1} of lactic acid. It was found that production of lactic acid finished after 52 hours and the highest yield of lactic acid was obtained at hydrolysate with adjusted pH.

Processes of individual fermentations are shown at the Fig. 1 and the Fig. 2. Fig. 3 shown graphical comparisons of various methods of fermentation.

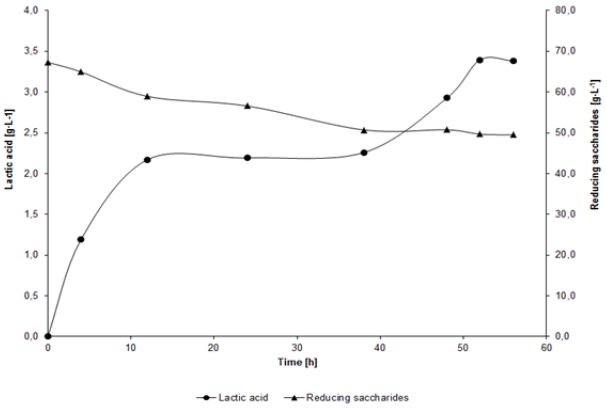

Fig. 6. **Graphical representation of fermentation process without pH adjustment**

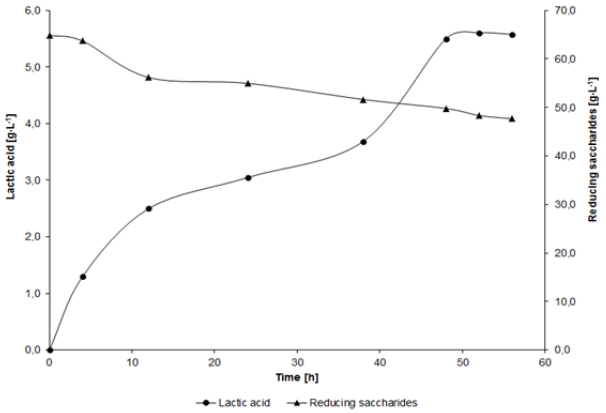

Fig. 7. **Graphical representation of fermentation process with pH 7**

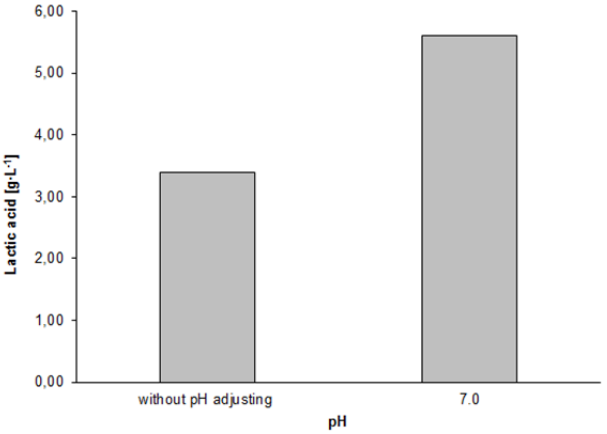

Fig. 8. **Comparison of various methods of fermentation**

Conclusion

In this study, lactic acid production using waste bread as nutrient source by *B. coagulans* (CCM 4318) was established. We were examinated two conditions of fermentation (with adjusting of pH to 7.0 and without adjusting). It was found that highest yield of ethanol was obtain at hydrolysates with adjusting pH (7.0). Final concentration of lactic acid was 5.60 ± 0.14 g·L^{-1}. It was found that waste bread is suitable for lactic acid production. By further research we would like to optimize the fermentations on this substrate and achieve higher yields of lactic acid.

REFERENCES

1. Zhao, B., Wang, L. M., Ma, C. Q., Yang, C. Y., Xu, P., Ma, Y. H: Bioresource Technology. 101, 6494–6498. (2010).
2. Lu, Z. D., He, F., Shi, Y., Lu, M. B., Yu, L. J.: Bioresource Technology. 101, 3642–3648. (2010).
3. Ouyang, J., Ma, R., Zheng, Z. J., Cai, C., Zhang, M., Jiang, T.: Bioresource Technology. 135, 475–480. (2013).
4. Gao, T., Wong, Y., Ng, C., Ho, K.: Bioresource Technology. 121, 105–110. (2012).

5. Qin, J. Y., Wang, X. W., Zheng, Z. J., Ma, C. Q., Tang, H. Z., Xu, P.: Bioresource Technology. 101, 7570–7576. (2010).
6. Kosseva, M. & Webb, C., in: Food industry wastes: assessment and recuperation of commodities, Elsevier/Academic Press, Singapore, (2013).
7. Ma, K., Maeda, T., You, H. & Shirai, Y.: Bioresource Technology. 151, 28–35. (2014).

DETERMINATION OF TOTAL POLYPHENOL CONTENT AND TOTAL ANTIOXIDANT ACTIVITY OF DIFFERENT CURRANT AND GOOSEBERRY CULTIVARS GROWN IN THE CZECH REPUBLIC

PAVEL DIVIŠ[a], SILVIA CHRISTOVOVÁ[a], JAROMÍR POŘÍZKA[a], MILENA VESPALCOVÁ[a] and ALEŠ MATĚJÍČEK[b]

[a]*Brno University of Technology, Faculty of Chemistry, Purkyňova 118, 612 00 Brno, CZ*
xcchristovova@fch.vutbr.cz
[b]*Research and Breeding Institute of Pomology Holovousy Ltd., Holovousy 1, 508 01 Hořice, CZ*

Currants and gooseberries have been known in Europe since the 14th century. They are consumed either fresh or as juices and jams or as fermented fruit beverages. Currant is a small shrub belonging to the family of Grossulariaceae of the genus Ribes. The currant bush grows up to a height of 1–1.5 meters. Its leaves are yellowish-green in colour and are arranged spirally on the stems in bunches of five. During each season the shrub bears pendulous chain of small berries. Depending on the berries colour, red, white and black currant varieties can be distinguished. Gooseberries are deciduous, fast growing shrubs reaching 1 m in height and 1.5 m in width under optimum conditions. The leaves are alternate, single, deeply lobed, and glossy dark green. The fruit, borne singly or in pairs at the axils, is a berry with many miniature seeds at the center. A gooseberry may be green, white, yellow, or in shades of red from pink to purple to almost black[1]. Currants and gooseberries are important source of biologically active substances and have essential importance for humans[2]. In this work the total concentration of polyfenolic compounds and the antioxidant activity of different cultivars of currants and gooseberries grown in the Czech Republic were determined.

All of the currants and gooseberries cultivars were grown in the Czech Republic, at the Research and Breeding Institute of Pomology Holovousy Ltd. (50°22′29″ N, 15°34′38″ E, 321 m alt.), in an experimental orchard established in autumn 2008[3]. The average annual temperature in the locality is 8.14 °C. The average annual rainfall is 655 mm and the average rainfall during the plant growing period is 379 mm. Fruits were harvested at full maturity and stored at −18 °C before the analysis. The analysed cultivars of black currant were ′Ceres′, ′Lota′, ′Ruben′, ′Ometa′, ′Fokus′, ′Démon′, ′Triton′ and ′Morávia′. Of the red gooseberry cultivars ′Alan′, ′Hinnonmaki Rot′, ′Karát′, ′Karmen′, ′Krasnoslawjankij′, ′Remarka′, ′Rolonda′ and ′Pax′ were analysed. The antioxidant activity of red gooseberries was determined by UV-VIS spectrometry using ABTS (2.2'-azino-bis(3-ethylbenzthiazoline-6-sulfonic acid)) and DPPH (1.1-diphenyl-2-picrylhydrazyl) method[4]. Trolox was used as a standard compound for construction of calibration curves. Absorbance was measured at wavelengths of 734 nm (ABTS) and 515 nm (DPPH) against the blank (methanol) after the time determined from the measured kinetic curves. The antioxidant activity of black currants was determined by electron paramagnetic resonance (EPR) spectrometry using the ABTS and DPPH methods[5]. The antioxidant activity in each sample was expressed as Trolox equivalent antioxidant capacity ($TEAC_{ABTS}$ and $TEAC_{DPPH}$) in the case of EPR measurement[5] and as Trolox equivalent (TE) in the case of UV-VIS measurement[4]. Total polyphenols were determined by UV-VIS spectrometry at the wavelength of 750 nm according to the Folin-Ciocalteu method[6]. Gallic acid was used as a standard for construction of calibration curve. All analyses were done in 3 replicates and the results were processed using statistical software XLSTAT and Statistica.

The results from the analyses are summarised in Table 1 and Table 2. The concentration of total polyphenols varied between the cultivars of currants and gooseberries and the differences were statistically significant ($p < 0.05$). In the terms of total polyphenol content, black currant cultivars ′Ometa′, ′Fokus′ and ′Démon′ were evaluated as the best. In the case of gooseberry cultivars ′Alan′, ′Krasnoslawjanskij′, ′Rolonda′ and ′Pax′ showed the highest concentration of total polyphenols.

Table 1
Total polyphenol content (TP) and antioxidant activity expressed as Trolox equivalent antioxidant capacity (TEAC) of black currant cultivars analysed in this study

Cultivar	TP ($mg \cdot kg^{-1}$)	$TEAC_{DPPH}$ (mM)	$TEAC_{ABTS}$ (mM)
′Ceres′	1971	27.3	13.7
′Lota′	1774	27.6	11.8
′Ruben′	1872	39.4	15.7
′Ometa′	2673	28.9	16.0
′Fokus′	2621	30.9	13.1
′Démon′	2704	31.3	13.9
′Triton′	2123	29.2	13.2
′Morávia′	2047	28.0	11.1

Table 2
Total polyphenol content (TP) and antioxidant activity expressed as Trolox equivalent (TE) of red gooseberry cultivars analysed in this study

Cultivar	TP ($mg \cdot kg^{-1}$)	TE_{DPPH} (mM)	TE_{ABTS} (mM)
′Alan′	2118	1.92	1.57
′Hinnonmaki Rot′	1655	1.05	0.84
′Karát′	1444	1.07	0.79
′Karmen′	2019	1.56	1.44
′Krasnoslawjanskij′	2125	1.22	1.17
′Remarka′	1415	0.59	0.56
′Rolonda′	2147	1.33	1.22
′Pax′	2229	1.56	1.49

Good correlation was found between the total polyphenol content (TP) and the antioxidant activity. In the case of red gooseberries the TP/TE_{DPPH} correlation coefficient was found to be 0.7912 and in the case of TP/TE_{ABTS} correlation was even better, $r = 0.9095$. Slightly weaker, but still significant correlation was found between the total polyphenol content of black currant and its antioxidant activity. Correlation coefficients were 0.7410 for $TP/TEAC_{DPPH}$ and 0.5613 for $TP/TEAC_{ABTS}$. High concentration of polyphenols and high

antioxidant activity of red gooseberries and black currants found in this study confirm that these fruits are rich source of health benefiting compounds. Free radicals in the human body contributes significantly to the development of diabetes, promote ageing, formation of eye diseases, inflammations, tumors, a series of lung diseases, skin diseases, neurodegenerative and immune disorders, and other health problems. Consumption of higher amounts of red gooseberries and black currants can help to reduce the oxidation stress in the human body.

In the present literature, there is only little information about the total polyphenol content in black currants and red gooseberries. Nour et al.[7] determined the total anthocyanins in 8 cultivars of black currant grown in Romania within the range of 1161−2878 $mg \cdot kg^{-1}$, which is comparable with our study. However, Hegedus et al.[8] found significantly higher concentration of total polyphenols, up to 12000 $mg \cdot kg^{-1}$ in ′Fertodi′, ′Otelo′ and ′Titania′ black currant cultivars grown in Hungary. Similar results have also been published by Pantelidis et al.[9] (12570 $mg \cdot kg^{-1}$ in ′Whinham's Industry′ gooseberry cultivar). The differences in values of total polyphenol content published by other authors and those determined in our study can be caused by different stage of maturity of analysed fruit.

This work was supported by the grant of the Ministry of the Agriculture of the Czech Republic No. QI111A141.

REFERENCES

1. Strik B. C., in: Berry Fruit Value-Added Products for Health Promotion, p.3. CRC Press, Boca Raton, 2007.
2. Karjalainen R., Anttonen M., Saviranta N., Stewart D., McDougall G. J., Hilz H., Mattila, P.: Acta Hortic., *839*, 301 (2009).
3. Diviš P., Pořízka J., Vespalcová M., Matějíček A., Kaplan J.: J. Element., *20*, 549 (2015).
4. Rop O., Mlcek J., Kramarova D., Jurikova T.: Afric. J. Biotechnol., *9*, 1205 (2010).
5. Polovka V.: J. Food Nutr. Res., *45*, 1 (2006).
6. Faller A. L. K., Fialho E.: J. Food Compos. Anal., *23*, 561 (2010).
7. Nour V., Trandafir I., Ionica M. E.: Fruits, *65*, 353 (2011).
8. Hegedus A., Balogh E., Engel R., Sipos B. Z., Papp J., Blazovics A., Stefanovits-Bányai E.: Hort. Sci. *43*, 1711 (2008).
9. Pantelidis G. E., Vasilakakis M., Manganaris G. A, Diamantidis G.: Food Chem., *102*, 777 (2007).

ASSESSMENT OF TRACE ELEMENTS IN FISH TISSUES AS TOOL FOR MONITORING POLLUTION IN THE AQUATIC ECOSYSTEM

CEZARA VOICA[a], ROXANA ELENA IONETE[b], MONICA CULEA[a], SONIA SUVAR[b] and ANDREEA MARIA IORDACHE[b]*

[a]*National Institute for Research and Development of Isotopic and Molecular Technologies, 67-103 Donat Str, Cluj-Napoca, Romania*
[b]*National R&D Institute for Cryogenics and Isotopic Technologies -ICIT, 4 Uzinei Str, Romania*
[3]*"Babes-Bolyai" University, Biomolecular Physics Department, M Kogalniceanu Str, Cluj-Napoca, Romania*
andreea.iordache@icsi.ro

An important part of the human diet, the fish is considered to be a reliable pollution marker of the aquatic ecosystem due to its feeding regime and living environment. Its ability to uptake and concentrate metals, either by ingestion of contaminated food (e.g. aquatic vegetation, invertebrates, and small fish) or through the gills and skin, and its location at the end of the aquatic food chain, makes it the ideal candidate to be used in assessing the heavy metal pollution of the aquatic environment.

High toxicity, bioaccumulation and their persistence in environment makes many metals to present health risks. In this work an assessment of several elements (Fe, Cu, Zn, Mn, Ni, As, Pb, Hg, and Cd) was performed on samples of fish collected from three different rivers in Romania and of squid purchased from the seafood market. Trace metals were determined by inductively coupled plasma mass spectrometry (ICP-MS) after microwave digestion. All nine elements were quantitatively recovered (over 80 %). The relative standard deviation was less than 10 %.

Introduction

Environmental pollution is seen as a major issue in all the countries around the world, no matter their stage of development[1]. Recent years have witnessed a significant concern due to environmental contamination problems caused by a wide variety of chemical pollutants, including trace metals. Metals from various natural and anthropogenic sources continuously affect the aquatic ecosystem and pose serious health threats to organism because of their toxicity, long persistence, bioaccumulation and biomagnification in the food chain[2].

Today, much attention is paid to study the content of essential and toxic trace elements in foodstuffs, as a result of a growing concern about the health benefits and risks of food consumption[3]. Particularly, fish is an important part of the human diet and a good indicator of pollution with trace metals in the aquatic ecosystem. Several analytical techniques are available for trace element determination in fish samples[4–8]. Quantification of trace elements in fish tissues is typically performed with inductively coupled plasma-mass spectrometry (ICP-MS), which is capable of simultaneously quantifying the large number of elements needed for stock discrimination[9–10].

In this study, determination of trace elements (toxic metals and trace elements) in three different highly consumed fish species in Romania was performed by ICP–MS, after microwave digestion.

Material and methods

Seventeen fish samples were collected from three rivers in Romania: Trout, Catfish *(Silurus glanis),* Common Roach *(Rutilus rutilus),* Carassius, Bleak *(Alburnus alburnus*), Common nase *(Chondrostoma nasus),* Common carp *(Cyprinus carpio),* Silver carp *Hypophthalmichthys molitrix*). Additionaly, three samples of squid *(Loligo vulgaris)* were purchased from the Romanian seafood market. The samples were stored at –20 °C until the analysis.

Prior to quantification in the ICP-MS, trace elements were extracted from fish tissues using a digestion method. The digestion method was chosen to ideally remove and avoid adding whatever may cause formation of polyatomic ions in the plasma and/or non-spectral interferences[11]. Samples digestion was carried out using a Mars 5 Microwave System (CEM Microwave). The aliquots were digested in an acids mixture at high pressure and temperature. The optimized method for fish digestion that we adapted was: HNO_3 (2 mL) + HF (0.3 mL) + H_2O_2 (2 mL), with sample weight of 0.15 g (dried sample). After cooling, the liquid was transferred quantitatively in a 50 cm^3 volumetric flask and brought to the required volume with ultrapure water.

Table 1
Microwave digestion programme for sample of fish

Step	Power (W)	% Power	Ramp min.	Pressure (PSI)	Temp. (°C)	Hold (min.)
1	800	100	10	350	200	10

The elemental analysis was performed by inductively coupled plasma quadrupole mass spectrometry (ICP-Q-MS). The following operating conditions were applied: nebulizer gas flow rates of 0.86 $L \cdot min^{-1}$; auxiliary gas flow of 1.2 $L \cdot min^{-1}$; plasma gas flow of 15 $L \cdot min^{-1}$; lens voltage of 7.25 V; 1100 W ICP RF Power; CeO/Ce = 0.027; and Ba++/Ba+ = 0.025.

Results and discussion

The sample extraction and analytical procedures were accompanied by the running of blanks and spiked standards. All samples were analyzed in three independent replicates to ascertain the reproducibility of the analyses. The accuracy of arsenic determination was examined by running Certified Measurements of the CRM (Atomic Spectroscopy standard: Multi-element calibration standard standard 10 $mg \cdot L^{-1}$ and Hg standard 10$\mu g \cdot mL^{-1}$ Perkin Elmer Pure); showed that the recovery after destruction in the digestion oven was over 80 %.

Trace element content in fish samples were found between 11.68 and 129.30 $mg \cdot kg^{-1}$ for zinc, 0.77–32.35 $mg \cdot kg^{-1}$ for copper, 0.007–2.43 $mg \cdot kg^{-1}$ for manganese, and 7.71–36.51 $mg \cdot kg^{-1}$ for iron (Table 2). Toxic elements content in fish samples were found as follows: < 0.001 for cadmium,

0.09–1.58 mg·kg^{-1} for arsenic, 0.06–2.03 mg·kg^{-1} for mercury, 0.03–0.41 mg·kg^{-1} for nickel, 0.03–0.72 mg·kg^{-1} for lead (Table 3).

Acording to these data, zinc has the highest concentration followed by iron, copper, manganese, arsenic, and lead.

Table 2
Trace elements in studied samples (mean ± standard deviation)

Fish type	Metal concentrations [mg·kg^{-1}]			
	Fe	Cu	Zn	Mn
Trout	31.48±1.57	32.35±0.99	28.23±1.68	0.34±0.01
Catfish	36.51±1.72	24.19±0.75	31.77±1.77	0.06±0.002
Roach	9.93±0.68	9.01±0.33	53.15±3.18	0.35±0.01
Carassius	7.71±0.44	3.11±0.17	129.30±7.74	2.43±0.07
Squid	10.08±0.75	1.05±0.03	14.18±0.85	0.52±0.01
Bleak	8.89±0.67	0.99±0.03	90.33±5.42	1.08±0.03
Common nase	24.43±1.23	1.97±0.05	43.30±2.59	0.47±0.01
Common carp	13.85±0.88	7.17±0.22	18.25±1.09	0.19±0.006
Silver carp	10.47±0.77	0.77±0.01	11.68±0.70	0.007±0.0002

Table 3
Toxic elements in studied samples (mean ± standard deviation)

Fish type	Metal concentrations [mg·kg^{-1}]			
	Ni	As	Pb	Hg
Trout	0.31±0.02	0.42±0.04	0.72±0.04	2.03±0.15
Catfish	0.41±0.03	0.28±0.02	0.55±0.03	0.91±0.06
Roach	0.08±0.006	1.12±0.10	0.10±0.006	0.61±0.04
Carassius	0.19±0.01	0.90±0.08	0.08±0.005	0.33±0.02
Squid	0.23±0.02	1.58±0.14	0.24±0.85	0.12±0.01
Bleak	0.16±0.01	0.09±0.008	0.15±0.01	0.69±0.05
Common nase	0.17±0.01	0.38±0.03	0.03±0.002	0.50±0.01
Common carp	0.03±0.002	0.20±0.023	0.23±0.02	0.21±0.02
Silver carp	0.07±0.003	0.14±0.01	0.05±0.003	0.06±0.004

Among the numerous inorganic elements found in nature, some, such as cadmium, mercury, lead and arsenic, are considered potentially dangerous for human health if absorbed beyond certain limits.

Arsenic (As) is an important element for speciation analysis, especially with regard to nutritional control. Human intake of arsenic occurs mainly via food chain, and it is closely related to the consumption of fish[12]. The provisional tolerable weekly intake (PTWI) for inorganic arsenic indicated by the Joint FAO/WHO Expert Committee on Food Additives is 0.015 mg·kg^{-1} body mass/week[13] and some authors demonstrated that more than 90 % of the total arsenic ingested comes from fish. However, less than 3 % of the arsenic in fish is present in the inorganic form (arsenite or arsenate)[14].

Cadmium (Cd) is a highly toxic metal with a natural occurrence in soil, but it is also spread in the environment due to human activities[1]. In the literature cadmium levels in fish samples have been reported in the range of 0.51–0.73 mg·kg^{-1} dry weight in fish species from Bangladesh[15]. In all fish samples from this study, the level concentration of cadmium was below 0.001 mg·kg^{-1}.

Mercury (Hg) accumulation in fish has received much attention internationally and many countries have fish consumption advisories related to Hg (e.g. UNEP, 2002)[16–17]. The most commonly recommended limit for consumption is 0.5 mg·kg^{-1}, although there are lower limits in some countries[18]. According to USEPA risk consumption limit tables[19], chronic systemic non-carcinogenic effects of mercury may be expected, even with concentrations much below 0.5 mg·kg^{-1}. In our work, four out of the twenty samples collected had concentrations slightly above 0.5 mg·kg^{-1}. The highest concentration was recorded in trout samples. Mercury bioconcentration in fish decreased in the following order: trout > catfish > bleak > roach > carassius > common nase > common carp > squid > silver carp.

Lead (Pb) is a non-essential element. It is well documented that Pb can cause neurotoxicity, nephrotoxicity, and many others adverse health effects[19, 20]. Lead is a metal with a clear Codex Alimentarius[21] standard of 0.2 mg·kg^{-1}, which is lower than the lowest international standard of 0.5 mg·kg^{-1}. In this work, the lowest and the highest levels of lead were registered for Common nase, of 0.03 mg·kg^{-1}, and 0.72 mg·kg^{-1} for trout, respectively.

The maximum levels of heavy metals permitted in Romania are 3.0 mg·kg^{-1} for arsenic, 0.1 mg·kg^{-1} for cadmium, 0.5 mg·kg^{-1} for lead, 50.0 mg·kg^{-1} for zinc and 5.0 mg·kg^{-1} (for predatory fish) and 0.5 for other species for copper according to the Order 975/1998[22]. The European Regulation on maximum residue levels in food (Commission Regulation EC 1881/2006), which is adopted in B&H legislation (Sl. list BiH, 37/09) sets the maximum allowed concentration (MAC) for Cd in edible fish tissue at 0.050 mg·kg^{-1} wet weight (0.10 mg·kg^{-1} for Mugil sp.)[23]. The limit for lead is 0.4 mg·kg^{-1} (ww) for bonito, common two-banded seabream, eel, grey mullet, grunt, horse mackerel or scad, sardine, sardinops, spotted sea bass, tuna and wedge sole and 0.2 mg·kg^{-1} (ww) for all other fish species.

Zinc (Zn) is found in almost every cell and in a wide variety of foods. It is present in seafood in milligrams per kilogram amounts and there have been no reports of concentrations in the edible parts of fish that form a hazard to health[24]. With an average zinc content of 3–5 mg·kg^{-1} wet weight, fish is a good source for this essential element[25]. The higher concentration of zinc was found in the carassius sample (129.30 mg·kg^{-1}).

Nickel (Ni) normally occurs at very low levels in the environment and it can cause a variety of pulmonary adverse health effects, such as lung inflammation, fibrosis, emphysema and tumours[26]. The lowest and highest nickel levels in fish species were found as 0.03 mg·kg^{-1} in common carp and 0.401 mg·kg^{-1} in catfish.

Copper (Cu) is required for iron utilization, and as a cofactor for enzymes involved in glucose metabolism and the synthesis of hemoglobin, connective tissue and phospholipids[27]. Numerous studies have been directed on copper metabolism in fish and there is a lot of concern about the toxic effects related to heavy-metal pollution in the aquatic environment[28]; however, copper is not toxic for humans in low concentrations[29]. The lowest and highest copper levels in fish samples were found as 0.77 mg·kg^{-1} in silver carp samples and 32.35 mg·kg^{-1} in trout samples, a value that exceeds the maximum level permitted for copper through food consumption (30 mg·kg^{-1}) for FAO (1983)[30].

Manganese (Mn) is an essential element for both animals and plants and its deficiency result in severe skeletal and reproductive abnormalities in mammals[31]. Manganese contents in the literature have been reported in the range of 0.09–0.35 mg·kg^{-1} [32], 0.5–8.8 mg·kg^{-1} [33], 0.11–0.37 mg·kg^{-1} [34]. Manganese, likewise, is an essential element, for which we did not find standards in fish. The average value of the studied samples was 0.605 mg·kg^{-1}, the maximum leves being found in carassius samples.

Conclusions

Nine elements consisting potentially toxic metals and trace elements were analyzed in 20 seafood products using ICP-MS. The levels for the toxic and trace elements in fish samples reported in the present study were in agreement with other studies from literature.

Accumulation of heavy metals in fish viscera and other organs may be considered as an important warning signal for fish health and human consumption.

In this work, the concentration of Zn was lower in Silver carp and higher in Carassius fish (18.30–124.9 mg·kg^{-1}). Four out of the twenty samples collected had Hg concentrations slightly above 0.5 mg·kg^{-1}. The highest concentration of Hg (of 2.03 mg·kg^{-1}), Pb (of 0.72 mg·kg^{-1}) and Cu (of 32.35 mg·kg^{-1}) was recorded in trout samples.

The contents of Cd in the investigated samples were more lower than the maximum permissible value.

REFERENCES

1. Ahmed M., K., Shaheen N., Islam M. S., Mamun H. M., Islam S., Mohiduzzaman M., Bhattacharjee L.: Chemosphere *128*, 284–292 (2015).
2. Orecchio S., Amorello D. J.: Hazard. Mater. *174*, 720–727 (2010).
3. Papagiannis I., Kagaloub I., Leonardos J., Petridis D. Kalfakakou V.: Environ. Int. *30*, 357–362 (2004).
4. Ikem A., Egiebor N.O.: J. Food Compos. Anal. *18*, 771–787 (2005).
5. Tuzen M.: Food Chem. Toxicol. *47*, 1785–1790 (2009).
6. Onsanit S., Ke C., Wang X., Wang K.J., Wang W.X.: Environ. Pol. *158*, 1334–1342 (2010).
7. Rahman M. S., Molla A. H., Saha N., Rahman A.: Food Chem. *134*, 1847–1854, (2012).
8. Thiyagarajan D., Dhaneesh K. V., Kumar T. T. A., Kumaresan S., Balasubramanian T.: Bul. Environ. Contam. Toxicol. *88*, 582–588 (2012).
9. Anan Y., Kunito T., Tanabe S., Mitrofanov I., Aubrey D. G.: Mar. Pollut. Bull. *51*, 882–888 (2005).
10. Yang K. X., Swami K.: Spectrochim. Acta B Atom. Spectrosc. *62*, 1177–1181 (2007).
11. Ashoka S., Peake B. M., Bremner G., Hageman K. J. Reid M. R.: Analytica Chimica Acta *653*, 191–199 (2009).
12. Montesinos P. C., Nilles K., Cervera M. L. de la Guardia M.: Talanta *66*, 895–901 (2005).
13. FAO/WHO Expert Committee on Food Additives, WHO Technical Report Series *759*, WHO, Geneva, Switzerland (1989).
14. Ysart G., Miller P., Croasdale M., Crews H., Robb P., Baxter M., de L'Argy C., Harrison N.: Food Add. Contam. *17,* 775 (2000).
15. Ahmed M.K., Ahamed S., Rahman S., Haque M.R., Islam M. M.: Terres. Aquat. Environ. Toxicol. *3*, 33–41 (2009).
16. UNEP 2002UNEP (United Nations Environment Programme). (2002). Global Mercury Assessment. UNEP Chemicals, Geneva, *70*, http://www.unep.org/gc/gc22/ Document/UNEP- GC22-INF3.pdf; Accessed 22.06.11.
17. Djedjibegovic J., Larssen T., Skrbo A., Marjanović A., Sober M.: Food Chemistry, *131*, 469–476 (2012).
18. Burgera J., Gochfeld M.: Environmental Research, *99*, 403–412 (2005).
19. Garcia-Leston J., Mendez J., Pasaro E., Laffon B.: Genotoxic effects of lead: an updated review. Environ. Int. *36*, 623–636 (2010).
20. Weber D. N., Dingel W. M.: Am. Zool. 37, 354–362 (1997).
21. Codex Alimentarius Commission, 2002. Codex Committee on Food Additives and Contaminants: Maximum level for lead in fish. Joint FAO/WHO Food Standards Programme. Document CL-2002 10- FAC. United Nations, Rome.
22. Romanian Order 975/1998 Health Food.
23. Commission Regulation (EC) No 1881/2006 of 19 December 2006 setting maximum levels for certain contaminants in foodstuffs.
24. Tuzen M.: Food Chem. Toxicol. *47*, 1785–1790 (2009).
25. Oehlenschläger J.: Identifying heavy metals in fish. In: Bremner HA (ed) Safety and quality issues in fish processing. Woodhead and CRC, Cambridge, UK, *95*–113 (2002).
26. Forti E., Salovaara S., Cetin Y., Bulgheroni A., Pfaller R. W., Prieto P.: Toxicol. in Vitro. *25*, 454–461 (2011).
27. Çelik U., Oehlenschläger J.: Eur Food Res Technol. *220*:37–41 DOI 10.1007/s00217-004-1104-1, (2005).
28. Lall S. P.: Macro and trace elements in fish and shellfish. In: Ruiter A (ed) Fish and fishery products. CAB International, 187–213, (1995).
29. Linder M. C., Hazegh-Azam M.: Am. J. Clin. Nutr. *63*:797– 811 (1996).
30. Food and Agriculture Organization (FAO). Compilation of legal limits for hazardous substances in fish and fishery products. FAO Fishery Circular No. 464, 5–10. Food and Agriculture Organization of the United Nations, Rome, (1983).
31. Sivaperumal P., Sankar T. V., Viswanathan N. P. G.: Food Chem. *102*, 612–620 (2007).
32. Thiyagarajan D., Dhaneesh K. V., Kumar T. T. A., Kumaresan S. Balasubramanian, T.: Bul. Environ. Contam. Toxicol. *88*, 582–588 (2012).
33. Biswas S., Prabhu R. K., Hussain K. J., Selvanayagam M., Satpathy K. K.: Environ. Monit. Assess. *184*, 5097–5104 (2012).
34. Pintaeva E. T., Bazarsadueva S.V., Radnaeva L. D., Pertov E. A., Smirnova O. G.: Content and character of metal accumulation in fish of the Kichera River (a tributary of Lake of Baikal). Contemp. Prob. Ecol. 4, 64–68 (2011).

STUDY OF AGAROSE GELATION PROCESS BY UNCONVENTIONAL LIGHT SCATTERING METHOD

MICHAL KALINA[a,*], JIRI SMILEK[a], ROMANA KRATOCHVILOVA[a], ŠÁRKA KRŇÁVKOVÁ[a], MARCELA LASTUVKOVA[a] and MARTINA KLUCAKOVA[a]

[a] *Brno University of Technology, Faculty of Chemistry, Materials Research Centre, Purkyňova 118, 612 00 Brno, Czech Republic*
**kalina-m@fch.vutbr.cz*

Abstract

Nowadays hydrogels represent material with broad application in different areas (medicine, agriculture, food…). One of the most important parameters of these systems is the knowledge of gelation temperature. The main purpose of this contribution was utilization of dynamic light scattering technique as novel tool for the study of gelation process. Agarose was selected as model thermoreversible hydrogel applied in experimental part of present study. The gelation process of this linear polysaccharide is well-known and discussed in literature. Results obtained from dynamic light scattering measurement were in good agreement with classical macrorheology (oscillation test and temperature ramp). Results of present work are indicating that described method of dynamic light scattering can provide simple and reasonably precise tool for deeper investigation of sol-gel transition behavior of different substances especially biopolymers and biocolloids and can be comparable with different conventional techniques.

Introduction

Nowadays many industrial mechanisms such as catalyst support, soil remediation, transport phenomenon, water purification, electrochemical processes and design of selective membranes are closely connected to the local nature of their environment, which is often made by porous materials (f. e. gels)[1, 2]. Even a slight change in the properties of these porous matrices, cause by the difference in its structure or also by often occurring degradation processes can lead to significantly lower yield of the final formulation, decrease in the kinetic of the process, or to the formation of unexpected product[3]. These gel based porous materials are often made by the sol-gel transition. This process can be initiated by change of the physical conditions (temperature, pH, ionic strength), by ultra-visible light or by addition of crosslinking agent[4]. During the sol-gel transition the formation of internal interactions (physically or chemically based) finally lead to the nucleation, growth and aggregation of all chains in the sample. This is gradually yielding in the formation of three dimensional structures.

Hydrogels represent probably the most significant group of gels. A hydrogel can be described as hydrophilic polymeric network cross-linked in some way to produce an elastic structure. Hydrogels can be prepared either from synthetic or natural polymers. The water holding capacity and permeability are often discussed as one of the most important characteristic features of a these systems[5]. Moreover, in accordance to the main applications of hydrogels in the area of agriculture, food and beverage production, pharmaceutical and biomedical field, tissue engineering and ophthalmology, the biocompatibility must be taken into account as crucial parameter[6].

Agarose is neutral polysaccharide generally obtained from marine red algae (Rhophyceae). This polysaccharide is formed by repeating units of agarobiose. Agarose represents one of the major food constituents and important part of products manufacturers of broad variety of different formulations mainly in the area of confectionery[7]. The process of formation of agarose hydrogels is well-known and described in literature[8, 9]. The sol-gel conversion involves rearrangement from fluctuating disorder coils in solutions to ordered structure of co-axial double helix in gel[10]. Agarose hydrogels are regarded as physical gels. Their stabilization is made completely by hydrogen bonding[11].

The process of the formation of an agarose hydrogel was studied in literature using different experimental approaches such as oscillation rheological measurements[7, 12], methods of x-ray diffraction[10], circular dichroism spectroscopy[8] or differential scanning calorimetry[8]. The main aim of present study is the application and further optimization of dynamic light scattering for purposes of determination of sol-gel transition point. For purposes of this work agarose, as an example of thermoreversible hydrogel, was selected.

Dynamic light scattering (DLS) represents optical method measuring the diffusion of particulate materials either in solution or in suspension. In basic, the method of DLS is detecting the time fluctuation of scattered light intensity caused by these moving particles in sample[13]. Obtained value of the diffusion coefficient can be easily recalculated on particle size (hydrodynamic diameter) using Stokes-Einstein relation[14]. The advantage of DLS method is its extremely high sensitivity on the presence of big particles in the samples even at lower concentration. The limiting factor of the application of light scattering methods is the optical access of studied systems[2]. Considering the problem with optical access through porous structure of hydrogel, method of dynamic light scattering can be also applied for investigation of translation diffusion of tracer particles added into studied samples. Movement of these particles with precisely defined particle sizes in solution is practically not influenced by surrounding. This is contrary to the gel sample, in which the movement of tracer particles is allowed only through its pores. As consequence of this, the whole process of translational diffusion is significantly hindered by three dimensional network of hydrogel resulting in the decrease of the rate of translational diffusion. All these findings create from dynamic light scattering perfect tool for determination and deeper investigation of sol-gel transition processes.

Experimental

Materials

In present study, agarose was selected as an example of thermoreversible biopolymer, which point of gelation was determined. Moreover polystyrene microparticles of defined particle size 100 nm, 500 nm, 1000 nm and 2000 nm were used as tracer particles in dynamic light scattering method. All utilized chemicals were purchased from Sigma-Aldrich (p.a. purity grade).

Methods

The main aim of present work was introducing and further optimization of the method of dynamic light scattering (Zetasizer Nano ZS; Malvern Instruments) as an easy tool for determination of point of gelation of thermoreversible biopolymer agarose. Obtained results were compared with data determined using the classical macrorheological methods (ARG2 Rheometer, TA Instruments).

Agarose hydrogel samples used in both parts of the work were prepared by dissolving of solid agarose powder in demineralized water at 85 °C. Final concentration of agarose in the studied hydrogels was 0.01, 0.05, 0.1 and 1 wt. %. In the case of rheological determination of gelation point, the heated samples were loaded on rheometer geometry (steel plate-plates, diameter 40 mm). The measurement was implemented from 90 to 20 °C (5 °C/min). The temperature ramp of agarose hydrogels was performed at fixed oscillation frequency (1 Hz) and at constant strain 0.1 % (this value was chosen from linear viscoelastic region). Consequently, the temperature of gelation for all studied samples was determined.

The second part of the work was dealing with determination of gelation point for agarose hydrogels using the method of dynamic light scattering. For purposes of the DLS analysis, agarose hydrogels contained also regularly distributed polystyrene size particle standards. All samples were heated up to the temperature 85 °C and transferred into preheated glass UV-VIS cuvettes. First part of the DLS determination of agarose hydrogel´s gelation point was focuded on finding of optimal concentration of polystyrene particles in the hydrogel. Consequently, the effect of size of applied polystyrene particles on determination of gelation point (100, 500, 1000 and 2000 nm) and the concentration of agarose (0.01, 0.05, 0.1 and 1 wt. %) in the sample was studied.

Results

Prepared agarose hydrogels were measured by classical rheology (oscillatory tests). The main purpose of these measurements was to determine the temperature of gelation and compare this specific temperature with data obtained from dynamic light scattering measurements.

First of all, the strain sweep measurement was performed. The aim of this measurement was to find out the linear viscoelastic region (LVR) for agarose hydrogels. The accurate value, included in LVR, is the necessary parameter for further oscillatory measurements (frequency sweep and temperature ramp). The LVR for 1 wt. % agarose hydrogel was determined in the range 0.01–2 % of strain.

The temperature of gelation was determined by oscillatory test – temperature ramp performed at constant frequency of oscillation and constant strain. The dependence of viscoelastic modulus as the function of temperature is shown on the Fig.1. From this graphical dependence, it is obvious, that the 1 wt. % agarose hydrogels exhibits elastic behaviour (elastic moduli represented by G' is almost 10× higher in comparison with viscous moduli G'') at lower temperature. Shift of the viscoelastic behaviour occurs in the range of 50–60 °C. The elastic moduli (G') slightly decreases indicating the change of hydrogel structure. At this temperature hydrogels chains are destabilized by heat and the structure of hydrogel become disturbed.

Transition between two states (semi-solid – hydrogel to liquid) is characterized by crossing point of both moduli. This crossing point takes place at 88.5 ± 0.6 °C in the case of 1 wt. % agarose. This critical temperature can be considered as melting point. If the temperature is lower, the hydrogel sample exhibits solid-like behaviour and contrary, if the temperature is higher than melting point, the sample is liquid-like.

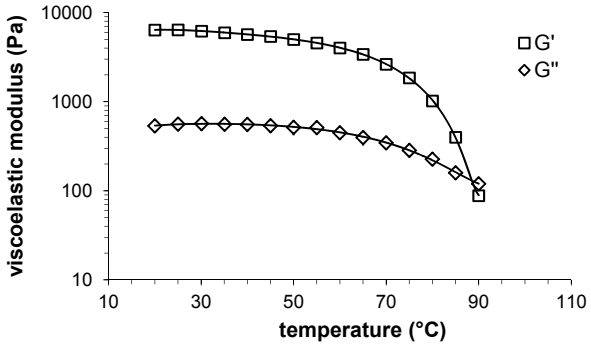

Fig. 1. **Viscoelastic modulus as the function of temperature for 1 wt. % agarose hydrogel** (increasing temperature trend)

The similar dependences were obtained also for other concentration of agarose in the hydrogel. The measured value of melting point is in good agreement with the melting point referred to material safety data sheet of the same type of agarose.

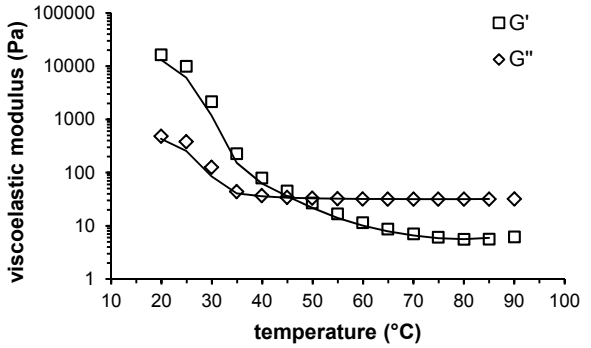

Fig. 2. **Viscoelastic modulus as the function of temperature for 1 wt. % agarose hydrogel** (decreasing trend)

After that the temperature ramp with same experimental setup was performed in opposite trend (with decreasing temperature of the system). The main purpose for this measurement was to determine the temperature of gelation. As it is obvious from the Fig. 2., the viscous modulus is higher in comparison with elastic modulus at higher temperature. Thecrossing point occurs at 43.2 ± 0.4 °C. At this point the contribution to the rheological behaviour of measured sample from viscous and elastic properties is totally same. At lower temperature, the elastic modulus exceeds the viscous modulus, which indicates solid-like behaviour of measured system. The temperature determined in the crossing point is proportional to the gelation temperature.

Subsequently the method of dynamic light scattering was used as a novel method for determination of gelation point. This method determines the fluctuation of the light caused by moving particles in the sample. DLS is extremely sensitive on presence of bigger particles. During the cooling down of agarose samples to the gelation temperature often small agarose particle aggregates are formed. The presence of these aggregegages significantly affect the whole analysis and increase the measurement uncertainty. Moreover the agarose particles represent really weak scatterers. The requirement for optical access in the case of DLS measurements must be also taken into account as important condition. To overcome all these problems, addition of tracer particles into analyzed samples can be implemented. For purposes of present work standard polystyrene particles were chosen. Their refractive index is much higher (n = 1.58 at 632.8 nm) in comparison with both agarose and used solvents, resulting in an intense scattering from these particles even at their low concentration in the sample. This leads to outshining of the scattering of agarose particles and their aggregates by added polystyrene particles. Consequently, DLS analysis can be used for simple monitoring of the movement of these tracer particles in studied sample. Moreover the mobility of these particles is highly dependent on the environment. In solutions the movement is not hindered on the other side in viscous solutions or in hydrogels the movement is significantly restricted by complex 3D structure of the environemnt. These basic findings can be applied for determination of sol-gel transition state of studied sample.

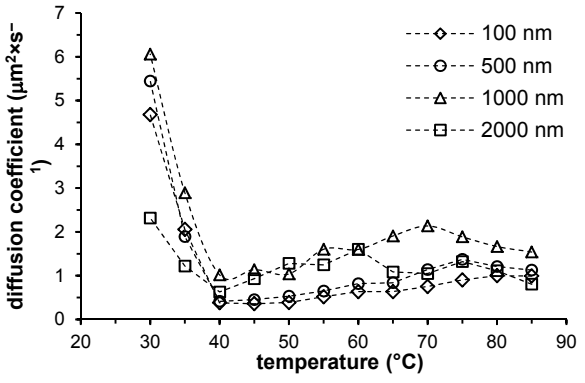

Fig. 3. **Temperature dependence of diffusion coefficient for all applied polystyrene tracer particles; data for 1 wt. % agarose hydrogel**

Comparison of measured temperature dependences of diffusion coefficients obtained by DLS for all utilized polystyrene tracer particles is shown in Fig. 3. All these dependences exhibit the same trend with the decrease of the diffusion coefficient of tracer particles with decreasing temperature up to the point of break on the curve. This point can be assumed as the point of gelation. From Fig. 3 is also obvious that all presented dependences for particular studied tracer particles show the break in their curves around the same temperature. The point of gelation from these dependences was determined by regression of linear sections under and above the gelation point temperature.

All calculated values of gelation point were practically similar. This finding was expected. In general it tells us that the there is no direct dependence of tracer particle size on the diffusion process. The only limiting factor of DLS analysis in the case of porous matrices is the pore size of the matrix.. According to the literature[15] 1 wt. % agarose hydrogel should have the pore size around 100 nm. This is in good accordance with observed data. In all cases the diffusion of tracer particles in agarose hydrogel was significantly influenced by sol-gel transition indicating formation of the agarose hydrogel.

Following part of the study was focused on the deeper research on the influence of agarose concentration in hydrogel (0.01, 0.05, 0.1 and 1 wt. %) on its gelation temperature.. Determined temperatures of sol-gel transition by DLS and their comparison with data obtained from rheological gelation point determination are listed in Table 1.

Table 1
Gelation temperatures determined by both techniques

agarose concentration [wt. %]	DLS [°C]	Rheology [°C]
1.00	40.22±0.35	45.20±0.13

Unfortunately, for DLS measurement, temperature of sol-gel transition was determined only for the 1 wt. % agarose hydrogel. The hydrogels with lower concentration of agarose did not display the break on the dependence of diffusion coefficient of tracer particles on the temperature. This means that the temperature of gelation for these samples was not possible to determine. Probably to low concentration of agarose in hydrogels cannot significantly influence the movement of tracer particles under the sol-gel temperature.

Comparison of both methods of determination of sol-gel transition in the case of 1 wt. % agarose shows the similar results. These values are also in good agreement with the data declared by the producer (36.0 ± 1.5 for hydrogel with agarose concentration 1.5 wt. %, Sigma-Aldrich[16]).

Conclusion

The results of present study confirm the applicability of the method of dynamic light scattering for purposes of determination of gelation point of thermoreversibile polysaccharide agarose. The values determined by this

technique were comparable to values determined using the conventional method of macrorheology and also to the values declared by the producer. All these finding hand by hand with low-cost and simple analysis are indicating that described method of dynamic light scattering can provide simple and reasonably precise tool for deeper investigation of sol-gel transition behavior of different substances especially biopolymers and biocolloids and can be comparable with different conventional techniques.

This work has been supported by Materials Research Centre at Faculty of Chemistry, Brno University of Technology – Sustainability and Development, REG Lo1211, with financial support from National Program for Sustainability I (Ministry of Education, Youth and Sports, Czech Republic).

REFERENCES

1. Taylor S. J., Haw J., Sefcik A. J.: Langmuir *30*, 10231 (2014).
2. Beschieru V., Rathke B., Will S.: Microporous Mesoporous Mater. 125, 63 (2009).
3. Kalina M., Chytilová A., Klučáková M.: *6th International Conference on Nanomaterials NANOCON 2014, Brno, 5-7 Nov. 2014*, Conference Proceedings, p. 844, TANGER Ltd, Ostrava 2014.
4. Ahmed E. M.: J. Adv. Res. 6, 105 (2015).
5. Carpi A.: *Progress in Molecular and Environmental Bioengineering - From Analysis and Modeling to Technology Applications*, Intech, GB 2011.
6. Anderson J. M., Langone J. J.: J. Controlled Release 57, 107 (1999).
7. Deszczynski M., Kasapis S.: Carbohydr. Polym. 53, 85 (2003).
8. Mohamemed Z. M., Hember M. W. N., Richardson R. K., Morris E. R.: Carbohydr. Polym. 36, 15 (1998).
9. Rees D. A., Morris E. R., Thom D., Madden J. K.: *The polysaccharides*, Academic Press, NY 1982.
10. Arnott S., Fulmer A., Scott W. E., Dea I. C. M., Moorhouse R., Rees D.A.: J. Mol. Biol. 90, 269 (1974).
11. Braudo E. E.: Food hydrocolloids 6, 25 (1992).
12. Braudo E. E., Muratalieva I. R., Plashina I. G., Tolstoguzov V. B.: Carbohydr. Polym. 15, 317 (1991).
13. Xu R.: Particuology 6, 112 (2008).
14. Brown W.: *Dynamic light scattering: The Method and Some Applications*, Kluwer Claredon press, Oxford 2011.
15. Holmes D. L., Stellwagen N. C.: Electrophoresis 1, 5 (1990).
16. Sigma Aldrich: *Agarose – Product information,* Available from: https://www.sigmaaldrich.com, downloaded 2015-07-13.

SOLID – PHASE DNA EXTRACTION USING VARIOUS TYPES OF MAGNETIC MICROPARTICLES

JANA KONEČNÁ[a], ALENA ŠPANOVÁ[a], DANIEL HORÁK[b] and BOHUSLAV RITTICH[a]

[a]*Brno University of Technology, Faculty of Chemistry, Department of Food Chemistry and Biotechnology, Purkyňova 464/118, 612 00 Brno, Czech Republic*
[b]*Institute of Macromolecular Chemistry, Academy of Sciences of the Czech Republic, Heyrovský Sq. 2, CZ-162 06 Prague, Czech Republic*
xckonecnaj@fch.vutbr.cz

1. Introduction

The polymerase chain reaction (PCR) has become an essential and indispensable tool for biological research and laboratory diagnostic applications[1]. However, numerous substances have been demonstrated to inhibit PCR[2]. Although a wide range of inhibitors is reported, the mechanisms and ways of action of many remain unclear[3]. The inhibitors generally make cause at one or more essential ways: (1) interfere with the cell lysis, which influences DNA extraction; (2) interfere by nucleic acid degradation; (3) inhibit polymerase activity[3]. The problem of pure DNA (PCR-ready DNA) isolation can be resolved by means of various isolation and purification techniques.

Strategies based on solid phase systems have become popular for the isolation of various biomolecules of interest. Magnetic microparticles find practical use in effective isolation and purification of biomolecules such as enzymes, antibodies[4–6] and nucleic acids[7]. The main advantages of their use is high capacity and simple separation from complex food samples containing PCR inhibitors[7]. The most obvious and common strategy is the functionalisation of particle surfaces with positively charged organic molecules which increase the electrostatic affinity for the phosphate backbone of DNA (which is negatively charged). The use of amino groups ($-NH_2$), which provide cationic surface charge, is mostly preferred for nucleic acid extraction and purification[7].

The aim of this work was to evaluate two different types of magnetic particles with $-NH_2$ groups for solid – phase DNA isolation. First type of magnetic microparticles were P(HEMA-GMA)-NH_2 microspheres; second type were poly (L-lysine) (PLL) modified iron oxide nanoparticles (F79/L3-PLL). Quality of extracted DNA was checked spectrophotometrically and by PCR .

2. Materials and methods

2.1. Chemicals

DNA from chicken erythrocytes was from Reanal (Budapest, Hungary) and DNA isolated from bacterial cells of *Lactobacillus gasseri* K7 from Collection of microorganisms, Chair of Dairy Science, Biotechnical Faculty, University of Ljubljana, Slovenia. Probiotic food supplement Linex® Forte was produced by Sandoz (Prague, Czech Republic). Agarose was purchased from Top-Bio (Prague, Czech Republic), ethidium bromide from Sigma (St. Louis, USA). The PCR primers were synthesized by Generi Biotech (Hradec Králové, Czech Republic), Taq1.1. polymerase was from Top-Bio (Prague, Czech Republic). The DNA marker (100 bp ladder) for gel electrophoresis was from Malamité (Moravské Prusy, Czech Republic). Magnetic P(HEMA-GMA)-NH_2 and poly (L-lysine) (PLL) modified iron oxide nanoparticles were prepared using methods published earlier[5, 8]. Specification of magnetic particles are shown in Table 1. The other common chemicals and solvents were of analytical grade.

Table 1
Specification of magnetic microparticles

Magnetic particles	Fe (%)	Dn	-NH_2 (mmol/g)	PDI
P(HEMA–co-GMA)-NH_2	6.5	1.27 µm	1.79	1.04
F79/L3-PLL	69.8	6.2 nm	0.28.	1.37

D_n - number average particle diameter, PDI-polydispersity index (ratio of weight- to number-average particle diameter)

2.2. Equipment

Spectrophotometric measurements of DNA were carried out on a UV spectrophotometer NanoDrop ND-2000/2000c (Thermo Scientific, Wilmington, USA). Magnetic particles were separated using an InvitrogenTM magnetic particle concentrator (Invitrogen Dynal AS, Oslo, Norway). The DNA in PCR mixtures was amplified in an Termocycler PTC-200 (BIO-RAD Laboratories, Richmond, USA). Agarose gel electrophoresis was carried out using equipment for electrophoresis Owl Easy-cast, model B1 (Thermo Scientific, Wilmington, USA), source voltage Enduro Power supplies, model E0303 (Labnet International, New York, USA). PCR products were visualised on a UV transilluminator TVR 3121 (Spectroline, Paramount, USA).

2.3. Methods

2.3.1. Preparation of crude cell lysates

Content of 1 capsule of food supplement Linex® Forte or cells from 1 ml culture were washed and resuspended in 1.5 ml of lysis buffer (10 mM Tris–HCl, pH 7.8, 5 mM EDTA, pH 8.0, lysozyme 3 mg/ml) for 1 hour. Crude cell lysates were prepared using 12.5 µl of 20% SDS, 10 µl of proteinase K (1 mg/ml) and incubation at 55 °C over night.

2.3.2. DNA reversible adsorption

DNA from chicken erythrocytes was used for method optimalisation before bacterial DNA isolation from Linex® Forte. The amounts of DNA in separation mixtures were measured by UV-VIS spectrophotometry. Separation mixture (100 µl) was prepared by mixing the following ingredients: 30 µl DNA (10 µg/ml), 20 µl phosphate buffer and 50 µl of magnetic microparticles (2 mg/ml). Phosphate buffer (0.067 mol/l KH_2PO_4, 0.067 mol/l $Na_2HPO_4.2H_2O$) of three different pH values (7.0, 7.6, 8.0) was used.

The particles with adsorbed DNA were rinsed twice by 300 µl of 70% ethanol and carefully dried before its elution.

2.3.3. DNA elution from the magnetic particle surfaces

DNA was eluted from magnetic particles with 100 µl TE buffer (10 mM Tris-HCl, pH 7.8; 1 mM EDTA, pH 8.0; end pH value 9.0 or 10.0). Elution buffer was also modified by adding of NaCl (end concentration 1 mM) or KCl (10 mM).

The elution of DNA was performed at various temperatures (23, 55, 70 and 90 °C) and various times (10, 30, 60 min, 18 h). The concentration of DNA was measured spectrophotometrically.

2.3.4. PCR amplification and detection of PCR products

Bacterial DNA eluted from magnetic microparticles was used as DNA matrix in PCR. PCR was performed using F eub a R eub primers specific to the domain *Bacteria*[9], which enabled the amplification of 466 bp long DNA fragment. Typically, the PCR mixture contained 1 µl of each 10 mM dNTP, 1 µl (10 pmol/µl) of each primer, 1 µl of DNA matrix, and 1 µl of Taq 1.1 polymerase (1 U/µl), 2.5 µl of buffer, and PCR water was added to a 25 µl volume. After 5 min of the initial denaturation period at 94 °C, amplification was carried out in 30 cycles of 30 s at 94 °C; 30 s at 55 °C, and 60 s at 72 °C. In the last cycle, the elongation step at 72 °C was prolonged to 10 min. PCR products were separated using agarose gel electrophoresis on 1.5% agarose gel in TBE buffer (45 mM boric acid, 45 mM Tris–base, 1 mM EDTA, pH 8.0). DNA was stained using ethidium bromide (0.5 µg/ml).

3. Results and discussion

The effect of pH on the quantity of DNA adsorbedon F79/L3-PLL nanoparticles is shown in Fig. 1. Tested values of pH have no effects on DNA adsorption. The higher amounts of DNA were eluted with TE buffer (pH 9.0), added KCl and heated to 90 °C. Results indicate that about 50 % DNA remain adsorbed on magnetic particles. Both types of tested magnetic particles showed similar behaviour during the isolation of DNA from chicken erythrocytes, bacterial DNA and DNA from real product.

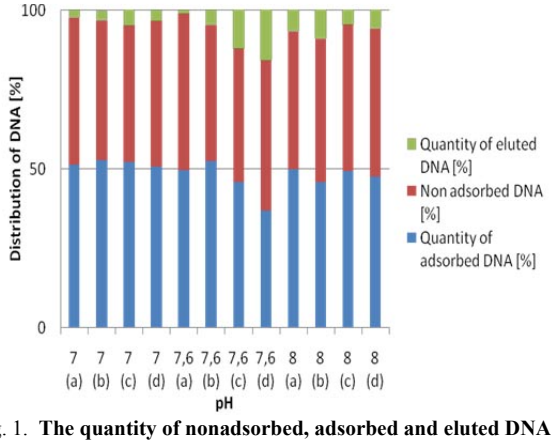

Fig. 1. **The quantity of nonadsorbed, adsorbed and eluted DNA** (chicken erythrocytes) **using separation mixtures with different pH values. Elution was carried out by TE buffer (ph 9.0) at 10 (a), 30 (b), 60 min (c) and 18 h (d)**

The presence of PCR inhibitors is an important problem in PCR identification of bacterial cells in real specimens[10]. DNA isolated from probiotic food supplement Linex® Forte was used for verification of DNA isolation method. Magnetic nanoparticles modified by poly (L-lysine) (F79/L3-PLL) were used for this purpose. The example of amplification of DNA isolated from probiotic food supplement is given in Fig. 2. Specific PCR products for domain Bacteria (466 bp) were detected.

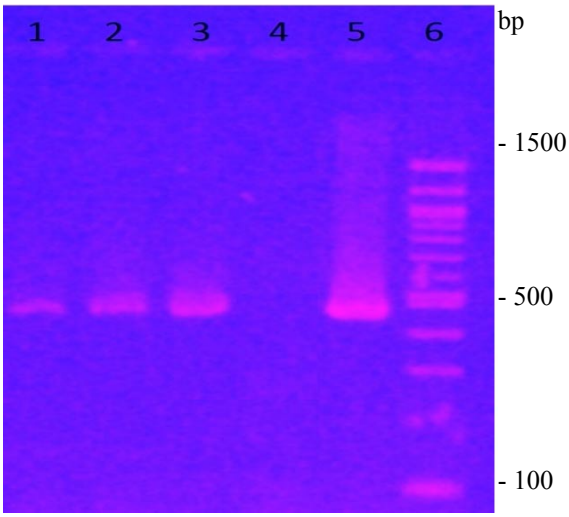

Fig. 2. **Agarose gel electrophoresis of PCR products obtained after amplification of DNA isolated from probiotic food supplement Linex® Forte using magnetic nanoparticles F79/L3-PLL.** Lanes 1–3: DNA isolated from Linex® Forte; lane 4: negative control; lane 5: positive control DNA (*L. gasseri K7)*; lane 6: DNA standard (100–1500 bp)

4. Conclusion

It was shown that the DNAs isolated from bacterial cells and food supplement using tested magnetic particles were in PCR-ready quality and could be used for conventional PCR applications.

The financial support of internal grant FCH-S-15-2827 is gratefully acknowledged.

REFERENCES

1. Rudi K., Kroken M., Dahlberg O. J., Deggerdal A., Jakobsen K. S., Larsen F.: Biotech. 22: 506–511 (1997).
2. Kemp B. M., Monroe C., Smith D. G.: Journal of Archaeological Science. 33: 1680–1689 (2006).
3. Wilson I. G.: Appl. Environ. Microbiol. 10: 3741–3751 (1997).
4. Bayramoglu G., Biritim V., Tunali Y., Arica M. Y., Akcali K. C.: Mat. Sci. Eng. C 33: 801–810 (2013).
5. Babič M., Horák D., Trchová M., Jendelová P., Glogarová K., Lesná P., Herynek V., Hájek M., Syková E.: Bioconjugate Chem. 19*:* 740–750 *(*2008).
6. Horák D., Kučerová J., Korecká L., Jankovičová B., Palarčík J., Mikulášek P., Bílková Z.: Macromol. Biosci.

12: 647–655 (2012).
7. Rittich B., Španová A. J. Sep. Sci. *36*: 2472-2485 (2013).
8. Horák, D., Španová, A., Tvrdíková, J., Rittich, B. Eur. Polym. J. *47*: 1090–1096 (2011).
9. Haarman, M., Knol J.: Appl. Environ. Microbiol. *72*: 2359 (2006).
10. Prodělalová J., Rittich B., Španová A., Petrová K., Beneš M. J.: J. Chromatogr. A 1056: 43–48 (2004).

IMPACT OF DIFFERENT PROCESSING ATMOSPHERES ON THE VOLATILES OF ORANGE JUICE WITH PULP

MÁRIA KOPUNCOVÁ[a, b], EMIL KOLEK[a] and JANA[a] SÁDECKÁ

[a]*National Agricultural and Food Centre, Food Research Institute, Department of Chemistry and Food Analysis, Priemyselná 4, 824 75 Bratislava, Slovak Republic*
[b]*Comenius University, Faculty of Natural Science, Chemical Institute, Mlynská dolina, Ilkovičova 6, 842 15 Bratislava, Slovak Republic*
kopuncova@vup.sk

Abstract

The effectiveness of three different processing atmospheres to preserve the volatiles of orange juice with pulp during its shelf life was investigated over two years. Application of conventional "air", and nitrogen atmosphere was evaluated in 2014; use of two inert gases, nitrogen and carbon dioxide, was monitored in 2015. Headspace-solid phase microextraction (HS-SPME), gas chromatography-mass spectrometry (GC-MS) and gas chromatography coupled to flame ionization detection and olfactometry (GC/FID-O) were used for extraction, and subsequently for analysis and identification of the volatile fraction composition. Results demonstrated that production of juices under inert atmosphere (nitrogen or carbon dioxide) can protect their standard organoleptic quality from changes caused by oxidative load or acid-catalysed reactions during storage.

Key words

Gas chromatography, inert atmosphere, orange juice, storage, volatiles

Introduction

Due to its pleasant aroma and nutritional value, orange juice is the most popular among the commercially manufactured fruit juices. The flavour of fresh hand-squeezed orange juice is generally considered as the most attractive and is used as a reference against which all juices are judged[1, 2]. However, different stages of industrial processing result in some alterations in original fresh juice aroma[1–4]. In addition, undesirable changes in juice composition can occur during its storage in retail chain[4–7]. Therefore, optimization of production and packaging process is necessary for the maintaining of high quality of the final product during its shelf life that can be up to several months.

Numerous studies were focused on the influence of temperature, time, oxygen content, light exposure and packaging material on organoleptic quality of orange juice[4–7]. At the same time, several compounds were found as important contributors to orange juice off-flavours formed during storage, which have been described as "aged" or "heated"[4].

The aromatic profile of orange juice can be modified by the formation of new compounds, through oxidation or acid-catalyzed reactions. Combined with other factors, as light or temperature, mainly oxygen strongly affects these reactions[5]. One potential way how to reduce the oxidative degradation of orange juice during storage can be its production under inert atmosphere. Thus, the aim of this paper is to evaluate the influence of the nitrogen and carbon dioxide application in production of orange juice with pulp on its key aroma compounds during 4-month shelf life.

Materials and methods

Samples of orange juice enriched with pulp were obtained from McCarter Ltd., Bratislava (production premises Dunajská Streda), Slovakia. This company imports raw unconcentrated juice in frozen state from country of origin, in this case Costa Rica. After unfreezing, juice is enriched with pulp, mixed, pasteurized at up to 95 °C during 20 seconds and filled aseptically into PET bottles.

First year (2014), one series of samples from the same batch of raw juice was produced under nitrogen atmosphere, and the second one by traditional technology in conventional "air" atmosphere. In the second year (2015), one series of samples was processed under nitrogen, and the second one under carbon dioxide atmosphere. Bottled samples were stored at 7 ± 1 °C during 4 months – that is the shelf life of the product declared by the producer. Analyses were performed on a monthly basis.

Extraction of volatiles was carried out by HS-SPME. Extracted mixtures of volatiles were separated and analysed by GC-MS, and parallel by the technique of GC/FID-O. Detailed conditions of extraction and analyses were described previously by Sádecká et al.[7]

Volatile compounds were identified on the basis of comparison of their mass spectra, linear retention indices, GC analysis of standards, and by comparison of data on occurrence and odour description with literature[3, 7, 8]. Linear retention indices (LRI) for individual compounds were calculated, confirmed and compared with LRI data obtained by measurements of standard substances and using C_7–C_{14} alkanes as reference standards according to Van den Dool and Kratz[9]. For this purpose, our in-house database of LRI data was used. Identification of compounds by comparison of mass spectra was done using Wiley and NIST MS libraries (National Institute of Standards and Technology, Gaithersburg, Maryland, USA). All chemicals used as reference standards for identification purposes of volatiles were donated from Bedoukian Research (Danbury, Connecticut, USA).

Relative content of individual compounds found by GC-MS was calculated by the method of internal normalization and expressed as percentage. Results of GC-O analyses were expressed as the average values of odour intensities in a scale from 0 to 3 with increments of 0.5 obtained from 3 independent measurements. The value of ± 0.5 was considered as measurement deviation.

Results and discussion

As it was described above, two series of orange juices with pulp were analysed in 2014 (conventional „air" and nitrogen atmosphere) and two series in 2015 (nitrogen and carbon dioxide atmosphere). This approach was chosen because production company introduced the new technology

including inert gas application step by step during two years and thus, it was not able to produce juices from the same batch of raw juice under three different atmospheres at the same time. Therefore, impact of the year of production on the quality of provided samples was significant, despite the fact that country of origin (Costa Rica) remained the same in both years.

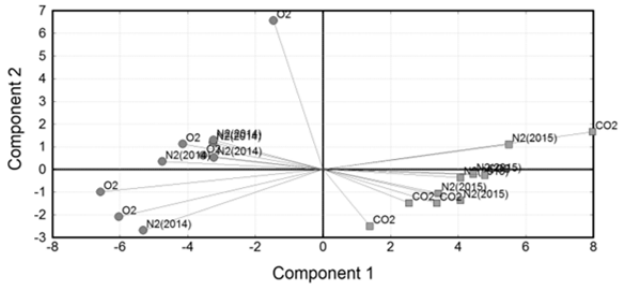

Fig. 1. **Plot of principal components demonstrating differentiation of orange juices with pulp processed under conventional "air" (O_2) and nitrogen atmosphere (N_2(2014)) in 2014, and under carbon dioxide (CO_2) and nitrogen atmosphere (N_2(2015)) in 2015 constructed on the basis of the relative contents of individual volatile compounds obtained by the GC-MS**

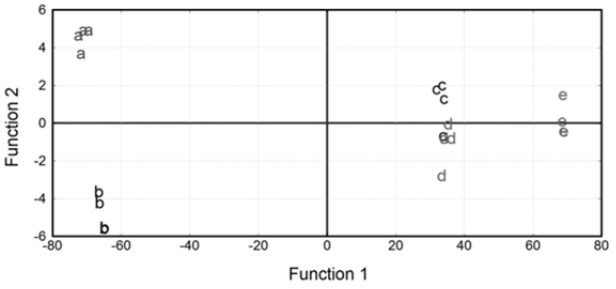

Fig. 2. **Discrimination of orange juice samples, irrespective of used production atmosphere, using the time of storage (0 up to 4 months) as discriminating criterion; a – fresh samples (0 month), b, c, d, e – samples stored for 1 up to 4 months. Plot of discriminant functions was constructed on the basis of the relative contents of individual volatile compounds obtained by the GC-MS**

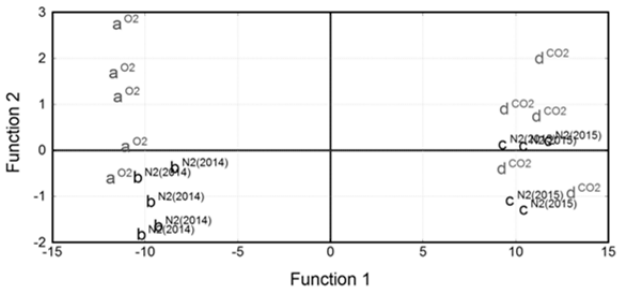

Fig. 3. **Discrimination of orange juice samples using the production atmosphere as discriminating criterion; a^{O2} – conventional "air" atmosphere, $b^{N2(2014)}$ – nitrogen atmosphere, year of production 2014, $c^{N2(2015)}$ – nitrogen atmosphere, year of production 2015, d^{CO2} – carbon dioxide atmosphere. Plot of discriminant functions was constructed on the basis of the relative contents of individual volatile compounds obtained by the GC-MS**

Regardless of used atmosphere, orange juice produced in 2015 had richer aroma. Total 54 compounds were identified in its volatile fraction in contrast with 32 volatiles identified in orange juice produced in 2014. In addition, differences in relative content of some compounds were observed. Significant variability between the two years is obvious from principal components analysis (PCA). Plot of principal components (Fig. 1) clearly indicates the existence of 2 differentiated groups of eigenvectors belonging to the samples from year 2014 and 2015.

Anova Tukey's HSD analysis of the GC-MS data confirmed the effects of storage on compositional changes of orange juices for all of the four sets of samples (three atmospheres). As regards concentration changes, the differences between fresh samples and samples stored for three and four months were found to be statistically significant ($p < 0.05$) for 14 compounds, namely ethyl butanoate, α-pinene + benzaldehyde, octanal + β-myrcene, p-cymene, D-limonene, 1-octanol, p-cymenene, nonanal, decanal, octyl acetate, carvone and perillaldehyde. Subsequent differentiation of samples according to the storage time by canonical discriminant analysis (CDA) classified samples into groups on the basis of compositional analysis with 100% correctness. As it can be seen from the plot of discriminant functions (Fig. 2), changes in orange juice composition occurred already in the first month of storage and continued during the entire monitored period. The discriminant scores of individual groups were different and, as a result, the existence of five groups of points belonging to the samples stored for four months is obvious from the plot of discriminant functions.

In the next step, differentiation of samples according to used production atmosphere was proved. Once again, CDA showed strong relationship between the composition of orange juice and year of its production. It is evident from the plot of discriminant functions (Fig. 3) where two opposite groups were formed belonging to the samples produced in 2014 and 2015. Nevertheless, within the samples from 2014, two smaller groups belonging to the samples produced under conventional and respectively nitrogen atmosphere, were separated. It indicates that use of these two atmospheres had different effect on the composition of orange juice volatiles. On the contrary, samples produced under nitrogen and carbon dioxide atmosphere in 2015 were not separated, suggesting that juices produced under nitrogen were closer to the juices produced under carbon dioxide by their properties. Moreover, correctness of classification into groups on the basis of compositional analysis for samples produced under carbon dioxide atmosphere was only 60 %. Thus, use of nitrogen or carbon dioxide as production atmospheres seems to have very similar effect on volatiles of orange juice during storage.

Observed worsening of organoleptic properties of juices produced in conventional atmosphere, and on the contrary, stable sensory character of juices produced under nitrogen or carbon dioxide during entire monitored period correlated with above mentioned results and indicated that application of inert gases could have protective effect on the flavour of orange juice with pulp.

In order to identify potential off-flavour compounds responsible for the negative changes in flavour of juices

processed in conventional atmosphere, all samples were analysed also by GC/FID-O.

On the basis of GC-MS analyses, mainly terpenic alcohols α-terpineol and terpinen-4-ol were supposed to be off-flavours, because of their significant increase only in conventional atmosphere. These compounds are degradation products of limonene and linalool, and as it was reported in several studies[4–6], α-terpineol was previously described as an off-flavour in stored orange juice. However, despite its higher relative content, α-terpineol was not detected by GC/FID-O. It implies that its respective concentration level did not achieve nasal odour threshold and its role as off-flavour in orange juice was not confirmed in our study. As regard terpinen-4-ol (with musty, waxy, earthy, woody odour description), it was sensorially active, but with the same odour intensity in all investigated atmospheres and no increasing trend was observed for this compound during storage. Similarly, α-terpinolene (mushroom, plastic odour) was detected in all samples, but its odour intensity was stable during storage irrespective of used atmosphere.

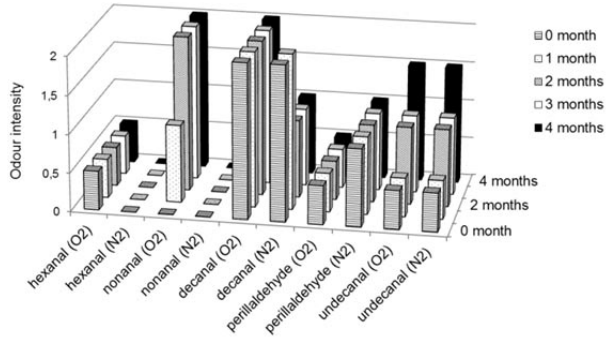

Fig. 4. **Changes in odour intensities of some aldehydes occurred during 4-month storage of orange juices with pulp produced under nitrogen (N_2) or conventional "air" atmosphere (O_2)**

Concerning the other compounds, considered as typical off-flavours, furaldehyde, which is created as degradation product of ascorbic acid[5] was detected by the GC-MS in our study, but its relative content was very low and it was not detected by olfactory perception. On the contrary, hexanal (green, nutty and bitter odour), and also nonanal (soapy, waxy, tallow-like odour) were detected by GC-O only in samples produced in conventional atmosphere. Perillaldehyde (smoked, cumin, spicy odour) was noticed in both atmospheres, but in conventional atmosphere showed higher odour intensity. Intensity of decanal (orange peel-like, waxy odour) dropped in nitrogen atmosphere, whereas in conventional atmosphere was stable. Only undecanal (fatty, citrus, aldehydic, waxy odour) showed increasing trend in both atmospheres. Differences in odour intensities of some aldehydes related to used atmosphere (Fig. 4) could explain increase of bitter and astringent taste along with certain loss of freshness and fruity sweetness which was observed for juices processed by traditional technology.

Conclusions

Statistical processing of GC-MS data proved that use of nitrogen atmosphere in the production of orange juice had different effect on the composition of its volatile fraction during 4-month storage than technological processing of the identical juice in the conventional "air" atmosphere. Effectiveness of the application of carbon dioxide as inert atmosphere was comparable with nitrogen but its acceptability by consumers have to be considered because of the sparkling character of final products.

None of investigated inert atmospheres was able to avoid all changes in the composition of volatiles during 4-month storage. However, parallel GC/FID-O analyses proved that these changes were not sensorially significant and they did not lead to the worsening of organoleptic properties of juices. On the contrary, negative sensory changes in flavour were observed for juices processed in conventional atmosphere. GC/FID-O analyses revealed that generation of some aldehydes could be responsible for the off-flavour phenomenon occurred during storage.

This work is a partial study of the research project "Improvement of nutritional and sensorial parameters of fruity and vegetable drinks via an inert gas application" – ITMS26220220175 supported by the Research and Development Operational Programme funded by the ERDF. *McCarter Ltd., Bratislava (production premises Dunajská Streda), Slovakia, is gratefully acknowledged for player friendly cooperation and samples provision.*

REFERENCES

1. Seideneck R., Schieberle P.: Eur. Food Res. Technol. *232*, 6 (2011).
2. Brat P., Rega B., Alter P., Reynes M., Brillouet J. M.: J. Agric. Food Chem. *51*, 11 (2003).
3. Averbeck M., Schieberle P.: Eur. Food Res. Technol. *229*, 4 (2009).
4. Averbeck M., Schieberle P.: Eur. Food Res. Technol. *232*, 1 (2011).
5. Bacigalupi C., Lemaistre M. H., Boutroy N., Bunel Ch., Peyron S., Guillard V., Chalier P.: Food Chem. *141*, 4 (2013).
6. Berlinet C., Brat P., Brillouet J.-M., Ducruet V.: J. Sci. Food Agric. *86*, 13 (2006).
7. Sádecká J., Polovka M., Kolek E., Belajová E., Tobolková B., Daško L., Durec J.: J. Food Nutr. Res. *53*, 4 (2014).
8. Cerdán-Calero M., Sendra J. M., Sentandreu E.: J. Chromatogr. A. *1241* (2014).
9. Van den Dool H., Kratz P.: J. Chromatogr. *11* (1963).

SUPERABSORBENT POLYMERS AND THEIR EFFECT ON SOIL WATER RETENTION

ROMANA KRATOCHVILOVA*, MARTINA KLUCAKOVA, PETR SEDLACEK, MARCELA LASTUVKOVA and MICHAL KALINA

Brno University of Technology, Faculty of Chemistry, Materials Research Centre, Purkyňova 118, 612 00 Brno, Czech Republic
**xckolajova@fch.vutbr.cz*

Abstract

Agricultural land is in a very bad condition in the Czech Republic nowadays. There is a problem of pollution caused by previous synthetic fertilizing. The land lost its natural property of water controlling. Rain has rather devastating than beneficial effect for the ground. Artificially applied nutrients are often flushed away and only a bit of them is transported to the targeted location. Solution of these problems can be found in application of natural fertilizer in form of hydrogel matrix. Superabsorbent polymers were used for this purpose in this work. The aim of this work is to develop superabsorbent polymer with incorporated fertilizer in its structure and confirm its ability to enable controlled release of fertilizer from hydrogel matrix. This system should also provide enhancement of natural ground humidity. Water retention tests were then also carried out. Several different samples of superabsorbent polymers based on acrylic acid were observed during our research. They differed in a basic composition of superabsorbent and mainly in a type of fertilizer. Common synthetic NPK fertilizer was used as natural lignohumate fertilizer as well. The role of dosage of these components was also studied. This work proves that novel form of agricultural preparation was developed. The superabsorbent polymer allows controlled release of variety fertilizers. Its role as the water reservoir system was proved as well. The usage of superabsorbent polymers in agriculture can have a very positive effect on crop yield.

Introduction

Many researchers are trying to solve the problem with continuous increasing degradation of agricultural lands. The ground is still more and more devastated mainly because of its wasteful cultivation and excessive fertilization. These facts have big impact on the loss of soil organic matter (SOM). The solution of these problems can be found in application of humic substances which constitute the most ubiquitous source of SOM in nature[1]. They have important role in soil fertility such as stimulating plant growth, enhancing the resistance of crops, improving soil structure and increasing soil retention of water and fertilizer[2].

Superabsorbent polymers (SAPs) are loosely crosslinked, three dimensional networks of flexible polymer chains that carry dissociated, ionic groups which cause their ability to absorb large quantities of water and other aqueous solutions without dissolving by solvation of water molecules via hydrogel bonds.

SAPs have wide range of usage. In the field of agriculture and environmental protection they are very often used as a water hanger during a dry season nowadays. In contrary they avoid to decay of plants' root system in the time of heavy rains. There is a new trend in a field of superabsorbent polymers and it is an incorporation of fertilizers into the gel structure. This can be consider as a functional system which allows controlled release of substances that support growing and maturing of plants. Such mechanism solves the problem with flushing of fertilizers into deep underground water and avoids to overferilize of ground as well[3, 4].

Experimental

Materials and method

Six different samples (A–F) were used in this work. All of them have a certain addition of NPK fertilizer. Some of them have an addition of humic substance (lignohumate) and they differ in a content of acrylamide in their structure as well.

Accurate representation of these selected substances can be found in Table 1.

Table 1
Composition of used samples

sample	A	B	C	D	E	F
NPK [%]	1	10	1	10	1	10
lignohumate	no	no	yes	yes	yes	yes
acrylamide	yes	yes	no	no	yes	yes

These samples were prepared in cooperation with company of Amagro s.r.o. company and their composition will not be more detailed specified because of intellectual property protection.

Measurements of water absorbency were carried out very easily. Samples (0.05 g) was immersed in excess distilled water (200 ml) at room temperature for 12 hours to reach swelling equilibrium. Swollen samples were then separated from unabsorbed water. Water absorbency in distilled water of the superabsorbent composite, Q, was calculated using the equation $Q = (m - m_0)/ m_0$, where m_0 and m are the weights of the dry sample and the swollen sample, respectively. Q is calculated as grams of water per gram of sample.

The mechanisms of potassium release from hydrogel carriers were observed in an environment of demineralized water for five days. Total content of potassium was determined by ICP – OES technology every 24 hours.

The artificial soil was prepared by mixing of fain grain peat free of visible debris (10 %) with kaolin of kaolinite concentration at least 30 % (20 %) and with main proportion of silica sand (70 %).

The water retention capacity (WRC) of artificial soil enriched by 1 % amount of SAP has been determined from long-term observation and compared with a WRC of pure artificial soil.

Results

Swelling behaviour of all SAP samples was determined due to measurement of water absorbency. The measurement of their water absorbency showed that all samples exhibit very good swelling properties, as it is displayed on Fig 1. Results showed very interesting findings. The samples differed from each other by special composition that is shown in Table 1. There is significant negative effect on SAP swelling properties caused by higher content of NPK in the structure of sample. These samples B, D and F reflect much lower ability to absorb surrounding water and they were not treated under the next procedure because of mentioned reasons. Samples with addition of lignohumate swelled significantly better than samples without lignohumate. That is caused by hydrophilic character of lignohumate.

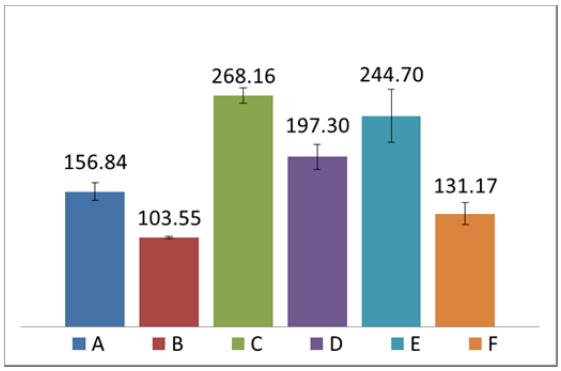

Fig. 1. **Water absorbency of SAP samples**

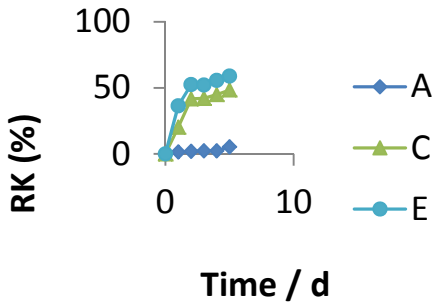

Fig. 2. **Release curve of potassium in SAP in water**

The experimental result for potassium release in the SAP was shown in Fig. 2. Sample A released potassium less than other two samples because of absence lignohumate which bounded molecules of NPK and improve their release make them release better. As is shown there, sample C and sample E behaved very similar, that's caused by their composition. They both contain lignohumate addition. The potassium released out in the period of first two days mainly existed in the SAP surface layer, because it would go into water without diffusing as soon as it was dissolved, so the release rate was fast. During time, the released phosphate was mainly incorporated inside of the SAP sample, because it not only needs to be dissolve but also to diffuse out of sample before it went into water, so the release rate was slow.

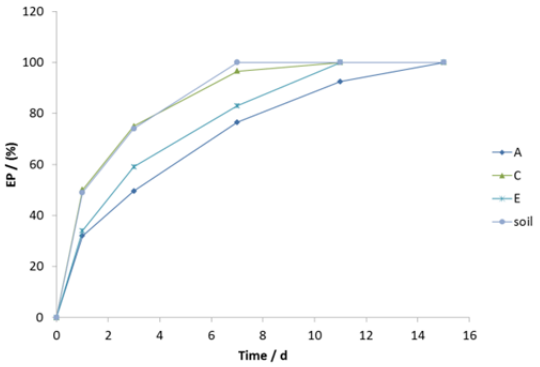

Fig. 3. **Water retention curve of SAP samples (A, C, E) – water + sample SAP + dry soil; (soil) water + dry soil**

The experimental result of water retention was shown in Fig. 3, where it could be found out that the water evaporation rate decreased after the addition of SAP in the soil. This is caused by excellent water absorbency of the SAP samples, so the water evaporation rate decreased. The slowest evaporation is displayed by the sample A which differed from other samples by absence of lignohumate. It is important to say that sampe A exhibits the slowest evaporation even though it has the lowest water absorbency capacity.

Sample C is not very good water hanger in the soil due to Fig. 3. The quick decrease of water content in the system soil – SAP – water can be caused by acrylamide – free SAP sensitivity on salinity which can be presented in the soil.

Conclusion

Novel superabsorbent composites for agricultural and environmental usage were investigated. There were several samples with various composition compared. The result of our experiments showed that we are able to prepare SAP polymers of various swelling behaviour, of specific releasing abilities and of varied absorbing capacity. From these findings result that we are able to prepare such products, which are their properties accurately meet with the needs of the certain plant.

This work has been supported by Materials Research Centre at Faculty of Chemistry, Brno University of Technology – Sustainability and Development, REG Lo1211, with financial support from National Program for Sustainability I (Ministry of Education, Youth and Sports, Czech Republic).

REFERENCES

1. Piccolo A. and Mbagwu H. S. C.: Agro Food Ind. Hi Tech. *8*, 2–4 (1997).
2. Lal R.: Science. *304*, 1623–1627 (2004).
3. Davidson D., Gu F. X. and Wilkins R. M.: J. Agric. Food Chem. *60*, 343–356 (2012)
4. Liu G., Zotarelli L., Li Y., Dinkins D., Wang Q. and Ozores-Hampton M.: Research report HS1255, Horticultural Sciences Department, UF/IFAS Extension, Florida 2014.

MORPHOLOGY OF PLANT CUTICLES AS THE LIMITING BARRIER FOR THE UPTAKE FERTILIZERS

MARCELA LASTUVKOVA[a,*], IRENA TURKEOVA[a], JIRI SMILEK[a], PETR SEDLACEK[a], ROMANA KRATOCHVILOVA[a], VERONIKA SCHMIEDOVA[a] and MARTINA KLUCAKOVA[a]

[a]*Brno University of Technology, Faculty of Chemistry, Materials Research Centre, Purkyňova 118, 612 00 Brno, Czech Republic*
**xclastuvkova@fch.vutbr.cz*

Abstract

The uptake of pesticides into plant foliage varies with plants and chemicals are based on adjuvants and environmental conditions. The penetration of nutrients into plant leaves relates to the physicochemical properties of the active ingredients (molecular size and lipophilicity). For the penetration studies of active ingredients thin layers – cuticles are usually used. These barriers are isolated by specialized methods (enzymatically and chemically) and itself can be used for evaluating the leaves surface permeability. However, the uptake rate of a compound or function can be influenced by isolation methods. During the isolation process the structure of the cuticles or the function of stomata in the cuticles can be changed.

The cuticles were characterized by Fluorescence Lifetime Imaging Microscopy (FLIM) and Isothermal Microcalorimetry (IMC). These methods enable to study the binding and interaction of the compounds with the cuticles surface. Optical Microscopy (OM) was used for the inner state structure of the cuticles and their changes involved by effect of water, air or potassium lignohumate (LHA). The change of the inner structure was studied by Fluorescence Microscopy (FM), because the cuticles are able to excite at different wavelength. The thicknesses of the cuticles were measured by Profilometer.

The knowledge obtained from this work is very important for the following research aimed on the improving of the foliar uptake and the problem with nutrients overloading in soil and degradation not only soil, but ground water as well.

Introduction

Despite the negative perception of the community, pesticides are still going to be used for many decades to ensure the food supply for the ever growing world population. One of the most important ways how to improve the efficiency of pesticides and minimize their impact on off-target living systems is through increasing the penetration of active ingredients into plant foliage[1].

The absorption of minerals by leaves of plants was demonstrated experimentally 100 years ago[2, 3]. The numerous works studied the uptake of mineral ions, fungicides, pesticides, etc. Root absorptions of nutrients were replaced by foliar fertilizers, which became the new method of absorption of the plant beneficial substances. Absorption by living folic cells of any foliar applied chemical (mineral nutrients, growth regulators, pesticides, antibiotics) must be proceeding by transcuticular penetration[4].

For these studies they use top and/or bottom part from the plant leaves – cuticles. It is the first barrier with many important functions (respiration, regulation of water, regulation of ions, penetration of nutrients, etc.). The permeability of the cuticle membrane for ions, herbicides, and pesticides has been discussed in several papers[5–7]. The foliar uptake of active ingredients is a complex process and depends on the leaf surface of plant, physicochemical properties of the chemicals structure or properties of cuticles[1]. An important role for the nutrient absorption plays the concentration of the additives as well as the environmental conditions. Wang and Liu[1] summarized the major progress of the foliar fertilization especially during the last 15 years. They wanted to clarify the pesticide uptake into plant foliage and influence of adjuvants[1].

The cuticles were obtained by two isolation methods – chemical and enzymatic methods. Enzymatically isolation methods (EIM) were demonstrated by Chayen[8] and Hohl[9], who used pectin enzymes as the macerating agents in anatomical and cytological studies. Orgel[10] tried to develop a simplified cuticle isolation procedure, which is based on the usage of commercially available pectin enzymes. Chemically isolation methods (CHIM) were demonstrated by Holloway and Baker[11], who used zinc chloride-hydrochloric acid solution. Edgington[12] was inspirited by this isolation method and he used isolated cuticles for his transcuticular movement of fungicides.

Our work is focused on the study of the cuticle morphology and their utilization for diffusion experiments. For these experiments, we used leaves of *Prunus laurocerasus*, which were characterized as strong and rigid. Results presented in this paper open the new view on the compounds penetration through plant cuticles and their usage for commercial application.

Experimental

Chemically isolation methods of cuticles

We stripped the rims from leaves of *Prunus laurocerasus* and prepared leaves were given into the square container with cover and volume 500 ml. These leaves were fixed by grid, to avoid floating to the surface of leaves. The fixed leaves were covered by 60 wt. % zinc chloride ($ZnCl_2$) dissolved in 35 wt. % hydrochloric acid (HCl). The container was covered, to avoid evaporation of solution and it was maintained at 25 °C. After 2 days leaves were transferred into the container with the distilled water for rinsing. After that cuticles were prepared for characterization.

Enzymatically isolation methods of cuticles

We stripped the rime from leaves of *Prunus laurocerasus* and prepared leaves were given into the container again. The leaves were fixed by grid, to avoid floating to the surface of leaves. This method is based on the 0.1 M citrate buffer solution by pH 3.5–4.5 and concentration of pectinase and cellulose enzymes was 5 wt. %. Then, sodium azide was added to the buffer solution in the container as disinfection agent. The container was covered, to avoid evaporation of solution and it

was maintained at 25 °C for 7 weeks. Then the cuticles were washed gently by distillated water. The cuticles were prepared for the characterization.

Measuring of Fluorescence Lifetime Imaging Microscopy

Isolated plant cuticles were cut on the squares (1.5 × 1.5 cm) and those were placed on microslides and they were covered by glass slide. Prepared samples were used for measuring by FLIM and the study of fluorescence lifetime groups present on plant cuticles. Cuticles were studied at different conditions – air, water and 0.5 wt. % LHA. Samples were measured at specified intervals – day after isolation, 1 to 3 days effect of LHA and after 11 days effect of LHA). This method was used for assessment of the stability of cuticles at different conditions and their abilities of interaction with LHA.

Measuring of Isothermal Microcalorimetry

Isolated plant cuticles were used for studies of interaction between substances (air, water and LHA) and cuticles. For these experiments, wet or dried cuticles were used. First experiment was based on fresh isolated cuticles, which were placed in ampoules with different conditions (air, water and 1 wt. % LHA). This experiment showed that cuticles and LHA interact together (pilot measurement).

The second experiment was based on dried cuticles, which were dried at 30 °C for 24 hours. These cuticles were placed in 4 ml measuring ampoules, which were filled with different concentrations of LHA solution (1 wt. %, 0.5 wt. % and 0.1 wt. %). The third experiment was based on study of clear condition. The ampoules contained water, 1 wt. % LHA and 0.5 wt. % LHA.

First two experiments served for studies of interactions between different conditions and wet/dried cuticles. The last experiment enables to clarify, that LHA is suitable matters for this research and where it has not impact on measurements. Experiments were performed measured at 25 °C.

Measuring of Optical and Fluorescence Microscopy

Optical microscopy is a simple technique for studying the structure of the thin layers for study of structure of thin layers and their partition on top and bottom cuticles. Optical microscopy enables the first observation of cuticle state and its conditions for the following experiments. The cuticles were placed on the microglass and they were covered by the microslide. The experiments were performed with fresh cuticles and cuticles, which were exposed to 0.5 wt. % solution of LHA for 1, 2, 3 and 11 days respectively.

The fluorescence microscopy is a method used for the study of cuticle structure. The important thing is that fluorescence of cuticles is spontaneous without usage of any common fluorescent. This characterization can be used for elementary research. Leaves used for diffusion processes cause changes of emission light by compounds present in cuticles and enable to determine depth of penetration of chosen materials.

Experiment for optical microscopy was based on the fresh isolated cuticles which they were exposed to water and air. For fluorescence microscopy we used the whole leaves which were placed in water solution 1 wt. % LHA.

Measuring of the thickness by profilometry

Profilometry is another method suitable for analyzation of morphology of leaf surface. This instrument enables to determine of thickness and surface profile of cuticles. Thickness of studied cuticles was determined by mechanical profilometer. Three isolated plant cuticles were placed on microglass and dried under laboratory temperature for 24 hours. It was prepared 4 microglasses (abaxial and adaxial) and for 2 isolated methods (enzymatically and chemically).

Results

Fluorescence Lifetime Imaging Microscopy

This method studied fluorescence lifetime of groups present on cuticles. From obtained data, the average values were determined for measured time and also the deviation. Graph (Fig. 1) shows stability of cuticles under air condition. They have the same behaviors after 11 days in the present environment. This is very important fact for further experiments.

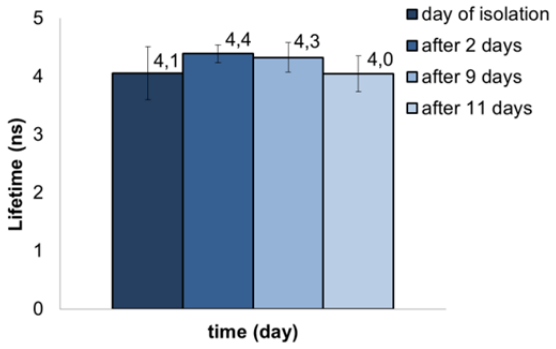

Fig. 1. **Lifetime of fluorescence groups under air condition**

Water is a natural environment for the cuticles, but we would like to know, how isolated cuticles behave under this condition and if there is no degradation in time or if there is any influence on properties of cuticles.

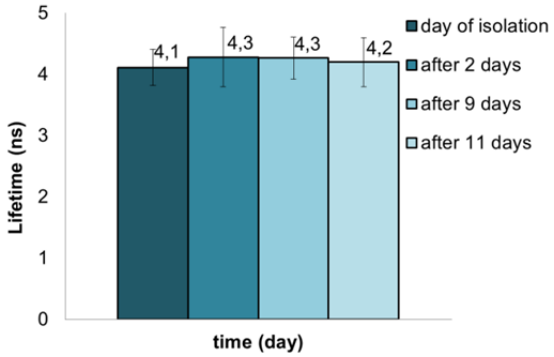

Fig. 2. **Lifetime of fluorescence groups in water condition**

From Fig. 2, it is obvious, that there is no change of fluorescent lifetime of cuticles in time. It can be seen that there is no degradation after 11 days and it is possible to use them for diffusion experiments. Moreover, we can show that the data

for air and water conditions are very similar, also cuticles are stable in this environment and we can use this material for the transport experiments.

The last graph (Fig. 3) shows cuticles under LHA conditions after 11 days. There is an exponential decrease of fluorescence lifetime. From data we can show exponential decrease of fluorescence lifetime groups in cuticles in measured time. From the graph is possible conclude the positive interaction between potassium lignohumate and cuticles. It is possible to conclude that there is interaction between K-LH and cuticles. The knowledge of fluorescence life time can help us to understand foliar uptake of fertilizers.

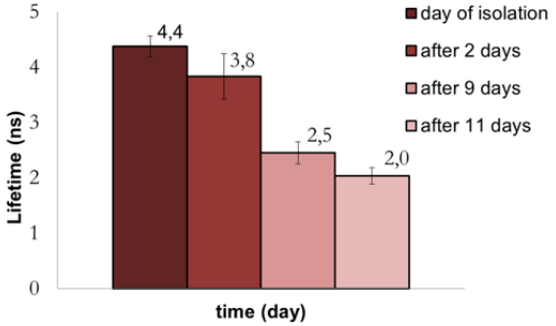

Fig. 3. **Lifetime of fluorescence groups in LHA condition**

Isothermal Microcalorimetry

This method serves as a comparison to FLIM measurement. The first measurement was the one, where cuticles with air and water do not react (constant line), but cuticles under 1 wt. % LHA condition showed increasing heat flow, also we can deduce specific interactions between the investigated maters. It brought the idea for further experiment (Fig. 4). The cuticles were put into the ampoules and the ampoules wee then filled with water and different LHA solutions (1, 0.1 and 0.05 wt. %).

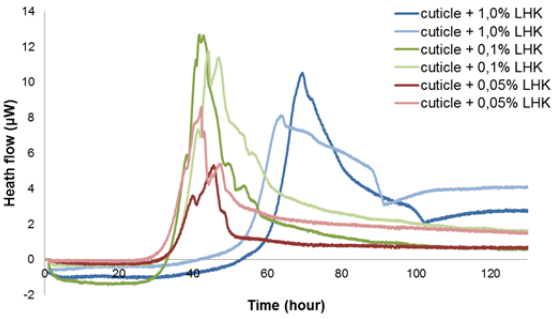

Fig. 4. **Isothermal microcalorimetry – cuticles and different concentration of LHA (1 wt. %, 0.1 wt. % and 0.05 wt. %)**

Moreover, the important finding is the time of the interaction, which it is in range 42 to 70 hours. This fact explained the ability of cuticles uptake.

Profilometer

The Thickness and the surface profile of the cuticles were studied by a mechanical profilometer. It was determined that the enzymatic and chemical isolated cuticles have the thickness about 9.8 ± 1.2 µm and the roughness of cuticles is 2.35 µm for both. It is caused by a very inhomogeneous surface.

Optical and Fluorescence Microscopy

The optical microscopy was used for assessment top or bottom cuticles (Fig. 5) and for studies of their structure or possible changes in the structure of cuticles by using LHA. For chemically isolated cuticles were made same images. Used method is not so useful for the determination of changes in structure of cuticles using LHA. Fluorescence microscopy enabled to establish spontanous fluorescence of cuticle or the whole leaves, which is possible by the nutrients uptake. Leaves were placed into the container with 1 wt. % LHA. From measuremnt were detected the fluorescence change on the cuticles in the time. Also, we can revealed, positive interaction between LHA and cuticles.

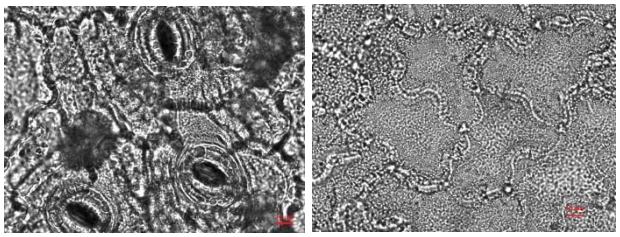

Fig. 5. **Bottom cuticle** (left) **and top cuticle** (right) **for EIC**

Conclusion

This work is focused on the morphology of the cuticles and their usage by foliar uptake. For this purpose, several methods were used. FLIM is the method, which it revealed establish LHA interactions with the cuticles. The results from FLIM measurements were correlated with the data obtained from microcalorimetry, which acknowledged the binding between the cuticles and LHA and moreover, it completed the start of substance penetration, which was used by diffusion experiments. For the first characterization optical and fluorescence microscopy were used. Optical microscopy is a suitable method for disaggregation the cuticles on top/bottom of leaves. Fluorescence microscopy was used for observation of the uptake of LHA and clarification of spontaneous fluorescence, which can be used in following experiments. The results obtained from this work will be used for future experiments, which focus on the plant uptake of nutrients.

This work has been supported by Materials Research Centre at Faculty of Chemistry, Brno University of Technology – Sustainability and Development, REG Lo1211, with financial support from National Program for Sustainability I (Ministry of Education, Youth and Sports, Czech Republic).

REFERENCES

1. Wang C. J., Liu Z. Q.: Pestc. Bio. And Physiol. *87*, 1–8 (2007).
2. Wittwer S. H., Teubner F. G.: Ann. Rev. Plant Physiol. *10*, 13–32 (1959).
3. Yamada Y., Wittwer S. H., Bukovac J.: Plant Physiol. *39*, 978–82 (1964).
4. Wittwer S. H.: Plant Sci. *8*, 161–82 (1964).
5. Okuda A., Yamada Y.: Proc. Japan Conf. on Radioisotopes *4,* 1083–90 (1962).
6. Schieferstein R. H., Loomis W. E.: Am. J. Botany *46*, 625–35 (1959).
7. Skoss J. D.: Botan. Gaz. *117*, 55–72 (1955).
8. Chayen J.: Nature *164*, 930 (1940).
9. Hohl L. A: Stain Technol. *23*, 129–131 (1948).
10. Orgel W. H.: Plant Physiol. *27*, 78–80 (1954).
11. Holloway P. J., Baker E. A.: Plant Physiol. *43*, 1878–1879 (1968).
12. Solel Z., Edgington L. V.: Phytopathology *63*, 505–510 (1972).

THE DEVELOPMENT OF VOLATILE FLAVOUR COMPOUNDS DURING RIPENING OF GOUDA CHEESE

MARTINA MAHDALOVÁ[a]*, EVA VÍTOVÁ[a], HANA RYGLOVÁ[a], KATEŘINA SŮKALOVÁ[a] and FRANTIŠEK BUŇKA[b]

[a]*Department of Food Chemistry and Biotechnology, Faculty of Chemistry, Brno University of Technology, Purkyňova 118, CZ-612 00 Brno, Czech Republic xcmahdalova@fch.vutbr.cz*
[b]*Department of Food Technology, Faculty of Technology, Tomas Bata University in Zlín, Nám. T. G. Masaryka 275, CZ-762 72 Zlín, Czech Republic*

Introduction

Cheeses, in general, are very popular dairy products. There are many types of them and also a lot of ways how to make them. Their flavour depends on many factors, e. g. milk type, milk heat treatment, starter cultures, the maturation period etc[1, 2]. In general, cheese undergoes the most significant changes during its ripening. Proteins, saccharides and fat are important for flavour formation. Biochemical changes in cheese may be grouped into primary (lipolysis, proteolysis and metabolism of residual lactose, lactate and citrate) or secondary (metabolism of fatty acids and amino acids) events. The flavour of cheese is a result of the interaction of starter bacteria, enzymes from milk, rennet, native lipases and secondary microflora. Fatty acids arise during lipolysis; they may be the precursors of the other compounds such as esters, lactones, ketones and aldehydes[1, 2].

Gouda cheese belongs to the Dutch type cheeses which are known for their unique and specific mild cheesy, sweetish, nutty taste and aroma[3, 4]. The aroma profile of Gouda cheese has been characterized by several authors before[3–5]. More than 600 volatile compounds have been identified so far, but only a small fraction of these compounds are responsible for cheese flavour[6, 7]. Volatile flavour compounds provide the characteristic flavour to food. They are substances with the low molecular weight and belong to the various chemical groups, such as alcohols, aldehydes, ketones, esters, lower fatty acids, terpenes, lactones etc[1, 2].

The aim of this study was to identify, quantify and compare the volatile aroma compounds of raw and ripened Gouda cheeses. The volatiles were extracted by solid phase microextraction (SPME) and assessed by gas chromatography with flame ionization detection (GC-FID).

Experimental

The model samples of Gouda cheeses (55 % dry matter, 45 % fat in dry matter) were produced in pilot plant using standard producing technology[1, 2] and ripened at 10 °C for 2 months. For confidentiality reasons, the exact process parameters and the ripening conditions are not completely revealed. Three modes of milk heat treatment: 65 °C 30 min. (sample 1); 80 °C 30 s (sample 2); and 74 °C 30 s (sample 3) were applied during production. The produced cheeses were sampled before and after ripening and all samples were then analyzed for content of volatile flavour compounds.

Volatile compounds were extracted by SPME, identified and quantified using standards by GC-FID. The SPME conditions were: SPME fiber CAR^{TM}/PDMS 85 μm (Supelco). Sample volume 1 g, extraction temperature 35 °C, equilibrium time 30 min., extraction time 20 min., desorption temperature 250 °C, desorption time 20 min. Gas chromatograph used was TRACE^{TM} GC (ThermoQuest, I), capillary column DB-WAX (30 m × 0,32 mm × 0,5 μm). GC conditions: injector 250 °C, splitless desorption 5 min, carrier gas N_2 0,9 ml·min^{-1}, FID at 220 °C, H_2 35 ml·min^{-1}, air 350 ml·min^{-1}, make-up N_2 30 ml·min^{-1}. The oven temperature was 40 °C for 1 min., 40–200 °C at 5 °C·min^{-1}, 200 °C for 7 min. Total analysis time was 42 min. The results were statistically treated using one way Wilcoxon test at $p < 0.05$ using Unistat version 5.5.

Results and discussion

The intention of this study was (i) to investigate the influence of milk heat treatment on selected volatiles in cheese and (ii) to judge their development during the production of Gouda cheeses. Simple and fast SPME as alternative to other long-lasting and/or expensive extraction methods was applied in this work; it has been used by many authors to measure the volatiles of foods. The fibre coating selected is the most often applied to extract volatile compounds[1–3].

In total 18 various volatile compounds were identified in the raw cheeses samples. All of them were present in sample 1: 3 aldehydes, 4 ketones, 7 alcohols, 1 ester and 3 acids; 17 compounds were identified in sample 2: 2 aldehydes, 4 ketones, 7 alcohols, 2 esters and 2 acids; and 15 of them were found in sample 3: 2 aldehydes, 4 ketones, 6 alcohols, 1 ester and 2 acids.

While in total 29 various volatile compounds were identified in the ripened cheese samples. All of them were presented in sample 1: 3 aldehydes, 4 esters, 6 ketones, 10 alcohols and 6 acids; sample 2 contained 21 compounds: 2 aldehydes, 3 esters, 4 ketones, 8 alcohols and 4 acids; and 20 compounds were found in sample 3: 2 aldehydes, 2 esters, 5 ketones, 6 alcohols and 5 acids. These results confirm generally known fact, that many new volatile compounds are formed during ripening of cheese[1, 2]. As expected, the raw cheeses contained low numbers, as well as the total quantity, of the volatile compounds. Samples are at the beginning of ripening, so they contain only the compounds present in raw material used (milk) and several substances were probably created during the production process because of lactose fermentation[1, 2]. The secondary processes (proteolysis, lipolysis) begin to run during cheese ripening and most of volatile aromatic compounds are the result of the processes[1, 2]. The comparison of total content of compounds identified in samples is expressed in Fig. 1. As can be seen the ripened cheeses contained much higher quantity of compounds identified in most cases.

In the case of raw cheeses sample 3 had the highest total content (711 ± 44 μg·g^{-1}) of volatile compounds identified, sample 1 the lowest (589 ± 65 μg·g^{-1}). The sample 1 was produced from milk pasteurized at lower temperature, but for a

long time (65 °C 30 min), while the short/fast heat treatement was applied on sample 2 (80 °C 30 s) and sample 3 (74 °C 30 s). The long duration of milk heat treatement will probably be the main factor which contributes to the low amount of compounds. The higher pasteurizing temperature can also contribute to this decrease to some extent, owing to the slightly lower content of compounds in sample 2 (80 °C) comparing to sample 3 (74 °C).

Regarding the ripened cheeses, different trend was observed; the highest total content of volatile compounds was found in sample 1 ($2\,111 \pm 102$ μg·g^{-1}) and the lowest in sample 2 ($1\,677 \pm 365$ μg·g^{-1}) (see Fig. 1). In this case pasteurizing temperature seems to be the main factor influencing the content of compounds formed during ripening.

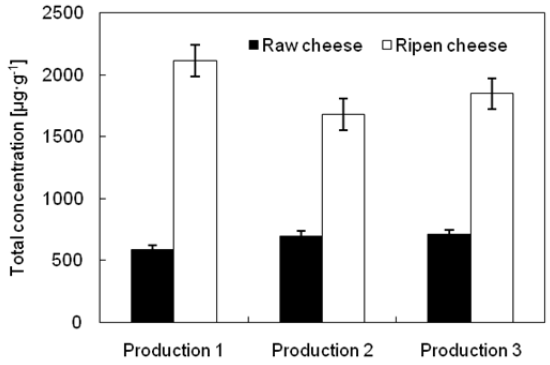

Fig. 1. **Total content (in μg.g^{-1}) of volatile compounds identified in Gouda cheese samples**

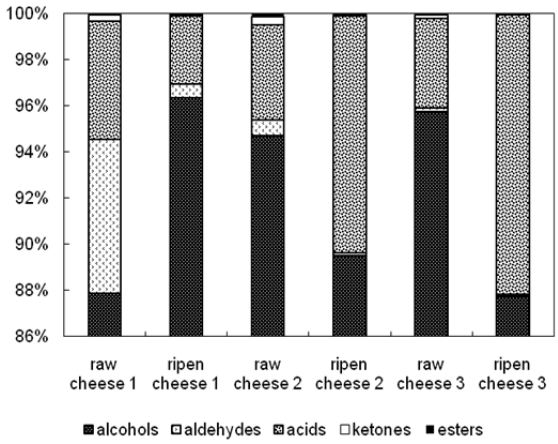

Fig. 2. **Percentage of the chemical groups of compounds identified in Gouda cheeses**

The comparison of chemical groups of compound identified in samples is given in Fig. 2. The significant ($p < 0.05$) differences were found between samples. The results indicate that alcohols create the highest percentage of the chemical groups in all samples. Ethanol represented the highest content of alcohols in all samples. It is formed during lactose fermentation in the first days of cheese ripening[1, 2]. Acids are the second most important group in almost all cheese samples, except raw cheese of production 1, where aldehydes are the second most represented group. Especially ethanoic acid was the most represented carboxylic acid, also butanoic acid creates a great part of all samples; isobutanoic, lactic and propionic acids belong to the acids identified in the samples. As can be seen in Fig. 2 amount of carboxylic acids rises in ripened cheeses (with the exception of production 1). Aldehydes are the third major chemical group. Among them ethanal and fenylmethanal were present in the all cheeses. Finally ketones and esters were represented minimally. However, mainly ketones are very imporant in cheese flavour, although at low concentrations[1, 2]. Butan-2,3-dione, butan-2-one and 3-hydroxybutan-2-one were present in all samples, they exhibit typical buttery and yogurt flavour[1, 2]. Major ester is ethyl ester ethanoic acid in Dutch type cheese.

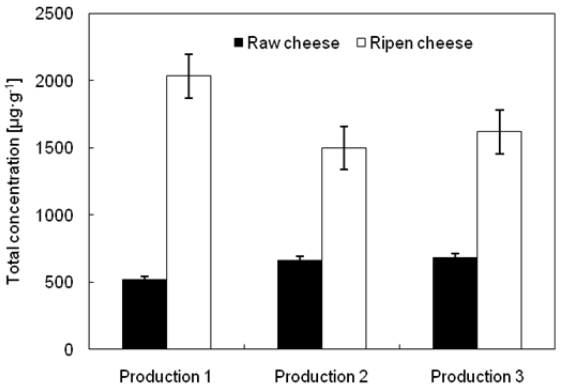

Fig. 3. **Comparison of alcohols in cheese samples**

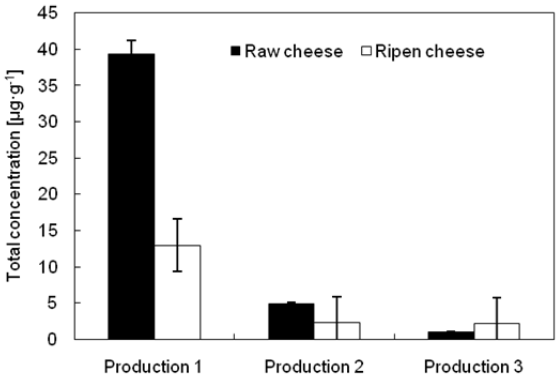

Fig. 4. **Comparison of aldehydes in cheese samples**

The above mentioned findings (Fig. 2) show the great dissimilarity of sample 1 (65 °C 30 min) such confirming the important influence of pasteurizing temperature on formation and composition of volatile compounds in cheese. For the better comprehensibility of differences among samples, the single chemical groups of compounds are given individually in Fig. 3–7. The amount of alcohols rises during production and ripening (see Fig. 3) in all samples. Mainly ethanol, propanol,

butan-1-ol, butan-2-ol and also other alcohols increased their concentrations after ripening. We can assume that lactose fermentation is the main reason[1, 2].

As Fig. 4 shows the concentration of aldehydes is very variable. Raw cheese of production 1 contained exceptionally high quantity of aldehydes, which sharply decreased during ripening. Also in sample 2 the mild decrease of aldehydes was observed. On the other hand the lowest amount of aldehydes was in production 3 with the slight rise after ripening.

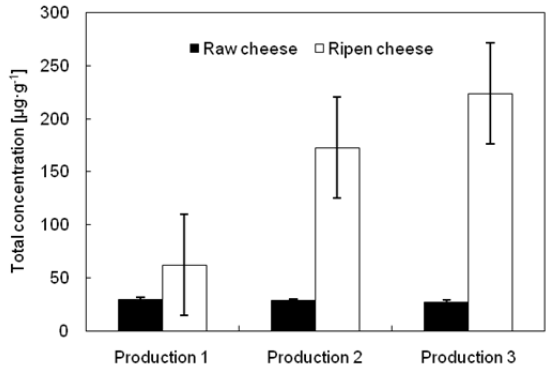

Fig. 5. **Comparison of acids in cheese samples**

The quantity of carboxylic acids increased during ripening in all samples, as Fig. 5 points. Mainly the concentration of ethanoic and butanoic acids, which are also produced during lactose fermentation[1, 2].

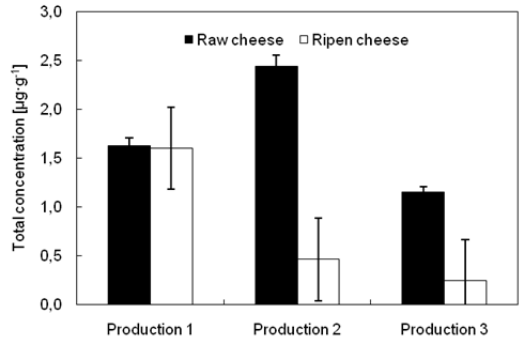

Fig. 6. **Comparison of ketones in cheese samples**

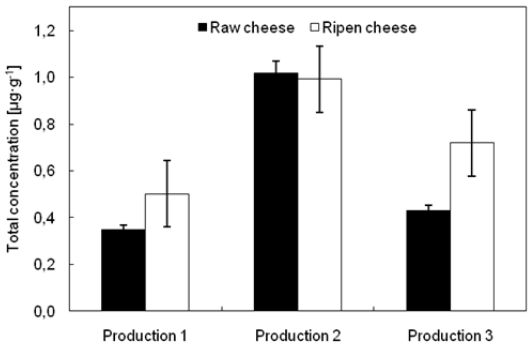

Fig. 7. **Comparison of esters in cheese samples**

The amount of ketones decreased during cheese ripenig (Fig. 6), especially apparently in sample 2 (high pasteurizing temperature 80 °C). This very interesting fact was probably caused by their transformation into alcohols and/or acids[1, 2].

The concentration of esters was generally very low as Fig. 7 indicates; their changes during ripenig were marginal.

To summarize, the development of volatile aroma compounds during ripening of experimentally produced model Gouda cheese was investigated in this study; various modes of heat treatment of milk used as raw material were applied and compared. In accordance with other studies[3–5], ripening has a clear effect on development of aroma compounds in Gouda cheese. The influence of heat treatment on development of compounds detected is variable and will need a deeper investigation.

This work was kindly supported by a Standard project of specific research No. FCH-S-15-2827.

REFERENCES

1. Sousa, M., Ardö, J. Y., McSweeney, P. L. H.: Advances in the study of proteolysis during cheese ripening. Int. Dairy J. *11*, 327 (2001).
2. Heaven, M. W., Nash, D.: Recent analyses using solid phase microextraction in industries related to food made into or from liquids. Food Control. *27*, 214 (2012).
3. Frank, D. C., Owen, C. M. Patterson, J.: Solid phase microextraction (SPME) combined with gas-chromatography and olfactometry-mass spectrometry for characterization of cheese aroma compounds. Food Sci. Technol.-LEB. *37*, 139 (2004).
4. Verzera, A., Ziino, M. Condurso, C., Romeo, V. Zappal, M.: Solid-phase microextraction and gas chromatography/mass spectrometry for rapid characterisation of semi-hard cheeses. Anal. Bioanal. Chem. *380*, 930 (2004).
5. McSweeney, P. L. H., Sousa, M.: Biochemical pathways for the production of flavour compounds in cheeses during ripening. Diary Sci. Technol. *80*, 293 (2000).
6. Yvon, M., Rijnen, L.: Cheese flavour formation by amino acid catabolism. Int. Dairy J. *11*, 185 (2001).
7. Marilley, L.: Flavours of cheese products: metabolic pathways, analytical tools and identification of producing strains. Int. J. of Food Microbiol. *90*, 139 (2004).

DETERMINATION OF NICOTINE IN DIFFERENT TYPES OF PRODUCT

PETRA MATOUŠKOVÁ, JANA PRAŽÁKOVÁ and IVANA MÁROVÁ

Brno University of Technology, Faculty of Chemistry, Department of Food Chemistry and Biotechnology, Purkynova 118, 612 00 Brno, Czech Republic
xcmatouskovap@fch.vutbr.cz

Abstract

Tobacco is a plant grown for its leaves, which are smoked, chewed, or sniffed. Tobacco contains the alkaloid nicotine, a drug classified as a stimulant. Pure nicotine is a hygroscopic, colorless oily liquid and it is a poisonous alkaloid.

Nicotine effects on the body are complex. The drug affects the brain and central nervous system as well as the hypothalamus and pituitary glands of the endocrine system. Nicotine to improve memory and concentration, and also increases the sensation of wakefulness. These beneficial effects may play a role in the initiation and maintenance of tobacco dependence. Withdrawal symptoms are a sense of emptiness, anxiety, depression, moodiness, irritability, and inattentiveness.

This work was focused on optimization of methods for the determination of nicotine in different kinds of products. Nicotine was determined by HPLC/PDA. For quantitative analysis of nicotine concentration were tested cartridges for electronic cigarettes, nicotine gums, nicotine spray, nicotine lozenges, nicotine ordispersible film and classic cigarettes. For each type of product was also the most appropriate method for extracting nicotine tested.

Finally, the encapsulation of nicotine was tested. As a material for particles preparation were used alginate, chitosan and alginate-starch. The particles were prepared by the method based on the principle of gelation and cross-linking polymers using the Büchi encapsulator B-395 Pro. The particles were exposed to model gastrointestinal conditions. After exposition, particles stability and amount of released nicotine was monitored. The stability of particles in the model food was studied too.

Introduction

Nicotine is the primary alkaloid found in tobacco. But more than 5300 different chemicals have been found in tobacco and tobacco smoke, including carbon monoxide, hydrogen cyanide, tar, formaldehyde, and benzene. So, tobacco smoke is harmful to smokers and nonsmokers and causes numerous types of cancer. Although smoking cessation is the most effective way to reduce the risk of tobacco-related diseases, nicotine withdrawal symptoms make quitting smoking difficult. To reduce the withdrawal symptoms, nicotine replacement therapy is useful for most people who are attempting to quit smoking[1].

The first commercial nicotine replacement technology was chewing gum. Nicotine gum is a type of chewing gum that delivers nicotine to the body. The nicotine is delivered to the bloodstream via absorption by the tissues of the mouth. Nicotine content is usually either 2 or 4 mg of nicotine[2]. Electronic cigarette or E- cigarette is a battery-powered device that contains a cartridge filled with nicotine, flavor and other chemicals. The e-cigarette turns the nicotine into a vapor that is then inhaled by the user. The user will puff on it, similar to a cigarette, and receive a vaporized solution of propylene glycol and nicotine. The e-cigarette often looks like a real cigarette. This product is often marketed as an alternative to smoking or an aid in quitting[3, 4]. Alternative nicotine replacement products include the nicotine patch, nicotine pastilles/lozenges and the nicotine inhaler[5].

The determination of nicotine is an important analysis for the tobacco industry, as the quality and usability of the product can be determined by its nicotine content. Several methods for the determination of nicotine and its metabolites have been reported, including high-performance liquid chromatography–ultraviolet detection (HPLC–UV), high-performance liquid chromatography–Diode Array detection (HPLC–DAD), liquid chromatography–mass spectrometry (LC–MS), liquid chromatography–tandem mass spectrometry (LC–MS/MS) and gas chromatography–mass spectrometry (GC–MS)[1, 6, 7].

Methods

Various methods have been employed to isolation the nicotine from tobacco products, including different solvent extraction followed by high-performance liquid chromatography with diode array detection (HPLC/PDA). Firstly, method for the determination of nicotine by HPLC/PDA was optimized. As the most suitable stationary phase was selected a Kinetex 5u C18 100A 150 × 4.6 mm column, as the optimal mobile phase was chosen a pure methanol with a flow rate of 1 $ml \cdot min^{-1}$ and a temperature of 25 °C. Analysis was performed by external calibration; nicotine standard was purchased from Sigma Aldrich. The objective of this study was evaluated and compared the nicotine content of cigarette and product of nicotine replacement therapy available in the market in Czech Republic. All samples were obtained from local stores in Brno.

Table 1
The amount of nicotine in cigarettes

cigarette brands	concentration of nicotine [mg/cigarette]	quantity declared on the packaging (recoverable amount) [mg/cigarette]
Marlboro red	13.9 ± 0.4	0.8
Winston classic	10.4 ± 0.3	0.8
Phillip Morris Ruby	9.51 ± 0.1	0.8
Sparta classic	8.4 ± 0.3	0.7
Start by Chesterfield	8.68 ± 0.1	0.7
Camel activate double	7.9 ± 0.2	0.6
LM loft blue	9.3 ± 0.4	0.6
Marlboro gold	9.0 ± 0.5	0.6
Davidoff shape	8.1 ± 0.1	0.6
Kiss super slims strawberry	7.5 ± 0.1	0.5

Results and discussion

This work was focused on optimization of methods for the determination of nicotine in different kinds of products using HPLC/PDA.

For the analysis of nicotine were chosen: 18 kinds of cartridges for electronic cigarettes, two kinds of nicotine gum, nicotine spray, nicotine pastilles, nicotine film and ten species of classic cigarettes. For each type of product the most appropriate method for extracting nicotine and its subsequent analysis by HPLC/PDA was found.

For tobacco 24 hour extraction in methanol and 10s ultrasound was selected. Declaration of recoverable amount was for most of cigarettes 10 % of real content of nicotine (Table 1). The highest amount of nicotine was measured for the strongest cigarettes in product Marlboro red (13.9 mg/cigarette).

Table 2
The amount of nicotine in snuff

product	concentration of nicotine [mg/10g]
Gletscher Prise Snuff	66.0 ± 0.4
Red Bull Strong Snuff	103.6 ± 0.7

For analysis were chosen two of the snuff products (Table 2). For product Gletscher Prise Snuff was found to contain 6.6 mg nicotine per g and a product Strong Red Bull Snuff had contained of nicotine 10.4 mg per g.

Table 3
The amount of nicotine in cartridges for electronic cigarettes

product	concentration of nicotine [mg/ml]
Desert Ship 0 mg	not detected
Desert Ship 6 mg	5.4 ± 0.3
Desert Ship 11 mg	10.4 ± 1.2
Desert Ship 16 mg	16.9 ± 0.7
Desert Ship 18 mg	11.2 ± 0.5
Desert Ship 24 mg	24.1 ± 0.5
Daf 0 mg	not detected
Daf 6 mg	6.59 ± 0.7
Daf 11 mg	9.6 ± 0.9
Daf 16 mg	15.7 ± 0.4
Daf 24 mg	23.9 ± 0.6
Banana 16 mg	14.0 ± 0.9
Straw-champ 16 mg	16.7 ± 0.6
Apple 16 mg	15.3 ± 0.3
Blueberry 16 mg	15.0 ± 0.7
Menthol 16 mg	15.4 ± 0.5
Water melon 16 mg	16.3 ± 0.6
Crème caramel 16 mg	15.8 ± 0.2

The nicotine spray and electronic cigarette refills without flavors were only diluted with methanol. Flavored refills were first diluted by sodium hydroxide and then with methanol. Content of nicotine in packaging of nicotine sprays (15 mL) was determined to 10.05 mg of nicotine. It was smaller than the quantity declared on the packaging. Manufacturer declared a quantity of 11–13.5 mg.

Content of nicotine in cartridges for electronic corresponded to the quantity declared on the packaging (Table 3). In product Desert ship (18 mg) only 11.2 mg of nicotine was measured.

Table 4
The amount of nicotine in nicotine chewing gum

nicotine gum	concentration of nicotine [mg/chewing gum]	quantity declared on the packaging [mg/chewing gum]
Nicorette menthol	3.98 ± 0.03	4
Nicorette fresh fruit	1.99 ± 0.04	2

For chewing gums, pastilles and nicotine film extraction with 5% sodium hydroxide was chosen. Content of nicotine in Nicorette gum corresponded to the quantity declared on the packaging (Table 4).

For chewing gum was measure after used the residual amount of nicotine. Determination of residual nicotine content was relatively high, for Nicorette menthol gum 68 % and for Nicorette fresh fruit gum 77 %. Differences may be also caused chewed with a different intensity.

In nicotine pastilles was measured 2.49 mg of nicotine per pastille. However the amount declared by the manufacturer was 4 mg. The amount of nicotine in nicotine film was determined to 1.67 mg of nicotine per film. Declared amount on the packaging was 2.5 mg nicotine.

In present study was designed new nicotine product, too. Nicotine has been encapsulated into polysaccharide capsules. As a material for particles preparation were used alginate, chitosan and alginate-starch. Particles were prepared by the method based on the principle of gelation and cross-linking polymers. The highest encapsulation efficiency was found in alginate-starch particles, almost 99 % (Table 5).

Table 5
Encapsulation efficiency of nicotine (%)

particles	encapsulation efficiency [%]
chitosan	88.74
alginate	95.79
alginate-starch	98.71

Prepared particles long-term stability in different model foods was evaluated. As the most suitable medium for storage the water medium was determined. For three weeks storage was released only 1.1 % of the amount of encapsulated nicotine.

Particles with encapsulated nicotine were exposed to model physiological conditions – artificial stomach and intestinal liquids and bile acids. In these environments the particles were partially disintegrated and the release of nicotine was evaluated. After passing through the artificial digestive system has been released from particles over 20 % of nicotine. Encapsulated forms of nicotine enables controlled release of nicotine in digestive system. It can be concluded that encapsulation procedures could be a suitable alternative for nicotine replacement therapy.

Fig. 1. **Alginate-starch particles with encapsulated nicotine**

The last part of this work was the consumer questionnaire. Questionnaire was designed to focus on the knowledge of people about nicotine and sources of nicotine, how many people smoke and what products used people who want to quit smoking.

It was found that three-quarters of smokers/former smokers smoke light cigarettes. It is interesting that only 50% of smokers knew concentrations of nicotine which they receive. More than half of non-smokers and former smokers believe that the electronic cigarette is healthier than regular cigarettes. In the case of smokers, it is only 40 %. Some of nicotine replacement therapy products help to quit smoking only for 13 percent of former smokers.

Conclusions

In present work was optimized method for determination of nicotine using high performance liquid chromatography. This method was very simple and fast, but in some types of products was a disadvantage in the long sample preparation. In the present population are a considerable number of people who are dependent on nicotine and smoking. Therefore, it is necessary to looking for possibilities that help with addiction. One way could be better informed about the consequences and the harmfulness of smoking. Another possibility is the design and production of new interesting nicotine replacement products which can be a substitute for effective smoking cessation.

This work was supported by project "Materials Research Centre – Sustainability and Development" No. LO1211 (Ministry of Education, Youth and Sport of the Czech Republic).

REFERENCES

1. Yasuda, M., Ota T., Morikawa A., Mawatari K., Fukuuchi T., Yamaoka N., Kaneko K., Nakagomi K. *Journal of Chromatography B*. 2013, 934: 41–45.
2. Elam M.J. *International Journal of Drug Policy*. 2015, 26(6): 536–542.
3. Pokhrel, P., Little M.A., Fagan P., Kawamoto C. T., and T. A. Herzog. *Addictive Behaviors*. 2014, 39(12): 1869–1873.
4. Etter J. F., Eissenberg T. *Drug and Alcohol Dependence*. 2015, 147: 68–75.
5. Carpenter, M. J., Jardin, B. F., Burris, J. L., Mathew, A. R., Schnoll, R. A., Rigotti, N. A., Cummings, K. M. *Drugs*. 2013, 73(5): 407–426.
6. Trehy M. L., Ye W., Hadwiger M. E., Moore T. W. Allgire J. F., Woodruff J. T., Ahadi S. S., Black J. C., Westenberger B. J. *Journal of Liquid Chromatography*. 2011, 34(14): 1442–1458.
7. Famele, M., Ferranti C., Abenavoli C., Palleschi L., Mancinelli R., Draisci R. *Nicotine*. 2015, 17(3): 271–279.

"VINUM REGNUM - REX VINORUM" ^{1}H NMR SPECTROSCOPY STUDY OF THE SLOVAK TOKAJ WINES

MILAN MAZUR*, LUCIA HUSÁRIKOVÁ, MICHAL KALIŇÁK and MARIAN VALKO

Faculty of Chemical and Food Technology, Slovak University of Technology in Bratislava, Radlinského 9, SK – 812 37 Bratislava, Slovak Republic
**milan.mazur@stuba.sk*

The present contribution analyses the characteristic properties of the Slovak Tokaj wines by high resolution ^{1}H NMR spectroscopy. The following original wines of various vintages were selected for NMR experiment: Tokaj Furmint, Tokaj Lipovina, Tokaj Yellow Muscat, Tokaj "samorodne" dry and sweet wine, Tokaj 2-, 3-, 4-, 5- and 6- puttony select wines, and Tokaj essence. All Tokaj wines were produced by classic Tokaj „oxidative" processing technology. Additionally, the Tokaj select wines and Tokaj essence were prepared using „cibebs" – grape raisins affected by noble rot Botrytis cinerea and were stored in Tokaj tuff cellars for 3–6 years of aging in oak wood barrels. In summary, the NMR spectroscopy can be used for the detection of organic and amino acids present in the Tokaj wines. The ^{1}H NMR spectra can be utilized as the unique "fingerprints" of the original Slovak Tokaj wines.

Keywords

NMR spectroscopy, Tokaj wines, minor compounds.

Introduction

The chemical analysis of the grape wines is becoming more important due to quality and safety food control in all European Union countries[1]. The determination of grape wine authenticity is very important and it is dependent on the wine variety, year of production (vintage) but mainly geographical origin. High resolution ^{1}H NMR spectroscopy can be used for the detection of organic and amino acids, phenolic compounds and sugars present in the wines and enables to see differences in their composition originating from different geographical area. NMR spectra can be used as a "*fingerprint"* for the monitoring of grape wines[2–4]. Numerous papers have been published about the NMR analysis of red and white wines[2–14]. However, only the few chemical studies are available about the Tokaj wines originating from both Hungary[15–18] and Slovakia[19, 20] with the status „Protected Designation of Origin". To the best of our knowledge, no NMR analysis of original Tokaj wines was published up to date.

In our previous papers[13, 14], the ^{1}H NMR spectra of white and red Slovak quality wines were measured. To continue our investigation, in the present contribution the ^{1}H NMR spectra of Slovak Tokaj wines were collected. The received NMR data enriched our basic wine „*fingerprint*" database of white and red Slovak wines with the original Slovak Tokaj wines of selected wine varieties and various years of production (vintages) with grape origin only from Slovak Tokaj region and distributed only by authorized Slovak Tokaj wine producers.

Experimental

Materials and sample preparation – *Original Slovak Tokaj wines from Slovak wine region of Tokaj used in this work are summarized in Table 1. All the wines were produced by Tokaj oxidative technology. Addition of deuterium oxide (Aldrich, 99.9 %) with 0.05 % sodium 3-(trimethylsilyl) propionate-2,2,3,3,-d_4 (TSP) as a chemical shift (0.0 ppm) was used.*

The wine samples were not pre-concentrated and so called "*direct analysis*" of the wine samples was used[13, 14]. That means the concentration of the dominant components in the Tokaj wine samples was not decreased at all. Thus, 0.6 ml of Tokaj wine was taken from a freshly opened bottle, transferred to 5 mm NMR sample tube and mixed with 0.1 ml D_2O for NMR field/frequency lock. Advantages and disadvantages of the wine sample pre-concentration by vacuum-distillation, frees-drying or under argon-flow are discussed in our previous paper[13].

NMR experiment – High resolution ^{1}H NMR spectra of Tokaj wines were recorded on a Varian INOVA 600 MHz NMR spectrometer using a 5.00 mm indirect detection pulsed field gradient probe operating at 599.75 MHz for ^{1}H nuclei. The sample temperature during NMR experiments was 25 °C. ^{1}H NMR spectra were recorded with the suppression of water signal by the presaturation pulses (pulse sequence PRESAT). The original program VnmrJ 2.1B (Varian) was used for post-recording manipulations and analysis of ^{1}H NMR spectra of Tokaj wines. The relative integrals of the selected peaks in the form of bins (0.1 ppm) in the aliphatic region (0.0–6.0 ppm) of ^{1}H NMR spectra were evaluated with a percentile error of 5 %. The peak intensities were normalized to the intensity of a standard TSP (marked by * in the histogram).

Table 1
An overview of the original Slovak Tokaj wines

Tokaj quality wines: Furmint, semi-sweet, 1997, Furmint, dry, 2000, 2004, Furmint, dry, 2004, 2005, 2006, Malá Tŕňa; Lipovina (Linden Leaf), semisweet, 1997, Lipovina, dry, 2000, Malá Tŕňa; Lipovina, dry, 2004, 2005, 2006, Muškát žltý (Yellow Muscat), dry, 2003, 2004, 2005, 2006, Veľká Tŕňa.

Tokaj cuvée wines: Svätý Urban, semisweet, Malá Tŕňa 2003, Omšové, dry, 1999, Tokaj *"samorodne"*, dry, 1996, Tokaj *"samorodne"*, sweet, 2003, Malá Tŕňa; Tokaj *"samorodne"*, dry, 1997, Tokaj *"samorodne"*, sweet, 1997, Viničky.

Tokaj select wines: 2-puttony, sweet, 1999, Malá Tŕňa, 3-puttony, sweet, 1993, Viničky, 3-puttony, sweet, 1997, 1999, Malá Tŕňa, 4-puttony, sweet, 1990, Viničky; 4-puttony, sweet, 1999, 5-puttony, sweet, 1999, 2001, Malá Tŕňa, 6-puttony, sweet, 1999, 2001, select essence, sweet, 1999, Malá Tŕňa.

Results and discussion

For illustration, the following representative examples were selected from each of the three sets of the Tokaj wines:

a) *Tokaj quality wines* – Fig. 1 shows the ^{1}H NMR spectra of quality wines Tokaj Furmint, dry, year of production 1997 and 2000, both prepared by special Tokaj oxidative

technology and relative integral intensities of minor compounds of various vintage wines (in histogram, bottom).

b) *Tokaj cuvée wines* – ^{1}H NMR spectra of cuvée wines Tokaj "samorodne" Omšové, dry, 1999, 2003 and Svätý Urban, semi-sweet, 2003 and relative integral intensities of minor compounds of various wines are given in the Fig. 2. Again, all the wines were produced in the Slovak wine region of Tokaj by oxidative technology.

c) *Tokaj select wines* – Fig. 3 depicts ^{1}H NMR spectra of Tokaj select wines 5-puttony, very sweet, 1999, 2001 vintages, produced in the Slovak wine region of Tokaj using oxidative technology. And again, relative integral intensities of minor compounds of various vintage wines are presented.

^{1}H NMR chemical shifts detected in the NMR spectra of dry, semi-sweet and very sweet Tokaj wines can be assigned according to literature data of Košír & Kirdič[5, 6] for grape wines and Pereira et al.[11, 12] for grape must as follows:

A. *Dominant compounds* – fructose (multiplets) at 3.63–3.72, 3.98–4.02, 4.09–4.12, glucose (α) at 4.64 ppm, (β) at 5.23 ppm, sucrose at 4.21 ppm, 5.41 ppm, ethanol (triplet, CH_3) at 1.17 ppm, (quartet, CH_2) at 3.67 ppm, glycerol (CH_2) at 3.63 ppm, (CH) at 3.79 ppm, butylenglycol (CH_3) at 1.13 ppm, (CH) at 3.64 ppm, water singlet at 4.80 ppm.

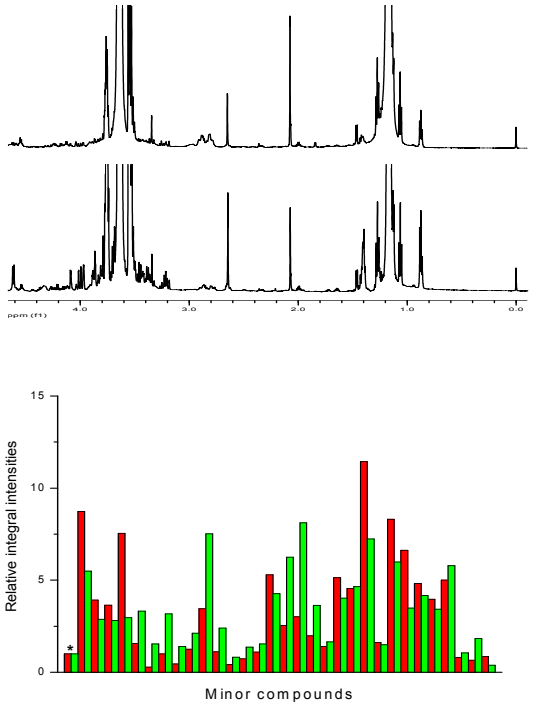

Fig. 1. **Part of the ^{1}H NMR spectra of quality wines Tokaj Furmint, dry, 1997 (top, red) and 2000 (bottom, green), Slovak wine region of Tokaj, Malá Tŕňa, oxidative technology. Histogram with integral intensities relative to TSP of bins (0.1 ppm) of the two vintage wines**

B. *Minor compounds* – a) organic acids: lactic acid (CH_3) at 1.42 ppm, (CH) at 4.44 ppm, acetic acid (CH_3) at 2.08 ppm, malic acid (CH_2) at 2.90 ppm, (CH) at 4.61 ppm, succinic acid (CH_2) at 2.66 ppm, tartaric acid (CH) at 4.77 ppm, citric acid (CH_3) at 2.74 ppm, 2.87 ppm. – b) amino acids: valine at 1.05 ppm, 2.33 ppm, 3.69 ppm, alanine at 1.49 ppm, 3.89 ppm, isoleucine at 0.94 ppm, 1.01 ppm, 1.46 ppm, 2.01 ppm, 3.76 ppm, proline at 2.08 ppm, 2.35 ppm, 3.42 ppm, 4.17 ppm, lysine at 1.45 ppm, 1.71 ppm, 1.89 ppm, 3.03 ppm, 3.82 ppm, citruline at 1.55 ppm, 1.88 ppm, 3.13 ppm, 3.75 ppm, arginine at 1.72 ppm, 2.02 ppm, 3.26 ppm, 4.11 ppm, asparagine at 2.98 ppm, 4.04 ppm, threonine at 1.36 ppm, 3.71 ppm, 4.26 ppm, leucine at 0.95 ppm, 1.70 ppm, 1.75 ppm, 3.82 ppm, histidine at 3.40 ppm, 4.147 ppm, tyrosine at 3.18 ppm, 4.07 ppm, phenylalanine at 3.14 ppm, 3.31 ppm, 4.02 ppm, glutamine at 2.18, 2.58 ppm, 3.91 ppm, glycine at 3.61 ppm, serine at 3.87 ppm, 3.97 ppm, methionine at 2.11 ppm, 2.21 ppm, 2.63 ppm.

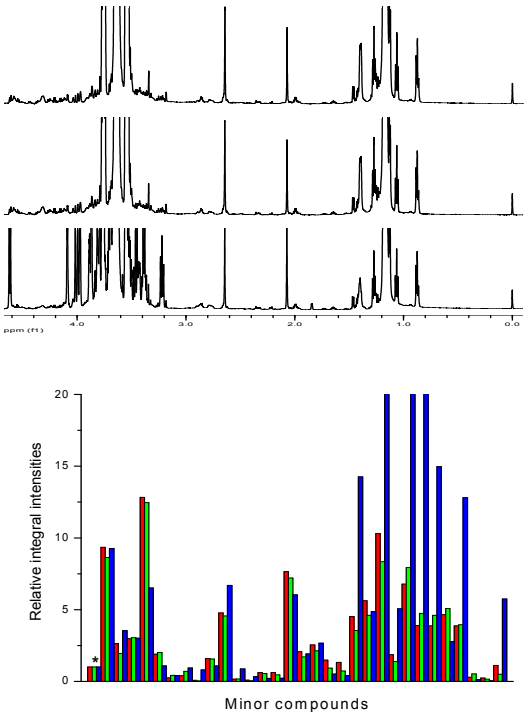

Fig. 2. **Part of the ^{1}H NMR spectra of cuvée Tokaj "samorodne" Omšové, dry, 1999 (top, red), Omšové, dry, 2003 (middle, green) and Svätý Urban, semi-sweet, 2003 (bottom, blue), Slovak wine region of Tokaj, Malá Tŕňa, oxidative technology. Histogram with integral intensities relative to TSP of bins (0.1 ppm) of three vintage wines**

Unfortunately, in the ^{1}H NMR spectra of the Tokaj wines, the small signals of minor compounds (organic and amino acids) are overlapped by very strong signals of dominant compounds (ethanol, glycerol and additionally at semi-sweet and very sweet Tokaj wines also by fructose, glucose and sucrose). The signal intensities of the dominant compounds can be 20 or more times bigger than those of minor compounds. Therefore, the precise assignment of individual peaks of minor compounds in such NMR spectra is very difficult.

It is obvious that, in the spectral region of 0.5–1.5 ppm of all the Fig. 1–3, the strong signals of ethanol and butylenglycol dominate, overlapping the small signals of valine, alanine, leucine and also lactic acid. In the region of 1.5–3.0 ppm, the resonances of acetic, succinic and malic acids, and likewise isoleucine, proline and lysine are clearly resolved. In the spectral region over 3.0 ppm of the dry Tokaj wines, the very strong signals of ethanol, glycerol and butylenglycol are dominant, so very small signals of amino and organic acids are fully overlapped. Additionally, in the case of semi-sweet and sweet Tokaj wines, the very strong resonances of fructose, glucose and sucrose in the region of 3.6–5.5 ppm are dominant. In the Fig 1, the histogram clearly shows the differences between relative integral intensity of the minor compounds in the dry Furmint samples of different vintages (1997 and 2000). In contrast, in the case of sweet Tokaj select wines of 1999 and 2000 vintages (Fig. 3) the very similar relative integral intensities were found. The same is true comparing 4-, 5-, 6-puttony Tokaj wines and a very sweet select Tokaj essence.

According to Brescia et al.[9], the aromatic part (6.2–8.2 ppm) of ^{1}H NMR spectra can map the phenolic compounds in grape wines. However, the resonances of the individual phenolic compounds (data not shown) in Tokaj wine samples can not be clearly distinguished and subsequently precisely assigned due to their signal complexity.

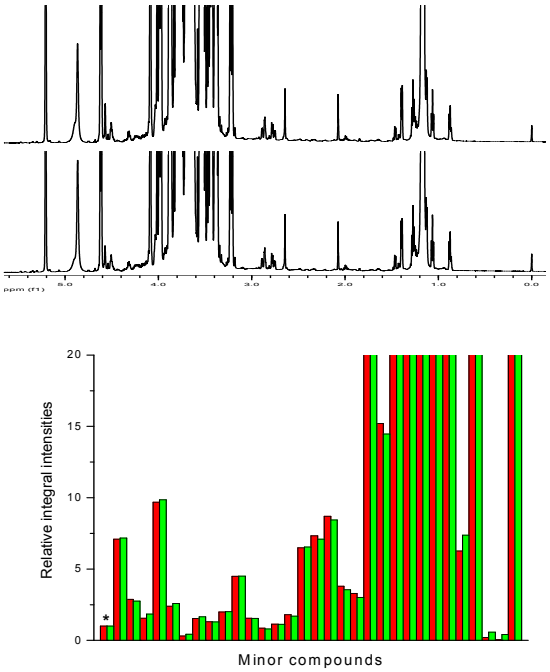

Fig. 3. **Part of the ^{1}H NMR spectra of Tokaj select wines 5-puttony, very sweet, 1999 (top, red), 2001 (bottom, green), Slovak wine region of Tokaj, Malá Tŕňa. Histogram with integral intensities relative to TSP of bins (0.1 ppm) of two vintage wines. Bins with cut-off peaks represent sugars**

Conclusions

The high resolution ^{1}H NMR spectroscopy using 600 MHz NMR spectrometer is an excellent technique for non-destructive analysis of the Tokaj wines and can successfully monitor ^{1}H NMR signals of dominant and minor compounds in the dry, semisweet and sweet Tokaj wines. The sample preparation (not pre-concentrated) retains original composition of Tokaj wines without any physical and chemical interference. Only the water signal suppression was applied during ^{1}H NMR spectra measurement by presaturation pulses. Such ^{1}H NMR spectra can be then used as unique „*fingerprints*“ of Slovak Tokaj wines in authenticity studies to differentiate wines according to the wine varieties, years of production (vintages) or geographical origin (Slovak Tokaj region).

This work was supported by the Scientific Grant Agency of the Slovak Republic (Projects VEGA 1/0765/14, 1/0041/15).

REFERENCES

1. Commission Regulation, No. 2676/90, *33*, L272 (1990).
2. Košir I. J., Kidrič J.: Analusis, *26*, 7797 (1998).
3. Košir I. J., Kocjančič M., Ogrinc N., Kidrič J.: Anal. Chim. Acta, *429*, 195 (2001).
4. Ogrinc N., Košir I.J., Kociančič M., Kidrič J.: J. Agric. Food Chem., *49*, 1432 (2001).
5. Košir I. J., Kidrič J.: J. Agric. Food Chem., *49*, 50 (2001).
6. Košir I. J., Kidrič J.: Anal. Chim. Acta, *458*, 77 (2002).
7. Brescia M. A., Caldaroda V., De Giglio A., Banedetti D., Fanizzi F. P., Sacco A.: Anal. Chim. Acta, *458*, 177, (2002).
8. Ogrinc N., Košir I. J., Spangenberg J. E., M., Kidrič J.: Anal. Bioanal. Chem., *376*, 424 (2003).
9. Brescia M. A., Košir I. J., Caldaroda V., Kidrič J., Sacco A.: J. Agric. Food Chem., *51*, 21 (2003).
10. Košir I. J., Lapornik B., Andrašek S., Wondra A.G., Vrhovšek U., Kidrič J.: Anal. Chim. Acta, *512*, 277 (2004).
11. Pereira G. E., Gaudillere J. P., Leuven C., Hilbert G., Lavialle O., Maucourt M., Deborde C., Moing A., Rolin D.: J. Agric. Food Chem., *53*, 6382 (2005).
12. Pereira G. E., Gaudillere J. P., Leuven C., Hilbert G., Maucourt M., Deborde C., Moing A., Rolin D.: Anal. Chim. Acta, *563,* 346 (2006).
13. Mazur M., Furdíková K., Kaliňák M., Žúbor V., Pronayová N.: Chem. Listy, *102*, s1089 (2008).
14. Staško A., Brezová V., Mazur M., Čertík M., Kaliňák M., Gescheidt G.: LWT-Food Sci. Technol., *41*, 2126 (2008).
15. Hajos G., Sass-Kish A., Szerdahelyi E., Bardocz S.: J. Food Sci., *65*, 1142, (2000).
16. Miklosy E., Kerenyi Z.: Anal. Chim. Acta, *513*, 177 (2004).
17. Pour M. S., Laszlo G., Dietrich H.: Food Chem.: *93*, 74 (2006).

18. Maciejewska M., Szczurek A., A., Kerenyi Z.: Sens. Actuat. B: *115*, 170 (2006).
19. Staško A., Polovka M., Brezová V., Biskupič S., Malík F.: Food Chem., *96*, 185 (2006).
20. Fikselová M., Kačániová M., Mellen M.: Acta Aliment. *39*, 256 (2008).

PROCESSING AND CHARACTERIZATION OF LONG FLAX/THERMOSET BIOCOMPOSITES WITH MODIFIED INTERPHASE

PŘEMYSL MENČÍK, RADEK PŘIKRYL, FILIP HAHN and EMIL LETAVAJ

Brno university of technology, Faculty of Chemistry, Purkyňova 118, CZ-612 00 Brno, Czech Republic
xcmencik@fch.vutbr.cz

Introduction

Polymer composites with fiber reinforcements are widely used as construction materials. Nowadays most of the fibers used in polymer composite industry are synthetic ones, like glass, aramid or carbon fibers. They are widely used especially for their high stiffness and strength properties. However, due to growing ecological and economic awareness, green materials have been developed. Typical examples of green materials are natural fibers. There are lots of types of natural fibers and most of them are readily available with usable mechanical properties[1].

Nevertheless, because of hydrophilic surface, natural fibers are not compatible with the majority of polymer matrices. This causes ineffective stress transfer across the fiber-matrix interface. Possible solution of this problem can be the surface treatment of fibers[2]. Fiber surface polarity can be changed by introducing specific functional groups prepared by grafting technologies. This kind of treatment can improve the fiber – matrix compatibility and leads to an improvement of composite mechanical properties and reduction of water absorption. Moreover, better wettability of fibers by matrix opens the door for new technologies of natural composites preparation.

The aim of this work is to prepare polymer composites of desired mechanical properties with low-twisted flax fiber reinforcement by the pultrusion process. Several chemical treatments of the flax fibers were tested[3].

Materials and Methods

Used materials

As the reinforcement low twisted flax fibers rowings supplied and treated by NaOH solution by Safilin (Poland) to remove the pollutants were used.

Used polyester matrix was based on isophtalic resin ISO 112-G (Poliver – Italy), vinyl ester matrix was based on vinyl ester – epoxy resin Derakene 470-HT (Ashland – USA). The curing reaction was initiated by benzoyl peroxide, bis(4-tert-butylcyclohexyl) peroxydicarbonate and tert-butyl peroxybenzoate.

The surface analysis of the flax fibers was performed by Scanning Electron Microscopy (EVO LS 10, Zeiss). The elemental composition of tested samples was determined by Energy-dispersive X-ray (EDS) detector.

The tensile properties were tested by Instron 5985 equipped with the extensometer. The flexural properties were tested by Zwick Z010 and the impact strength was measured by Labtest CHK 50J-I.

Water absorption of the composite samples was tested according to ISO 62 standard. Three samples of each tested series were dried for 12 hours at 60 °C and their weight after drying was recorded. Those dried samples were immersed in water and their weight was measured until the constant mass value was observed.

Fiber treatment methods

The wet treatment was used to improve the chemical compatibility with the thermoset matrix. Maleic anhydride (MA), itaconic anhydride (ITA), triethoxyvinylsilane (VS), (3-Methacryloxypropyl)trimethoxysilane (MS) and (3-Glycidyloxypropyl)trimethoxysilane (GS) were used as coupling agents.

MA and ITA treatments were carried out by immersing the fibers into acetone with 10 wt. % of appropriate anhydride. The solution was boiled 60 minutes. Treated fibers were rinsed in acetone and dried at 70 °C for 12 hours.

Silane fiber treatments VS, MS, GS were performed in an ethanol/water mixture in a volume ratio 4:1 with 3 wt. % of appropriate silane. The pH = 4 adjustment of prepared solutions was arranged by acetic acid. The fibers were immersed in the solutions and heated until the solutions started to boil. The solutions with fibers were cooled down to laboratory temperature after 2 hours of boiling and the fibers were rinsed twice by cool solvent. Treated fibers were dried in a dry box at 70 °C for 12 hours. The nomenclature of tested samples is described in Table 1.

Table 1
Nomenclature of the samples

UP	Polyester resin
VE	Vinyl ester resin
Ref	Fibers treated only by NaOH from supplier. Raw material for all other treatments
MAF	Fibers treated by maleic anhydride
ITAF	Fibers treated by itaconic anhydride
VSF	Fibers treated by triethoxyvinylsilane
MSF	Fibers treated by (3-Methacryloxypropyl)trimethoxysilane
GSF	Fibers treated by (3-Glycidyloxypropyl)trimethoxysilane

Specimen processing and preparation

Natural composite profiles were prepared by the pultrusion process using the experimental pultrusion device developed at the Brno University of Technology. During this process the flax fibers were impregnated by thermoset resin and pulled into heated steel die, where the material was shaped into rectangular profile and cured at two temperature zones 100 and 160 °C. The pulling speed was set to 0.25 $m \cdot min^{-1}$. At the end of this process the final material was cut to specific length required by ASTM testing standards.

Results and discussion

Chemical treatments of natural fibers are used to improve the chemical interaction between polymer matrix and fiber reinforcement and to reduce the sorption and diffusion of water molecules into the structure of natural fibers as well4.

Tensile and Flexural properties

Prepared composite samples were tested by tensile and flexural tests. In Fig. 2 the tensile modulus of elasticity ΔE and the tensile strength Δσ are described (treated fibers value/untreated fibers value). The improvement of tensile modulus for MAF and ITAF samples with both matrixes was observed from the results of tensile test. Recent improvement of tensile modulus was also observed for all samples treated by silanes, but it was not as high as for the samples with MAF or ITAF. On the other hand we can see massive decrease of tensile strength for MAF and ITAF samples. MSF and GSF samples show no (or not significant) decrease of tensile strength. For VSF-VE and VSF-UP samples lower values of tensile modulus and strength were measured compared to other silane treatments.

Very similar data were measured by the flexural test. The samples with MAF, respectively ITAF showed reduced flexural strength and increased flexural modulus for both matrixes. MSF samples also showed similar trend to GSF samples and VSF had no effect on the improvement of flexural properties.

Because of the destructive effect of MA and ITA treatments and no effect of VS treatment on the mechanical properties of fibers, further attention was focused on the MS and GS treatments.

SEM and XPS analysis

The SEM analysis was performed as a surface analysis for the flax fibers treated by MS and GS. The attention was focused on the silane layer structure. The surface of the fiber was rough and covered by separated areas of silane multilayer. However, treated fibers were not covered fully by consistent silane monolayer, as was expected. This effect was even more pronounced on fibers treated by GS. There were evident multilayer areas of GS on the surface of the fiber. Moreover, those multilayers were more non-consistent, full of defects and more rough than the MS layer.

The silane-origin of the areas was confirmed by the elemental XPS analysis via EDS detector. This method detected several mass percent of Si atoms, which does not correspond to common content of the flax fibers. For MS higher content of C atoms from methacrylate functional groups was detected. For GS an increasing content of O atoms due to glycidyl functional end group of the silane chain was detected.

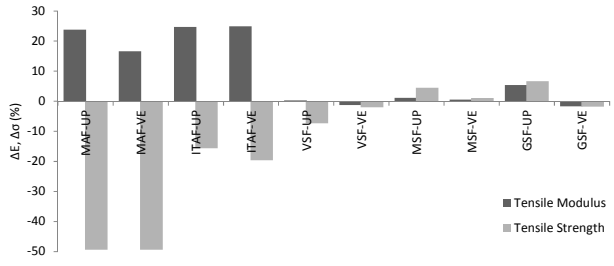

Fig. 1. **Tensile test results of the treated fibers with UP respective VE matrix compared to the reference**

Impact toughness

Another method for testing the interphase quality, performed on the samples with MSF and GSF was the Charpy impact test. The results of the UP and VE samples with MSF and GSF were compared to those of samples with untreated Ref fibers. The MSF-UP and MSF-VE samples showed the decrease of the impact strength up to 7 % and 11 %, respectively. On the other hand the GSF-UP and GSF-VE samples gave the values of impact strength higher up to 11 % and 12 %, respectively, compared to the reference.

Fiber volume fraction effect

The flexural and tensile properties of the composites were investigated as a function of the fiber volume fraction. For this experiment UP composite with Ref fibers was chosen. In the graph of flexural properties shown in Fig. 2 an increase of the flexural modulus with fiber volume fraction is evident. The flexural strength increases with the volume fraction up to 63 vol. % of the fibers. Beyond this value, at higher volume fraction, the flexural strength is constant, or slightly decreases. A similar trend was observed also for the measurements of tensile properties.

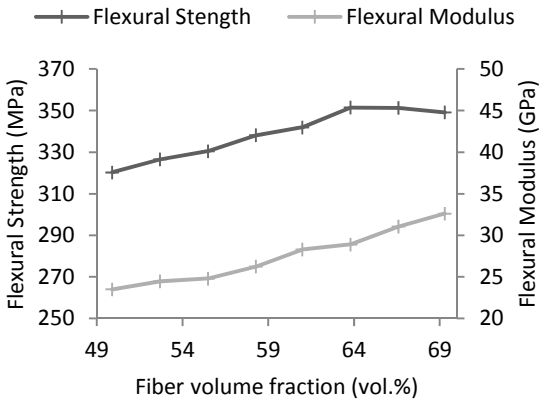

Fig. 9. **Flexural properties of the Ref-UP composite as a function of the fiber volume fraction**

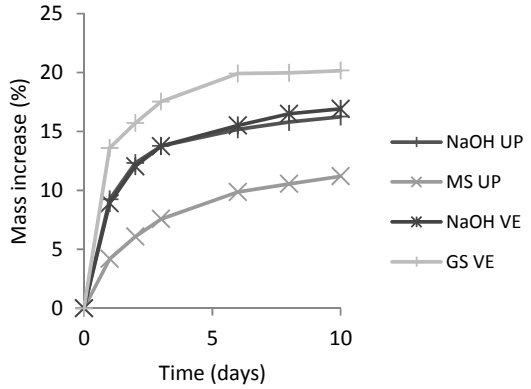

Fig. 3. **Time dependence of water absorption**

Water absorption test

One of the effects of the surface treatment should also be the reduction of water absorption. The composite samples with silane treated fibers were tested for the water absorption. The time-dependencies of the water absorption for the Ref-UP and Ref-VE samples were very close to each other, and can be taken as a reference for this test. Better results of the water resistance were reached for the GSF-UP samples (not displayed) and the best result, the lowest increase of the samples weight, was observed for the MSF-UP composite. Slightly worse water resistance was shown by MSF-VE samples compared to the reference (not displayed). The highest water absorption results provides GSF-VE composite sample.

Conclusion

The flexural and tensile tests were performed on prepared composite samples. From the results we can deduce some improvement of the composite interfacial compatibility for MSF and GSF and no improvement for VSF for both matrixes. MAF and ITAF improve the compatibility much more than silane coupling agents, but they strongly damage the fibers. The tensile strength of those fibers is lower and from this reason the improvement of interfacial compatibility cannot race up the composite strength. Since GSF provides worse mechanical properties compared to MSF, the methacrylate group is much more suitable for used UP, respectively VE matrix.

The SEM photographs show non-consistent silane multilayers and separated silane areas. This is because of a non-optimal method of treatment for flax fibers. Those small silane areas shows only slightly improved mechanical properties described earlier as well. With better treatment procedure much better properties of the composites with MSF and GSF can be expected.

The improvement of the interphase interaction in the composite leads to the increase of brittleness and to the decrease of impact strength. The decrease of the impact strength for the MSF-UP and MSF-VE samples means better coupling properties of MS for Flax-UP or VE composites.

The results of the fiber volume fraction effect on the mechanical properties show the value of 63 vol.% as an optimum. Below this value the flexural and tensile properties increase with increasing fiber fraction and above 63 vol.% the properties are constant or, even, worse. At higher volume of fibers the matrix saturation is insufficient for an effective transfer of the outer stress into the fibers. Moreover, low matrix content cannot perform its bonding function.

The decrease of water absorption should be one of requested achievements of the fiber treatment. MSF-UP composite samples provide the lowest values of water absorption. On the other hand, GSF-VE samples even increase the water absorption compared to the reference.

The most effective and useful fiber treatment method appears to be the MS treatment combined with UP matrix and containing 63 volume % of the fibers reinforcement.

This work was supported by Safilin company (www.safilin.pl) and by the Ministry of Education, Youth and Sports of the Czech Republic, Project No. LO1211.

REFERENCES

1. Kalia S., Kaith B. S., Kaur I., *Cellulose fibers: bio- and nano-polymer composites*, part. 1, (4). Springer, New York (2011).
2. Kabir M. M., Wang H., Lau K. T., Cardona F.: *Composites: Part B*, 43, 2883 (2012).
3. Menčík, P.; Přikryl, R.; Hahn, F. *In Proceedings of the 2nd International Conference on Chemical Technology*. 1. 2014. p. 303–308. ISBN: 978-80-86238-64- 7.
4. Mishra, S., J.B. Naik, Y.P. Patil. T. *Composites Science and Technology*. 2000; 60 (9) 1729.

BINDING OF SURFACTANT TO POLYELECTROLYTE IN NON-STANDARD CONDITIONS – FLUORESCENCE STUDY

MONDEK JAKUB*, MRAVEC FILIP and MILOSLAV PEKAŘ

Brno University of Technology, Materials Research Centre, Faculty of Chemistry, Purkyňova 118, CZ-612 00 Brno, Czech Republic
xcmondek@fch.vutbr.cz

Abstract

Steady-state and time-resolved fluorescence and UV−vis techniques were used to study the formation and dissociation of dodecylacridine orange in order to investigate hyaluronan (polystyrene sulfonate – PSS)−dodecylacridine orange, hyaluronan−CTAB (cetyltrimethylammonium bromide), polystyrenesulfonate−acridine orange, and polystyrenesulfonate−CTAB interactions in aqueous solution. Steady-state and time-resolved fluorescence and the dimer:monomer absorbance ratio of dodecylacridine orange (DAO) were used to determine dimer formation on polymer chains of polyelectrolytes. After the addition of surfactant, we observed an enhancement of fluorescence intensity, indicating the dissociation of DAO dimers into monomers and the replacement of dodecylacridine orange on polymer chains by surfactant molecules. Importantly, we show that surfactant molecules bind to polymer chains before the critical micelle concentration (CMC) is reached and form the so-called "bottle-brush" structure.

Introduction

The aggregation of acridine dyes is a well described phenomenon[1–4]. Negative charge, represented for example by a polyelectrolyte or surfactant, added into a solution of acridine dye causes aggregation of these molecules into dimers due to Van der Waals forces and the strong coupling of molecular transition dipole moments. Coupling causes a wavelength shift in the absorption spectrum. When red or blue shift occurs, aggregates are called J-aggregates or H-aggregates, respectively[2]. The H-type of aggregates have forbidden radiative decay from the excited state and their absorption band is blue shifted. From a spectroscopic point of view, fluorescence of the sample at nearly 530 nm decreases with an increasing amount of dye aggregate; the probability of absorption at 492 nm (monomer band, the α-band) decreases with a concomitant increase in absorption at 465 nm (dimer band, β-band) and at 450 nm (oligomer band, the γ-band). The formation of dye aggregates is, of course, concentration dependent and in the case of acridine orange (AO) the aggregates appear at and above its concentration of $5{\cdot}10^{-5}$ ml·L^{-1} in aqueous solution1. In the presence of a negative binding site – for example, the negative charge of a surfactant or a polyanion – monomers of AO condense on these sites and the dimer form of AO is preferred, which changes its fluorescence intensity and a dimer fluorescent peak appears in the fluorescence spectrum at around 657 nm[2]. Acridine orange aggregates were used to study negatively charged polyelectrolytes[2], probe-DNA interactions[5–7] and probe-protein or protein-surfactant interactions[8–9].

We used acridine orange in our previous study to label hyaluronan binding sites and to observe the increase of fluorescence intensity when cationic surfactant was added into the system[10]. The purpose of this work is to apply the behaviour of acridine orange to its amphiphilic equivalent dodecyl acridine orange and to verify the binding of single surfactant molecules to polyelectrolyte.

Materials and methods

All reagents and solvents were used as received and their purity was higher than 97 %. Samples for acridine orange and polyelectrolyte interaction were prepared as follows: 25 μL of dodecyl acridine orange stock solution were added to plastic vials and a fluorescence probe was diluted with an appropriate volume of hyaluronan (PSS) and solvent to achieve a concentration range for hylauronan from $5{\cdot}10^{-4}$ ml·L^{-1} to 15 g·L^{-1} and for polystyrene sulfonate, from $1.25{\cdot}10^{-5}$ g·L^{-1} to. 3.6 g·L^{-1} Samples for polymer-surfactant interaction were prepared with a constant concentration of dodecyl acridine orange and polymer (respective equivalence point for each polymer determined by formation of acridine orange dimer) and with an increasing concentration of surfactant ranging from $9{\cdot}10^{-5}$ mol·L^{-1} to $2{\cdot}10^{-5}$ mol·L^{-1}. All samples were stirred overnight to ensure equilibration.

Results and Discussion

A Brief Introduction to AO-HyA (PSS)-Surfactant Interactions

Acridine orange was used as a fluorescence label attached to oppositely charged functional groups of biopolymer hyaluronan. The labeling changed the fluorescence and absorption properties of dye molecules due to the formation of AO dimers. The ratio of the number of polymer binding sites to the number of dye molecules (P/D) at the equivalence point was determined at the point of fluorescence intensity minimum.

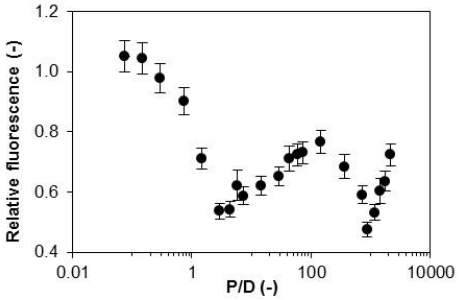

Fig. 10. **Dependency of the relative fluorescence intensity on the P/D of the system with a constant concentration of acridine orange of $1.7{\cdot}10^{-5}$ mol·L^{-1}.** Fluorescence is relative to the sample in which hyaluronan is not present. The concentration of hyaluronan covers the range from 0.5 mg L^{-1} to 15 g L^{-1}

The dissociation of AO dimer upon the addition of surfactant to the system corresponding to the equivalent P/D

value was then used to study polymer-surfactant interactions. The interactions between hyaluronan and AO or surfactant were found to be weaker than the interactions with polystyrene sulfonate, probably due to the high hydration of hyaluronan chains. Critical aggregation concentrations of CTAB determined by the fluorescence method were $3 \cdot 10^{-5}$ M for hyaluronan and $4 \cdot 10^{-6}$ M for PSS. In the presence of polyelectrolyte, surfactant molecules were pulled into the solution before the critical micelle concentration was reached.

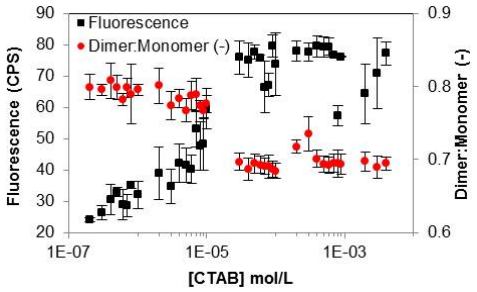

Fig. 11. **Dependencies of the fluorescence intensity and dimer:monomer ratio as a function of CTAB concentration in AO-hyaluronan-CTAB system (concentrations of AO and hyaluronan correspond to the equivalence point $(P/D)_e = 3$)**

According to the fluorescence and absorption spectra of acridine orange in the presence of polystyrene sulfonate (PSS), we suppose that acridine orange forms dimers in the presence of polystyrene sulfonate (See in Mondek et al.[10]). As in the case of hyaluronan, the fluorescence intensity of AO decreased with a concomitant increase in PSS concentration; the minimum was very shallow and it was not easy to determine the equivalence point. The equivalence point was determined as $(P/D)_e = 4$.

From the plot of fluorescence intensity as a function of CTAB concentration, it is obvious that after the addition of a micromolar concentration the fluorescence intensity increased (Fig. 3). The increase in fluorescence intensity means that monomeric surfactant molecules replaced acridine orange dimers.

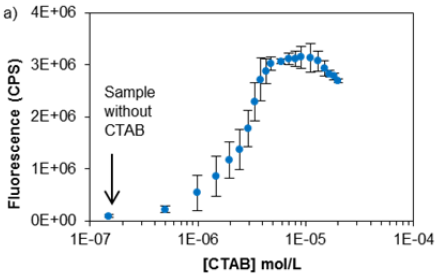

Fig. 3. **Plot of acridine orange fluorescence intensity as a function of increasing CTAB concentration**

Interaction of Dodecylacridine Orange and Hyaluronan

As well as in the case of acridine orange, dodecyl acridine orange (DAO) was used as a fluorescence label attached to oppositely charged functional groups of biopolymer hyaluronan. The labeling changed the fluorescence properties of dye molecules due to the formation of DAO dimers. The ratio of the number of polymer binding sites to the number of dye molecules (P/D) at the equivalence point was determined at the point of fluorescence intensity minimum.

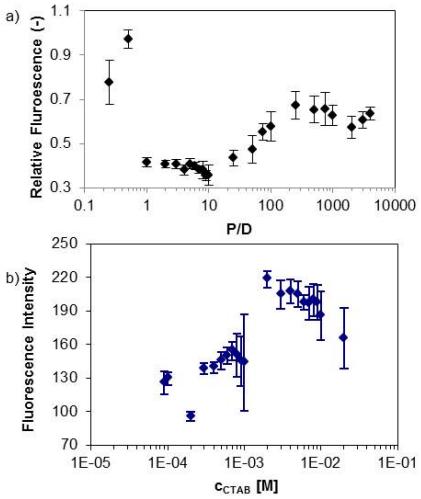

Fig. 4. **a) Dependency of the relative fluorescence intensity on the P/D of the system with a constant concentration of dodecyl acridine orange of $1.7 \cdot 10^{-5}$ mol·L^{-1}.** Fluorescence is relative to the sample in which hyaluronan is not present. b) Dependency of the fluorescence intensity as a function of CTAB concentration in DAO-hyaluronan-CTAB system (concentrations of DAO and hyaluronan correspond to the equivalence point $(P/D)_e = 9$)

The minimum of relative fluorescence intensity can be found in the dependency in Fig. 4a. This minimum is considered as a point of equivalence, the point where all probe molecules condense as dimers on the accessible binding sites of the polymer. If all carboxylic groups are taken into account as possible binding sites and the (dodecyl) acridine orange molecules condense to form dimers, a value of 0.5 for the point of equivalence can easily be predicted (for each carboxylic anion, two probe molecules are necessary). As is obvious from Fig. 4a, the fluorescence intensity minimum is found at a value of P/D = 9. This means that only around 6 % of carboxylic groups are accessible to the DAO molecules. The value of the equivalence point can be explained in a way, that hyaluronan is not fully dissociated or DAO dimer formation is prevented due to interchain interactions. The third reason is that interactions between hyaluronan and DAO are weak, which could also contribute to the high value of equivalence point. Dissociation of hyaluronan is probably not the reason of high equivalence point, because pH of samples suggests full dissociation of hyaluronan. Calculation of the accessibility of polymer binding sites is based on the assumption that, for fully dissociated polymer, each carboxylic group possesses two molecules of dodecyl acridine orange to form dimers and to obtain the minimum of fluorescence intensity. As well as in the previous work with acridine orange[10], it should be noted that the real concentration of hyaluronan in the sample at this equivalence point is 60 mg L^{-1}. At this concentration we are dealing with a highly diluted polymer regime; therefore, the polyelectrolyte hyaluronan should be stretched and fully dissociated[11]. However, in the presence of oppositely charged acridine

orange, a similar phenomenon of a partial collapse may occur, as observed in polyelectrolyte-surfactant systems[12], in which the chain extension is decreased, which may also result in the hiding of hyaluronan carboxylic groups.

Steady-state fluorescence was further used to study the interaction of CTAB with the DAO-hyaluronan system (Fig. 4b). The fluorescence intensity of dodecyl acridine orange in a sample at the equivalence point $(P/D)_e$ without the addition of CTAB was significantly smaller than the fluorescence intensity in the presence of CTAB at the lowest concentration used, which indicates that, at the equivalence point, there should be significant occupation of carboxylic groups of hyaluronan by DAO dimers. This increase in fluorescence intensity could be ascribed to the electrostatic interaction between hyaluronan and CTAB and to the dissociation of DAO dimers. When the surfactant concentration was around its CMC, the fluorescence intensity decreased (see Fig. 5b). Such a phenomenon may be caused by the aggregation of some AO monomers into dimers again due to the formation of micelles or other micelle-hyaluronan aggregates. Experiments with DAO agrees well with the experiments with acridine orange, meaning, that DAO confirms the assumption, that before the critical micelle concentration was reached, the electrostatic interaction caused the molecules of the surfactant not to remain at the air-water interface but to bind to carboxylic groups of hyaluronan[10, 12, 13].

Interaction of Dodecylacridine Orange and Polystyrene sulfonate

In DAO-PSS system occured similar phenomenon as well as in case of DAO-hyaluronan or AO-hyaluronan (PSS) systems (Fig. 5a). Firstly, fluorescence intensity decreased with increasing P/D value. Equivalence point was determined as $(P/D)_e = 3$. Above the P/D_e, the number of available polymer binding sites increases with a concomitant increase in the fluorescence intensity because of the dissociation of acridine orange dimers. But at high P/D values, there is significant difference between hyaluronan and PSS. We observe fluctuations in fluorescence intensity with increasing P/D value (polymer concentration) in case of hyaluronan. In our previouse study[10] is stated that when the concentration of binding sites increases nearly thirty times (from P/D~3 to P/D~90), the fluorescence intensity measured for P/D~90 is lower than the values at low P/D. This suppressed fluorescence intensity may be caused by conformational changes in hyaluronan. The experiment with AO-PSS and DAO-PSS confirms above stated assumption, because the fluorescence intensity was increasing in DAO-PSS system, until the system reached the free probe-like fluorescence intensity.

Interaction of CTAB with the DAO-PSS system was further studied (Fig. 5b). Again, the fluorescence intensity of dodecyl acridine orange in a sample at the equivalence point $(P/D)_e$ without the addition of CTAB was significantly smaller than the fluorescence intensity in the presence of CTAB at the lowest concentration used, which indicates significant occupation of PSS binding sites and the replacement of DAO dimers with CTAB molecules.

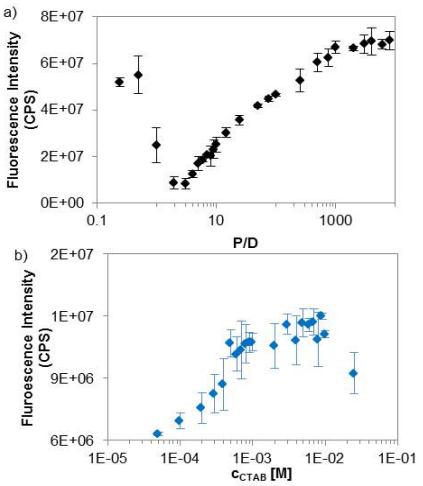

Fig. 5. **a) Dependency of the relative fluorescence intensity on the P/D of the system with a constant concentration of dodecyl acridine orange of $1.7 \cdot 10^{-5}$ mol·L^{-1}.** Fluorescence is relative to the sample in which PSS is not present. b) Dependency of the fluorescence intensity as a function of CTAB concentration in DAO-PSS-CTAB system (concentrations of DAO and PSS correspond to the equivalence point $(P/D)_e = 3$)

Conclusions

Dodecyl acridine orange was used as a fluorescence label attached to oppositely charged functional groups of biopolymer or synthetic polyelectrolyte – hyaluronan and polystyrene sulfonate, respectively, and as a comparison to previous work performed with acridine orange. Results with dodecyl acridine orange confirmed the formation of dimers on the binding sites of polymers and, most importantly, the experiment confirmed the replacement of DAO dimers with single surfactant molecules before critical micelle concentration was reached. The conformational changes of hyaluronan above the equivalence point were suggested when compared to PSS experiments. The formation and dissociation of dodecyl acridine orange dimer exhibited the formation of the "bottle-brush" structure caused by the adsorption of surfactants on the polyelectrolyte chain.

This work was supported by the Materials Research Centre at FCH BUT- Sustainability and Development, REG LO1211, with financial support from the National Programme for Sustainability I (Ministry of Education, Youth and Sports).

REFERENCES

1. Costantino, L.; Guarino, G.; Ortona, O.; Vitagliano, V., Journal of Chemical & Engineering Data 29, 1 (1984).
2. Peyratout, C.; Donath, E.; Daehne, L., Journal of Photochemistry and Photobiology A: Chemistry, 142, 1 (2001).
3. Lamm, M. E.; Neville, D. M., The Journal of Physical Chemistry 69, 11 (1965).
4. Antonov, L.; Gergov, G.; Petrov, V.; Kubista, M.; Nygren, J., Talanta 49, 1 (1999).

5. Lauretti, F.; Lucas de Melo, F.; Benati, F.; amp; x; cio, J.; de Mello Volotão, E.; Santos, N.; Linhares, R. E. C.; Nozawa, C., Journal of Virological Methods 114, 1 (2003).
6. Ito, F.; Kakiuchi, T.; Nagamura, T., The Journal of Physical Chemistry C 111, 19 (2007).
7. Sarkar, D.; Misra, T. N., Biomaterials 10, 3 (1989).
8. Smal, J.; Kathuria, S.; De Meyts, P., FEBS Letters, 244, 2 (1989).
9. Wang, F.; Yang, J.; Wu, X.; Wang, X.; Feng, L.; Jia, Z.; Guo, C., Journal of Colloid and Interface Science, 298, 2 (2006).
10. Mondek, J., Mravec, F., Halasová, T., Hnyluchová, Z., Pekař, M., Langmuir, 30, 29 (2014).
11. Matteini, P.; Dei, L.; Carretti, E.; Volpi, N.; Goti, A.; Pini, R., Biomacromolecules, 10, 6 (2009).
12. Bain, C. D.; Claesson, P. M.; Langevin, D.; Meszaros, R.; Nylander, T.; Stubenrauch, C.; Titmuss, S.; von Klitzing, R., Advances in Colloid and Interface Science, 155, 1–2 (2010).
13. Goddard, E. D., Journal of Colloid and Interface Science, 256, 1 (2002).

BIOTECHNOLOGICAL PRODUCTION OF POLYHYDROXYALKANOATES ON VARIOUS LIGNOCELLULOSE-BASED AGRICULTURAL WASTES

STANISLAV OBRUCA, DAN KUCERA, TEREZIA DINGOVA, PAVLA BENESOVA, JAROMIR PORIZKA and IVANA MAROVA

Faculty of Chemistry, Brno University of Technology, Purkynova 118, 612 00 Brno, Czech Republic
obruca@fch.vutbr.cz

The exponential growth of human population has led to accretion of huge amounts of non-degradable waste materials of plastic origin across the globe. Hence, attention is paid to biodegradable alternatives of synthetic polymers. Among these biodegradable materials, bacterial polyesters – polyhydroxyalkanoates (PHAs) are considered as the very promising materials[1]. PHAs are accumnulated as carbon and energy reserve materials by a wide variety of bacterial strain. When extracted from bacterial cells, their properties reminds of those of polyethylene or polypropylene[2]. Generally, mechanical and technological properties of PHAs depend on monomer composition. The most common member of PHAs family – poly(3-hydroxybutyrate) possesses highly crystalline structure that makes it relatively stiff and brittle. Nevertheless, the mechanical properties of PHB can be significantly improved by the incorporation of other monomer units into the PHA structure. For instance, the incorporation of 3-hydroxyvalerate results in the material (poly(3-hydroxybutyrate-co-3-hydroxyvalerate), P(3HB-*co*-3HV)) with increased flexibility and decreased melting point[3].

Generally, the main obstacle preventing PHAs from entering the market massively is their production cost. The analysis and economic evaluation of the bacterial PHAs productions suggested, that the cost of substrate (mainly carbon source) contributed the most significantly (up to 50%) to the overall production cost. Thus, cheap waste substrates attract the attention of both scientific researches and industrial companies in as they reduce the PHAs production cost and make this environmental friendly product also more economically feasible[4].

Lignocellulose biomass includes agricultural and forestry residues, portions of municipal solid waste as well as herbaceous and woody crops. With the annual generation of 80 billion tons, lignocellulosic materials have a great potential for the production of a wide variety of industrial and commodity products including paper, lumber, bioethanol, biodegradable polymers (e.g. PHAs) and a range of fine chemicals. Such materials are abundant and competitive in price with petroleum, and, therefore, lignocellulose biomass can provide a sustainable resource also for fermentative production of PHAs[5].

This work deals with identification of potential strategies for biotechnological production of PHAs from various lignocellulose-based waste materials (such as apple fiber, corn stover, spent coffee grounds, spend malt grains and wine pomace) employing *Burkholderia cepacia*, *Bacillus megaterium* and *Burkholderia sacchari*.

Lignocellulose materials were subjected to enzymatic and/or diluted acid (1 % H_2SO_4, 120 °C, 20 min.) hydrolysis prior to their utilization as waste carbon substrates for cultivation. Composition of the hydrolysates was analysed by HPLC-RID/PDA (sugars, furfurals) and ion chromatography (organic acids). The first cultivations were conducted in Erlenmeyer flasks, hydrolysates of lignocellulose materials were used as sole carbon sources and medium was supplemented with mineral salts as described elsewhere[6]. At the end of cultivation, biomass concentration was determined gravimetrically and PHAs content in bacterial cells was assayed by GC-FID as described previously[7]. The cultivations on the most promising waste materials were also performed in laboratory bioreactor. Since we discovered capability of *B. cepacia* to excrete lignocellulytic enzymes and utilize non-hydrolyzed lignocellulose materials, we also characterized its hydrolytic enzyme cocktail by enzymatic assays and PAGE-SDS.

At first, we performed diluted-acid-mediated hydrolysis of lignocellulose materials and the liquid hydrolysates were used as an energy and carbon source in the production medium for PHAs production employing two bacterial strains – *Burkholderia cepacia* and *Bacillus megaterium* the results are shonw in Table 1. Generally, significantly higher growth as well as PHAs titers was gained with *B. cepacia*. Moreover, *B. cepacia* was able to accumulate copolymer poly(3-hydroxybutyrat-*co*-3-hydroxyvalerate) [P(HB-*co*-HV)] having more desirable properties than homopolymer poly(3-hydroxybutyrate) produced by *B. megaterium*. Levulinic acid present in hydrolysates probably served as the precursor of 3HV for the copolymer biosynthesis.

Table 1
PHAs production from hydrolyzates of lignocelloses by *B. megaterium* and *B. cepacia*

Material	***Bacillus megaterium***		
	CDW[1] [g·l^{-1}]	PHA in CDW [%]	PHA [g·l^{-1}]
control[2]	1.3 ± 0.0	17.2 ± 2.5	0.2 ± 0.0
coffee grounds	1.2 ± 0.1	*n.d.*	*n.d.*
apple pomace	2.0 ± 0.1	41.6 ± 3.1	0.8 ± 0.1
rapeseed pomace	1.7 ± 0.0	8.8 ± 0.3	0.2 ± 0.0
wine pomace	2.1 ± 0.2	31.3 ± 3.5	0.7 ± 0.0
Material	***Burkholderia cepacia***		
	CDW[1] [g·l^{-1}]	PHA in CDW [%]	PHA [g·l^{-1}]
control[2]	4.4 ± 0.0	52.2 ± 4.7	2.3 ± 0.2
coffee grounds	3.2 ± 0.1	19.6 ± 1.8	0.6 ± 0.0
apple pomace	5.0 ± 0.8	34.1 ± 3.1	1.7 ± 0.1
rapeseed pomace	3.9 ± 0.2	5.6 ± 2.4	0.2 ± 0.1
wine pomace	3.7 ± 0.2	23.1 ± 0.7	0.8 ± 0.0

[1] CDW stands for cell dry weight
[2] Glucose (20 g l^{-1}) based medium was used as a control in the experiment

Further, we were surprised that *B. cepacia* was capable of utilization of non-hydrolyzed lignocellulose materials and growing in the mineral medium with these solid materials as the only carbon source (Fig. 1). This indicates that *B. cepacia* is capable of excretion of hydrolytic enzymes (celulases, hemicelulases, proteases and lipases) which might be considered as interesting biotechnological products. Co-production of extracellular enzymes and intracellular PHAs on cheap waste substrates; hence, also deserves particular experimental attention as interesting biotechnological strategy.

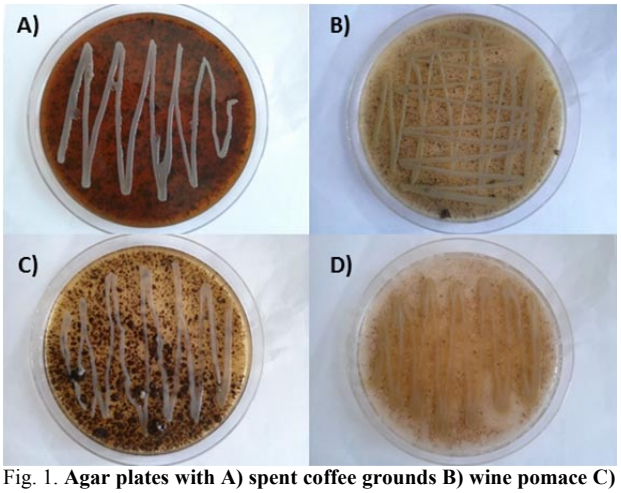

Fig. 1. **Agar plates with A) spent coffee grounds B) wine pomace C) rapeseed D) apple pomace**

Therefore, in our further experiments we focused on study of co-production of selected extracellular enzymes and PHAs. In these experiments we utilized spent coffee grounds (SCG) as a substrate because we had experience with utilization of this agricultural waste stream for production of PHAs[6] and carotenoids[8]. Moreover, unlike other lignocellulse materials, SCG do not contain free sugars and; thus, the growth of the bacterial culture can be entirely attributed to enzymatic hydrolysis of lignocellulose material.

We compared the influence of the method of hydrolysis – chemical hydrolysis by diluted acid, enzymatic hydrolysis by enzymatic system of *B. cepacia* and combination of diluted acid hydrolysis and enzymatic hydrolysis. In case of acid hydrolysis, SCG were removed from cultivation broth after hydrolysis prior to inoculation. When acid hydrolysis was combined with enzymatic hydrolysis, the procedure was the same as for acid hydrolysis, but the SCG were left in the medium during cultivation to be hydrolyzed by extracellular enzymatic system of *B. cepacia*. The last collection of samples was not subjected to hydrolysis by diluted acids and bacterial culture was cultivated on SCG without any pretreatment. After the end of cultivation (72 h), biomass and its PHAs content was determined (Fig. 2) and also activity of selected hydrolytic enzymaes was measured (Fig. 3). Generally, the highest titers of PHAs as well as biomass were achieved in the medium were SCG were hydrolyzed by diluted acid and removed from the medium before cultivation. There is a significant decrease in yields using a combination of acid and consequently the enzymatic hydrolysis. This is probably caused by substances in the SCG inhibiting the growth of the culture which were released from SCG during cultivation.

Gas chromatography of the samples identified two different types of PHAs. Besides PHB, 3-hydroxyvalerate was observed in the samples pretreated by diluted mineral acid. It is very likely that some component which was formed during hydrolysis of SCG by diluted mineral acids served as precursor of 3-hydroxyvalerate. From the spectrum of potential precursors it can be expected that it was levulinic acid – product of degradation of hexoses, which enabled accumulation of P(HB-*co*-HV) copolymer.

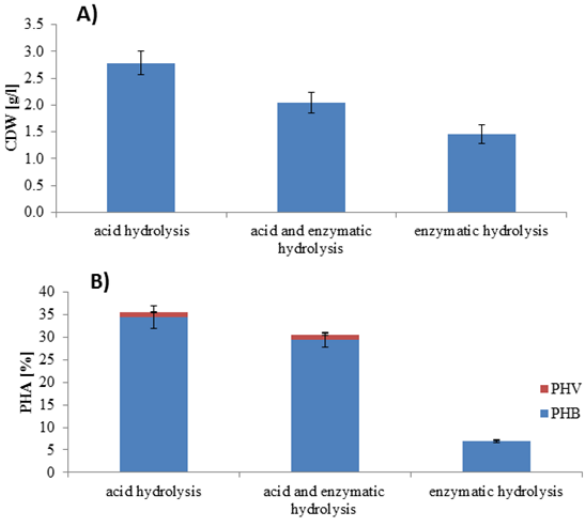

Fig. 2. **Biomass (A) and PHAs (B) concentrations obtained on SCG treated by different approaches**

Fig. 3 shows effect of the hydrolysis method on the activities of selected biotechnologically important extracellular enzymes of *B. cepacia*. In general, we can say that the enzymatic activity was lowest in the sample, where the medium did not contain solids of SCG. The reason is obvious - the bacteria did not need to produce lignocellulose degrading enzymes. This hypothesis explains the highest biomass yield, the bacteria that can fully "focus" on the production of PHAs as a storage polymer utilizing simple sugars. Furthermore, it is apparent that in the medium after acid hydrolysis with solid SCG is much greater cellulase activity than in the last sample. Hydrolysis by diluted acid is able to cleavage hemicelluloses but not highly resistant cellulose. On the other side, hydrolysis of hemicelluloses made cellulose much more accessible to action of enzymatic hydrolysis. This may explain why the highest cellulose activity was observed in the sample where SCG were exposed to acid hydrolysis. On the contrary, when SCG was not hydrolyzed prior to cultivation, bacterial culture was able to excrete the highest amount of lipase and protease, which represent important industrial enzymes. Therefore, the pretreatment of SCG can be used as a tool to control spectrum of the products of the intended technology. Acid hydrolysis with subsequent removal of SCG prior to cultivation results in the highest PHAs yields. On the other side, when SCG are

leaved in the cultivation, bacterial culture produces also high amount of PHAs, but also high amount of extracellular enzymes, in particular, production of cellulose is enhanced significantly. Finally, when SCG are not hydrolyzed by diluted acid, bacterial culture accumulates only low amount of PHB (up to 10 % of CDW) but it is able to produce sustainable amount of extracellular hydrolytic enzymes – especially lipase and protease.

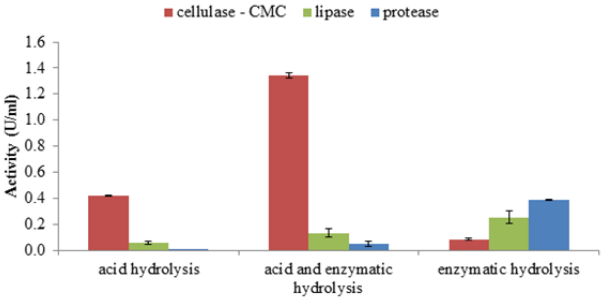

Fig. 3. **Activities of selected extracellular hydrolytic enzymes produced by *B. cepacia* on SCG by different cultivation approaches**

In conclusion, we identified *B. cepacia* as a very promising candidate strain for biotechnological production of PHAs from lignocellulose materials. Not only that this bacteria is capable of utilization of wide spectrum of diluted-acid pretreated lignocelluloses while producing P(HB-*co*-HV) copolymer, but this bacteria also revealed ability to excret hydrolytic enzymes which are of biotechnological interest (cellulose, lipase, protease) when cultivated on non-pretrated solid lignocellulose materials. Hence, co-production of intracellular PHAs and extracellular enzymes from cheap waste materials is possible and pretreatment of the lignocellulose material and adopted cultivation strategy can be used to control the prevalent product of the process (PHAs or enzymes).

This work was supported by the project "Materials Research Centre at FCH BUT – Sustainability and Development" No. LO1211 of the Ministry of Education, Youth and Sports of the Czech Republic and by the project GP15-20645S of Czech Science Foundation.

REFERENCES

1. Philip S., Keshavarz T., Roy I.: J. Chem. Technol. Biotechnol. *82* , 233 (2007).
2. Sudesh K., Abe H., Doi Y.: Prog. Polym. Sci. *25*, 1503 (2000).
3. Lee W. H., Loo C. Y., Nomura C. T., Sudesh K.: Bioresource Technol. *99,* 6844 (2008).
4. Choi J., Lee S. Y.: Appl. Microbiol. Biotechnol. *51*, 12 (1999).
5. Obruca S., Benesova P., Marsalek L., Marova I.: Chem. Biochem. Eng. Q. *29* , 151 (2015).
6. Obruca S., Benesova P., Petrik S., Oborna J., Prikryl R., Marova I. Process Biochem *49*, 1409 (2014).
7. Obruca S., Marova I., Snajdar O., Mravcova L., Svoboda Z.: Biotech Lett. *32*, 1925 (2010).
8. Petrik S., Obruca S., Benesova P., Marova I. Biochem. Eng. J. *90*, 307 (2014).

SMALL BERRIES AS AN IMPORTANT SOURCE OF ANTIOXIDANTS.

ZUZANA OLSOVCOVA, MILENA VESPALCOVA, PAVEL DIVIS, JITKA MATEJICKOVA, JIŘÍ KAPLAN, and ALES MATEJICEK

Brno University of Technology, Faculty of Chemistry, Purkynova 118, CZ – 612 00 Brno
xcolsovcova@fch.vutbr.cz

Small fruit contains high levels of beneficial effects of substances on human organism. It is mainly the amount of polyphenolic substances from flavonoids, phenolic acids, proanthocyanidins and anthocyanins, which give fruits characteristic color and are able to eliminate free radicals from the cells[1]. Furthermore organic acids which give the typical acidic flavor of fruits, and a number of vitamins and minerals. Last but not least fruits contain simple carbohydrates that give fruit sweet taste[1, 2].

Blackcurrants (Ben Hope and Moravia species) are usually grown like deciduous shrub that produces small dark berries with significantly high content of vitamin C and in terms the content flavonoids of blackcurrant beyond only the fruits like blackberries, raspberries, rose hips and sea buckthorn. In the Czech Republic is growing at 17 major species of blackcurrant[3, 4]. Jostaberry and Jocheline are crosssbreeds of blackcurrants and gooseberries. Visually they are looking like both nature species. They are deciduous shrubs thornless. Fruits are dark purple color as well as black currant contains a high content of vitamin C[5, 6]. Black Negus, with its dark fruit belongs to gooseberry among deciduous shrubs. It also contains a high content of vitamin C, polyphenols and fiber[3]. They join in other fruits, which containing low pectines for the production of jams and marmalades[2]. Elderberry (Sambo and Weihenstephan species) is also numerically grown deciduous broad-leaved shrub[7]. Cultivated species of elderberries are 17 in the Czech Republic. Wild species are appearing in the fields or upon edge of the forest. Its fruits are small, black, round, shiny drupe, which begin to ripen in late August. The juices from these fruit are mainly used as a food coloring[7, 8]. Honeysuckles (Blue Triumph and Helfstyn species) are ones of the less known fruits[9]. In our conditions they are grown only very rarely. We knew about 180 kinds of these modest deciduous shrubs[10]. Juice of elongated fruit is most commonly used as a food dye[9, 10]. Rowan berries (Likernaja and Granatina species) are widespread shrubs or trees in the northern hemisphere[11]. It is known about 150 different kinds of berries modest soil conditions[12]. Dark fruits cranes are the result of intersecting. They contain relatively large amounts of organic acids, simple carbohydrates, and polyphenols[11].

The last few years, the consumption of these small berries are very significant in terms of potential health benefits associated mainly with antioxidant properties of substances which are largely appear in fruits[1]. Also acts against inflammations, suppresses fever, relieve pain, and detoxify the body. Acts against the effects of aging and the substances contained in them helps prevent antidiabetic and cancer[1,2].

In this work, we focused on comparing the content of some of the aforementioned biologically active substances in small, often ignored fruit. We chose the colored, dark red and black fruit that contain anthocyanin pigments and that can grow in our climate. We analyzed blackcurrant, jostaberry, jocheline, variety of gooseberry Black Negus, superior breeding elderberry, honeysuckle and Rowan berry, harvested in 2015.

Total content of polyphenols. Samples were obtained by homogenizing 4.7 g of berries and diluted to the final volume of 25 ml. To the tubes were pipetted 0.1 ml of Folin-Ciocalt reagents, 1.8 ml of distilled water and 0.1 ml of diluted sample. To the solutions were added a solution of 1 ml of 7% sodium carbonate after 5 min. The prepared samples were left at room temperature for 2 hours, and then samples were measured in a spectrophotometer at 750 nm. Each sample was measured three times. The concentration of polyphenols based on the concentration of gallic acid.

Content of anthocyanins. Juices for determining the content of anthocyanin pigments are the same as for the determination of polyphenols. To one tube was pipetted 2.9 ml of potassium chloride buffer at pH 1 and 0.1 ml of sample. Into next tube was pipetted 2.9 ml sodium acetate buffer at pH 4.5 and 0.1 ml of sample. The contents of the tubes were mixed thoroughly and immediately measured in a spectrophotometer at 510 and 710 nm. Each sample was prepared in triplicate. The final concentration of anthocyanin pigments is converted to cyanidin 3-glucoside.

Determination of vitamin C by HPLC. Samples were prepared by homogenizing 4.7 g of fruits with metaphosphoric acid to volume of 25 ml. Chromatographic conditions were defined as flow rate of 1 ml/min, Gemini C18 column (150 × 4.6 mm and 5 μm particles), which was thermostated at 30 °C, detector wavelength set to 254 nm. The mobile phase was made up of a solution of potassium dihydrogenphosphate and methanol 9:1 and a volume of sample which was injected to loop was 10 μl.

Table 1
Content of polyfenolics (TCP), anthocyanins (TCA) and vitamin C in mg/100 g fresh fruits in small berries

Variety	TCP	TCA	TCP/TCA	Vitamin C
Black Negus	263.2	94.7	2.8	34.4
Josta	379.1	106.9	3.6	91.3
Jocheline	288.3	43.3	6.7	82.1
Ben Hope	478.5	126.1	3.8	238.5
Moravia	433.9	119.9	3.6	152.9
Sambo	569.3	297.9	1.9	144.6
Weihenstephan	681.2	319.8	2.1	178.7
Likernaja	2115.2	752.9	2.8	3.5
Granatina	2624.3	895.3	2.9	7.1
Blue Triumph	424.9	228.3	1.8	33.4
Helfstyn	723.6	399.4	1.9	10.8

From the Table 1 and Fig. 1 is evident the subsequent good correlation of the content of anthocyanin pigments and total polyphenols. The biggest content of polyphenols was determined in rowan berries, from 2115.2 to 2624.3 mg/100 g of fresh fruit. The minimum content was represented by gooseberry Black Negus, 263.2 mg/100 g of fresh fruit. The most of anthocyanin pigments from 752.9 to 895.3 mg/100g were also detected in rowan berries. At crosssbreeds and their native species, blackcurrants and gooseberries (Black Negus) 94.7 mg/100 g were detected the lowest amount of anthocyanins. The lowest ratio of total polyphenols and anthokynů was found in honeysuckles and elderberries, ranging from 1.8 to 2.1. The ratio shows the representation content of anthocyanins in the total polyphenols.

As another substance for the initial screening of small fruits were vitamin C and its contents. At first sight is obvious that large amount of vitamin C were in the blackcurrants, from 152.9 to 238.5 mg/100 g and the least L-ascorbic acid was found in rowan berries, it was about units of mg per 100 g fresh fruits.

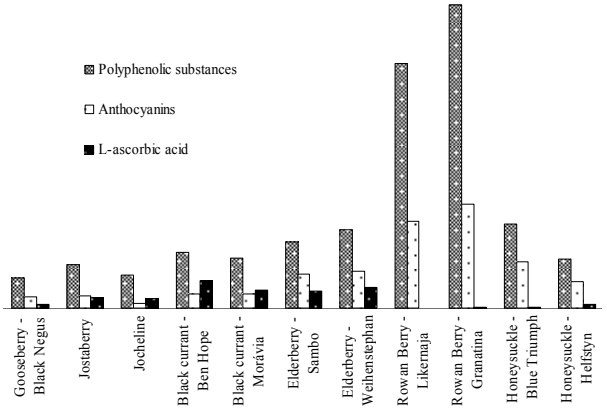

Fig. 1. **Representation of contents of the specified values of selected biologically active compounds in small fruits**

Ones of the most consumed small fresh fruits are undoubtedly currants, gooseberries and their crossbreds. They are a good source of vitamin C and important polyphenols which also include anthocyanins. More suitable for consumption to appear elderberries products, which are currently comes to the forefront on the Czech market.

The study was financially supported by the project no.QI111141 MA.

REFERENCES

1. Mitchell, C., Brennan, R. M., Cross, J. V. and Johnson, S. N.: Agric. For. Entomol. *13*, 3 (2011).
2. Ramadan, M. F.: Food Res. Int. *44*, 7 (2011).
3. Pantelidis, G., Vasilakakis, M., Manganaris, G., Diamantidis, G.: Food Chem. *102*, 3 (2007).
4. Vagiri, M., Ekholm, A., Oberg, E., Johansson, E., Andersson, S., Rumpunen, K., Hajduch M., Šarek J.: J. Agric. Food Chem. *69*, 39 (2013).
5. Hempfling, K., Fastowski, O., Celik, J., Engel, K. H.: J. Agric. Food Chem. *61*, 38 (2013).
6. Khanal, B. P., Grimm, E., Knoche, M.: Sci. Hortic. *128*, 3 (2011).
7. Ozgen, M., Scheerens, J., Reese, R. N., Miller, R. A.: Pharmacogn. Mag. *6*, 23 (2010).
8. Johnson, M. C., Thomas, A. L., Greenlief, C. M.: J. Agric. Food Chem. *63*, 23 (2015).
9. Bonarska-Kujawa, D., Pruchnik, H., Cyboran, S., Zylka, R., Oszmianski, J., Kleszczynska, H.: J. Membr. Biol. *247*, 7 (2014).
10. Kusznierewicz, B., Piekarska, A., Mrugalska, B., Konieczka, P., Namiesnik, J., Bartoszek, A.: J. Agric. Food Chem. *67*, 7 (2012).
11. Hukkanen, A. T., Polonen, S. S., Karenlampi, S. O., Kokko, H. I.: J. Agric. Food Chem. *54*, 1 (2006).
12. Mlcek, J., Rop, O., Jurikova, T., Sochor, J., Fisera, M., Balla, S., Baron, M., Hrabe, J.: Cent. Eur. J. Biol. *9*, 11 (2014).

PRINCIPAL COMPONENT ANALYSIS OF NIR SPECTRAL DATA USED AS FORENSIC METHOD FOR INKJET PRINTED DOCUMENT

MICHAL ORAVEC*, LUKÁŠ GÁL and MICHAL ČEPPAN

Faculty of Chemical and Food Technology, Slovak University of Technology in Bratislava, 812 37 Bratislava, Slovak Republic
michal.oravec@stuba.sk

This paper is focused on analyzing documents by combination of fiber optic reflection spectra in Near Infrared Region (NIR) and multivariate statistical method – Principal component analysis (PCA)[1]. The approach of non-destructive method can be used to verify the authenticity of documents or to identify inks on questioned documents.

The aim of this work was to study the interrelationships of 19 samples prepared by inkjet devices from three different manufacturers Canon, Epson and HP. Samples were printed on the same type of office paper by black ink only. The spectra were obtained by Ocean Optics system in two spectral regions i.e. overtones 1000–1600 nm and combination bands 1600–2300 nm separately. The spectrophotometer was calibrated on the blank paper. The most important output of PCA is scatter plot of the component scores[2]. The goal of this paper was to classify the samples into groups. The groups of samples were highlighted with regard to similarity of the shape of the spectra. Next step of the experiment was confrontation of the groups with the information which we have about questioned devices. The most substantial facts were originality of used ink in inkjet device, type of printer and manufacturer. The results show inconsistency between samples of the same type of manufacturer and their locations in several groups in scatter plots of PCA (PCA models). Spectra of Canon manufacturer differ from each other and do not create one group. Also OEM (original equipment manufacturer) and third party inks used for printing samples were examined in the PCA models. We notice that loading graphs can be helpful in our investigation as indicates major differences of examined spectra shape in the PCA models.

The results suggests, that the combination of non-destructive methods of molecular spectroscopy in NIR region and chemometric method PCA with a sufficiently large and diverse database can be useful tool for analyzing of inkjet printed documents. The measured set of data collected in this study has established the database of the samples printed by inkjet devices. This database will be extended in the near future.

Experimental

In our experiment 19 samples of inks of 3 manufacturers (Canon, Epson and HP) of inkjet devices (Table 1) were analyzed. Every sample was prepared on the office paper (Xerox Performer 80 g/m^2) and consists of full squares printed by black ink only. The squares were measured using the fiber optics spectrophotometer Ocean Optics NIR256-2.5 in the range of 1000–2300 nm. The reflex probe adapter with beam geometry 45°/45° was used to eliminate specular reflections. For each measurement, the detector was calibrated on the blank paper – near the inked area.

In this way we create database NIR spectra of contemporary inkjet devices. The database contains OEM inks and also third party inks. Both groups of spectra was pre-processed and analyzed by PCA separately. For this transformation the software The Unscrambler X was used. The important part of this work was to design an appropriate procedure of pre-processing of raw spectral data for our experiments in PCA.

The combination of transformation methods were selected with regard to optimal results in PCA models. Our aim was to achieve the variance described by the first two principal components as high as possible.

Table 1
Overview of the inkjet printers used for preparation of the samples

Sample	Manufacturer	Type of Print Device
C1	Canon	IP 3000
C2	Canon	Pro 9500 II
C3	Canon	IP 4300
E1	EPSON	SX 425
E2	EPSON	PMD 800
E3	EPSON	PM 830c
E4	EPSON	PX 730WD - OEM ink
E5	EPSON	DX 7400
E6	EPSON	PX 730 WD - third party ink
E7	EPSON	P50 - third party ink
E8	EPSON	P50 - OEM ink
E9	EPSON	SX 130 - third party ink
E10	EPSON	L 210
H1	HP	Photosmart C4580
H2	HP	Photosmart 3210
H3	HP	Photosmart C3180
H4	HP	DeskJet 920C
H5	HP	Photosmart C1410
H6	HP	Office jet Pro 8100

For NIR spectra were used pre-processing transformation methods e. g. smoothing filter Sawitsky–Golay[3], de-trending[4] and baseline correction[5] etc. The detail procedure of pre-processing transformation is described in the paper[6].

Therefore, inputs of PCA method were pre-processed spectra. PCA method provides the output information in various forms.

For our experiments very important output of PCA are PCA models. The samples, in this plot, were localized based on their mutual differences. In the two dimensional space, of the scatter plot, the samples were classified into groups with regard to pre-processed spectra of the samples. In this way the human factor of sorting samples is reduced.

Important step of analysis was confrontation of created groups of samples with available information about inkjet

devices. We noticed information such as manufacturer, originality of used ink and type of print device.

Results and discussion

Collected spectra were pre-treated as described above. Based on the scatter plot of PCA, some spectra were divided into groups. The spectra of the samples of different groups were analysed by mutual visual comparison. The groups were generated with regard to similarity in shapes of spectra. We found out that NIR spectra vary in their shapes, but individual peaks are located close to one to the other. This is the reason, why mere visual resolution of NIR spectra is not suitable[7]. Due to relative high described variance of the first two principal components, our PCA are prepared for a valuable and successful interpretation of sample relations. However, in the PCA model 1600–2300 nm, the variance described by first two principal components was only 79 %. Remaining PCA model described 96 % of variance. In spite of lower level of variance in PCA model 1600–2300 nm there is a group of spectra G3 with the same samples as are in group G2. Group G2 is in model 1000–1600 nm. Both of the groups were marked with regard to spectra comparison. Considering the equality of G2 and G3, we suppose, that the variance 79 % in 1600–2300 nm model is sufficient for analyzing our samples.

In the PCA model 1000–1600 nm were marked two groups G1 and G2 (Fig. 1). It is evident that spectra of these two groups are different (Fig. 2). Group G2 is more compact then G1. Loading graph (Fig. 4) of first principal component indicates positives and negative correlations of spectra. Wavelengths with negative correlation, below –0.7 represent regions with better visual distinctness and vice versa. Spectra E3 and E7 (Fig. 2) are very similar, particularly, in the first half of the wavelength range. The other half range were decisive for non-inclusion the samples into G2. Spectrum C3 differs from the spectra of G2 i.e. C3 is not in any group. Samples E6 and E9 are not included into G1 because of diffrences in the second half range (Figure 3). In the scatter plot of the component score (Fig. 1) E6 and E9 are shifted to G1 along the first and second principal components. Samples E6, E9 and E7 were prepared from third party inks used in Epson devices.

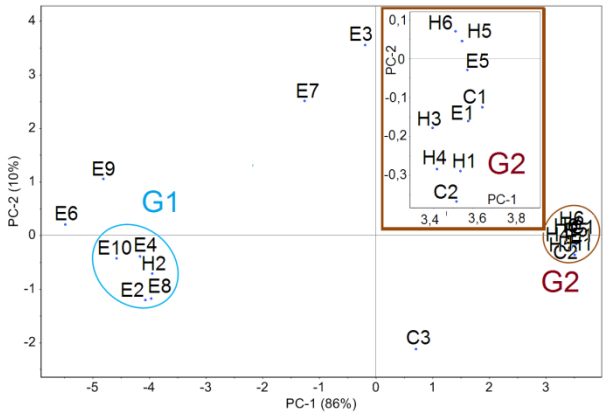

Fig. 1. **PCA model in the range of 1000–1600 nm**

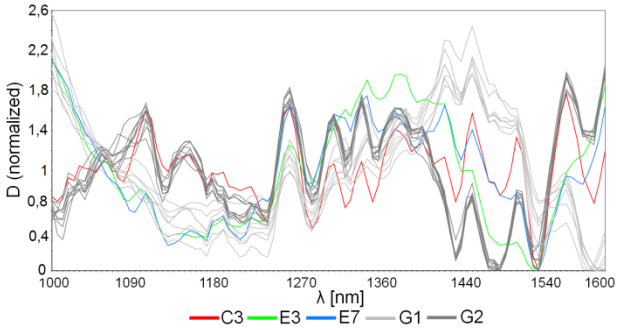

Fig. 2. **Comparison of spectra C3, E3 and E7 with G1 and G2**

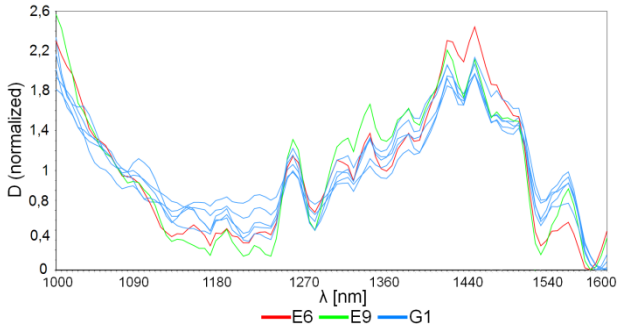

Fig. 3. **Comparison of spectra E6 and E9 with G1**

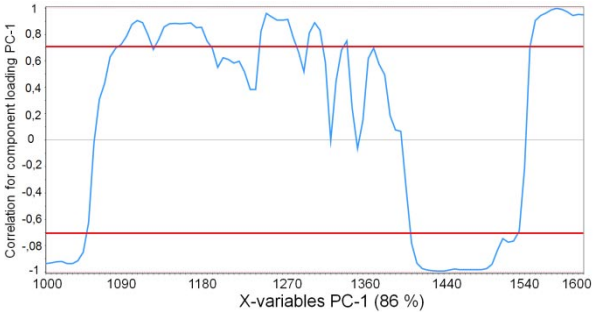

Fig. 4. **Loading graph of first principal component**

In the PCA model 1600–2300 nm was marked only one compact group G3 (Fig. 5). Compactness of the group is evident on Fig. 6. Remaining samples were scattered in the left half of the plot. In G2 are samples of 3 manufacturers and several types of their devices which indicates that PCA did not divided samples strictly, according to manufacturers. On the Fig. 8 is example of comparison only one manufacturer inks. Three spectra of Canon are compared. Sample C3 is not in G3. In this comparison, C3 differs from C1 and C2, especially in the range from 1950 to 2300 nm. However, in the G3 are collected all types of print devices Photosmart C marked H1, H3 and H5. Sample H2, which is not in G3, has not character C in the type of print device. Also in the G3 is sample H5 which indicates that Deskjet C and Photosmart C probably use inks of alike nature. Sample H6 represents Office jet Pro and it is also in G3. This discrepancy could be explained by the fact that H6 is relative new model which could have similar chemical

components of ink as Photosmart C or Deskjet C. Third party type of ink represents E9 (Fig. 7). This spectrum differs from the remaining spectra in almost all the spectral range.

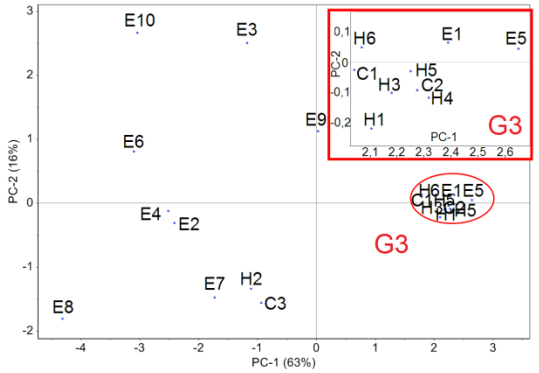

Fig. 5. **PCA model in the range of 1600–2300 nm**

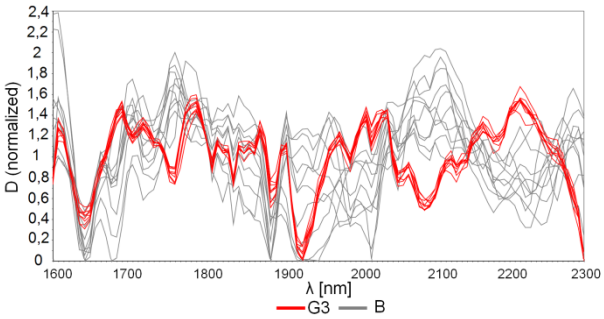

Fig. 6. **Comparison of spectra G3 with remaining spectra**

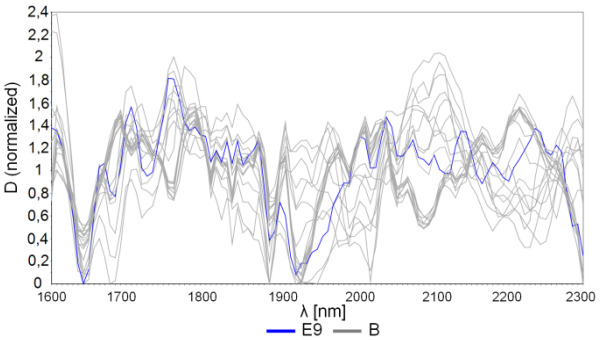

Fig. 7. **Comparison of E9 with remaining spectra**

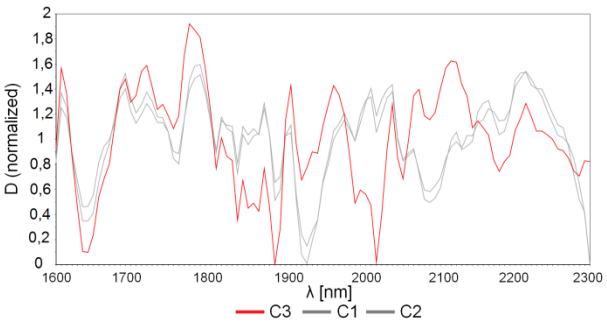

Fig. 8. **Comparison of spectra of Canon manufacturer**

Conclusion

The aim of this work was to study interrelationships of NIR spectra by PCA. There were created two PCA models. We gained the variance, described by first two principal components, 79 % in examined region 1600–2300 nm and 96% in region 1000–1600 nm. Groups G2 and G3 of both spectral regions include the same samples. In this gorups are not samples prepared by the same manufacturer or type device. Scatter plot of component score in PCA did not create extra group for third party inks. However, the groups in the scatter plot of the component score are marked with regard to shapes of spectra. Another form of PCA output is loadings plot. In the case of PCA model 1000–1600 nm, loading graph of first principal component indicate positives and negative correlations of spectra. Wavelength with negative correlation, below –0.7 represents regions with better visual distinctness and vice versa.

Our results suggest that the combination of spectroscopy in NIR region and chemometric method PCA, with a sufficiently large and diverse database, can be a useful tool for questioned inks differentiation.

This work was supported by the Slovak Research and Development Agency under the contract no. APVV-0324-10.

This publication is the result of the project implementation: Center of Excellence for Security Research ITMS code: 26240120034 supported by the Research & Development Operational Program funded by the ERDF.

Michal Oravec was also supported by an internal STU grant.

REFERENCES

1. Pearson, K.: On Lines And Planes Of Closest Fit To Systems Of Points In Space, Philosophical Magagazine, 2, pp. 559–572 (1901).
2. Meloun, M., Militký J., Hill M.: Počítačová analýza vícerozměrných dat v příkladech, Academia, ISBN: 80–200–1335–0, Praha, (2005).
3. Savitzky, A., Golay, M., J., E.: Anal. Chem., 36 (1964).
4. Barnes R. J., Dhanoa M. S., Susan J. Lister,: Standard Normal Variate Transformation and De-trending of Near-Infrared Diffuse Reflectance Spectra, Appl. Spectrosc. 43, pp. 772–777 (1989).
5. Eesbensen, K.: Multivariate Data Analysis – In Practice. 5., Oslo, 2002, CAMO Pro-cess AS.
6. Oravec M., Gál L., Čeppan M.: Pre-processing of inkjet prints NIR spectral data for principal component analysis. Acta Chimica Slovaca, 8, pp. 191–196, DOI: 10.1515/acs-2015-0031 (2015).
7. Oravec M., Gál L.: The Vis-NIR Spectroscopy with Chemometric Processing of Spectral Data in Forensic Analysis of Inkjet-printed Documents, Student Professional Conference Chemie is life in 2014, pp. 86, ISBN 978-80-214-5077-6.

GROWTH DYNAMICS CHARACTERIZATION OF *SETLICOLA PHILIPPINA* GEN. ET SPEC. NOV. (TREBOUXIOPHYCEAE, CHLOROPHYTA), PERFORMED IN TWO TYPES OF PHOTOBIOREACTORS

KATEŘINA PERÚTKOVÁ[a*], JANA STEINOVÁ[b], ZLATICA NOVOTNÁ[a], JAN ČERVENÝ[c] and MARTIN TRTÍLEK[a]

[a]*Photon Systems Instruments, 664 24 Drásov 470, Czech Republic*
[b]*Charles University in Prague, Faculty of Science, Department of Botany, Benátská 2, 128 01 Praha 2, Czech Republic*
[c]*Global Change Research Centre, Academy of Sciences of the Czech Republic, Bělidla 986/4a, 603 00 Brno, Czech Republic*
**perutkova@psi.cz*

Introduction

In our study, we focused on novel *Chlorella*-like algae *Setlicola philippina.* This algae was isolated from Taal Volcano Crater Lake, which is the largest lake on an island in a lake on an island in the world. The Taal Volcano shows increased seismic activity in the last 20 years, which is reflected by changes in water temperature and by the bubbling or boiling activity in the Crater Lake[1]. Surviving of autotrophic organims in such atypical contidions is often associated with production of specific metabolic compounds , especially lipids, polysaccharides, pigments, enzymes, vitamins and minerals[2]. These products are widely used in biotechnology. Therefore, we decided to describe this new algae and characterize its growth dynamics and potential metabolites. In following paragraphs we present preliminary results of physiological characterization obtained from algae cultivation performed in two types of photobioreactors.

Methods

The new strain was isolated from freshwater bentic biofilm from Taal Volcano Crater Lake, Philippines. To determine phylogenetic position 18S rDNA sequence was used[3]. First step of growth characterization was performed in multicultivator MC1000-OD with white LED illumination and 2 % CO_2 (Photon Systems Instruments, Brno, Czech Republic) (Fig. 1). To determine the optimal cultivation condition we initially tested growth dynamics in different light intensities (50, 100 and 150 μmol m^{-2} s^{-1}) and temperatures (20, 25, 30, 40 and 50 °C). Second stage of growth dynamics characterisation was conducted in photobioreactor FMT 150 (Photon Systems Instruments, Brno, Czech Republic) in temperature 25 °C and in 150 μmol m^{-2} s^{-1} of white and 25 μmol m^{-2} s^{-1} of red LED illumination (Fig. 2). FMT 150 continuously measured optical density (OD), fluorescence, pH and dissolved O_2. All culture experiments were performed in modified liquid BBM medium with the triple addition of sodium nitrate and magnesium sulfate (Bischoff & Bold, 1963). pH was optimized to 7.5 using 17 mM HEPES.

OD measurement data was used to growth rates and doubling time calculation of *Setlicola philippina* cultivated in both types of photobioreactors[4].

$$\text{Growth rate} = \frac{\ln \text{OD2} - \ln \text{OD1}}{\text{t2} - \text{t1}}$$

$$\text{Doubling time} = \frac{\ln 2}{\text{growth rate}}$$

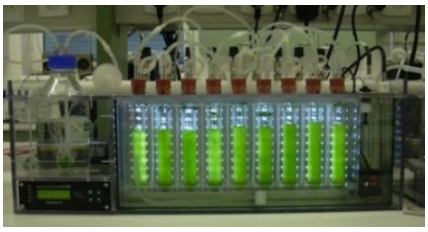

Fig. 1. **Multicultivator MC1000-OD**

Fig. 2. **Photobioreactor FMT 150**

Results

In MC 1000-OD *Setlicola philippina* reached shortest doubling time 12.22 hours in exponential phase at 25 °C and relatively high light intensity of 150 μmol m^{-2} s^{-1} (Table 1). These conditions were default for next characterization step made in FMT 150. For cultivation in FMT 150 was calculated doubling time in exponential phase about 18.5 hours. The growth curve measured in OD_{680} (red colour in Fig. 3–5) and in OD_{720} (dark red colour in Fig. 3) had long lag phase, which indicates a long adaptation phase of *S. philippina*. Exponential growth phase started at OD_{680} 0.3 and ended at OD_{680} 24 (Fig. 3). Amount of dissolved oxygen (blue colour in Fig. 4) was growing during the exponential phase and reached local maxima at the end of this growth phase. Increase of pH (green colour in Fig. 4) correlated with increase of biomass. Chlorophyll fluorescence parameter determined in quantum yield (QY) also showed its maximum at the end of exponential phase. Fluorescence sensitivity was identical for wavelength 450 nm (blue color) and 620 nm (red colour) used by QY measurements (Fig. 5).

Table 1
Doubling time of exponential phase in hours reached in different culture conditions (data from MC 1000-OD)

Cultivation temperature	Light intensity (white LED) 50 µmol m^{-2} s^{-1}	100 µmol m^{-2} s^{-1}	150 µmol m^{-2} s^{-1}
20 °C	71.25	85.96	N/A
25 °C	22.58	19.05	12.22
30 °C	35.13	24.38	21.17
40 °C	no growth	no growth	no growth
50 °C	no growth	no growth	no growth

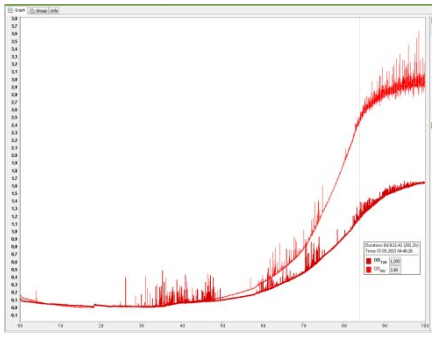

Fig. 3. **Growth curve measured in OD680 (red colour) and OD720 (dark red colour). Printscrean from FMT 150 software**

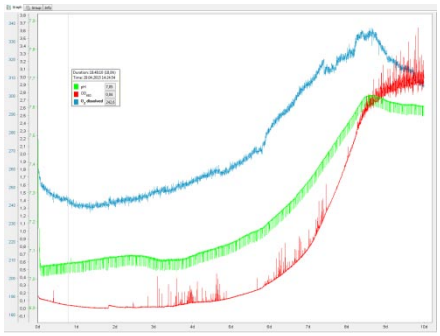

Fig. 4. **Growth curve measured in OD680 (red colour), dissolved oxygen (blue colour) and pH (green colour). Printscrean from FMT 150 software**

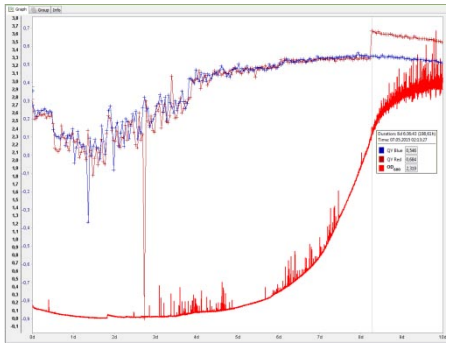

Fig. 5. **Growth curve measured in OD680 (red colour), blue QY (blue colour) and red QY (dark red colour). Printscrean from FMT 150 software**

Discussion

According to atypic conditions in Crater Lake reflected by water temperature changes, high temperature resistence of *Setlicola philippina* was tested using MC 1000-OD. Growth dynamics showed at the mesophilic character of studied organism with the ability to high illumination tolerance. Higher temperatures effected culture sedimentation and degradation of photosynthetic pigments.

The 680 nm radiation is absorbed by the chlorophyll a (major photosynthetic pigment of green algae) as well as by cell structures, while 720 nm are absorbed by cell structures only[5]. Thus OD_{680} was chosen as the indicator of growth monitoring. During the cultivation in FMT 150 OD_{680}/OD_{720} was maintained at the value 2:1, which indicated no increase of bacterial growth in the culture and no changes of chlorophyll content in algae cells.

QY is the ratio of photons absorbed to photons emitted through fluorescence[6]. It means that QY reflect viability of the culture. QY maximum of *S. philippina* was around 0.55. Efficiency of photosystem II could bee higher compared to other *Chlorella*-like species utilized in biotechnologies[7].

Conclusion

The results of this study show preliminary growth characteriazation of novel genus and species *Setlicola philippina* conducted in two different photobioreactors. Optimal cultivation conditions were determined. Next characterization step should be focused on metabolic products, its potential usage and prospective industrial production in large-scale photobioreactors.

This work was supported by the Ministry of Education, Youth and sports of CR within the National Sustainability Program I (NPU I), grant number LO 1415.

REFERENCES

1. http://www.taalvolcano.org/
2. Seyfabadi J., Ramezanpour Z. & Khoeyi Z. A. (2011) Protein, fatty acid, and pigment content of *Chlorella vulgaris* under different light regimes. Journal of Applied Phycology, Volume 23:4 , 721–726.
3. Škaloud, P., Němcová, Y., Pytela, J., Bogdanov, N. I., Bock, C. & Pickinpaugh, S. H. (2014) *Planktochlorella nurekis* gen. et sp. nov. (Trebouxiophyceae, Chlorophyta), a novel coccoid green alga carrying significant biotechnological potential. Fottea 14(1): 53–62.
4. Hirsch, H. R. & Engelberg, J. (1965) Determination of the cell doubling-time distribution from culture growth-rate data. Journal of Theoretical Biology, Volume 9:2, 297–302.
5. Zavřel, T., Sinetova, M. A., Búzová, D., Literáková, P. & Červený, J. (2015) Characterization of a model cyaobacterium Synechocystis sp. PCC 6803 autotrophic growth in a flat-panel photobioreactor. Engineering in Life Sciences, Volume 15, 122–132.
6. Parkhill, J., Maillet, G. & Cullen, J. J. (2001) Fluorescence-based maximal quantum yield for PSII as a diagnostic of nutrient. Journal of Phycology, Volume 37:4, 517–529.

7. Masojídek, J., Kopecký, J., Giannelli, L. & Torzillo, G. (2010) Productivity correlated to photobiochemical performance of *Chlorella* mass cultures grown outdoors in thin-layer cascades. J Ind Microbiol, Volume 38, 307–317.

ON THE QUALITATIVE PARAMETERS OF FRUIT JUICES AND POSSIBILITIES OF THEIR IMPROVEMENT VIA TECHNOLOGICAL MODIFICATIONS

MARTIN POLOVKA[a], BLANKA TOBOLKOVÁ[a], ELENA BELAJOVÁ[a] and JÁN DUREC[b]

[a]National Agricultural and Food Centre, VÚP Food Research Institute, Department of Chemistry and Food Analysis, Priemyselná 4, SK-824 75 Bratislava, [b]McCarter, Ltd., Bajkalská 25, SK-821 01 Bratislava, Slovak Republic; production premises: Budovateľská 1247/7, SK-929 01 Dunajská Streda, Slovak Republic
polovka@vup.sk

Introduction

Fruit juices belong to the most popular drinks worldwide. Besides vitamins and minerals they represent rich source of phenolic compounds recognized for their antioxidant activity. Pineapple and orange juices belong to the most preferable by the consumers, covering altogether more than 42 % of the overall fruit juices production[1].

Pineapple (*Ananas comosus*, L.) is the most important species of the Bromeliaceae family grown commercially for its fruit. It is native to South America, where wild relatives occur. Commercially grown cultivars (Cayenne, Queen, Spanish, Pernambuco, and Perolera) are nearly or completely seedless. This is an advantage for production of fresh juices with pulp[2]. The fruit is used either as fresh or processed. Processed products are most frequently juice, canned slices, dried pieces, jam, and glaze. Pineapple is rich source of various phytochemicals, such as vitamins A, B and C, carotenoids, flavonoids, isoflavones, flavones, anthocyanins, catechins and other phenolic compounds. Flavonoids are present as coloring pigments and also function as antioxidants[3]. Pineapples also contain significant amount of bromelain, proteolytic enzyme with varied use. Bromelain is used for tenderizing meat, preventing cold haze in beer and for medicinal purposes.

Sweet oranges (Citrus sinensis) are most abundant citrus species produced worldwide. Citrus originated in China and spread mostly throughout the Asian continent. Nowadays, citruses are grown in subtropical regions all around the world [2]. Oranges are non-climacteric fruit. When reaching appropriate ripeness, they are harvested mostly by hand and can be stored at 5–10 °C for 6–8 weeks. Minimum safe temperature for their storing is 3–5 °C. During the storage, oranges produce very small amount of ethylene, less than 0.1 ppm. Respiration rate is 7–13 mg $CO_2 \cdot kg^{-1} \cdot h^{-1}$ [4].

Analyses of oranges have revealed the presence of approximately 224 phytochemicals, including 23 monoterpenoids, 15 sesquiterpenoids, 13 diterpenoids, 32 flavones, 13 flavanones, 6 flavanols, 9 anthocyanins, 3 chaconnes, 4 phenolic acids, 15 carotenoids and 4 coumarins[5]. Citruses are also rich source of phenolic compounds, mainly flavonoids. Orange contains high amount of flavonoid hesperidin and small amounts of flavonoids narirutin and didimin. Occasionally, aromatic and aliphatic acids, methylenedioxyl or isoprenyl groups also attach to the flavonoid nucleus and their glycosides. Other flavonoids that can be only found in citruses are polymethoxyflavones and glycosylated flavones[6]. Orange also contains vitamin C and folic acid. Most health promoting carotenoids in oranges are α-carotene, β-carotene, lutein, β-cryptoxanthin and zeinoxanthin. Color of orange is mainly influenced by its carotenoid content[7].

Increasing consumer's demands towards high quality and safe food products push their producers to increase the production and qualitative standards of the products.

Quality of fruit juices and juices produced without any additives is determined beside the other factors, by the quality of feedstock. Generally, sour and juicy fruit with higher sugars content and distinctive aroma is preferably used for nectars and fruit juices production. Fruit quality is fundamentally influenced by several factors, especially by its ripeness (mutual sugar/acid ratio and contents of flavouring substances)[8, 9]. In addition, quality of the juice during its processing, filling into packaging material, and finally during the transport and storage is also influenced by the hygiene during the filling and packaging, physico-chemical conditions of the storage (here the action of oxygen, light, temperature should be taken into consideration) or potential interactions of the product with packaging material or its components. The contact of fruit juice with oxygen may lead to the degradation of several unstable vitamins and other substances of antioxidant character result in colour changes and may also lead to changes in taste (development of off-flavour products). Oxygen may be dissolved in juice, itself, but usually it is also present in the upper part of the inner-package space (headspace). The concentration of oxygen dissolved in juice may be reduced during the processing step involving various techniques[10–14].

Recent innovations in juices production resulted in modification of production conditions, comprising the modification of composition (e.g., via the addition of fruit pulp and/or small fruit pieces), innovations in packaging materials, as well as the production atmosphere modification.

In view of what is written above, in this contribution, the study on the effects of production conditions of fresh orange juices with pulp and pineapple juices and their modification (i. e., the production under the Ar, CO_2 and N_2 atmosphere), as well as the effect of their long-term storage on selected qualitative characteristics (antioxidant activity, color changes and concentration of selected phytochemicals) dominantly assessed by EPR and UV-VIS spectroscopy is presented.

Materials and methods

Samples

100% juice from freshly pressed pineapples and oranges with pulp were provided by McCarter a.s. Dunajská Streda, the reputable Slovak fresh fruit juices producer. Juices were cold-processed and treated by light pasteurization (95 °C, 20 s). Analyzed juices were processed both with, and without the modified atmosphere application during the processing. After the pasteurization, juices were aseptically filled into the PET bottles and closed with cap containing oxygen scavengers (SK38/16-O_2S; BeriCap, Budenheim, Germany). Bottled samples of respective fruit juices (from the same batch) were

delivered to the laboratory immediately after their production in sufficient number and stored at defined conditions (7 ± 2 °C) in darkness in the refrigerator between the experiments. Respective fruit juice samples were centrifuged at 10 000 g at the temperature of 5 °C for 10 minutes in order to separate the solid matter before the analysis. The supernatants were stored at 7 °C in the darkness between the experiments. Sample was always prepared from new bottle/bottles just prior the measurement. All experiments were performed in duplicates.

Experimental setup

UV-VIS experiments were performed on UV-VIS-NIR spectrophotometer Schimadzu 3600 with accessories (Schimadzu, Japan). Total polyphenolic compounds (TPC) concentration was estimated by modified Folin – Ciocalteu method. Color characteristics in CIE L*a*b* color system were calculated by processing the absorbance spectra of respective sample by ColorLite Panorama Shimadzu software (LabCognition Analytical Software, Köln, Germany) as previously described by Tobolková et al.[15].

For EPR measurements, portable EPR spectrometer e-scan (Bruker, Germany) with accessories was used. The entire measurements were realized with flat quartz cell designed for EPR experiments with polar solutions. $ABTS^{\bullet+}$ and TEMPOL assays were utilized to characterize the antioxidant and radical-scavenging ability of juices samples and their changes resulting from different production conditions and/or storage. The experiment and data evaluation procedure was identical to that previously described by Tobolková et al.[15].

Ascorbic acid and hesperidin concentration were determined by means of HPLC, involving Agilent Technologies 1100 Series chromatograph (Agilent Technologies) equipped with diode array detector (DAD), quaternary pump, degasser, column thermostat and autosampler. Juice samples were diluted tenfold and twentyfold, filtrated through a 0.45 μm syringe filter and subsequently analyzed on HPLC. The separation conditions and conditions of analysis were identical to these, previously described by Sádecká et al.[16].

Data evaluation

Kinetics of changes of the selected qualitative parameter was evaluated, on the basis of repeated measurements performed in regular time intervals (2 times a week, at minimum). For the purposes of quantitative evaluation of the studied effects, the experimental characteristics of the samples recorded immediately after the juice production and at 90 ± 5 days after the juice production were taken into consideration.

Statistical calculations were performed by means of Unistat v. 6.0 (Unistat, London, United Kingdom) statistical package. Analysis of variance (ANOVA) and multivariate statistics were used to compare, explore and discriminate the complex dataset of experimental characteristics.

Multiple comparisons were performed by ANOVA Tukey's HSD test at the level of significance of $P \leq 0.05$. The differences in means of individual compared characteristics were recognized as highly significant at $P < 0.001$.

Principal component analysis (PCA) and canonical discriminant analysis (CDA) were used in order to define, interpret and visualize the differences between the compared juices in terms of production atmosphere effects, seasoning effect and/or sample origin. Using the CDA, the recognition ability was calculated as the percentage of correctly classified samples in the original data set in which all the samples were of known properties for the classification model.

Results and discussion

UV-VIS experiments

Total polyphenol content is traditionally accepted as a basic parameter of juices of natural origin characterization, particularly in connection with antioxidant or radical-scavenging properties of the evaluated juice samples. In the experiments, the effect of production atmosphere on TPC content as well as the effect of long-term post-production storage on the concentration of total polyphenols was characterized. TPC values recorded for orange and pineapple juice samples of different production atmosphere at the respective time of their storage revealed their expected gradual decrease during the storage, probably as a result of the oxidation and polymerization of polyphenols, thus reducing the number of free hydroxyl groups measured by the Folin-Ciocalteu assay[17]. As regards the effects of the production atmosphere on TPC concentration, it is obvious that application of modified N_2 or CO_2 atmospheres positively influence the TPC in comparison to samples produced without the modified atmosphere. The obtained results indicated that the application of Ar atmosphere led surprisingly to the most significant decrease in TPC. The effect of CO_2/N_2 application on polyphenols protection is comparable. Kinetic rate constants evaluated from TPC changes during the storage are in good correlation with changes observed during the storage of juices. However, kinetic evaluation is rather complicated by the fact, that the calculation is affected by the variability of the experimental characteristics. Also the factors as fruit origin, season of production must be considered.

Color of fresh fruit juices is important qualitative parameter since consumers' often associate color of juice with its freshness and quality. Color characteristic can be also used for evaluation of bioactive compounds responsible for juice color[18, 19]. As follows from the previously published papers, color characteristics are mainly influenced by changes in particle size during the processing and by heat accelerated non-enzymatic browning reactions (i.e. Maillard reactions) during the pasteurization step[19]. During the long-term storage, color characteristics are mainly influenced by non-enzymatic browning reactions[20].

Changes of color characteristics resulting from the storage were evaluated in terms of total color difference (TCD) as previously suggested by Cserhalmi et al.[21]. The results obtained confirmed that the effect of the modified atmosphere production on changes in color characteristics of orange juices during their storage is influenced significantly by the sample homogeneity and the presence of solid particles in the juice solution, or the turbidity of the samples caused e.g., by the presence of proteins. Seasoning effect cannot be

underestimated in this context, as well. From general point of view, the effect of modified atmosphere on color changes is rather positive. The comparison of TCD of samples produced under the respective atmospheres revealed the following positive effect (in decreasing order according to TCD values at 90th day of storage): Ar> (CO_2≈N_2). The TCD changes of CO_2 and N_2 produced samples are comparable, as shown also for TCD.

EPR experiments

Ascorbic acid (AA) content is important qualitative parameter in fruit juices. AA content is mainly affected by the dissolved oxygen. Its degradation in juices is a result of aerobic and anaerobic mechanisms that occurs simultaneously. Main degradation reactions are oxidation and hydrolysis. Degradation of AA to dehydroascorbic acid also affects color characteristics of fruit juices. Changes in the ascorbic acid concentration in juices during the storage were evaluated by TEMPOL assay, as this stable free radical/ its water solution is sensitive to the presence of low-molecular organic acids of corresponding redox potential, forming EPR silent hydroxylamine. It was previously successfully applied e.g., for the indirect detection of the AA presence in fortified beers[22]. Results were expressed in terms of ascorbic acid equivalents, AAE, as previously described by Tobolková et al.[15].

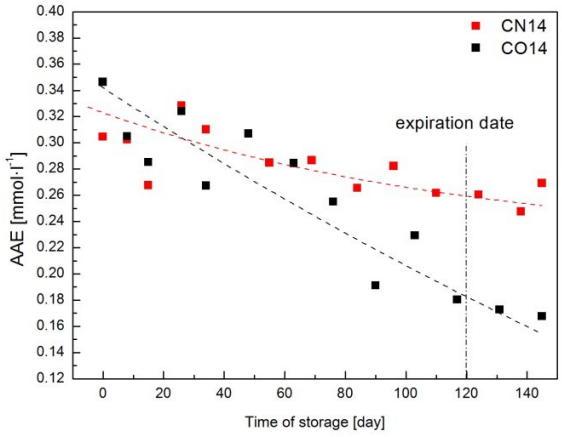

Fig. 1. **Changes of AAE values in orange juice samples produced under the conventional air (CO14) and nitrogen (CN14) atmosphere during the storage. Dotted line represents the fit of experimental data to the model of the 1st order kinetic equation**

As follows from the experimental results, the application of N_2 modified atmosphere leads to effective protection of low-molecular organic acids present in the pineapple and orange juice, slowing the deterioration of the radical-scavenging activity of the samples in comparison to those produced under the conventional air atmosphere. As regards the efficacy of CO_2 and N_2 atmosphere, it is apparent that the application of CO_2 modified atmosphere proved to have similar effect as the N_2 modified atmosphere. These results are in good correlation with the results described above for TPC and color value changes. It should also be noted here, that significant seasoning effect was noticed especially for orange juices, as the higher AAE values of orange juices processed in 2015 were noticed at the start of experiment and at the 90th day of storage, than for orange juices made in 2014.

Calculated rate constants and half-lives proved unambiguously the observed effects of modified atmosphere application in terms of AA and other low/molecular organic acids protection against oxidation and subsequent deterioration. It is evident, that in case of orange juices with pulp, the application of modified atmosphere suppress the degradation processes, the effects of N_2 and CO_2 atmospheres are comparable. However, the seasoning effect and samples homogeneity affect the precision of the kinetic evaluation.

Trolox-equivalent antioxidant capacity (TEAC) expresses the ability of antioxidants present in respective juice samples to scavenge the $ABTS^{\bullet+}$ cation-radical. The observed decrease in EPR spectra intensity resulting from the reaction of sample components with the cation-radical is the most frequently evaluated by comparing the radical-scavenging ability of the sample to that of TROLOX, synthetic water-soluble vitamin E derivate, in terms of Trolox-equivalents – TEAC values. TEAC value is often used for evaluation of the antioxidant and radical-scavenging properties of sample in a semi-quantitative scale.

Similarly like in the previously described assays, the effect of production atmosphere and long-term post-production storage on TEAC content was characterized. Experiments performed clearly proved that the application of N_2 led to general protection of samples against the oxidation, via eliminating or slowing down the deterioration of their antioxidant and radical-scavenging properties. Results obtained also confirmed very similar impact of the application of N_2 and CO_2 on TEAC values during storage. Seasoning effect was confirmed, as well. In comparison to juices produced in 2014, those of 2015 production exhibited overall higher TEAC values, probably due to seasonal variance during the growth of oranges, as mentioned also above in other assays.

Additional remark should also be done when considering the variability in experimental data, not only TEAC. In spite of the worse results of all the parameters evaluated for juices produced under Ar atmosphere, one phenomenon should be highlighted, i.e., the fact that the Ar-produced samples exhibited the lowest variability within the measurements and between the samples, obvious from time-dependent measurements presented in the study. It is hardly to discuss, whether observed lowered variability is the result of sample homogeneity, variety, season or origin. It can be only concluded on the basis of these results, that the lowered variability brings better predictability of the sample behavior at different time of storage, what could be effectively used for e.g., juice composition modulation in terms of reaching the defined values of certain nutrients/antioxidants at the desired time after the juice production. Of course, additional experiments in a wider scale performed on extended group of samples would be desirable to verify and evaluate the observed trends in a more complex way.

HPLC measurements

HPLC analysis was focused on direct monitoring of AA and of hesperidine concentration, typical representative of

flavonoids in orange juices, and their changes resulting either from production technology modification or long-term post-production storage. In accord with expectations, the highest AA concentrations were detected in freshly prepared juices at the beginning of the experiments. The lowest AA concentration was registered for juices produced in 2013 under the Ar atmosphere, followed by the samples produced in 2014 and the highest concentration of AA was noticed in both types of juices produced in 2015. The described trends clearly illustrate the seasoning effect and also the variability of the experimental results, affecting the standard deviation values. In addition, it is also obvious, that when the measurement uncertainty is taken into account, the initial concentrations of AA determined in both type of juice samples produced in 2014 (O_2 vs. N_2) and 2015 (N_2 vs. CO_2) are comparable. At the 90th day of storage, the highest decrease of AA concentration was detected in CO14 samples produced conventionally, reaching approx. 69 %, followed by samples produced under Argon in 2013. In fact, changes in AA concentrations determined by HPLC correlate well with changes in AAE values during the storage discussed above. AA concentration in pineapple juices produced under N_2 modified atmosphere exhibited 24.9 % decrease during the first 90 days of the storage, after which only slight decrease was observed. These results are comparable to our previously published studies[15, 16].

The values of hesperidin concentration determined in orange juice samples of different production atmospheres at the respective time of their storage exhibited that hesperidin content gradually decreased during the storage, what is the expected trend, in good agreement with gradual TPC decrease assessed by UV-VIS. The only exception was noticed for juices produced under the Ar modified atmosphere, for which 0.7 % increase was observed. However, this slight increase is within the measurement uncertainty, thus, it can be concluded, that in case of juices produced in 2013 under argon, practically steady-state of hesperidin concentration during the storage was determined.

Statistical evaluation

ANOVA Tukey HSD analysis of the experimental data proved that all the compared experimental characteristics are significantly different in dependence on the effect of storage, the year of production, the origin of sample or production atmosphere, with some exception. The test was performed on the significance level of $\alpha = 0.05$. These results are in good agreement with the behavior of the samples described above. Detailed insight is given by the multivariate statistical analysis. Of course, some exceptions (non-significant differences) were occasionally noticed for all parameters and both monitored factors, but without practical effect on general observations/trends.

Results attained were processed by multivariate statistics in order to evaluate the effects of sample origin and season or production technology on the monitored characteristics as well as an overall quality of fruit juices. As follows from the results of statistical analysis, the year of production is strong discriminant factor as on the basis of all the monitored characteristics, absolute discrimination of the samples by canonical discrimination analysis was achieved. As regards raw material origin, only partial differentiation, although with high classification score was obtained. Problematic was particularly the differentiation of the blend sample from that originating from Costa Rica.

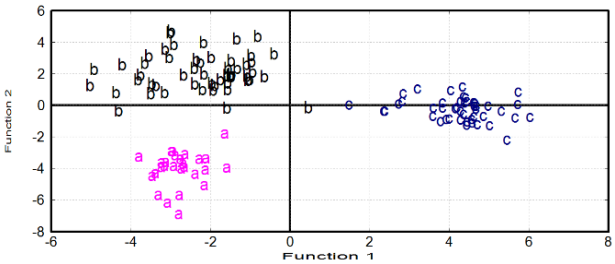

Fig. 2. **Discrimination of orange juice samples by canonical discriminant analysis, on the basis of the entire group of experimental characteristics. The year of production was used as the discrimination criterion (a- 2013, b-2014, c-2015)**

As regards the effect of production technology, partially successful differentiation of samples according to the inert gas applied was obtained, both for orange and pineapple juices. The acquired results will help the juice producer in optimization of the juice production conditions in order to obtain the product with maximum beneficial properties kept during the whole expiration period. Its length can also be optimized on the basis of the presented results.

Conclusion

On the basis of the presented results, general conclusion can be made, that inert gases application may improve the quality of fruit juices; however utilization of certain gas is the compromise of the expenses on technology modification and the effects obtained. Factors including the potential physical and\or chemical interactions of gas with juice components should also be considered carefully. Seasoning effects and the sample origin affect the properties of juices significantly, as well.

This contribution is the results of the project "Improvement of nutritional and sensorial parameters of fruity and vegetable drinks via an inert gases application – ITMS 26220220175" implementation, supported by the Research and Development Operational Programme funded by the European Regional Development Fund.

REFERENCES

1. European Fruit Juices Association AIJN 2014 Liquid Fruit Market Report. Available online from www.aijn.org
2. Tropical and Subtropical Fruits: Postharvest Physiology, Processing and Packaging. Siddiq, M., ed. 2012, Ames, Iowa: Wiley. ISBN 978-0-8138-1142-0.
3. Hossain, M. A., Rahman, S.M.M.: Food Res. Int. *44*, 672 (2011).
4. Yahia, E. M.: Postharvest biology and technology of tropical and subtropical fruits. Vol. 1. 2011: Woodhead Publishing. 534. ISBN: 978-1-84569-733-4.
5. Skinner, M., Hunter, D., González-Aguilar, G. A.: Bioactives in fruit: health benefits and functional foods.

2013, Chichester, West Sussex, UK: John Wiley. 517. ISBN: 978-0-470-67497-0.
6. Rosa, L. A., Alvarez-Parrilla, E. González-Aguilar, G. A.: Fruit and vegetable phytochemicals: chemistry, nutritional value and stability. 2010, Ames, Iowa: Wiley-Blackwell. 367. ISBN: 978-0-8138-0320-3.
7. Meléndez-Martínez, A. J., Escudero-Gilete, M. L., Vicario, I. M., Heredia F. J.: Food Res. Int. *43,* 1289 (2010).
8. F.A.I.M. – Food Authenticity – Issues and Methodologies. Michele Lees (ed.): Eurofins Scientific (1998). ISBN 2-9512051-0-4.
9. Sinha, N. K., Sidhu, J. S., Barta, J., Wu, J. S. B., Cano, M. P.: Handbook of fruits and fruit processing. 1st ed. Oxford: John Wiley & Sons, 2012, 727 p. ISBN 978-0-8138-0894-9.
10. Bacigulapi, C., Lemaistre, M. H., Boutroy, N., Bunel, C., Peyron, S., Guillard, V., Chalier, P.: Food Chem. *141*, 3827 (2013).
11. Zerdin, K., Rooney, M., Vermuë, J.: Food Chem. *82*, 387 (2003).
12. Ros-Chumillas, M., Belissario, Y., Iguaz, A., López, A.: J. Food Eng. *79*, 234 (2007).
13. Aday, M. S., Caner, C.: LWT – Food Sci. Technol. *52*, 102 (2013).
14. Aday, M. S., Caner, C., Rahvali, F.: Postharvest Biol. Tec. *62*, 179 (2011).
15. Tobolková, B., Durec, J., Belajová, E., Mihalíková, M., Polovka, M., Suhaj, M., Daško, Ľ., Šimko, P.: J. Food Nutr. Res. *52*, 181 (2013).
16. Sádecká, J., Polovka, M., Kolek, E., Belajová, E., Tobolková, B., Daško, Ľ., Durec, J.: J. Food Nutr. Res. *53*, 371 (2014).
17. Laorko, A., Tongchitpakdee, S., Youravong, W.: J. Food Engin. *116*, 554 (2013).
18. Wibowo, S., Vervoort, L., Tomic, J., Santiago, J. S., Lemmens, Agnese Panozzo, Tara Grauwet, Marc Hendrickx, L., Van Loey, A.: Food Chem. *171*, 330 (2015).
19. Stinco, C. M., Fernández-Vázquez, R., Escudero-Gilete, M. L., Heredia, F. J., Meléndez-Martínez, A. J., Vicario, I. M.: J. Agric. Food Chem. *60*, 1447 (2012).
20. Bharate, S. Bharate, S.: J. Food Sci. Technol. *51*, 2271 (2014).
21. Cserhalmi, Z., Sass-Kiss, Á., Tóth-Markus, M., Lechner, N.: Innov. Food Sci. Emerg. Technol. *7*, 49 (2006).
22. Brezová, V., Polovka, M., Staško, A.: Spectrochim. Acta A. *58*,1279 (2002).

PREPARATION OF SORBENTS FROM TAR DEPOSITS

ADRIAN PRYSZCZ[a], BARBORA GRYCOVÁ[a], IVAN KOUTNÍK[a] and MAŁGORZATA RUTKOWSKA[b]

[a]VSB-TU Ostrava, Institute of Environmental Technologies, 17. listopadu 15, 708 33 Ostrava-Poruba, [b]Jagiellonian University, Ingardena 3, 30-060 Kraków, Poland
adrian.pryszcz@vsb.cz, barbora.grycova@vsb.cz, ivan.koutnik@vsb.cz, ma.rutkows@gmail.com

Keywords
Tar, Tar deposits, Extraction, Activation, Surface area.

Introduction

From the chemical point of view tar is a complex mixture of hydrocarbons, with 1–5 ring aromatic compounds, and hetero compounds containing oxygen, nitrogen and sulfur[1].

Tar properties vary according to the source of their origin. The major part of tars is formed from the thermal conversion of coal (coal tar), the second part is formed during pyrolysis or gasification of biomass. During the last years, due to efforts to use renewable sources of energy instead of fossil fuel, new technologies for pyrolysis and gasification have been developed, especially for thermal processing of biomass. For the thermal decomposition of biomass, there are two basic technical designs. Conversion of biomass to gas (biomass to gas – BTG) and conversion of biomass to liquid (biomass to liquid – BTL)[2, 3, 4].

Tar removal or conversion is considered technologically an extremely challenging problem. Tar can condense or polymerize into more complex structures, which can lead to clogging pipes or heat exchangers. Tar elimination from the gasification product is necessary before additional usage[5].

Coal tar is obtained mainly from the process of coal carbonization, and accounts from 2.5 to 4.0 mass % of the feed coal. Coal tar contains more high molecular compounds than tar generated from biomass and it is an important source of aromatic compounds. 15 to 25 % of BTX (benzene, toluene, xylene) is obtained from coal tar, 95 % of multi-ring hydrocarbon can be obtained from coal tar and more than 90 % of anthracene, acenaphthene, pyrene, phenol and most of heterocyclic aromatic compounds is gained from coal tar. Nearly 100 % of carbazole, quinoline and thiophene is from coal tar[1, 6].

For tar deposits (pitch) it is not possible to determine exact compound composition, and therefore mostly group analysis is carried out. Tar Deposits can be divided into 4 groups: carboids, carbenes, asphaltenes and pre-asphaltenes. From carboids to pre-asphaltene ratio of C/H and heteroatoms content is decreasing. The heaviest group, carboids, are insoluble in quinoline (pyridine), carbenes are insoluble in toluene (benzene). Asphaltenes are soluble in toluene and pre-asphaltenes are soluble in n-hexane[7].

Experimental part

For experimental part tar deposits, formed by polymerization and condensation reactions, from storage tank for tars were chosen. At first the initial analyzes of tar deposits (elemental, thermogravimetric and calorimetric analysis) were performed.

Table 1
Elemental analysis of tar deposits

C^r (wt %)	H^r (wt %)	N^r (wt %)	S^r (wt %)	O^r (wt %)
70.33	2.28	1.07	0.55	0.27
C^d (wt %)	H^d (wt %)	N^d (wt %)	S^d (wt %)	O^d (wt %)
88.74	2.69	1.31	0.70	0.32

Upper index "d" refers to dry sample, upper index "r" refers to initial state of the sample. Oxygen was calculated.

Table 2
Thermogravimetric and calorimetric analysis of tar deposits

W^r (wt %)	V^r (wt %)	FC^r (wt %)	A^r (wt %)	HHV^r ($kJ \cdot kg^{-1}$)
15.30	35.21	44.21	5.28	31848
V^d (wt %)	FC^d (wt %)	A^d (wt %)	HHV^d ($kJ \cdot kg^{-1}$)	
41.58	52.19	6.23	37600	
$LHV(kJ \cdot kg^{-1})$				
31027				

Next step was an extraction of tar deposits in the Soxhlet extractor, using sequentially extraction solvents: acetone, toluene, pyridine and quinoline.

Table 3
Sequentially extraction of tar deposits

Extraction solvent	Extracted amount (wt %)
Acetone	50.9
Toluene	7.2
Pyridine	5.0
Quinoline	1.9
Insoluble residue	35.0

The results show, that for the preparation of sorbent should be sufficient to carry out extraction only with acetone or toluene and solvents such as pyridine and quinoline could be omitted. Subsequently three comparative extractions with acetone, toluene and quinoline were performed. These prepared extracted residues were activated by KOH. Approx. 15 g of sample was activated in a ratio of sample: KOH: distilled water 1: 3: 10, then the mixture was thermally treated in an inert atmosphere of nitrogen at 850 °C for 1 h. After cooling, the activated sample was neutralized by HCl, filtered and finally

washed with water. After drying, the activated sample was ready for subsequent surface analysis.

Table 4
Extraction yield of tar deposits

Extraction solvent	Acetone	Toluene	Quinoline
	(wt %)		
Extraction residue	49.6	44.0	41.6

Table 5
Activation yield of the extracted tar deposits

Sample extracted with	Acetone	Toluene	Quinoline
	(wt %)		
Activated amount	55.3	61.3	57.3

Table 6
Elemental and thermogravimetric analysis of extracted and activated samples of tar deposits

Sample	C^d (wt %)	H^d (wt %)	N^d (wt %)	S^d (wt %)	A^d (wt %)
Acetone	78.3	2.06	1.38	0.85	13.9
Toluene	77.4	1.85	1.58	0.85	14.5
Quinoline	77.1	1.70	1.62	0.84	15.0
Activated acetone	75.3	0.35	0.83	0.39	18.7
Activated toluene	75.9	0.31	0.89	0.40	16.2
Activated quinoline	75.4	0.30	0.82	0.22	16.5

After activation of samples, determination of surface area was performed. Measurements were carried out on 3Flex Surface Characterization Analyzer (Micromeritics). Approx. 1 g of non-activated samples and 0.1 g of activated samples were used for adsorption analysis. After weighing, the sample was degassed under the reduced pressure at 350 °C. Afterwards N_2 at 77 K was sorbed on the sample.

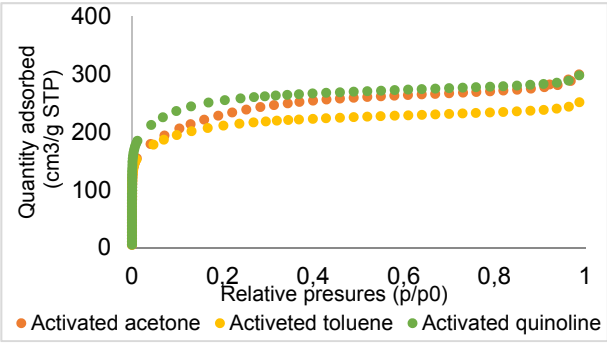

Fig. 1. **Adsorption isotherms of activated samples**

The specific surface area of the samples was evaluated using two methods: (i) single point measurement at $p/p_0 = 0.2$ and (ii) BET (Braunauer-Emmett-Teller) method. Wile, micropore and external surface areas were calculated based on the t-plot analysis (carbon black model). Two rows of activated and non-activated samples were measured.

Table 7
Surface area of the activated samples

Sample	Activated acetone	Activated toluene ($m^2 \cdot g^{-1}$)	Activated quinoline
t-Plot Micropore Area	753	709	867
t-Plot external surface area	63	64	74
Single point surface area at p/p° = 0.20	794	736	885
BET Surface Area	817	772	941

Table 8
Surface area of the non-activated samples

Sample	Acetone	Toluene ($m^2 \cdot g^{-1}$)	Quinoline
t-Plot Micropore Area	0	0	0
t-Plot external surface area	2	2	2
Single point surface area at p/p° = 0.20	2	3	2
BET Surface Area	2	3	2

The measured data shows that non-activated samples have almost zero sorption properties, but the activated samples of have sorption properties close to higher quality activated carbon (see Table 7, 8), surface area of comercial activated carbons is in the range from 500 to 1500 $m^2 \cdot g^{-1}$.

Conclusion

Based on the laboratory results conclude that it is possible to use tar deposits for the preparation of sorbents. It.can be stated that non-activated sorbents have almost zero sorption capacity. On the other side activated sorbents reach properties close to higher quality activated carbon. From the carried out experiments it is assumed, that major effect on the total surface area has well carried out activation. The selection of extraction solvent (acetone, toluene, quinoline) has negligible effect on the surface area.

This article was created with the financial support of the Ministry of Education, Youth and Sports within targeted support program „Národní program udržitelnosti I“, projekt LO1208 „TEWEP“.

REFERENCES

1. Chunshan L., Kenzi S., Resources, properties and utilization of tar, Resources, Conservation and Recycling, Volume 54, Issue 11, September 2010, p. 905–915.

2. Świerczyński D., Libs S., Courson C., Kiennemann A., Steam reforming of tar from a biomass gasification process over Ni/olivine catalyst using toluene as a model compound, Applied Catalysis B: Environmental, Volume 74, Issues 3–4, 31 July 2007, p. 211–222.
3. Jílková L., Ciahotný K., Černý R., Technologie pro pyrolýzu paliv a odpadů, Paliva 4, 2012, 3, p. 74–80.
4. Holocová P., Kaloč M., Hodnocení vlastností pyrolýzních produktů z odpadní biomasy, Úprava nerostných surovin, VŠB TU Ostrava 2006, p. 63–71.
5. Chunshan L., Kenzi S., Tar property, analysis, reforming mechanism and model for biomass gasification – An overview, Renewable and Sustainable Energy Reviews, Volume 13, Issue 3, April 2009, p. 594–604.
6. Schobert H. H., Song C., Chemicals and materials from coal in the 21st, Fuel 81 (2002), p. 15–32.
7. Esser S., Andrésen J. M., Properties of Fuels, Petroleum, Pitch, Petroleum Coke, and Carbon Material in: G. E. Totten, S.R. Westbrook, R.J. Shah, Fuels and Lubricants Handbook: technology, properties, performance and testing, 2003, p. 759–787.

CHARACTERIZATION OF NANOPOROUS MEMBRANES WITH CONTROLLED PERMEABILITY

JIŘÍ SMILEK*[a], HANA KYNCLOVÁ[b], PETR SEDLÁČEK[a], JAN PRÁŠEK[b] and MARTINA KLUČÁKOVÁ[a]

[a]*Brno University of Technology, Faculty of Chemistry, Materials Research Centre, Purkyňova 118, 612 00 Brno, Czech Republic*
[b]*Brno University of Technology, Central European Institute of Technology, Smart Nanodevices, Technická 3058/10, 616 00 Brno, Czech Republic*
[c]*Brno University of Technology, Faculty of Electrical Engineering and Communication, Technická 3058/10, 616 00 Brno, Czech Republic*
**xcsmilek@fch.vutbr.cz*

Abstract

Thin two-dimensional nanostructured films are abundantly used for the development of the whole range of sensors especially biosensors. Growing interest about usage of nanoporous materials in sensory analysis is given mainly by their specific permeability, which is primary driven by pore size and shape. These important parameters can be influenced by the modification of preparation process. Necessary assumption for practical utilization of these nanoporous membranes is their characterization especially with regard to their transport properties – determination the critical size of particle, which are able to penetrate through membrane undisturbed. Promising methodology for the study on penetration of chosen diffusion probe through nanoporous membranes seems to be diffusion cell technique. Diffusion of suitable probe (potassium chloride) will be realized through prepared nanoporous membranes and fundamental transport parameters, such as effective diffusion coefficient, will be calculated from the concentration change of chosen diffusion probe in acceptor part of diffusion cell. The change of concentration will be determined by UV-VIS spectroscopy and by conductivity. Results obtained from these experiments will contribute to the draft of electrochemical microsensor for detection of various substances in solutions and pores as well.

Introduction

Nanostructured membranes based on anodic aluminum oxide (AAO) with highly organized nanopores (nanocolumns) are abundantly studied because of their unique physical properties[1] and wide range of potential application. AAO can be utilized in optical[2], electronic or electrochemical branches as a tool for sensing of gases, biosensors, catalysis, selective separation of molecules, filtration, purification[3].

The physical properties of anodic alumina oxide membranes are strongly influenced mainly by the morphology of the final product. The change of physical-chemical properties such as permeability can be driven during the anodization process[4]. The main parameters which are able to influence the permeability are *pore size* (alumina membranes obtained by anodization method have nanopores with diameter in range from 4 nm to 250 nm), *thickness* (in the range 1–200 μm) and *density of pores* (typically 10^9–10^{12} pores/cm^2). Dimensions of pores can be easily controllable by changing of procedure conditions (current density, time of anodization, type of electrolyte or applied voltage)[5].

Growing interests about the usage of nanoporous membranes in sensor technologies is given mainly by their specific permeability for different solutes. This permeability is influenced primary by shape and size of nanopores in alumina membranes and also by the size of diffusing solutes. One of the most important facts for practical usage of anodic alumina oxide nanoporous membranes is the detailed knowledge of their transport (permeability) properties. Methodology, usually used for the determination of these fundamental penetration parameters, is well known and described in literature.

Kipke and Schmid[6] studied the diffusion processes realized through alumina membranes with pore size in range 20–200 nm. Organic dye crystal violet (C.I. 42555) encapsulated in the micelles of sodium dodecyl sulfate (SDS). They used horizontal diffusion cell (Franz diffusion cell) for the realization of the transport experiments. They observed absolutely no influence of the pore width on the delivery speed. Romero et al.[7] studied the penetration of sodium chloride through nanoporous membranes based on alumina. They studied mainly the interactions between diffusing probes (low molecular ionic compounds) with alumina membranes.

In this study, the permeability of different alumina membranes was determined by the change of concentration of chosen diffusing probes through membranes. Potassium chloride as a representative of low molecular ions compounds and methylene blue as a representative of basic organic dyes were chosen as a suitable diffusion probes. The change of concentration of potassium chloride was determined by conductivity measurements and the change of methylene blue (C.I. 52015) was measured by UV-Vis spectroscopic measurements. Methylene blue, as cationic organic dye, was chosen purposefully, because the authors have wide experience with the usage of this dye for penetration experiments. Sedlacek et al.[8, 9] studied the mobility of methylene blue through hydrogels samples with addition of humic acids. This cationic dye is able to interact with anionic supramolecular humic acids and fundamental diffusion parameters such as effective diffusion coefficient, break-through time (lag time) and sorption capacity of agarose hydrogel with/without addition of humic acids can be calculated. All experiments were realized in horizontal diffusion cells (Fig. 1).

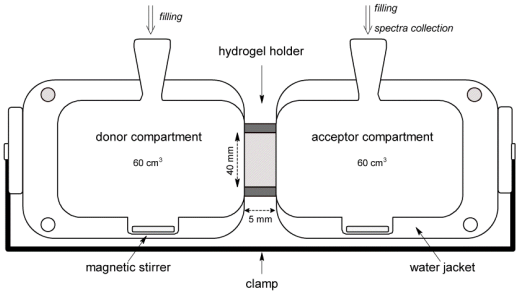

Fig. 1. **Schematic draw of horizontal diffusion cell**

Experimental

The synthesis of alumina membranes was performed by anodic oxidation in weakly acidic environment. Precise procedure of the preparation is summarized by Li et al.[10] Experimental setup for preparation of alumina membranes is given in Table 1.

Table 1
Experimental setup for preparation of alumina membranes

Alumina membranes	Applied voltage	Anodization solvent	Time of anodization
Sample 1	40 V	oxalic acid	4 hours
Sample 2	40 V	oxalic acid	6 hours
Sample 3	20 V	sulfuric acid	8 hours

First of all, alumina membranes were characterized by fundamental physical-chemical methods. The exact thickness of membranes was measured by profilometry (DektakXT, Bruker), the measurement of roughness was performed by elipsometry (Uvisel, Horina JobinYvon). Homogeneity, shape and the pore size was studied by scanning electron microscopy (Tescan FE MIRA II LMU with detectors EDX and WDX). Applied voltage during SEM measurements was 12.5 kV, magnitude was 100 000×. Specific surface area values were determined by using a Quantachrome NOVA 2200 analyser (Quantachrome Instruments). The samples were degassed and evacuated. The evacuated chamber with sample was filled by pure nitrogen. The measurements were repeated three times. The penetration experiments were realized in the water-jacketed horizontal diffusion cells (PermeGear, Inc.). Schematic draw (without dimensions) of horizontal diffusion cell is shown below (see Fig. 1).

Potassium chloride (> 99.0 wt. %, Sigma Aldrich®) was used as suitable diffusion probes without further purification. The cell volumes were 50 cm^3 in each compartment of diffusion cell. All experiments in diffusion cells were realized at constant temperature 25 °C. The temperature was controlled and maintained at constant value by circulating water bath. The stirring of both solutions (acceptor and donor compartment of diffusion cell) was arranged by magnetic stirrer (constant rate 350 rpm).

Results and discussion

Thickness and roughness of alumina membranes

The thickness of alumina membrane can be varied by changing of experimental conditions during preparation of membranes. The highest impact on the thickness of alumina membrane has the applied voltage and the time of anodization. If we will compare sample 1 (40 V, oxalic acid, 4 hours) with sample 2 (40 V, oxalic acid, 6 hours), it is obvious, that the thickness of alumina membranes decrease with increasing time of anodization.

The roughness of alumina membranes can be varied especially by changing of anodization solvent. Sample 4 was prepared by anodization process in sulfuric acid instead of other samples, which were prepared by anodization in oxalic acid. Sample 3 have lower roughness (at least 5×) in comparison with all other samples. The knowledge of roughness is one of the most important parameter for the accurate description of diffusion processes.

Table 2
Thickness and roughness of alumina membranes

Alumina membranes	Thickness (μm)	Roughness (μm)
Sample 1	160 ± 5	3.4
Sample 2	43 ± 2	4.4
Sample 3	103 ± 2	0.5

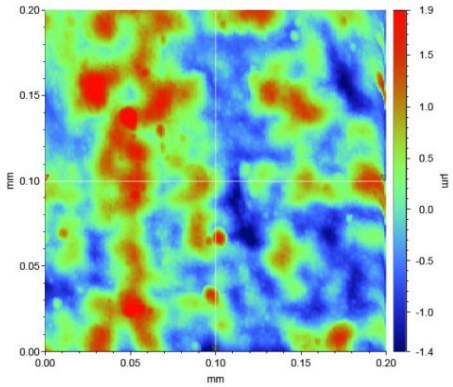

Fig. 2. **Surface profile for sample 1 determined by elipsometry** (Uvisel, Horina JobinYvon)

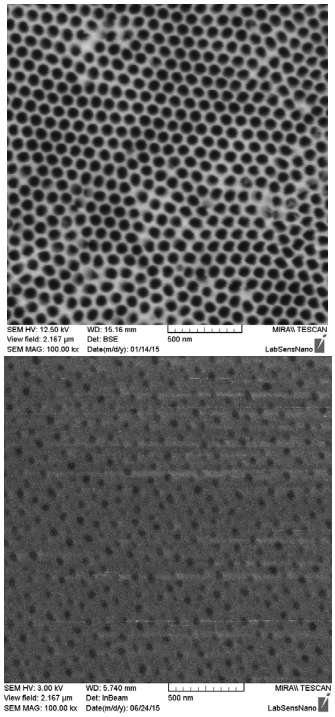

Fig. 3. **Scanning electron microscopy of nanoporous alumina membranes anodized in oxalic acid (left) and sulfuric acid (right)**

Scanning electron microscopy of alumina membranes

Nanoporous alumina membranes were characterized by scanning electron microscopy to determine the morphology and mainly the distribution of pores. The main purpose for this characterization was to determine the influence of anodization solvent for the morphology of fabricated membranes.

It is obvious, that the alumina membranes anodized in oxalic acid (Fig. 3 on the left) dispose higher pore size in comparison with alumina membranes anodized in sulfuric acid (Fig. 3 on the right). But the differences in pore size are not so significant. The barrier properties of alumina membranes are influenced mainly by distribution of pores. Density of pores for alumina membranes anodized in oxalic acid is much higher in comparison with membranes anodized in sulfuric acid (see Fig. 3)

Ionic permeability tests

Simple through-diffusion experiments in diffusion cells were performed in order to evaluate permeability of the prepared membranes for model low-molecular ions. Break-through curves, determined for the diffusion of potassium chloride, are presented in Fig. 4. Obviously, structural differences of the tested membranes resulted in a correspondingly altered barrier properties. Regression of the linearly increasing part of a breakthrough curve provides two important parameters which allow evaluation of membranes' transport properties in a quantitative way, as was addressed in details in our previous work[8].

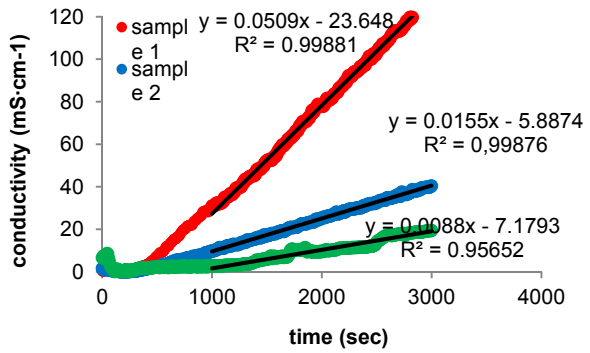

Fig. 4. **The change of conductivity as the time function. Break-through curves determined for the diffusion of potassium chloride**

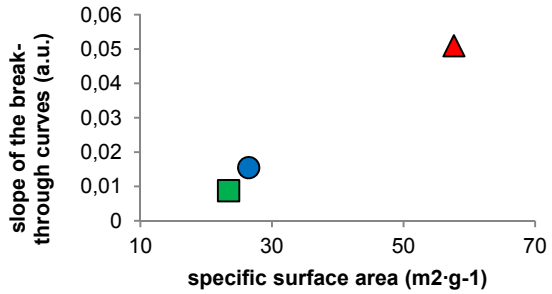

Fig. 5. **The slope of the break-through curves as the function of specific surface area. ▲ represents sample 1, ● shows sample 2 and ■ is sample 3**

Slope of the increasing part of the breakthrough curve represents a major experimental outcome as far as the membrane permeability is concerned. Furthermore, the slope should be crucially affected by the structure of the material, mainly its porosity. This expectation was experimentally confirmed.

The slope increases with specific surface area of the membranes as it is shown in Fig. 5 – i.e. with their increasing microporosity.

On the other hand, the break-through time (determined as the *x*-axis interception of the regression line) the time needed by the solute to penetrate the membrane. It is affected by the total thickness of the membrane in combination with the particular pathway of the solute transport in the individual pore (i.e. by the tortuosity of the transport). As can be seen in Fig. 6, no clear correlation was found between the break-through times and corresponding membrane thicknesses. This indicates that in spite of the fact that a simply tubular shape of the membrane pores is assumed for the prepared membranes and no significant differences in the pore diameters were detected by means of SEM, the specific diffusion pathway may differ for particular membranes.

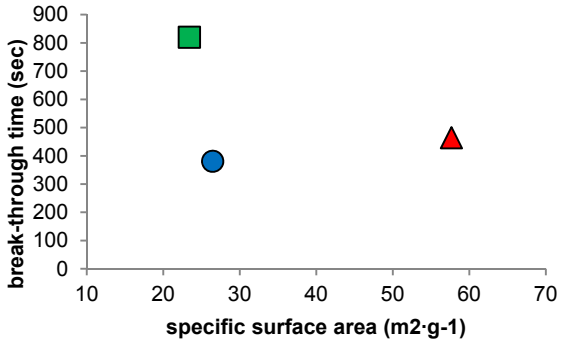

Fig. 6. **Break-through time as the function of specific surface area. ▲ represents sample 1, ● shows sample 2 and ■ is sample 3**

Conclusion

The barrier properties of alumina membranes were studied by horizontal diffusion cell technique by diffusion of potassium chloride. Penetration ability of potassium chloride through nanoporous alumina membranes is strongly dependent on the *specific surface area* (the linear increase of the slope of the break-through curve with increasing specific surface area was observed). The permeability is also strongly dependent on the *pore size* and the *distribution of pores* in the structure of membrane. This expectation was experimentally confirmed by correlation of scanning electron microscopy with diffusion experiments (the slope of the break-through curve is the lowest for membrane anodized in sulfuric acid. This sample disposes totally different distribution of pores in comparison with samples anodized in oxalic acid).

This work has been supported by the project FCH/FEKT-J-15-2663 IGA Development of sensors based on nanoporous membranes with controlled ion permeability, by project FEKT-S-14-2300 A new types of electronic circuits and sensors for

specific applications and by project "Materials Research Centre at FCH BUT – Suistainability and Development" No. LO1211 of the Ministry of Education, Youth and Sports of the Czech Republic.

REFERENCES

1. Yang, C. J., Liang, S. W., Wu, P. W., Chen, C., Shieh, J. M.: Electrochem. Solid-State Lett. 10, (12) 2007.
2. Sarkar, J., Khan, G. G., Basumallick, A.: Bull. Mater. Sci. *30*, 3 (2007).
3. Stroeve, P., Ileri, N.: Trends Biotechnol. *29*, (6) 2011.
4. Schneider, J. J., Engstler, J., Budna, K. P., Teicher, C., Franzka, S.: Eur. J. Inorg. Chem. *10*, (12) 2007.
5. Poinern, G. E. J., Ali, N., Fawcett, D.: Materials. *4*, (3) 2011.
6. Kipke, S., Schmid, G.: Adv. Funct. Mater. *14*, (12) 2004.
7. Romero, V., Vega, V., García, J., Prida, V. M., Hernando, B., Benavente, J.: J. Colloid Interface Sci. *376*, (1) 2012.
8. Sedlacek, P., Smilek, J., Klucakova, M.: React. Funct. Polym. *73*, (11) 2013.
9. Sedlacek, P., Smilek, J., Klucakova, M.: React. Funct. Polym. *75*, (-) 2014.
10. Li, Y., Zheng, M., Ma, L., Shen, W.: Nanotechnology. *17*, (20) 2006.

ANALYSIS OF TIRE COMPOSITION FOR FURTHER DETECTION OF TIRE MARKS ON THE ROAD

TOMÁŠ SOLNÝ[a], PAVEL DIVIŠ[a], PETR PTÁČEK[a], VLADIMÍR ADAMEC[b], MARTIN BILÍK[b], ALBERT BRADÁČ[b] and BARBORA SCHÜLLEROVÁ[b]

[a]*Brno University of Technology, Faculty of Chemistry, Purkyňova 118, 612 00 Brno, CZ*
xcsolny@fch.vutbr.cz
[b]*Brno University of Technology, Institute of Forensic Engineering, Údolní 244/53, building U2, 602 00 Brno, CZ*

Tire related particles are generated by interaction of the tire with the roadway surface. Tire marks on the road composed from the tire particles are one of the main tool for the analysis of car accident. Based on the length of tire mark the actual speed of the vehicle can be determined[1]. With increasing technical equipment of vehicles and with the introduction of the ABS system, tires marks on the road are becoming almost invisible to the human eye. Given that the braking track is one of the important aspects for the analysis of accident, their easy and accurate detection is very important. Individual corporations producing tires have different mixtures for making the tire. In conventional types of tire, which weighs about 10 kg, about 30 kinds of synthetic rubber, about 8 kinds of natural rubber and carbon materials, steel belts, polyester and nylon fibers, 40 different kinds of chemicals, waxes and oils can be found. Based on the knowledge of the chemical composition different types of tires within a track on the road can be identified and assigned to a specific vehicle. In the recent years application of laser break-down induced spectroscopy (LIBS) was investigated for the identicication of tire marks on the road[2]. For using this technique good marker (analyte) must be selected. Most often, zinc is used for such purpose. However in the present literature some information about the tire dust composition can be found[3, 4], there is a lack of information about the composition of various types of tires. In this preliminar study analysis of different types of tires was done by XRD and ICP-OES techniques and any differences in the chemical composition of tires were monitored. Based on this study broader analysis of more than 30 different tires will be performed and the database of chemical composition will be crated. This database will help to choose the alternative marker for the analysis of tire marks on the road by LIBS technique.

For the analysis only the top layer of the tire without the steel and nylon fibers was used. The tire was directly analysed by XRF (Xenemetric EX – 6600 SSD) Each of the sample was adapted to the appropriate size and measured directly under vacuum for 5 minutes with colimator, current 450 μA and voltage 20 Kv. For the analysis on ICP-OES (Horiba JY, Ultima 2, France) 1 g of the tire sample was dissolved in 30 ml of concentrated nitric acid. The sample with the nitric acid was placed on the heating plate and heated for 5 h. The temperature during the decomposition was set to 80 °C. After the decomposition created suspension was filtrated through a pre-weighed filters and filtrate was collected to the 25 ml volumetric flask. The volumetric flask was then filled up to the mark with ultrapure water. The setting of an ICP-OES instrument is summarized in Table 1. Carbonaceous fraction captured on the filter was dried and used for quantification of the amout of carbonaceous fraction, respective for the amounts of leachable substances from tires.

Table 1
Settings of an ICP-OES instrument used in this study

Power	1300	W
Pump rotation	18	rpm
Plasma gas	13.0	l/min
Sheat gas	0.2	l/min
Nebuliser pressure	0.3	MPa
Emission lines (nm):		
Al 396.152; Ba 230. 424; Cr 205.552; Cu 327.396; Fe 259.940; Mg 285.213; Mn 257.610; Ni 231.604; P 213.618; Si 251.611; Ti 334.941; Zn 206.191		

Before the tire analysis on ICP-OES a qualitative analysis was done on XRF. The typical spectrum from XRF analysis is shown on the Fug. 1.

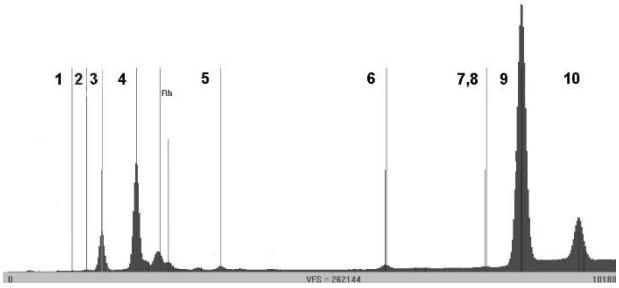

Fig. 1. **XRF spectrum of tire sample**

Table 2
Evaluation of XRF spectrum shown in Fig. 1

Peak		Energy (keV)	Peak		Energy (keV)
1	$K\alpha_1$Mg	1.254	6	$K\alpha_1$ Fe	6.403
2	$K\alpha_1$Al	1.487	7	$K\alpha_2$ Cu	8.027
3	$K\alpha_1$ Si	1.740	8	$K\alpha_1$ Cu	8.047
4	$K\alpha_1$S	2.307	9	$K\alpha_1$ Zn	8.638
5	$K\alpha_1$Ca	3.690	10	$K\beta_1$ Zn	9.571

In the spectre shown on figure 1 it is possible to find three types of peaks. There are peaks corresponding to standard energy transitions (Kα1, Kα2, Kβ1, Kβ2, Lα1, Lβ1 and LI). In addition to standard peaks it is also possible to find an escape and a sum peaks in the spectrum. Escape peaks occurs when Si in the detector absorbing some of the energy from a X-ray. Sum peaks occurs when two X-ray photons arriving at the

detector at the same time. In the spectra can be seen: major elements peaks (Si, S, Ca, Fe and Si), minor elements peaks (Mg, Al and Cu) and peaks caused by the use of rhodium X-ray tube for X-ray induction. All the important peaks (outside of rhodium peaks) were numbered. Evaluation of numbered peaks is shown in the table II. The relative concentration of metals measured on XRF is summarized in table III. The relative concentration of all studied elements varied between the analysed tires samples and the differences were statistically significant ($p < 0.05$). The highest relative concentrations were recorded for zinc and sulphur. Zinc in the form of zinc oxide and sulphur are used as an agents simplifying the process of vulcanization. Other metals detected at significant levels were silicon, calcium and aluminium. Silicon is added to the tire because it has excellent thermal properties, strong mechanical and corrosive reistance. Detected calcium and aluminium can be attributed to calcium carbonate and aluminum hydroxide which are used in tire manufacturing process.

Table 3
Relative concentration (%) of selected elements detected on XRF

	Tire1	Tire2	Tire3	Tire4	Tire5
Mg	0.992	1.195	1.285	1.053	0.874
Zn	40.39	50.89	44.13	49.25	39.28
Cu	0.099	0.619	0.069	0.094	0.158
Fe	0.291	1.352	0.783	0.367	0.464
Ca	6.235	2.494	3.645	2.539	0.863
S	47.22	33.89	39.46	44.39	30.66
Si	4.122	7.184	8.331	1.714	26.54
Al	0.648	2.376	2.292	0.581	1.159

After the analysis on XRF, tires samples were decomposed in nitric acid and analysed by ICP-OES. Decomposition of tires samples does not produce clear solution, however, by further analysis it was demonstrated that the solid residue is composed only from carbon. The amount of carbonaceous fraction does not differ in analysed tires and it was 98.0 ± 0.2 %. Results from the ICP-OES analysis are summarized in table IV. Concentration of Zn, Al, Fe, Mg, P, Si and Ti varied between the analysed tyre samples and the differences were statistically significant ($p < 0.05$) while the difference in concentration of other detected elements (Ba, Cr, Cu, Mn and Ni) was statistically insignificant. The elemental composition of tires is not described in detail in the present literature. The most studied element is zinc. The concentration of zinc in the tires ranges from 8.4 to 15.5 $mg.g^{-1}$ [2]. In the present study the zinc concentration in tires varied between 4.1 and 6.6 $mg.g^{-1}$. Concentration of other elements detected in tyre samples analysed in this study can be compared only with the concentration of the same elements found in the tire dust. Other data for the comparison of results obtained in this study are unfortunatelly not available. Concentration of selected elements is in some cases comparable with the road dust composition, for most of the elements however the metals concentrations in tire dust are much higher. This difference is caused by contribution of other particles (not only the tire particles) to the road dust. The road dust contains also particles from breaks and mineral dust from the road surface[5].

Table 4
Concentration of selected elements ($mg.g^{-1}$) analysed by an ICP-OES technique in different tires samples

	Tire1	Tire2	Tire3	Tire4	Tire5
Zn	5.081	4.807	6.638	4.673	4.071
Al	0.066	0.052	0.129	0.052	0.029
Ba	0.006	0.007	0.006	0.006	0.004
Cr	0.001	0.002	0.001	0.001	0.001
Cu	0.005	0.005	0.004	0.003	0.003
Fe	0.024	0.040	0.077	0.037	0.016
Mg	0.048	0.061	0.102	0.063	0.078
Mn	0.001	0.001	0.002	0.001	0.002
Ni	0.003	0.006	0.001	0.005	0.001
P	0.020	0.044	0.051	0.027	0.014
Si	0.029	0.020	0.022	0.035	0.018
Ti	0.166	0.195	0.145	0.188	0.179

From the results of this study it can be concluded that the elemental composition of different tire types may be significantly different. Searching of other marker than zinc for the analysis of tire marks on the road surface will be an intricate task requiring more detailed analysis.

This work was supported by Junior Internal Grant of Brno University of Technology. Registration number: J-15-2807.

REFERENCES

1. Heinrichs B. E., Allin B. D., Bowler J. J., Siegmung G. P.: Accident Anal. Prev., *36*, 829 (2004).
2. Prochazka D., Bilik M., Prochazkova P., Klus J., Porizka P., Novotny K., Ticova B., Bradac A., Semela M., Kaiser J.: Spectrochim Acta B, *108*, 1 (2015).
3. Kreider M. L., Panko J. M., McAtee B. L., Sweet L. I., Finley B. L.: Sci. Tot. Environ., *408*, 652 (2010).
4. Kreider M. L., Panko J. M., McAtee B. L., Sweet L. I., Finley B. L.: Sci. Tot. Environ., *408*, 652 (2010).
5. Dall´Osto M., BeddowsD. C. S., Gietl J. K., Olatunbosun O. A., Yang X., Harrison R. M.: Atmos. Env., *94*, 224 (2014).

TESTING OF SPECIAL BINDERS FOR IMMOBILIZATION OF TOXIC ELEMENTS

THEODOR STANĚK[a] and PETR SULOVSKÝ[b]

[a]*Research Institute for Building Materials, Hněvkovského 65, 617 00 Brno, Czech Republic*
stanek@vustah.cz
[b]*Department of Geology, Faculty of Science, Palacký University, tř. 17. listopadu 12, 771 49 Olomouc, Czech Republic*
petr.sulovsky@upol.cz

The paper deals with development of cementitious binders that would be able to efficiently immobilize toxic elements contained in various types of wastes. The basic component of the proposed binders are clinkers with phosphorus incorporated into the structure of clinker silicates, mixtures of cement with ash containing hydroxylapatite and belite-rich clinkers activated with sulfate anions. The prepared binders were mixed with water doped with various toxic elements; after a defined period of cement stone hydration the specimens were subjected to long-term testing of leachability of individual toxic elements. The research methods involved besides leaching tests were also optical and electron microscopy.

1. Introduction

The main goal of stabilization or solidification (s/s) is steady reduction of the mobility of toxic substances contained in processed wastes[1]. Stabilization lies in a change of physical and/or chemical properties of wastes by mixing them with proper additives[2]. Currently, s/s technique is recognized as one of the solutions to fix contaminants and has been identified by the US EPA (Environmental Protection Agency) as the Best Demonstrated Available Techniques for 57 regulated hazardous wastes[3]. Depending on the nature of the waste and the type of utilized admixtures, various physico-chemical reactions occur in the treated waste materials – sorption, substitution, hydration, precipitation, encapsulation. The stabilized waste can be disposed in a landfill or utilized in a suitable way – e. g. as building material – without introducing a risk of ensuing contamination of the environment.

The aim of this research project is development of special binders for immobilization of certain toxic elements or groups of elements (oxyanions-forming elements, heavy metals, amphoteric elements). The base of the binders for stabilization of cationic and certain anionic contaminants will be clinkers with phosphorus incorporated into the structure of clinker minerals. Hydration of such binders results in formation of phases with the apatite structure, which is known to be able to immobilize hazardous elements[4, 5] and belite and alite structures for formation of binding hydrosilicates, ensuring the physical compactness of the hydrated matter and also the fixation of some toxic elements.

The main object of research is dicalciumsilicate and tricalciusilicate with isomorphous admixture of Al/Ca phosphates („phosphobelite“ or „phosphoalite“); to a lesser extent, other types of anionic substitutions in C_2S and C_3S or other solid-solution mineral phases („sulfobelite“) or other cement types (e. g., calciumaluminate) or other supplementary additives (sorbents, additives changing redox state of hazardous elements) can be utilized to bind toxic elements.

2. Materials and methods

In order to assess the immobilization efficiency of different simple and blended binders, test bodies were prepared with mixing water enriched with soluble salts of toxic elements. Their concentrations had two constraints: one is the fact that high contents of heavy metal cations (for example Cu, Zn, Sn, Cd) with highly insoluble hydroxy compounds in alkaline solutions retard setting[6]. One of the constraints were the detection limits of the method of leachate analysis. This does not make much problems with leachates obtained by the so called batch („shaken“) method, but can be difficult in case of the long-term, monolithic („tank“) test. The resulting compromise was 1000–2500 mg/kg dry binder paste.

The large number of binders to be tested led to choosing toxic elements representative of the main groups of toxic elements: cations-forming Cd, Ni (true “heavy metals”), Pb and Zn (amphoteric heavy metals) and anions-forming metals and metalloids (Cr, V, As). The soluble salts used were combined in the following way: $Pb(NO_3)_2$ + $CdNO_3.4H_2O$, $ZnSO_4.7H_2O$ + $NiCl_2.6H_2O$, K_2CrO_4+NH_4VO_3 and $NaAsO_2$ was used alone. Each salt was added in amount corresponding approximately to 2 grams of each toxic element per 1 kg of binder. The chemicals were first dissolved in a constant volume of demineralized mixing water assigned for processing of the given binder. Pastes prepared from individual cement binders were cast in forms with dimensions 2 × 7 × 10 cm and stored in humid environment, and matured for 28 days. More than 100 hydrated test bodies were prepared for long-term monolithic testing. Collaterally, the same number of test bodies was prepared for determination of the contents of studied elements in dry matter by ICP-OES and for determination of toxic elements leachability by the batch method.

The properties of mortars were confronted with the control – ordinary Portland cement CEM I 52.5N. The commercial cements were used alone or blended together with cement included OPC, Portland blast furnace cement, calcium aluminate cement (CAC) and white Portland cement. The specially prepared phosphorus-doped clinkers were developed within another project, aimed at safe disposal of meat-and-bone meal by utilizing both as alternative fuel and as calcium-rich raw material[7]. Other specially prepared cements were made from low-saturated clinkers doped with sulfur[8] and reference alite-rich and belite-rich clinkers not doped with P or S. Ten kilograms of each raw meal was mixed in the calculated proportions and grinded in order to obtain amount of clinker sufficient for performing planned testing of cements made of them. Sulfur-doped low saturated clinkers with prevalent belite were burned at 1350 °C, the other clinkers at 1450 °C in superkanthal furnace with

holding time individually chosen to keep the content of residual free lime low enough not to cause unwanted volume changes during hydration. The phase composition was quantified using microscopic point counting.

The burned clinkers with gypsum added as setting regulator were grinded to cements with the same specific surface of 400 m^2/kg. The following parameters were determined for them: specific gravity, specific surface, particle size distribution, setting and volume stability according to EN, setting according to Tussenbrock, heat of hydration, measured by adiabatic calorimeter, dissolution heat according to EN and compressive and tensile strengths after 2, 7, 28 and 90 days of hydration according to EN.

In the ensuing phase, test bodies were prepared from various binders with added pure chemical compounds of the toxic elements for the purpose of study of their leachability. The binders that were used in this step can be divided into five groups (see Table 1).

Table 1
Overview of cem. binders for testing of PHE immobilization

Group	Binder
Reference binders	CEM I 52.5N, CEM II/B-S 32.5R, White CEM I CAC – Gorkal 40, Gorkal 50 A97S0 – high alite clinker, not doped B80S0 – high belite clinker, not doped
Cements from clinkers doped with P_2O_5	AP1 (cement from alite clinker with 1% P_2O_5) AP2 (cement from alite clinker with 2% P_2O_5) CAC 70% + AP1.5 30% (clinker with 1.5% P_2O_5) AP7/MKM (alite clinker with 7% P_2O_5 as granules of MBM ash)
Cements with addition MBM ash	9 – CEM I 52.5N (90%) + MBM ash (10%) 10 – White CEM I (90%) + MBM ash (10%) 17 – CAC (95%) + MBM ash (5%) 11 – CAC (90%) + MBM ash (10%) – 11 12 – CEM I 52.5N (50%) + CAC (40%) + MBM ash (10%)
Cements with addition of diatomite	18 – CAC (80%) + calcined diatomite (20%) 27 – CEM I 52.5N (75%) + diatomite (20%) + MBM ash (5%) 21 – CEM I 52.5N (80%) + diatomite (20%) 24– CAC (75%) + calc. diatomite (20%) + MBM ash (5%) 20 – CAC (80%) + diatomite (20%) 40 – CAC (75%) + diatomite (20%) + MBM ash (5%) 42 – CEM I 52.5 N (70%) + CAC (10%) + diatomite (20%)
Clinkers doped with SO_3	B89S5, B83S8, A92S8, B90S6MA2.5 – cements made from clinkers doped with SO_3, those do not contain yeelemite (numbers after S correspond to SO_3 concentration in %)

Despite the distinct decrease in early strength and other technological performance the long-term strengths of all cements, even the lowest ones in sulfobelite B83S8, are suitable for solidification purposes.

In the batch leaching test, the hydrated (min. 28 days) test bodies were crushed <10 mm, the material was mixed with distilled water at S/L = 1:10 and shaken "over head" for 24 hours. The decanted leachates were filtered through a 0.45 μm pore filter. The leachates were analyzed by ICP-MS (Agilent).

In the long-term semi-dynamic test, performed according to NEN7345, a monolithic specimen is subjected to leaching in a closed tank to evaluate surface area related release. The leachant demineralized water is renewed after 8 hours and 1, 2, 4, 9, 16, 36, 64 days using a leachant to product volume ratio (L/V) of 5. The leachate was also filtered and analyzed by ICP-MS.

For the purpose of assessing the (re)distribution of the used toxic elements upon hydration, fragments of cement paste after 28 days of hardening were embedded in epoxy resin (Araldite®), polished and studied by optical microscopy methods. Furthermore, the polished sections were coated with carbon and analyzed with electron microscopy and WDX analysis, using microprobes CAMECA SX 100 and Jeol JXA8600. The study involved acquisition of X-ray maps of the main binder constituting elements (Ca, Mg, Si, Al, Fe, S, P) and respective trace elements given above.

3. Results and Discussion

3.1 Results from the Batch Test

The leachant pH in experiments with calcium aluminate cements is about 1 to 1.5 units lower than the leachant from OPC reference. In all experiments, the concentration in the leachate was compared with the concentration in leachate from reference OPC; both normalized with the contents in the dry mortar (as these are only roughly equal). The results from chosen mortars are given in Table 2.

From the data in Table 2 several possible conclusions can be drawn:

- Calculations of Pearson´s correlation coefficient from 2 × 2 correspondence tables have shown that the presence of calcium aluminate cement in the s/s binder has a strong positive effect on the immobilization of all abovementioned toxic elements. The positive effect of CAC on the immobilization (as compared with OPC) can be explained by the substitution of the toxic elements in the products of hydration of the main CAC clinker phases[9] or simply by the fact that most of these elements show the solubility minimum in pH ranges slightly below the range in OPC, but equal to that found in pore solutions in CAC[11].
- White cement compared with common Portland cement (PC) shows lower leachability of Pb, Cd, Zn, Cr, Ni and V, but increases leachability of As.
- From the phosporus-doped cements (AP1, AP2, AP7/MBM), the lowest leachability shows in the case of Pb and As the one with the lowest P_2O_5 content (AP1). Chromium and zinc, on the contrary, are least leachable from the cement with the highest P_2O_5 content (AP7/MBM). Anyway, all tested P-enriched binders show leachability of all studied hazardous element lower than those in the reference binder CEM I 52.5N.
- Sulfobelite cements very strongly increase the leachability of all anions-forming elements (Cr, V and in two cases

As) and in one case also that of Pb and in another case of Zn. The toxic elements have probably been substitutionally incorporated into ettringite and subsequently released upon its transformation to monosulfate. Increased leachability of some elements from clinkers doped with sulfur can also be caused by a slow hydration and hardening of belite which is present in predominant amount.

- The addition of diatomite has certain positive effect on the immobilization of toxic elements – an effect that can probably be explained by the release of reactive silica into the hydrating mortar, which changes the C/S ratio of the C-S-H product, discussed in Richardson[10], towards the composition better fixing the toxic elements.
- The results obtained with blended binders have shown that the addition of MBM ash decreases the leachability of Zn, Ni and As, but in one case increases that of Cr (binder 27 in Table 2) and in another (binder 17 in Table 2) of V.
- The most promising combinations occurred to be the combination of 90 wt. % of calcium aluminate cement with 10% of MBM ash, which releases distinctly lesser amounts of all PHEs, in case of Pb, Cd, Zn, Ni, Cr and As to less than 28 % of that observed in the reference PC. Another promising is a blend of 70 % CAC with 30 % of P-doped clinker AP1.5. The fixation of these elements can probably be attributed to formation of discrete microaccumulations of insoluble metal hydroxides, in case of phosphorus-enriched clinkers of precipitates of analogues of apatite, where the toxic elements substitute both Ca (Zn, Ni, Pb, Cd) and PO_4^{3-} groups (VO_4^{3-}, CrO_4^{3-}, AsO_4^{3-})

Table 2
Leachability of individual toxic elements in % of leachability of reference binder (CEM I 52.5N)

No	Binder description	Pb	Ni	Zn	Cr	V	As
1	CEM I 52.5N	100	100	100	100	100	100
33	CEM II/B-S 32.5R	183	92	81	46	51	33
2	White CEM I	65	<3	50	45	43	153
44	CAC - Gorkal 50	0.6	35	23	13	0.1	44
6	AP1	49	<3	34	54	62	55
7	AP2	89	<3	23	53	81	94
8	AP7/MKM	60	<3	26	46	43	88
13	B89S5	37	30	<3	342	233	40
15	B83S8	107	51	<3	188	188	36
9	see table 1	58	<3	21	48	41	52
10	see table 1	69	<3	35	70	68	112
17	see table 1	2	58	21	7	136	20
11	see table 1	1	4	17	27	0.1	3
12	see table 1	18	79	25	46	22	10
18	see table 1	0.1	<3	14	2	55	89
27	see table 1	23	<3	<7	165	75	7
21	see table 1	13	27	7	117	123	59
24	see table 1	0	35	10	1	46	20
20	see table 1	1	29	7	4	0.2	70
40	see table 1	0.3	30	12	0.4	0.3	10
26	see table 1	0.1	<3	5	2	62	1
42	see table 1	1	40	25	170	19	29

3.2 Long Term Leachability Experiments

The mode of leaching is studied with the use of long-term monolithic "tank" tests according to NEN EU 7375. The leaching of toxic elements is diffusion controlled; the overall thickness of the surficial layer from which they are leached over 3 months does not exceed 0.2 mm. Cumulative long-term (64 days) release lower than in the reference CEM I 52.5N was observed in case of zinc in large majority of tested binders. On the contrary, long-term release of chromium was lower only in a few of them; the exceptions are binders from P-doped clinkers (AP1, AP1.5), binders containing MBM ash and binders from sulfobelite clinkers.

3.3 X-ray Mapping

The electron microprobe study through the acquisition of X-ray maps and BSE images of mapped areas has shown, that in most cases the hazardous elements, though applied dissolved in water, eventually form discrete microaccumulations. In binders based on P-doped clinkers, Cr and Ni precipitated as discrete microparticles, while V and Zn occur finely distributed in the matrix. Ni forms microaccumulations also in other types of binders, especially in CAC-based binders. Vanadium and nickel occur in most studied mortars homogenously distributed. Arsenic was dispersed in the hydrated binder matrix relatively homogenously, with moderately increased concentrations observable around grains of MBM ash as well as relict CA clinker grains. In most binders studied by X-ray mapping, cadmium occurs to form microaccumulations or increased concentrations in porous MBM ash particles.

4. Summary

All above described test methods have shown that the immobilization properties of the ordinary Portland cement are weaker than those of binders containing calcium aluminate cements and/or cement enriched with phosphorus; among the latter, cements based on phosphorus-doped clinkers are more efficient than binders with MBM ash addition. In OPC-based cements, addition of diatomite can help to improve the immobilization of toxic elements by changing the Ca/Si ratio of C-S-H hydrates.

This research was done within the project No. P104/12/1494 financed by the Czech Science Foundation.

REFERENCES

1. Means J. L.: *The application of solidification/stabilization to waste materials*. Boca Raton, Lewis Publishers, 1995.
2. Kafka Z., Vošický J.: (in Czech), Chem. listy *92,* 789–793 (1998).
3. Shi C., Spence R.: Sci. Technol. *34,* 391–417 (2004).
4. Gómez del Río J., Sanchez P., Morando P.J., Cicerone D. S.: Chemosphere *64*, 1015–1020 (2006).
5. Vega E. D., Pedregosa J. C., Narda G. E.: J. Argent. Chem. Soc. *97*, 1–12 (2009).
6. Tashiro C.: The effect of several heavy metal oxides on the hydration and the microstructure of hardened mortar of C_3S, in: Proc. 7th Inter. Cong. of Chem. of Cem. *11,* Edit. Septima, Paris, 1137 (1980).
7. Staněk T., Sulovský P.: Mater. Char. *60,* 749–755 (2009).

8. Staněk T., Sulovský P.: Advances in Cem. Res. *24,* 233–238 (2012).
9. Navarro-Blasco I., Duran A., Sirera R., Fernandez J. M., Alvarez J. I.: J. of Hazard. Mat. 260 (2013) 89–103.
10. Richardson I. G.: Cem. and Concr. Res. *29,* 1131–1147 (1999).
11. Bhattacharyya D., Jumawan A. B., Sun G., Sund-Hagelberg C., Schwitzgebel K.: in: Bennett G.F. (Ed.): Water-1980, AIChE Symposium Series *209*, New York, 31–38 (1981).

INFLUENCE OF VEGETABLE OILS ON FATTY ACIDS COMPOSITION IN PROCESSED CHEESE ANALOGUES

KATEŘINA SŮKALOVÁ*, EVA VÍTOVÁ, FRANTIŠEK BUŇKA and MARTINA MAHDALOVÁ

Department of Food Chemistry and Biotechnology, Faculty of Chemistry, Brno University of Technology, Purkyňova 118, 612 00, Brno, Czech Republic
sklenarova.katerina@gmail.com

Processed cheese analogues are cheese-like products manufactured by blending various edible oils/fats, proteins, other ingredients and water into a smooth homogeneous blend with the aid of heat, mechanical shear and emulsifying salts. They also may be labelled as cheese substitutes or imitations, in which milk fat, milk protein or both are partially or wholly replaced by non milk based components, principally of vegetable origin[1, 2]. They were developed in the United States in the early 1970s to create cheaper substitutes for the industrial and catering cheese sectors; their designation and labeling should clearly distinguish them from cheese. They are more and more used as advantageous product, because they can offer several health benefits to consumers comparing to classical cheese. E.g. milk fat is known to be rich in saturated fatty acids (SFA) and cholesterol[1], analogues can be produced with low content of saturated fat and cholesterol free[2, 3]. Knowledge of the individual fatty acid composition of neutral lipids in processed cheese and processed cheese analogues is important in terms of health aspect as well as consumer acceptance. Fatty acids (FA), especially polyunsaturated fatty acids (PUFA) originating from vegetable oils, added to the processed cheese, may offer benefit to the final consumer in the form of higher nutritive value of products. As mentioned before processed cheese analogues can be obtained by means of partial replacement of dairy fat with fats of vegetable origin[1]. Replacement by unusual vegetable oils, having a higher content of PUFA and their derivatives, could be very useful alternative, because they are important essential nutritives in mammals, especially in humans[2, 3].

Free fatty acids (FFA), their content and composition, could also be the important indicator of sensory quality and/or durability of product. They are generally produced by lipolysis during technology as well as storage procedure, contributing directly to cheese flavour, especially in the case of short- and medium-chain FFA. In addition, they also act as substrates for further reactions producing highly flavoured catabolic end products[4, 5].

Very scarce information can be found about FA composition of processed cheese and processed cheese analogues; e.g. the work of Kim et al.[6] could be mentioned. So the aim of this work was to assess the total FA and FFA content in the model samples of processed cheese analogues produced with addition of different vegetable oils (apricot kernel, blackcurrant, flaxseed and grape seed oils). The FA composition was then compared with standard processed cheese (without addition of vegetable oil). The lipid extraction and FA determination was made according to ISO standards; for obtaining FFA the lipid extracts were fractionated using Solid-phase extraction (SPE) method before esterification process. SPE is a widely used sample-preparation technique for the isolation of selected analytes, usually from a mobile phase (gas, fluid or liquid). The analytes are transferred into the solid phase where they are retained for the duration of the sampling process. The solid phase is then isolated from the sample and the analytes recovered by elution using a liquid or fluid, or by thermal desorption into the gas phase[7, 8].

Experimental part

The model samples of processed cheese analogues were produced at laboratory (pilot plant) conditions using standard producing technology[1, 2] with addition of different vegetable oil (apricot kernel (PCA-AO), blackcurrant (PCA-BO), flax seed (PCA-FO) and grape seed oils (PCA-GO). Standard processed cheese (without addition of vegetable oil (PC-S)) was produced at the same conditions. The model samples were produced using a Vorwerk Thermomix TM 31-1 (Vorwerk & Co., GmbH,Wuppertal, Germany) with indirect heating; melting at 90 °C for 10 min. Raw material used: Edam cheese (30 % fat in dry matter), butter (approximately 84%, w/w, dry matter and 82 %, w/w, fat), commercial emulsifying salt (sodium salts of phosphates and polyphosphates; Fosfa a.s., CZ), water and various types of oils (see above) obtained commercially. Declared values of analogues: 40 % (w/w) dry matter, 50 % (w/w) fat in dry matter. After 10 days of storage (< 6 °C), the FA and FFA were measured. Each variant of the sample was measured three times.

Extraction of fat from cheese samples was carried out according to the Official Method of Cheese Analysis (ISO 1735) with some modifications. 1 g of cheese sample was heated and mixed with 5 mL of a hydrochloric acid solution and after cooling, 5 mL of ethyl alcohol were added. After that extraction reagents (diethyl ether and petroleum ether) were added and the mixture was stirred for 5 min. The suspension was then rested for 30 min to allow phase separation. This extraction protocol was repeated 3 times. Three organic extracts were pooled, dried over anhydrous sodium sulfate, filtered with a cellulose filter and evaporated under reduced pressure in a rotary evaporator. Fatty acid methyl esters (FAMEs) were prepared according to ISO 5509 using methanolic KOH and isooctane. For obtaining FFA the lipid extracts were fractionated using Solid Phase Extraction method before esterification process. For confidentiality reasons, the exact conditions are not completely revealed. The GC analyses were performed with Trace GC (ThermoQuest S.p.A., Italy) with flame ionization detection system. The column DB-23 (60 m × 0.25 mm × 0.25 μm) was used. The injector and detector temperatures were 250 °C. The oven was firstly maintained at 60 °C for 10 min and then increased at 12 °C/min to 200 °C (held for 10 min), then increased at 5 °C/min to 220 °C (held for 15 min) and then increased at 10 °C / min to 240 °C (held for 10 min).

The results were statistically treated using parametric one way analysis of variance and subsequently by Duncan´s test at $p < 0.05$ using Unistat version 5.5 (Unistat, London, United

Kingdom; the results are expressed as mean (n = 3), RSDs < 10 %.

Results and discussion

Fatty acids profile

The fatty acid composition of triglycerides was measured in four samples of processed cheese analogues with different vegetable oils and compared with traditional processed cheese. Table 1 shows the average fatty acids composition of samples. Following FA were present in all samples in highest quantity: oleic (C18:1), palmitic (C16:0), stearic (C18:0), linoleic (C 18:2) and myristic (C14:0). The significant differences ($p < 0.05$) were found among samples for several fatty acids. As can be seen, analogue with flaxseed oil, together with apricot kernel oil, resembled the most traditional (standard) cheese with its total fatty acid composition. Processed cheese analogues are known to be characteristic by a relatively high content of monounsaturated fatty acids (MUFA) and PUFA and by a favourable ratio of n-6 to n-3 fatty acids.[2] For this reason the comparison SFA:MUFA:PUFA is showed in Fig. 1. Interestingly no significant differences between samples were found.

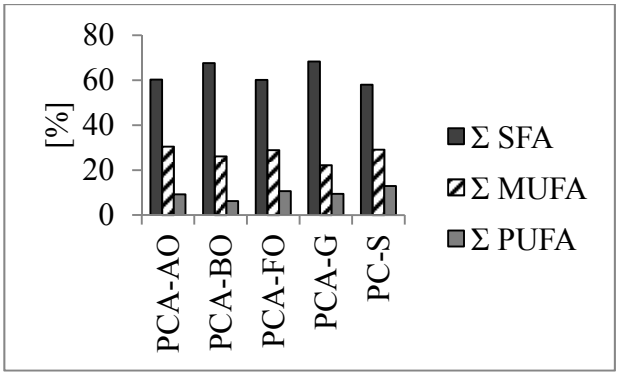

Fig. 1: **The sum content of saturated (SFA), monounsaturated (MUFA) and polyunsaturated fatty acids (PUFA) in processed cheese and processed cheese analogues; for sample labeling see Experimental part**

Free fatty acids profile

The most abundant FFAs were oleic (C18:1), palmitic (C16:0), stearic (C18:0), linoleic (C 18:2), capric (C10:0) and myristic (C14:0) acids, which together accounted for about 85 % of total FFAs. Butyric acid was the main short-chain FFA present (mean: 3.9% of total FFAs). These results agree with those reported by Kim et al.[6]. The significant differences ($p < 0.05$) were found between cheese vs. analogue; when measuring the FFA for PC-S, the most represented were SFA – palmitic (C 18:0), stearic (16:0) and myristic (C 14:0); while in the case of cheese analogues unsaturated fatty acids – oleic (C18:1) and linoleic (C 18:2) were the most abundant FFAs. This is in accordance with literature[1, 2].

Table 1
Selected FA identified in processed cheese and processed cheese analogues (in %).

Fatty acid	PCA-AO	PCA-BO	PCA-FO	PCA-GO	PC-S
C 6:0	0.11	0.16	0.20	0.23	2.12
C 8:0	2.00	2.42	2.02	2.60	1.84
C 10:0	4.05	4.88	3.95	5.09	3.77
C 11:0	0.09	0.10	0.10	0.11	0.08
C 12:0	3.85	4.54	3.85	4.80	3.65
C 13:0	0.13	0.15	0.13	0.16	0.13
C 14:0	10.68	12.08	10.95	12.59	10.14
C 14:1 (c9)	0.89	1.00	0.91	1.05	0.84
C 15:0	1.10	1.24	1.15	1.25	1.03
C 15:1 (c10)	0.25	0.28	0.26	0.28	0.23
C 16:0	29.32	31.96	30.77	31.93	26.97
C 16:1 (c9)	2.00	1.57	1.98	1.72	1.45
C 17:0	0.56	0.58	0.57	0.56	0.51
C 17:1 (c10)	0.27	0.27	0.27	0.22	0.23
C 18:0	8.12	9.39	6.20	8.84	7.57
C 18:1 (t9)	0.85	0.00	0.85	0.78	0.72
C 18:1 (c9)	25.97	22.92	24.43	18.05	24.07
C 18:2 (t 6)	0.30	0.09	0.33	0.69	0.31
C 18:2 (c9,12)	8.03	4.87	5.12	7.96	6.30
C 18:3 (c6,9,12)	0.09	0.29	0.22	0.08	0.40
C 18:3 (c9,12,15)	0.56	0.69	4.74	0.46	5.66
C 20:0	0.26	0.13	0.23	0.16	0.15
C 20:1 (c11)	0.19	0.07	0.18	0.09	1.34
C 20:3 (c8,11,14)	0.08	0.00	0.08	0.08	0.06
C 20:4 (c5,8,11,14)	0.09	0.09	0.10	0.10	0.08
C 20:3 (c11,14,17)	0.00	0.10	0.00	0.00	0.00
C 20:5 (c5,8,11,14,17)	0.07	0.03	0.03	0.05	0.06
C 22:0	0.03	0.02	0.03	0.03	0.00
C 22:1 (c13)	0.03	0.00	0.02	0.00	0.21
C 24:0	0.00	0.00	0.00	0.00	0.03
C 22:6 (c4,7,10,13,16,19)	0.03	0.04	0.03	0.04	0.03

For sample labeling see Experimental part; RSDs < 10%

Conclusion

The most abundant FAs and FFAs in all samples of processed cheese analogues were oleic, palmitic, stearic and linoleic acids. The significant differences were found among samples for several FAs and FFAs. Interestingly no differences were found between samples during comparison SFA:MUFA:PUFA.

This work was supported by a Standard project of specific research No. FCH-S-15-2827 and by "Materials Research Centre – Sustainability and Development" project Nr. LO1212 of the Ministry of Education, Youth and Sports.

REFERENCES

1. Guinee, T. P., Caric´, M., Kaláb, M., *Cheese: Chemistry, physics and microbiology. Major cheese groups*. London, New York: Elsevier Applied Science, 2004.
2. Bachmann, H. P.: Cheese analogues: a review. Int. Dairy J. *11*, 505 (2001).
3. Buňka, F., Buňková, L., Kráčmar, S. *Základní principy výroby tavených sýrů (The basic principles of processed cheese production)*. Brno: Mendelova zemědělská a lesnická univerzita v Brně, 2009.
4. Collins, Y., McSweeney, P. L. H., Wilkinson, M. G.: Lipolysis and free fatty acid catabolism in cheese: A review of current knowledge. Int. Dairy J. *13*, 841 (2003).
5. Hauff, S., Vetter, W.: Quantification of fatty acids as methyl esters and phospholipids in cheese samples after separation of triacylglycerides and phospholipids. Anal. Chim. Acta, *636*, 229 (2009).
6. Kim, N. S., Lee, J.H., Han, K. M., Kim, J. W., Cho, S., Kim, J.: Discrimination of commercial cheeses from fatty acid profiles and phytosterol contents obtained by GC and PCA. Food Chem. *143*, 40 (2014).
7. Poole, C. F.: New trends in solid-phase extraction. TrAC Trends Anal. Chem. *22*, 362 (2003).
8. Chu, B.-S., Nagy, K.: Enrichment and quantification of monoacylglycerols and free fatty acids by solid phase extraction and liquid chromatography–mass spectrometry. J. Chromatogr. B. *932*, 50 (2013).

COMPARISON OF NUTRIENTS COMPOSITION OF SOME VEGETABLE OILS

SONIA SUVAR[a], ANDREEA MARIA IORDACHE[b]*, CEZARA VOICA[c], ROXANA ELENA IONETE[b], RAMONA BLEIZIFFER[a] and MONICA CULEA[a]

[a] *"Babes-Bolyai" University, Biomolecular Physics Department, M Kogalniceanu Str, Cluj-Napoca, Romania*
[b] *National R&D Institute for Cryogenics and Isotopic Technologies -ICIT, 4 Uzinei Str , Romania*
[c] *National Institute for Research and Development of Isotopic and Molecular Technologies, 67-103 Donat Str, Cluj-Napoca, Romania*
andreea.iordache@icsi.ro

Several vegetable (e.g. linseed, poppy, grape, hemp, nuts, soya, pumpkin, sesame and olive) oils used as food supplements, purchased on the Romanian market of organic products, were compared in terms of their content in fatty acids and certain metal ions. The obtained values of fatty acids were compared with those found in trout meat. Measurements were performed by GC/MS (capillary gas chromatography-mass spectrometry) for fatty acids and ICP-MS (inductively coupled plasma mass spectrometry) for metal ions (Na, Mg, K, Mn, Cd, Cu and Cr).

Introduction

Gas chromatography coupled with mass spectrometry (GC/MS) is one of the widely used best techniques for fatty acids identification and quantitation[1–5]. The fatty acids composition is a characteristic of plant species and has nutritional, biochemical and technological importance. Vegetal oils are known as a good source of polyunsaturated fatty acids, especially linoleic acid that belongs to the familly of „essential" fatty acids[5, 6].

Nowadays, when a growing concern is noticed regarding food composition and the demands for healthy foods has expanded, organic vegetable oils have become more and more attractive in terms of nutrition due to the phytochemical and antioxidant properties of their active compounds[7–12].

The fatty acids composition of oils is very important since lipids are one of the three major constituents of food. Their roles in the biological tissues are: source of energy, components of biological membranes, precursors of many different molecules and transport vehicle for vitamin A, D, E and K.

The aim of this paper was to assess and compare the fatty acids and the metals ions present in different vegetable oils.

Fatty acids were also compared with the nutritional important fatty acids present in the fish meat[8], the conclusions being appropriate for the description of the natural compounds. Furthermore, the knowledge on heavy metals content is essential to prevent excessive build–up of these elements in the human food chain.

Material and methods

Analysis of total fatty acids in some vegetal oils was performed by gas chromatography-mass spectrometry (GC/MS) technique[1–6]. Fatty acids were derivatized as methyl ester derivatives, separated by GC and identified by MS techniques. Some vegetable oils used as food supplements, purchased on the organic market in Romania and coming from different European countries, including Romania, were compared in terms of fatty acid composition and some metal ions. The studied oil samples were of linseed, poppy, grape, hemp, nuts, soya, pumpkin, sesame and olive.

For assessing their content in fatty acids a Trace DSQ ThermoFinnigan quadrupole mass spectrometer coupled with a Trace GC was used. The oil samples were derivatized as fatty acid methyl esters (FAME) and separated on an Rtx-5MS capillary column, 30 m × 0.25 mm, 0.25 μm film thickness. Temperature program used was: 50 °C, 2 min, 8 °C/min at 310 °C (10 min); the carrier gas was helium 6.0 at a flow rate of 1 ml/min. The following conditions were followed: transfer line temperature 250 °C, injector temperature 250 °C; ion source temperature 250 °C; Splitter: 10:1. Electron energy was 70eV and the emission current, 100 μA.

Derivatization and separation steps were as follows: vegetable oil samples (20 μl) were converted to fatty acids methyl esters (FAME), for GC analysis, by esterification with 200 μl methanol: acetyl chloride (4:1 v/v) for 20 min at 80 °C. The derivatives were evaporated to dryness in a nitrogen stream at 60 °C and then dissolved in 500 μl dichloromethane. 1μl was automaticaly injected into GC. The identification of fatty acids was obtained by comparison of fatty acids methyl esters mass spectra, recorded in the m/z range 35–500, with the mass spectra of FAME standards of NIST library.

The elemental analysis was performed by inductively coupled plasma quadrupole mass spectrometry (ICP-Q-MS). The following operating conditions were applied: nebulizer gas flow rates of 0.86 $L \cdot min^{-1}$; auxiliary gas flow of 1.2 $L \cdot min^{-1}$; plasma gas flow of 15 $L \cdot min^{-1}$; lens voltage of 7.25 V; 1100 W ICP RF Power; CeO/Ce = 0.027; and Ba++/Ba+ = 0.025.

Results and discussion

The method was validated by using fatty acid standard samples. The developed GC/MS method has provided good validation parameters. The linear correlation coefficients on individual compounds were between 0.982–0.993. Precision gave R.S.D. values lower than 10 % for the important fatty acids determined.

Fig. 1 presents the comparative chromatograms of fatty acid methyl esters identified in hemp and grape seed oils.

High amounts of unsaturated fatty acids (UFAs), ranging from 71.49 % (olive) to 89.51 % (linseed seed), were found in the investigated vegetable oils. The sequence was as follows: olive < sesame (76.94) < pumpkin (78.16) < soya (82.92) < nuts (83.7) < hemp (86.19) < grapes (87.61) < poppy (88.93) < linseed. The lowest value of 68.96 % (Table 1 and 2) was found in trout meat UFAs.

The ratios of UFAs/SFAs (saturated fatty acids), ranging from 2.51 (olive) to 8.52 (linseed seed), had registered similar variation as UFAs. For trout meat the ratio was 2.22 (Fig. 2).

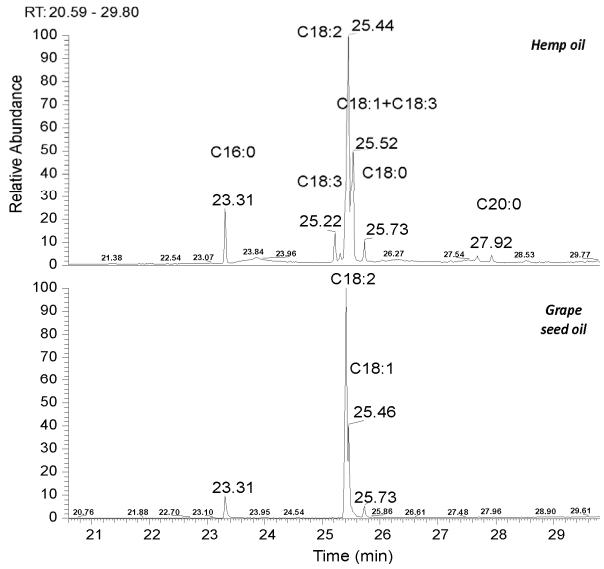

Fig. 1. **Chromatograms of FAME separation in hemp and grape seed oils**

Table 1
Fatty acid methyl esters in vegetal oils

FAME	linseed	poppy	grape	hemp	nuts
C16:1	0.06	0.39	0.15		0.27
C16:0	7.15	9.06	9.08	10.05	12.09
C18:2	18.34	71.93	63.1	58.35	59.32
C18:1	68.34	14.83	24.4	11.78	10.83
C18:3				16.06	9.46
C18:0	3.35	2	3.32	3.75	3.11
EPA	1.77	1.78			3.85
C20:1	1				
C20:0					
DHA					
C22:0					

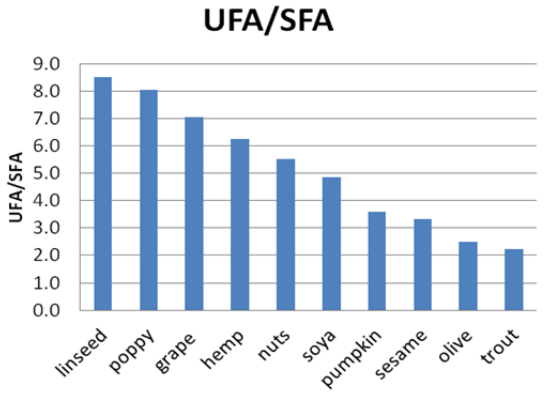

Fig. 2. **UFA/SFA ratio comparison in the studied samples**

Polyunsaturated fatty acids (PUFAs) determined in the vegetable oils ranged from 3.32 % (olive) to 74.41 % (hemp), in the following sequence: olive < linseed (20.11 %) < sesame (42.88 %) < soya (54.94 %) < pumpkin (57.42 %) < grapes (63.11 %) < nuts (72.6 %) < poppy (73.71 %) < hemp. Trout meat PUFAs value was 44.43 %. Except for linseed oil, these levels are comparable to those of PUFA-rich vegetable oils, such as grape seed (65.40 %), sunflower (66 %), paprika seed (67.80 %), perilla (69.90 %), linseed (71.80 %), blackcurrant seed (75.30 %), safflower (77.30 %) and hemp seed (79.10 %) oils[5]. Lenoleic acid (C18:2) had the highest value in all the studied vegetable oils, except linseed and olive oils where oleic acid (C18:1) was the most important. Linolenic acid (C18:3) was present only in hemp (16.06 %) and nuts (9.46 %). DHA fatty acids are the highest in trout meat and not found in vegetal oils, but EPA, of 8.51 % in fish meat, showed low value in vegetal oils, of 3.85 % in nuts, 1.78% in poppy and linseed and 0.65 % in sesame oil.

Table 2
Fatty acid methyl esters in vegetal oils

FAME	soya	pumpkin	sesame	olive	trout
C16:1		0.52	0.61	2.09	2.19
C16:0	12.4	17.18	15.62	22.7	24.8
C18:2	54.31	57.42	42.23	3.32	7.81
C18:1	27.98	20.22	32.54	65.2	22.3
C18:3					
C18:0	3.89	4.65	5.48	4.43	6.27
EPA			0.65		8.51
C20:1			0.91	0.87	
C20:0	0.38		0.89	1.35	
DHA	0.63				28.1
C22:0	0.42		1.08		

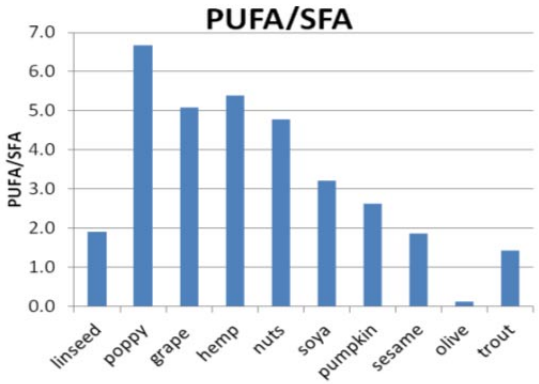

Fig. 3. **PUFA/SFA ratio comparison in the studied samples**

The ratios of PUFAs/SFAs, ranging from 0.12 (olive) to 6.66 (poppy seed), were found in the following order: olive < sesame < linseed < pumpkin < soya < nuts < grape < hemp < poppy (Fig. 3).

To prevent excessive metals in human food chain, monitoring the heavy metals in oils is essential. The nutritive quality of metal concentration content was tested using the Perkin Elmer ICP-MS instrument.

The important macro elements measured are ranging as followed: K: sesame < hemp < nuts; Mg: linseed < nuts < olive and Na: hemp < nuts < grape. In Fig. 4 are presented the determined metals in the studied vegetable oils.

The nutritional value of the vegetal oils expressed by the fatty acids content and by the concentration of metals (Na, Mg, K, Mn, Cd, Cu and Cr), proved their good quality to be used as food supplements. The heavy metals content (Cd, Pb and As) of the investigated vegetable oils were sufficiently low as to pose no risk to human health.

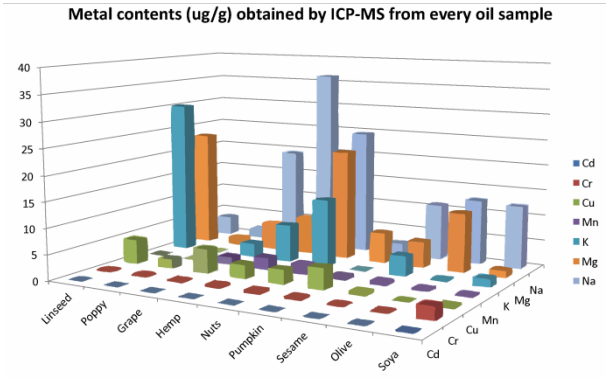

Fig. 4. **Comparison of metal contents (µg/g) in the oils studied**

Conclusions

GC-MS method showed interesting results in fatty acids comparison study of vegetable oil samples: oils UFA values exceed trout meat UFA and the majority oils showed PUFAs higher than trout meat PUFA value, except olive, linseed and sesame oils.

The nutritional value of the vegetal oils expressed by the fatty acids content and the concentration of metal ions proved their good quality to be used as food supplements but the control of heavy metals is important.

The methods are suitable for routine analysis of low quantities of food samples and the results may be used for different purposes as: food quality control, food processing control, nutritional labeling, animals' diet control and metabolic studies.

This work was possible due to the financial support of the Sectorial Operational Program for Human Resources Development 2007–2013, co-financed by the European Social Fund, under the project number POSDRU/159/1.5/S/132400 with the title „Young successful researchers – professional development in an international and interdisciplinary environment".

REFERENCES

1. Christie W. W., in: Advances in Lipid Methodology – *Two*, Oily Press, Dundee, 195 (1993).
2. Cocan D., Horj E., Culea M., Miresan V., Pintea A.: Bulletin UASVM Agriculture, *67*, 137 (2010).
3. Iverson S. J., Lang S.L.C., Cooper M. H.: *Lipids, 36*, 1283 (2001).
4. Pintea A., Varga A., Stepnowski P., Socaciu C., Culea M., Diehl H. A.: Phytochem. Anal., *16,* 188 (2005).
5. Scrob S., Culea M., Muste S., Rom. J.: Biophys. *23*, 107, (2013).
6. Pop C., Bara L., Horj E, Iordache A, Laslo C., Culea M.: Bulletin UASVM Agriculture, *67*, 373, (2010).
7. Freije A., J.: Oleo Sci., *58*, 379 (2009).
8. Shapira N., Weill P., Sharon O., Loewenbach R., Berzak O.: J. Agric. Food Chem., *57*, 2249 (2009).
9. Dulf F. V., Oroian I., Vodnar D. C., Socaciu C., Pintea A.: Molecules, *18*, 11768 (2003).
10. Mihoc M.**,** Pop G., Alexa E., Radulov I.: Chem. Central J. *6*, 122 (2012).
11. Dubois V., Breton S., Linder M., Fanni J., Parmentier M.: Eur. J. Lipid. Sci. Technol. *109*, 710 (2007).
12. Petersen Rodriguez M. A., Petrini J., Ferreira E. M., Barreto Mourão L. R. M., Salvian M., Cassoli L. D., Pires A. V., Machado P. F., Barreto Mourão G.: Food Chemistry, *156*, 170 (2014).

THERMODYNAMICS OF METAL ION INTERACTION WITH HUMIC ACIDS

IRENA TURKEOVA[a]*, VOJTECH ENEV[a], MARTINA KLUCAKOVA[a], JITKA KROUSKA[a] and MARCELA LASTUVKOVA[a]

[a]*Brno University of Technology, Faculty of chemistry, Materials Research Centre, Purkynova 464/118, 612 00 Brno*
**xcturkeovai@fch.vutbr.cz*

Abstract

Humic substances presented in soil are capable to bond with pollutants, water and nutrients. Considering their bonding with pollutants it is generally observed, that humic substances are able to bond heavy metals ions in nature. Study of thermodynamics of these reactions significantly improves our knowledge about reactivity of humic substances. The object of our study were two various samples of HA.

HAs were isolated from two different organic origin – compost and South Moravian lignite. Isolation of soil HA was performed according to the procedure recommended by the International Humic Substances Society (IHSS). All samples of HA were characterized by elemental analysis (EA).

The reactivity (thermodynamics) of humic acids (HAs) and metals was studied by isothermal titration calorimetry (ITC). As model metals were chosen Cu (II) and Pb (II) ions. Reaction enthalpy of systems were calculated and discussed as well as amount of metal binding by specific humic acid.

Introduction

Isothermal titration calorimetry is the only one capable of measuring not only the magnitude of the binding affinity but also the magnitude of the two thermodynamic terms that define the binding affinity: the enthalpy (ΔH) and entropy (ΔS) changes[1].

The general principle of ITC is based on measuring the heat which is generated or absorbed in the interaction between two molecules. ITC was used to determine the stability constants, stoichiometry, interaction enthalpy, under certain conditions, entropy, Gibbs free energy, and this may be change is detected by the thermal capacity[2].

Humic acid under research[3] occur in many places in nature. They are presented in all types of soils, sediments, peat, coal, rivers. Humic acids are capable of interaction with wide range of substances, such as metals, organic and inorganic pollutants in soils and waters. Another very important feature of humic acids presence in the soil is their high buffering ability in a wide range of pH values[4]. Humic acids are essentially large system of polyfunctional groups such as lipids, carbohydrates, aromatic compounds, and others. These compounds differ significantly in content of functional groups of the humic acids according to their origin and formation. According to the group of authors[5] these groups are responsible for their reactivity as they are capable of ionization. Among these functional groups oxygen, nitrogen and sulfur forming carboxylic, phenolic, hydroxyl, amine and thiol functional groups are presented.

In view of the frequent use of humic substances in the environment, for example: in remedial technologies, it is important to know the binding interaction of substances with contaminants, pollutants, heavy metals, which are present in the environment. Of explored the properties of humic materials and from known information about the structure we can deduce about possible linkage interaction-ionic bond, coordination bond, hydrogen bonds, hydrophobic interactions[6]. Extensive studies point to the fact that only few HL occurs in the soil in free form, but many of them are bound to clay or other mineral components of the soil. Interactions with HL compounds in soil is caused by interactions with salts of low molecular weight organic acids, alkali metals and alkaline earth metal complexes[7].

Materials and methods

Materials

Humic acids were isolated in the process of alkaline extraction from Moravian compost and South – Moravian lignite. Isolation of soil HA was performed according to the procedure recommended by the International Humic Substances Society (IHSS). Humic sols were prepared by the dissolution of the humic acid powder (lignite HA, compost HA) in the 0.1 M KOH solution. Obtained samples were stirred overnight. To neutralize KOH[8], the appropriate amount of 0.1 M HNO_3 was added to each solution. The resulting sols had the concentration of humic acids of 1.25 $g \cdot dm^{-3}$.

Metals applied in experimetal works were purchased from Sigma-Aldrich (p.a. purify grade). For the study of the interaction with HAs, metals ($Cu(NO_3)_2$, $Pb(NO_3)_2$) were dissolved in 0.1 M KNO_3. Solutions were also stirred overnight. The concentration of metal solution was 8 $g \cdot dm^{-3}$.

Methods

Characterization of humic acids

For characterization of studied HAs were used elemental analysis and thermogravimetry. Composition of HAs was obtained using a EURO EA Elementar analyzer (EURO Vector Instruments and software). The content of ash and humidity was obtained using TGA (TGA, Q5000, TA Instruments). Obtained results are listed in Table 1.

The total content of acid functional groups of HAs and the content of carboxylic functional groups was determined by using a conductometric and potenciometric titration. For determination of total acidity, solid HAs were suspended in water (ratio 0.1 g of HAs in 100 cm^3 of water) and titrated using 0.1 M NaOH. The value of total acidity of HAs was obtained using conductometric and potentiometric detection of inflex points during titration[8]. (Klucakova and Pekar, 2005). The content of carboxylic functional groups was measured using standard acetate method (Schnitzer and Khan, 1972; Stevenson, 1994). Obtained results are listed in Table 2.

Isothermal titration calorimetry (ITC)

The experiments were performed with an isothermal titration calorimeter (TAM III, TA instruments) with a sample and the reference cells. The reference cell contained miliQ water. The cell (1 ml) contained the solution of HA. In the syringe was titrant – metal solution. Experiment consisted of injecting 4.974 µl (50 injections). The titrant was injected at 10 min interval. Each injection lasted 10 s. The temperature was set on 298, 15 K. For homogeneous mixing in the cell, the stirrer speed was kept constant at 90 rpm. The data were processed with TAM assistant software and NanoAnalyze software, both from TA instruments.

Results and discussion

Characterization of humic acids

Table 1
Elemental composition, ash and humidity of used HAs

	C (at. %)	H (at. %)	N (at. %)	S (at. %)	O (at. %)	ash (w. %)	humidity
lignite HA	43,42	36,89	0,79	0,44	18,46	0,45	4,012
compost HA	37,28	44,14	3,06	0,26	15,27	0,44	5,923

It was determine from titration that higher total acidity and carboxylic acidity have lignite humic acid (Table 2). From these results, we can assume that lignite HAs will have better binding properties with metal ions.

Table 2
α total acidity and β carboxylic acidity of used HAs

	α (mmol/g)	β (mmol/g)
lignite HA	5,4 ± 0,24	3,62 ± 0,07
compost HA	3,81 ± 0,24	2,62 ± 0,06

Isothermal titration calorimetry

The representative type of results from ITC is showed in Fig. 1. It demonstrate the isotherm of Pb^{2+} ion binding to compost humic acid. All titration with metals were exothermic-results from heat flow had possitive. In settings of TAM III means positive heat flow – exothermic reaction. The resulted data were fitting with least-squares fitting model for one-site binding model. From fitting results we received thermodynamic parameters – binding constant K_a, reaction enthalpy ΔH, reaction entrophy ΔS, Gibbs energy ΔG (Table 3).

In Fig. 2 are thermodynamic responses in interaction of compost HAc with Pb, Cu. Both reaction were favorable ΔH, characteristic of hydrogen bond formation, and an unfavorable TΔS. Little bit higher enthalpy had reaction of compost HAs with copper ion. On the other side higher binding property was found with plumbum ion. In Fig. 3 are thermodynamic responses between interaction of lignite HAs with metals. Results are in Table 3. ΔG is change in free energy, negative value is for spontaneous reaction. More negative means higher affinity. ΔH measure of the energy content of the bonds broken and created. The dominant contribution is form hydrogen bonds. Negative value indicates enthalpy change favoring the binding. ΔS is positive for entropically driven reactions-favoring binding is hydrophobic interactions. Higher Gibbs energy had reactions with Pb.

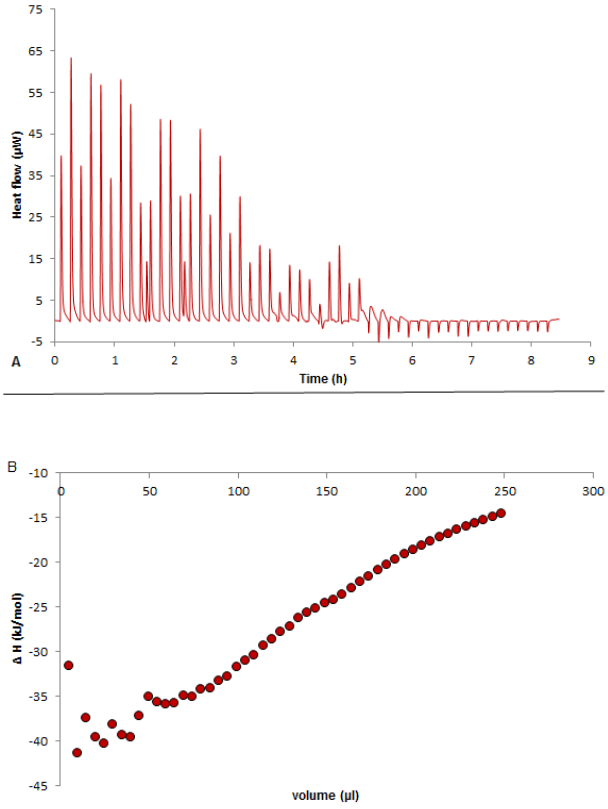

Fig. 1. **Isothermal titration calorimetry (ITC) measurement of binding to compost HA. A) Raw ITC data for injection of 24 mM Pb^{2+} ions into HA. B) ΔH from titration versus added volume of titrant**

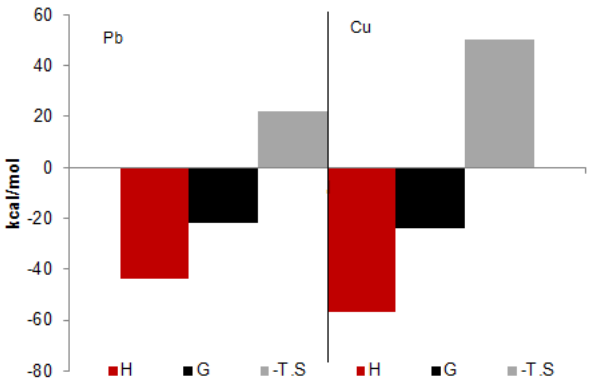

Fig. 2. **Thermodynamic response – compost HAs with Pb, Cu**

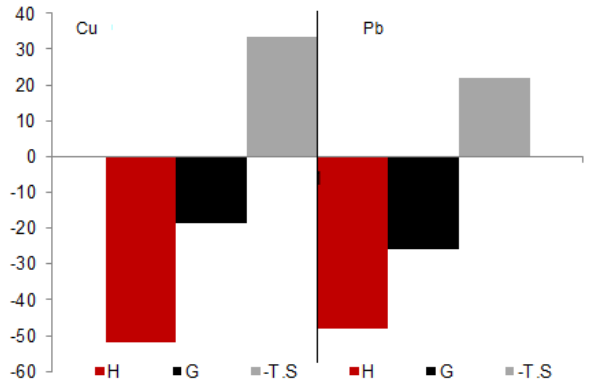

Fig. 3. **Thermodynamic response – lignite HAs with Pb, Cu**

Table 3
Thermodynamics parameters from isothermal titration calorimetry

Reaction	Ka (M^{-1})	Δ G (kJ/mol)	Δ S (J/(k.mol))	Δ H (kJ/mol)	adsorbed amount of ions (μmol)
compost HA-Pb	6.1×10^3	–21.618	–74.003	–43.7	4.05
compost HA-Cu	1.5×10^4	–23.843	–110.09	–57	3.61
lignite HA-Pb	1.3×10^3	–18.592	–111.943	–52	4.29
lignite HA-Cu	3.6×10^4	–25.994	–74.224	–48	3.44

Conclusion

The thermodynamics of interaction of metal ions with humic acids in sols was studied using isothermal titration calorimetry. ITC provides complete thermodynamic characterization of the binding reaction. It was used two models of ions – Pb, Cu, because they are pollutants in environment. We observed a good response from systems and it is good starting line for another humic research, but not only for interactions with metals. Its applicable for further organic and inorganic interactions with humic acids. It was found that metal ions can be adsorbed not only by acidic functional groups.

Acknowledgement: This work was supported by project Nr. LO1211, Materials Research Centre at FCH BUT-Sustainability and Development (National Programme for Sustainability I, Ministry of Education, Youth and Sports).

REFERENCES

1. Leavitt S., Freire E.: Curr. Opin. Struc. Biol. *11*, 560 (2001).
2. Bouchemal K.: Drug Discov. Today. *13*, 21 (2008).
3. Jansen S. A., Malaty M.: Mat. Sci. Eng. C. *4*, 175 (1996).
4. Cechova E.: Diploma thesis, BUT (2008).
5. Andelkovic T.: Maced. J. Chem. Chem. Eng. *25*, 131 (2006).
6. Dercova K.: Chem. Listy. *102*, 338 (2008).
7. Weber J.: Humintech, *online* (2011).
8. Klucakova M.: Environ. Eng. Sci. *31*, 612 (2014).

COMPARISON OF SENSORY QUALITY OF MODEL SWISS CHEESE WITH COMMERCIALLY OBTAINED CORRESPONDING PRODUCT

EVA VÍTOVÁ*, KATEŘINA SŮKALOVÁ, MARTINA MAHDALOVÁ, LENKA BUTOROVÁ, LENKA MUSILOVÁ and ESTER PECINOVÁ

Department of Food Chemistry and Biotechnology, Faculty of Chemistry, Brno University of Technology, Purkyňova 118, 612 00 Brno, Czech Republic
vitova@fch.vutbr.cz

Swiss cheese is a generic name for several related varieties of cheese resembling the true Emmental, whose name comes from the location where it supposedly originated, Emme valley in the canton of Bern in Switzerland[1].

Swiss cheese types have ivory to light yellow colour, firm, slightly elastic texture, characteristic mild, nutty, sweetish flavour and a distinctive appearance; some cheeses have round regular holes known as "eyes", while some do not (known as "blind"). In general, the larger the eyes in a Swiss cheese, the more pronounced its flavour because a longer fermentation period gives the bacteria more time to act[2, 3].

Three types of bacteria are typically used to make Swiss cheese (these can vary slightly depending on the manufacturer): *Streptococcus salivarius* subsp. *thermophilus*, *Lactobacillus* spp. (*Lactobacillus helveticus* or *Lactobacillus delbrueckii* subsp. *bulgaricus*), and *Propionibacterium freudenreichii* subsp. *shermanii*). In a late stage of cheese production, the propionibacteria consume the lactic acid excreted by the other bacteria and release acetate, propionic acid, and carbon dioxide. The carbon dioxide forms the bubbles that develop the "eyes", the acetate and propionic acid give Swiss its nutty and sweet flavour. Historically, the holes were seen as a sign of imperfection and cheese makers originally tried to avoid them by pressing during production. In modern times, the holes have become an identifier of the cheese[1–3]. Interestingly, the size of the holes in the United States is regulated, which was caused by the lobbying of commercial American Swiss cheese producers, who were having problems with cutting cheese using their mechanical slicers. This law is widely criticized by many Swiss cheese manufactures outside of the U.S., particularly in Switzerland, which claim that the regulations produce an inferior flavoured Swiss cheese[1, 2].

The acceptability of cheese depends largely on the sensory quality, mainly on flavour formed during ripening. The flavour profiles of cheeses are complex and region- or manufacturer-specific which have made it challenging to understand the chemistry of its development. Several authors have focused especially on sensory quality of Swiss cheese, which have been mostly investigated using descriptive sensory methods, and several articles have been published so far[4–7].

Today Swiss cheeses are produced in many countries and a great variety is available on the world market. The aim of this work was to produce new type of Swiss cheese with the comparable or even better sensory quality than commercially available corresponding products. The sensory quality of model samples was compared with standard Swiss cheese purchased on the Czech market.

Experimental part

Model samples of Swiss type cheese (69 % dry matter, 44 % fat in dry matter – FDM) were analysed in this work; raw milk in "bio" quality was used as the raw material, inoculated by commercial starter bacterial culture (*Lactobacillus thermophilus*, *Streptococcus thermophilus*, *Lactococcus mesophilus*). Cheeses were produced at laboratory (pilot plant) conditions using standard producing technology[1, 2] and ripened at 15 °C for 3 months. Standard Swiss cheese (60 % dry matter, 45 % FDM) was purchased on the local market. All samples were stored < 6°C until analysis (max 3 days).

The basic chemical characteristics were assessed using standard ISO methods (ISO 5534:2004; ISO 1735:2004).

The sensory analyses were carried out in a sensory laboratory (ISO 8589:2008). The assessors were selected from staff and doctoral students of the department, in total 23 judges were used for evaluation. About 20 g of the sample was served in 50 ml glass covered containers, marked with 4-digit codes, in random order. Tap water was provided to rinse mouth between samples.

The sensory attributes were evaluated using five point ordinal hedonic scale (1-excellent, characteristic for Swiss cheese ⇒ 5-unsatisfactory). The list of attributes comprised of appearance, colour, odour, taste (flavour) and texture. Paired preference test (ISO 5495:2005) was used to evaluate preferences of assessors/consumers and overall acceptability of the samples.

The results were statistically treated by means of Kruskall-Wallis test followed by Nemenyi multiple comparison test at $p < 0.05$ using Unistat version 5.5 (Unistat, London, United Kingdom); they are expressed as median (n = 23).

Results and discussion

The main aim of this work was to develop a new type of Swiss cheese, produced from raw milk in "bio" quality. Increasing incidence of lifestyle diseases leads to increasing interest of Czech consumers in novel, natural foods, and our "bio" product has a great potential from this point of view. More and more people look for traditional natural farm products, produced in clean and peaceful environment, without chemical additives, with additional value of interesting history, even though they have higher price and sometimes lower sensory quality. Cheeses are one of such products, the principle of their producing technology has been known for many years[2].

Traditional cheese originates from a complex system which results in unique sensory characteristics. The development of these unique characteristics is linked to several factors: the environment, the climate, the natural pasture, the breed of the animals, the use of raw milk and its natural microflora, the cheesemaking technology with the unique role of human beings rather than automated technology, historical tools as well as the natural aging conditions[8]. However, in many countries, including Czech Republic, traditional products are almost banned; issues relating to "food safety" are

frequently given as a "false" argument to explain the banning of traditional products.

In accordance with Giuseppe[8] we would like to demonstrate the importance of reintroduction of traditional cheesemaking to offer Czech consumers the opportunity to compare the natural aroma/flavour with the classical industrial products. Overall sensory quality of model samples was evaluated by selected assessors, the sensory characteristics were then compared with commercial Swiss type cheese of similar composition (dry matter, FDM), which was considered as standard of sensory quality.

To evaluate relationships/dependence of sensory properties on chemical composition and judge nutritional quality of samples, cheeses were also analyzed for basic chemical composition (dry matter, total lipids and protein content). Generally said dry matter is the good indicator of cheese nutritional as well as sensory quality. The higher dry matter content means higher content of calcium and other nutrients, simultaneously the texture is harder. Based on texture in relation to low moisture content Swiss cheese could be classified as hard cheese[2, 3]. Swiss type cheeses accessible on the Czech market have dry matter content in range about 60–65 % and FDM mostly 45 %. Dry matter of the produced model cheese (69 %) indicates its quite hard texture. Based on fat content Swiss cheese could be classified as full fat cheese (45–55 % FDM). Fat is very important component of cheese, it contributes significantly to taste, influences texture and is also the source of energy[1, 2]. The model cheese had slightly lower fat content (44 % FDM) than above stated interval, which probably also contribute to its firm texture, firmer than it is usual in this type of cheese. Similarly the lower content of proteins (14 %) was found than in the standard cheese (25 %). The low values of all basic characteristics in model cheese, indicating lower nutritional quality, are probably caused by producing technology which will need several improvements to reduce losses of nutrients. However, the sensory quality of samples was good. The comparison of main sensory characteristics of model vs. standard cheeses is provided in Fig. 1.

Fig. 1. **The comparison of main sensory characteristics of model vs. standard Swiss cheese. The results are expressed as median (n = 23); scale used (1-excellent ⇒ 5-unsatisfactory)**

As can be seen in Fig. 1 no differences were found in colour and appearance of samples; both samples were evaluated as very good. Swiss cheese types should have ivory to light yellow colour and distinctive appearance with the "eyes"[2, 3]. The model cheeses had a little darker yellow colour than standard cheese; however this fact apparently did not significantly influence evaluation of samples. Appearance of model cheeses (when cut) was different from standard, practically no eyes were visible on the slices; these types of Swiss cheese are called as "blind"[2, 3]. This fact was expected because eyes are formed by acting of propionibacteria producing carbon dioxide[2, 3], however, this type of culture was not used for production of model cheese. In such case the ripening process is rather different from classical Swiss cheese resulting also in formation of a little different flavour. Surprisingly this dissimilarity was not perceived negatively by assessors, the appearance of model samples was well evaluated.

However, significant differences ($P < 0.05$) were found between standard vs. model cheese in odour, flavour and texture. Swiss cheese types should have characteristic mild, nutty, sweetish flavour[2, 3]; the taste and odour of model samples were quite strong and piquant, which is caused by absence of propionibacteria, more intense ripening process and probably also influenced by lower fat content, which would soften taste perception. That was probably the reason of worse evaluation (evaluated as good), while standard was evaluated as very good in flavour and odour.

Texture of Swiss cheese should be firm, smooth, slightly elastic[2, 3]. The texture of standard was evaluated as excellent, however, owing to the high dry matter and low fat content, texture of model cheeses was firm, a little crumbly, evaluated only as very good.

Finally paired preference test confirmed the results of descriptive sensory profiling; because the acceptability of cheese depends largely on the flavour[4, 5] the model cheeses were less preferred by conservative Czech consumers/assessors because of their unusual dark yellow colour, firm texture and mainly very sharp piquant flavour. However, prospectively they could be offered at the Czech market as a new nontraditional natural cheese product.

This work was supported by a Standard project of specific research No. FCH-S-15-2827.

REFERENCES

1. Fox, P. F., Guinee, T. P., Cogan, T. M., Mcsweeney, P. L. H.: *Fundamentals of Cheese Science*. Gauthersburg (Maryland, USA): Aspen Publication, 2000.
2. Roginski, H., Fuquay, J. W., Fox, P. F.: *Encyclopedia of Dairy Science*. London: Academic Press, 2002.
3. Codex Standard for Emmental, Codex Standard 269-1967. Codex Alimentarius Commission, Joint FAO/WHO Food Standards Programme, Rome, Italy.
4. Kocaoglu-Vurma, N. A., Eliardi, A., Drake, M. A., Rodriguez-Saona, L. E., Harper, W. J.: Rapid Profiling of Swiss Cheese by Attenuated Total Reflectance (ATR) Infrared Spectroscopy and Descriptive Sensory Analysis. J. Food Sci. *74*, S232 (2009).

5. Kocaoglu-Vurma, N. A., Harper, W. J., Drake, M. A., Courtney, P. D.: Microbiological, chemical, and sensory characteristics of Swiss cheese manufactured with adjunct Lactobacillus strains using a low cooking temperature. J. Dairy Sci. *91*, 2947 (2008).
6. Ben Lawlor, J., Delahunty, C. M., Wilkinson, M. G., Sheehan, J.: Swiss-type and Swiss-Cheddar hybrid-type cheeses: effects of manufacture on sensory character and relationships between the sensory attributes and volatile compounds and gross compositional constituents. Int. J. Dairy Technol. *56*, 39 (2003).
7. Rychlik, M., Bosset, J. O.: Flavour and off-flavour compounds of Swiss Gruyere cheese. Identification of key odorants by quantitative instrumental and sensory studies. Int. Dairy J. *11*, 903 (2001).
8. Giuseppe, L.: Worldwide traditional cheeses: Banned for business ? Dairy Sci. Technol. *90*, 357 (2010).

AVAILABILITY OF SOIL NITROGEN MEDIATED BY RHIZOSPHERE "TRADE"

JAROSLAV ZÁHORA

Mendel University in Brno, Zemědělská 1/1665, 613 00 Brno, Czech Republic
e-mail: zahora@mendelu.cz

Introduction

The surface of plant roots along with the closely adhering soil particles called rhizoplane, is one of the most interesting sites of contacts between the living and nonliving nature. It is the site which is decisive for plant production, for the richness of plant communities and for the protection against plant pathogens. There is also decided about the partitioning of photosynthetically derived assimilates between above and below ground parts of plants as well as about the regeneration of soil organic matter via releasing organic compounds by root exudation and by releasing dead root tissue, both accelerating the turnover of accompanied soil organisms. This loss of organic compounds from roots is often termed rhizodeposition and is on average 15 % of the total assimilated C for cereals[1], and at least twice as much for pasture plants. Understanding to the relationships between the plants and the key players on the rhizoplane is the most important step in understanding to the essence of soil fertility.

The first scientist who recognized the importance of increased activity of soil organisms associated with the presence of root system and who in 1904 proposed for the area of influence of plant roots in the soil the term "rhizosphere" was Lorenz Hiltner, director of the Bavarian agri-botanical institute in Munich[2]. The term "rhizosphere" originating partly from the Greek word "rhiza", is designated to the plant-root interface, to root region of undefinable size or shape, consisting of a gradients of chemical, biological and physical properties which change both radially and longitudinally along the root.

In his rhizosphere concept, Hiltner also envisioned, that beneficial bacteria are not only attracted by the root exudates but that there are also "uninvited guests," that adjust to the specific root exudates. Based on his observations he hypothesized that "the resistance of plants towards pathogenesis is dependent on the composition of the rhizosphere microflora." He even had the idea, that the quality of plant products may be dependent on the composition of the root microflora[2].

In addition to his scientific work, Hiltner was very interested to applied research, such as improvement of the inoculum of nitrogen fixators, diazotrophic bacteria *Rhizobium* preparations, leading to farmer's independency on extra added nitrogen. His emphasis on understanding microbes in the context of their micro-habitat, the rhizosphere, made him a pioneer in microbial ecology. In the centennial symposium of Hiltner's definition of the "Rhizosphere" in Munich in September 2004, more than 450 scientists gave tribute to his founding work on the rhizosphere and presented studies that continue on many of the ideas first brought to light by Hiltner [2].

Apart from a few soil microbiologists, though, soil scientists in general took some time to incorporate this concept into their mainstream thinking. As Gregory[3] relates, the role of roots in determining plant accessibility to nutrients received little attention throughout the early 1900s when availability of nutrients to plants was defined by use of chemical extractants[4].

In the 1820s and 1830s, German scientist Carl Sprengel refuted the humus theory and postulated the theory of mineral nutrition of plants, which states that plants require mineral elements to develop; and he formulated the Law of the Minimum, which was later popularized by his countryman and colleague Justus von Liebig. It states that plant growth is controlled not by the total amount of resources available, but by the scarcest resource (limiting factor). To avoid a dispute on priorities and impacts and to recognize and commemorate the achievements of both pioneering scientists, the international community of agronomists proposed at 1999 that the Law of the Minimum should be henceforth called the Sprengel-Liebig´s Law of the Minimum[5].

Sprengel-Liebig´s theory of mineral nutrition plant begins to apply in the industrial, conventional agriculture after World War II. Of the 10,000 years of human agricultural activity, it is only a very short time, but sadly marked by the change in priorities overlooking the biological nature of soil fertility. The only criterion is to maximize yields and minimize costs. Proponents of industrial agriculture persuaded themselves, farmers, politicians and consumers by the myth that: "Industrial agriculture is the only way to feed the world."

Such an approach to agriculture must be supported by political decisions and arguments about the inevitability and efficiency. Neither is true. The model of industrial agriculture is neither effective nor does it constitute the tip of modern agriculture. In 1940 were produced 2.3 calories in food per calorie of fossil fuel used while the industrialization of our agricultural and food systems can now get one calorie of food per every 10 calories used in the form of fossil fuel, which is 23 times lower efficiency. Depending on the available energy and chemical inputs we have forgotten how to farm.

No wonder that the anthropogenically derived nitrogen (N) produced mainly intentionally for synthetic nitrogen fertilizers has a central role in global environmental changes, including climate change, biodiversity loss, air pollution, greenhouse gas emission, water pollution, as well as food production and human health.[6] Even now, in the era of genome and postgenome analysis with our better understanding of plant nutrition and soil bacteriology, the ideas and contributions of Lorenz Hiltner are as fresh as they were more than 100 years ago[2], and rhizosphere concept can offer a promising solution for recovery of soil fertility.[2]

Rhizosphere

The rhizosphere is the area of influence of plant roots in the soil (according to Lorenz Hiltner[7]). This is an area of active interchange between plants and soil bacteria, where photosynthate fuels microbial growth and activity, ultimately resulting in the stimulation of nitrogen mineralization locally and leading thus to the net plant nitrogen assimilation.[8]

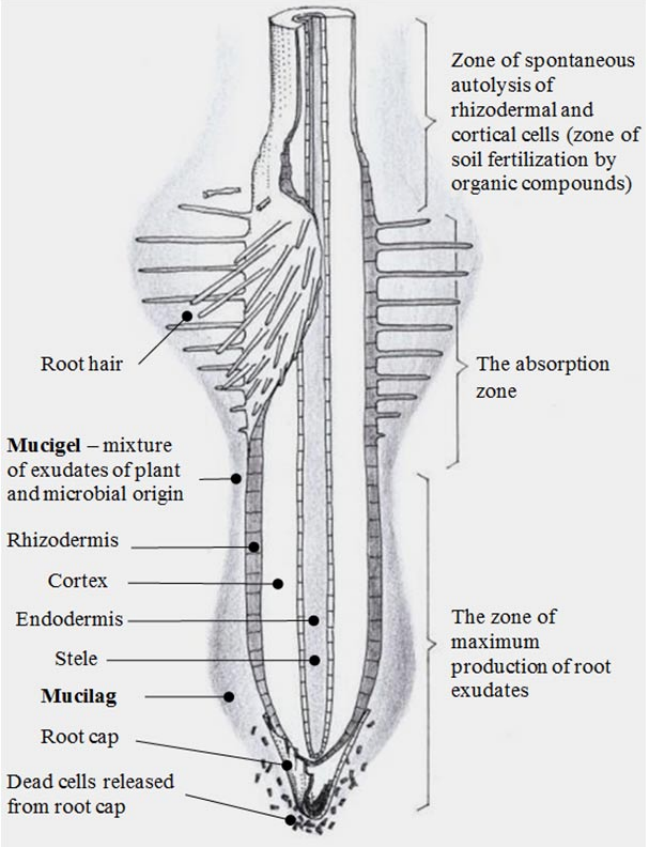

Fig. 1. Rhizosphere – **the root and its environment. The root cap, protective shields for the apex, outer cells are easily shed and are continually renewed.** Mucilag**, gelatinous compound produced by the cells of the root cap and rhizodermis.** Stele**, central part of the root containing conductive tissues of plants, the xylem and the phloem.** Cortex**, the zone of the root between its epidermis (**rhizodermis**) and the stele. More detailed explanations of the zones in the text. Modified according to Gobat et al., 2004**[9]

Sequence of characteristic zones and/or processes for nutrient acquisition by occupation of new soil volume is shown on the Fig. 1. During root growth, different root zones release rhizodeposits of different compositions. The first zone of maximum production of root exudates corresponds to the area of carbon and energy investments by plants via easily available rhizodeposits. Stimulated microbial activity accelerates the decomposition of soil organic matter (SOM) for additional N mineralization (real priming effect)[10].

In the absorption zone are the carbonaceous investments from the first zone valuated by the plants. The uptake of attractive root exudates by microorganisms was followed by their rapid growth and by corresponding increase of their nutrient needs. To obtain an extra amount of nutrients, especially nitrogen for their needs, they produce extracellular enzymes for the mineralization of soil organic matter. Despite the initial uptake of N mineralized from SOM by microorganisms, their much shorter life cycle compared with that of plant roots leads to the release of acquired N back into the soil; this mineral N is then available for root uptake in higher amounts than at the beginning[10].

In the third zone, the zone of spontaneous autolysis of rhizodermal cortical cells is generally accepted, that this lysis occurs under genetic control of the plant and is not affected by rhizosphere microorganisms. Dead root cells nourish the food chain and release organic and mineral substances to the soil[9]. Root death and consequent loss of mass are very difficult to characterize, even more so than production of biomass.

In general: roots provide microorganisms with C, and they in turn obtain nutrients, because these microorganisms efficiently acquire nutrients from sources that are chemically or spatially unavailable to plants[1]. In other words – *plants dominate in soil environment by providing energy and carbon while soil microorganisms dominate by control of biochemical processes in soil.*

"**Sleeping Beauty Paradox**"

Microorganisms are primarily carbon limited in soil; this limitation is partially relieved by exudates delivered by the root moving through soil space, converting bulk soil to rhizosphere soil[8].

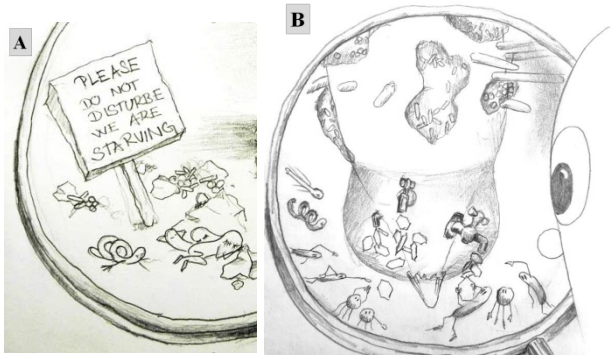

Fig. 2. **"Sleeping Beauty Paradox"**[11] – the contrast between the potential of soil microorganisms for an extremely fast turnover of organic matter and the field reality. Explanations in the text

Explanation of the Fig. 2: (**A**) Non-rhizosfere soil, in which the surviving microorganisms are suffering with minimal activities while involuntarily protecting still incompletely decomposed part of soil organic matter. Apparent "starvation" of soil microorganisms has been empirically proven already in the seventies of the 20th century, based on the conflict between short generation times of microorganisms (approx. 20 hrs) and the time of their life in the soil (1–1.5 years). The starvation associated with the utilization of organic substances and with the preservation of the natural fertility of the soil, is caused not only by the lack of key biogenic elements, but also by the synergy of several factors, such as physical, chemical and biological characteristics of the soil, competitive links between soil microorganisms, complexity of the trophic networks and bonds, concentration of signal substances, etc.

(**B**) Rhizosphere soil, in which the plant root releases rich and diverse source of energy and carbonaceous substances

(symbolically shown with open faucets in mucilage, from which are glucose molecules flowing) which stimulates explosive activity of soil microorganisms resulting in benefits for both, for soil invertebrates and for plants. The contrast between the potential of soil microorganisms for an extremely fast turnover of organic matter and the field reality has been called the "Sleeping Beauty Paradox"[11]. Macroorganisms that have the ability to change environmental conditions at the scale of microorganisms can interrupt this dormancy (acting as "Prince Charming"), providing assimilable substrates (root exudates) that initiate the metabolic capabilities of microorganisms. Hence, they appear to be major regulators of microbial activities.

Quorum sensing

In complex environments, such as a rhizosphere, should bacterial populations act co-operatively and do so by emitting and detecting small diffusing compounds (the most-studied bacterial autoinducers are N-acyl-homoserine lactones -AHL), whose concentration is crucial for a coordinated behavior. This process, known as quorum sensing (QS), allows a bacterial population to evaluate its size and to express specific genes at a threshold cell density, i.e. when a 'quorum' is reached[11].

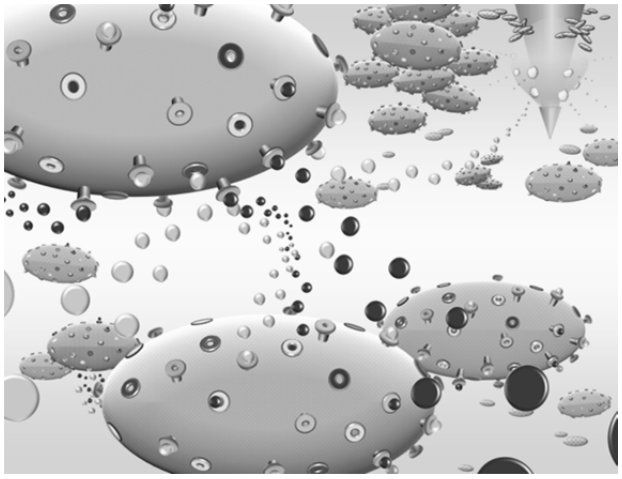

Fig. 3. **Complexities of bacterial regulatory signaling.** Bacteria naturally exist in communities where they constantly monitor their surroundings and coordinate behavior through intraspecies (light colored spheres) and interspecies (dark colored spheres) signaling. Altered bacterial behavior based on activation or the repression of target genes occur when high cell densities are perceived. Bacterial autoinducers also intermingle with eukaryotic hormones or mimic compounds (white spheres emitting from root – in the upper right corner in the background). Modified according to Carter et al., 2012[12]

In natural environments, microorganisms form communities where AHL-producing bacteria interact with other organisms that are able to degrade AHLs. Processes interfering with cell–cell communication are known as quorum quenching. The inactivation of AHLs can not only provide a source of nutrients but also prevents and mitigates QS signaling in neighboring bacteria which should provide a competitive advantage to the corresponding bacteria[11]. Some bacteria, although they do not produce any AHL, can detect these signals and induce specific genes accordingly, and so act as eavesdroppers[11].

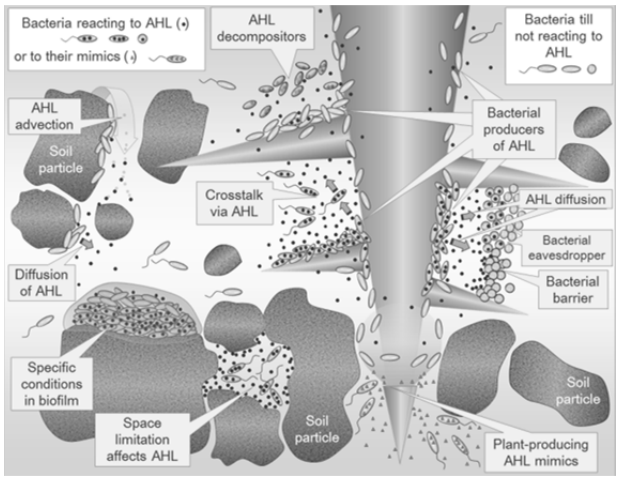

Fig. 4. **Schematic representation of environmental factors affecting the synthesis, stability, diffusion and perception of AHL signals in a rhizosphere.** There are bacterial AHL producers, AHL degraders, AHL eavesdroppers and bacteria acting as an AHL barrier. Influence of eukaryotes, such as plant-producing AHL mimics is also depicted. Modified according to Boyer et Wisniewski-Dyé, 2012[11]

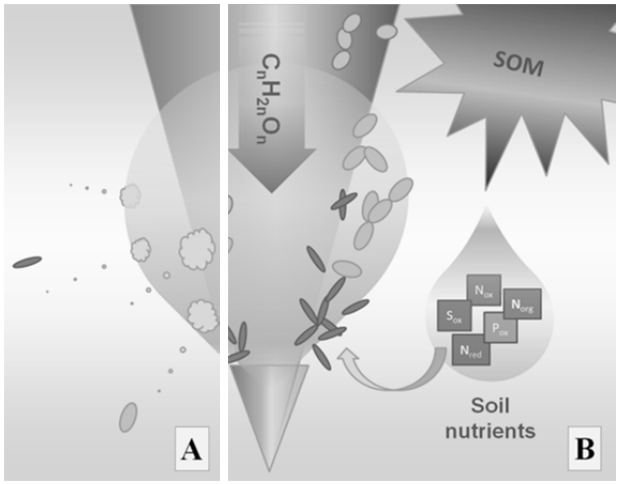

Fig. 5. **Sequence of processes when ingrowing roots occupy new soil volume.** (**A**) Sensitive tissue on root top and following thickening root tissue zone of a ingrowing roots are protected by root cap and by gel high-molecular weight substances (polysaccharides, proteins), so-called "mucilage" against mechanical damage and infection by soil pathogens. According to complexity of regulatory networks and the number of factors affecting QS signalling friendly microbes predominate in colonizing specific plant roots. (**B**) Besides mucilage, the plant root releases rich and diverse source of energy and carbonaceous substances, here representing by a model saccharide $C_nH_{2n}O_n$. As fast as possible are the microbes taking nutrients which are still present in the soil solution for creating their own microbial biomass. In this step are the friendly microbes strongly competing with the host plants about available nutrients. In following interactions will play the quality and quantity of SOM an increasingly important role

Root growth into the soil

Root growth into the soil is accompanied by the competition between plants and microorganisms for available nutrients. The microorganisms stimulated by available C from rhizodeposition begin capturing available nutrients from the soil solution earlier than the roots (Fig. 5). This leads to a temporary decrease in the available nutrients for the roots, and this nutrients limitation in turn stimulates them to release additional C. Although the mechanisms underlying the stimulation of C release by roots as a result of nutrient limitation remain unclear, the increase in C is associated with the development of more abundant fine roots, and consequently higher rhizodeposition. Following the uptake of root exudates, microorganisms use the C for growth and maintenance respiration[1].

As nutrients are limited even for microorganisms, they produce certain extracellular enzymes for the mineralization of poorly available C sources, such as less labile recalcitrant organics from SOM, to obtain insufficient nutrients. It should be mentioned, that microorganisms are not only passive decomposers, they influence SOM cycling also because microbial products are themselves important components of SOM[13].

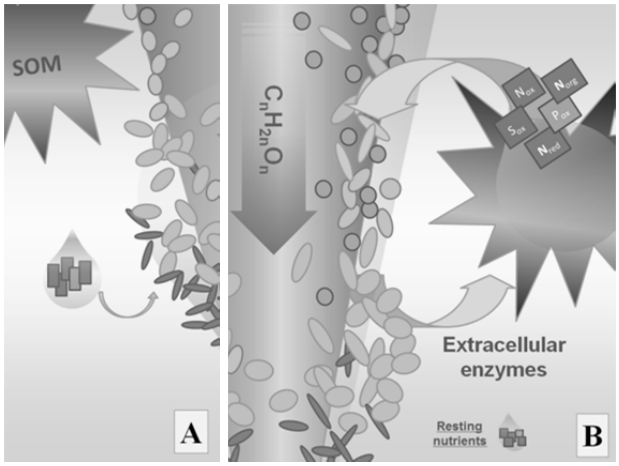

Fig. 6. (**A**) Preferential capturing of available nutrients from the soil solution by increasing number of microorganisms stimulated by rhizodepositions. (**B**) The uptake of root exudates by microorganisms is followed by their rapid growth, activity and respiration. Soon are the current sources of available N exhausted. Microorganisms respond to this pulse by production of extracellular enzymes for the mineralization of insufficient nutrients from poorly available part of soil organic matter (SOM)

The depolymerizing extracellular enzymes break down polymers and generate dimers and monomers that are soluble and available for microbial uptake. Because microbial turnover in the rhizosphere is very rapid (a few days), the C losses by respiration are very high. Consequently, these microorganisms become energy-starved and try to obtain their energy from amino acids. Amino acids can also be used directly by roots, although compared with microorganisms, plant roots are often not very efficient competitors for this N source[1]. Microorganisms strip off the N from the amino acids, thereby making the C skeletons available for energy and growth. Finally, NH_4^+ is released as a waste metabolite in this process (ammonification). And if there is sufficient amount of NH_4^+ ions accumulated, the process of nitrification may follow releasing NO_3^-. Similar pathways of mineralization make other key nutrients available. This form of available N and other key nutrients can be already absorbed by roots.

As a result of this trade, the net N release from starving or dying microorganisms is higher than the initially available N content because of microbial mining for extra N from SOM during root growth[1].

The Microbial Loop in Soil

The soil volume occupied by micro-organisms is considerably less than 1 %, and this occupied volume is distributed heterogeneously in small-scale habitats, connected by water-saturated or unsaturated pore space.

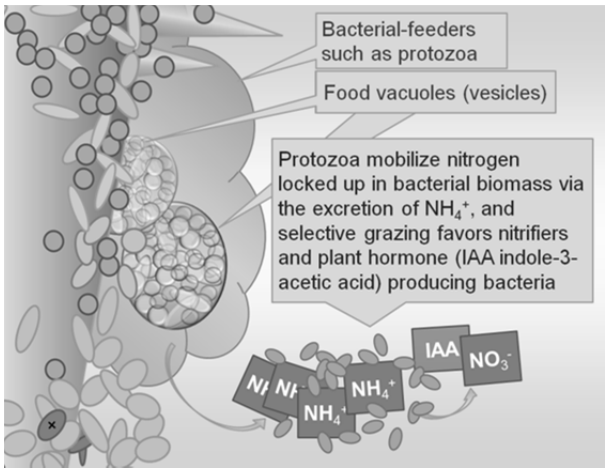

Fig. 7. A large amount of soil microbial biomass attracts predators, in this case soil protozoa, for which the bacterial cells and their elemental composition are stochiometrically very similar and to a great extent also easier to digest than plant biomass residues

The availability of spatially and temporally diverse habitats probably gives rise to the biodiversity that we see in soil[13]. Although diverse microorganisms occupy only a small portion of soil volume, they take up the labile organics compounds almost immediately and consume them within a few hours, and as a result, process rates are up to two orders of magnitude faster than in bulk soil[15]. Such small soil volumes with much faster process rates and much more intensive interactions compared to the average soil conditions were newly (in 2015) defined by Yakov Kuzyakov and Evgenia Blagodatskaya as **microbial hotspots**[15].

The scenario of microbial hotspots fits perfectly on rhizosphere, where removing the limitation by labile C stimulates the rapid microbial growth[1]. However the stimulation of microbial activities is quite costly; it has been observed in different plant-microbial interactions that through root-derived carbon, through this trade with plant C-investment, plants may release up to half of their total fixed carbon to fuel microbial interactions in the rhizosphere[14].

Due to improved understanding of rhizosphere in recent years, namely of the recognition that microbial signals are enhancing the efflux of carbon from roots, the nitrogen nutrition of plants seems to be partly driven by protozoan grazers[14]. Microbial hotspots in rhizosphere represent stochiometrically atractive microbial biomass for subsequent microfaunal grazers, where numbers of bacterial feeding protozoa and free-living nematodes may increase up to 30-fold compared with bulk soil[14]. Consequently, beneficial effects of protozoa on plant growth have been assigned to nutrients released from consumed bacterial biomass, that is, the „microbial loop“[14] (Fig. 7, 8).

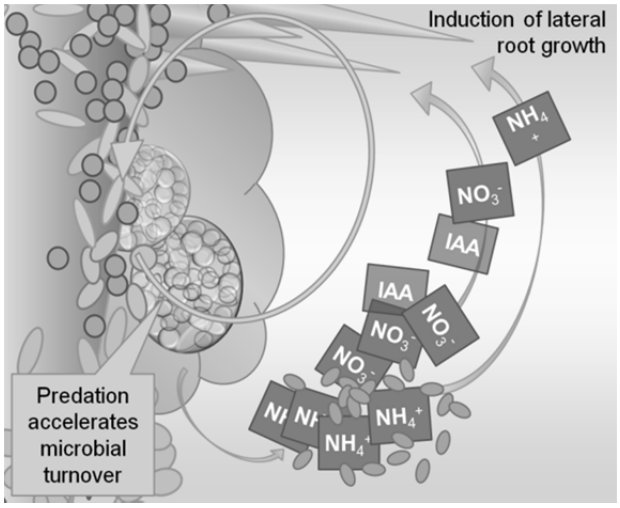

Fig. 8. Protozoan grazing can stimulate nitrifying bacteria, presumably through predation on their faster-growing bacterial competitors, resulting in high concentrations of NO_3^-, and in some cases through stimulation of indole-3-acetic acid (IAA+) producing bacteria. Positive feedbacks may also arise through selective grazing and consequent changing of rhizosphere microorganisms

Recent investigations indicate that the nutrients released from microbial biomass are only a small part of an intimate, but indirect symbiosis of bacterivores with plant roots[16]. Understanding of this complex of multitrophic interactions is tightly connected with identification of the genetic control points which determine these interactions and to determine how the interactions between multiple plant symbionts and their microbial hotspots and hot moments are coordinated[16, 15].

Conclusion

The mechanisms related with the natural soil fertility and soil organic matter regeneration described here as a mechanisms of carbonaceous stimulation by roots in rhizosphere and consequent cascade of microbial activities and processes removing N limitation remain mostly unclear despite the fact that higher rhizodeposition in the case of insufficient sources of available nitrogen in soil is evident.

Nevertheless, clarifying the C release by roots as a result of N limitation could significantly contribute to our understanding of mutualistic mechanisms within a community of microorganisms and invertebrates that has been selected through long-term ecosystem evolution. Highlighting these mechanisms in rhizosphere focused our attention on the quality and structure of soil organic matter, especially its easily available part. It indicates that, over long periods, plants in natural ecosystem tend to acquire increasing amounts of N, which had already passed through a microbial cycle(s) and was initially stored in the SOM.

On the contrary, the soil fertility in intensive agriculture is based on the addition of synthetic fertilizers in accordance with the Sprengel-Liebig´s theory of mineral nutrition, not on the mechanisms of the carbonaceous stimulation of soil environment. An excess of mineral N added as fertilizers that cannot be trapped by microorganisms because of the absence of available C, is causing high N losses by leaching in agricultural soils, and other consequent agroecosystems disturbances. Therefore, nitrogen losses from intensive agriculture are associated not only with high doses of mineral fertilizers (the annual N turnover in many natural ecosystems is even higher than in croplands) but also with the particular inability of microorganisms to retain excess of mineral nitrogen.

Abstract

Understanding to the relationships and interactions between the soil, plants and soil organisms in the rhizosphere is the most important step in understanding to the essence of soil fertility. According to the rhizosphere concept, firstly formulated by Lorenz Hiltner in 1904, rhizosphere is an area of active interchange between plants and soil bacteria, where photosynthate fuels microbial growth and activity, ultimately resulting in the stimulation of specialized microorganisms. In extremely heterogeneous environment such as soil act bacterial populations co-operatively and do so by the process, known as quorum sensing (QS). Immediate capturing of available nutrients from the soil solution by microorganisms is followed by their rapid growth and activity. Soon are the current sources of available N exhausted. Microorganisms respond to this pulse by production of extracellular enzymes for the mineralization of insufficient nutrients from poorly available part of soil organic matter (SOM). Despite the initial uptake of N mineralized from SOM by microorganisms, their much shorter life cycle compared with that of plant roots leads to the release of acquired N back into the soil; this mineral N is then available for root uptake in higher amounts than at the beginning. Presented concept of soil fertility stemming from the interactions in the environment surrounding plant roots is by the intensive agriculture unfortunately overlooked.

This work was supported by the National Agency for Agricultural Research of Czech Republic (NAZV): QJ1220007 - Possibilities of retention of reactive nitrogen from agriculture in the most vulnerable water resource area.

REFERENCES

1. Kuzyakov, Y., Xu, X. 2013. Competition between roots and microorganisms for nitrogen: mechanisms and ecological relevance. New Phytologist 198: 656–669.

2. Hartmannn, A., Rothballer, M., Schmid, M. 2008. Lorenz Hiltner, a pioneer in rhizosphere microbial ecology and soil bacteriology research. Plant Soil 312:7–14.
3. Gregory, P. J. 2006. Roots, rhizosphere and soil: the route to a better understanding of soil science? European Journal of Soil Science 57, 2–12.
4. Gregory, P. J. 2010. A history of rhizosphere research – roots to a solution. 19th World Congress of Soil Science, Soil Solutions for a Changing World, 1–6 August 2010, Brisbane, Australia. Published on DVD. 5–7.
5. Van der Ploeg, R. R., Böhm, W., Kirkham, M.B. 1999. History of soil science – On the origin of the theory of mineral nutrition of plants and the low of the minimum. Soil Sci. Soc. Am. J. 63: 1055–1062.
6. Shibata, H., Branquino, C., McDowell, W.H., Mitchell, M. J., Monteith, D. T., Tang, J., Arvola, L., Cruz, C., Cusack, D. F., Halada, L., Kopáček, J., Máguas, C., Sajidu, S., Schubert, H., Tokuchi, N., Záhora, J. 2015: Consequence of altered nitrogen cycles in the coupled human and ecological system under changing climate: The need for long-term and site-based research. Ambio 44:178–193.
7. Hiltner, L. 1904. Über neuere Erfahrungen und Probleme auf dem Gebiete der Bodenbakteriologie unter besonderer Berücksichtigung der Gründüngung und Brache. Arbeiten der Deutschen Landwirtschaftlichen Gesellschaft 98, 59-78.
8. DeAngelis, K. M., Lindow, S. E., Firestone, M. K. 2008. Bacterial quorum sensing and nitrogen cycling in rhizosphere soil. FEMS Microbiol Ecol 66: 197–207.
9. Gobat, J. M., Aragno, M., Matthey, W. 2004: *The Living Soil, Fundamentals of Soil Science and Soil Biology* – Science Publishers, Inc. Enfield. pp 603.
10. Lavelle, P., Gilot, C. 1994. Priming effects of macroorganisms on microflora: A key process of soil functions? In: *Beyond the Biomass*, (Ed. by K. Ritz, J. Dighton and K. Giller), Wiley-Sayce, Chichester, UK. pp. 176–181.
11. Boyer, M., Wisniewski-Dyé, F. 2009.Cell-cell signalling in bacteria: not simply a matter of quorum. FEMS Microbiol. Ecol. 70: 1–19.
12. Carter, K. K., Valdes, J.J., Bentley, W. E. 2012. Pathway engineering via quorum sensing and sRNA riboregulators – Interconnected networks and controllers. Metabolic Engineering 14: 281–288.
13. Schmidt, M. W., Torn, M. S., Abiven, S., Dittmar, T., Guggenberger, G., Janssens, I. A., Kleber, M., Kögel-Knabner, I., Lehmann, J., Manning, D. A., Nannipieri, P., Rasse, D. P., Weiner, S., Trumbore, S. E. 2011. Persistence of soil organic matter as an ecosystem property. Nature. 478: 49–56.
14. Bonkowski, M. 2004. Protozoa and plant growth:the microbial loop in soil revisited. New Phytologist 162: 617–631.
15. Kuzyakov, Y., Blagodatskaya E, 2015. Microbial hotspots and hot moments in soil: Concept & review. Soil Biology & Biochemistry 83: 184–199.
16. Bonkowski, M., Villenave, C., Griffiths, B. 2009. Rhizosphere fauna: the functional and structural diversity of intimate interactions of soil fauna with plant roots. Plant Soil 321: 213–233.

Autorský rejstřík

CZECH CHEMICAL SOCIETY SYMPOSIUM SERIES • ročník/volume 13 (2015), čís./no. 2 • ISSN 2336-7202 (Print), ISSN 2336-7210 (On-line) • evidenční číslo MK ČR E 21999 • Vydává Česká společnost chemická jako časopis Asociace českých chemických společností ve spolupráci s VŠCHT Praha, s ČSPCH a ÚOCHB AV ČR za finanční podpory Rady vědeckých společností ČR, Akademie věd ČR, Nadace Český literární fond a kolektivních členů ČSCH • IČO 444715 • Published by the Czech Chemical Society • VEDOUCÍ REDAKTOR/EDITOR-IN-CHIEF: P. Chuchvalec • REDAKTOŘI/ EDITORS: J. Barek, Z. Bělohlav, P. Drašar, P. Holý, J. Horák, Z. Kolská, B. Kratochvíl, J. Podešva, P. Rauch; Webové stránky: P. Zámostný • TECHNICKÁ REDAKTORKA/EDITORIAL ASSISTANT: R. Řápková • Redakce čísla (ISSUE EDITOR) O. Zmeškal • ADRESA PRO ZASÍLÁNÍ PŘÍSPĚVKŮ/MANUSCRIPTS IN CZECH, SLOVAK OR ENGLISH CAN BE SENT TO: Chemické listy, Novotného lávka 5, 116 68 Praha 1; tel./phone +420 221 082 370, +420 222 220 184, e-mail: chem.listy@csvts.cz • PLNÁ VERZE NA INTERNETU/FULL VERSION ON URL: http://www.ccsss.cz • TISK: Garamon s.r.o., Wonkova 432, 500 02 Hradec Králové • SAZBA, ZLOM: ČSCH, Chemické listy • Pokyny pro autory najdete na http://www.ccsss.cz , zkratky časopisů podle Chemical Abstract Service Source Index (viz http://cassi.cas.org/search.jsp) • Molekulární námět na obálce: Vladimír Palivec • Dáno do tisku 10.12.2015.